THE DOMAINS OF FLAVOCYTOCHROME b_2

Claire Elaine Brunt

A thesis presented for the degree of
Doctor of Philosophy

University of Edinburgh

1993

IN MEMORY OF MY FATHER,

BRIAN BRUNT

1934 -1987

The best years of my life have been passed in the ardent study of ... chemical science. Chemistry, especially, has always had irresistible attractions for me, from the enormous, the illimitable power which the knowledge of it confers. Chemists, I assert it emphatically, might sway, if they pleased, the destinies of humanity.

Wilkie Collins
"The Woman in White"

DECLARATION

I hereby declare that, except where specific reference is made to other sources, the work presented in this thesis is my own original work, some of which has been performed in collaboration with other researchers. I identify myself as the author of this thesis. Some of the work presented in this thesis has already been published.

ACKNOWLEDGEMENTS

I thank the University of Edinburgh for the gift of a Dewar Research Studentship and for the use of University facilities.

Research is not a task which can be performed in isolation. I would therefore like to acknowledge and thank the many colleagues and friends without whose help, patience, support and encouragement this thesis would never have been written, and who helped to make the last few years so happy and memorable for me.

Dr. Stephen Chapman, for being the best supervisor possible, in every sense;

Dr. Graeme Reid, for help, advice and discussion;

Drs. Geoff Moore, Andy Thurgood and John Parkinson, and Mark Cox, for a fruitful and enjoyable NMR collaboration;

Dr. Graeme Pettigrew, for help and advice, and for allowing me to carry out redox potentiometry in his laboratory;

The Chapman group, past and present, for friendship, support and general lunacy, especially Patricia White for proof-reading;

Ros Ibberson, who should really take the blame;

My mother, Anne Brunt, for love, support and especially for her tireless work in typing this thesis from a muddled manuscript; and

David Maden, for being there.

ABSTRACT

Flavocytochrome $\underline{b}_2$ is a respiratory enzyme found in the intermembrane space of yeast mitochondria, where it catalyses the oxidation of L-lactate to pyruvate, transferring electrons to cytochrome $\underline{c}$. The enzyme is a tetramer. Each subunit comprises two functionally-distinct domains, one containing flavin mononucleotide and the other containing protohaem IX. The lactate-binding site of the enzyme is located within the flavin-containing domain. This domain is essential for L-lactate dehydrogenase activity. The haem domain is essential for electron transfer to cytochrome $\underline{c}$.

The haem- and FMN-containing domains of flavocytochrome $\underline{b}_2$ have now been expressed independently in E.coli. This thesis describes the development of effective purification procedures for the two independently-expressed domains and their characterization by biophysical and biochemical techniques. The characterization of a point mutant of the isolated $\underline{b}_2$-flavin domain is also discussed.

The independently-expressed haem domain was purified to a high level by column chromatography. The isolated protein was found to be monomeric with a molecular weight of 10 500. It had no detectable enzyme activity and failed to accept electrons from either the isolated $\underline{b}_2$-flavin domain or the holoenzyme. Isolated $\underline{b}_2$-haem domain was found to be stable over a wide temperature and pH range. Its redox potential was found to be -31+/-2mV, in agreement with a previously-determined value for a similar fragment isolated from the holoenzyme by proteolytic methods. High-field ^{1}H-NMR studies have been carried out on the isolated $\underline{b}_2$-haem domain. The pK_A values of the haem propionates were found by NMR to be 4.8

and 4.6, consistent with these groups being exposed to solvent. NMR studies were also used to determine an electron self-exchange rate constant of $2.3 \times 10^{6} M^{-1} s^{-1}$ for the $\underline{b}_2$-haem domain. The interactions of cytochrome $\underline{c}$ with both the holoenzyme and the isolated haem domain were studied by NMR. It was found that, whereas cytochrome $\underline{c}$ bound to the holoenzyme, it failed to bind to the isolated haem domain.

The independently-expressed flavin domain of flavocytochrome $\underline{b}_2$ was also purified by column chromatography and was found to be a tetramer, with a subunit molecular weight of 47 000. It was found to have L-lactate dehydrogenase activity with ferricyanide as the electron acceptor but not with cytochrome $\underline{c}$. k_{cat} and K_m values were determined for the isolated $\underline{b}_2$-flavin domain under steady-state and pre-steady-state conditions. The rate-determining step for the isolated flavin domain was found by steady-state kinetic isotope effect studies to be similar to that observed in the holoenzyme. Stopped-flow studies found FMN reduction to be monophasic in the isolated $\underline{b}_2$-flavin domain, in contrast to the holoenzyme. The effects of various inhibitors on the isolated flavin domain are also discussed.

The role of tyrosine 143 in the isolated $\underline{b}_2$-flavin domain was probed by replacing it with phenylalanine. The mutant enzyme was then investigated by steady-state and pre-steady-state kinetics. Under stopped-flow conditions, FMN reduction in the mutant enzyme was found to be biphasic, unlike FMN reduction in the native $\underline{b}_2$-flavin domain. Inhibition studies using oxalate, an analogue for the transition state in flavocytochrome $\underline{b}_2$, suggested that Tyr 143 is important for transition state stabilisation.

ABBREVIATIONS AND UNITS

AMINO ACIDS

Amino acids are represented by single-letter and three-letter codes:

Amino acid	Three-letter abbreviation	One-letter symbol
Alanine	Ala	A
Arginine	Arg	R
Asparagine	Asn	N
Aspartic acid	Asp	D
Glutamine	Gln	Q
Glutamic acid	Glu	E
Histidine	His	H
Lysine	Lys	K
Methionine	Met	M
Phenylalanine	Phe	F
Proline	Pro	P
Serine	Ser	S
Tyrosine	Tyr	Y

OLIGONUCLEOTIDES

The purine and pyrimidine bases are abbreviated to A (adenine), G (guanine), C (cytosine) and T (thymine).

ENZYMES

$\underline{b}_2$-flavin domain	the isolated flavin domain of flavocytochrome $\underline{b}_2$ expressed independently in E.coli.
$\underline{b}_2$-haem domain	the isolated haem domain of flavocytochrome $\underline{b}_2$ expressed independently in E.coli.
HE/Y143F	holo-flavocytochrome $\underline{b}_2$ in which the tyrosine at position 143 (Y143) in the amino-acid sequence has been replaced by phenylalanine (F).
FD/Y143F	$\underline{b}_2$-flavin domain in which Y143 has been replaced with F.

KINETIC PARAMETERS

K_m	Michaelis constant
k_{cat}	enzyme turnover number
V_{max}	limiting value for reaction rate
K_I	inhibitor constant

OTHER ABBREVIATIONS

DNA	deoxyribonucleic acid
E.coli	Escherichia coli
EDTA	ethylenediamine tetraacetic acid
EPR	electron paramagnetic resonance
FAD	flavin adenine dinucleotide
FMN	flavin mononucleotide
FPLC	fast protein liquid chromatography
H.anomala	Hansenula anomala
lactate	L-[2-^{1}H] lactate (unless otherwise stated)
M_r	relative molecular weight
NMR	nuclear magnetic resonance
PMSF	phenylmethylsulphonyl fluoride
S.cerevisiae	Saccharomyces cerevisiae
SDS-PAGE	sodium dodecyl sulphate-polyacrylamide gel electrophoresis

UNITS

Units used in this thesis include

Å	Angstroms	K	Kelvin
g	grams	ppm	parts per million
G	Gauss	V	volts
H	Hertz	Ω	ohms

All relative molecular masses are given in Daltons.

Other unit abbreviations include

s^{-1}	first order rate constant
$M^{-1}s^{-1}$	second order rate constant
$M^{-1}cm^{-1}$	molar extinction coefficient

LIST OF CONTENTS

LIST OF FIGURES

LIST OF TABLES

CHAPTER 1

INTRODUCTION

1.1 INTRODUCTION

1.1.1 FLAVOCYTOCHROME b_2

Flavocytochrome b_2 (L(+)-lactate:cytochrome c oxidoreductase) is found as a soluble component of the intermembrane space of yeast mitochondria, where it catalyses the oxidation of L-lactate to pyruvate, subsequently transferring electrons to cytochrome c [1], [2]. The enzyme contains two prosthetic groups, flavin mononucleotide (FMN) and protohaem IX [1] (Figure 1.1), bound in two functionally-distinct domains, and is thought to be the evolutionary result of a fusion of one gene coding for a cytochrome and another coding for an FMN-binding dehydrogenase [3].

1.1.2 CYTOCHROMES

Cytochromes are electron-transporting proteins which contain protohaem IX (Figure 1.1(a)) or one of its derivatives. They are usually single-electron carriers which function by alternating between reduced (ferrous, Fe^{2+}) and oxidized (ferric, Fe^{3+}) redox states, and therefore play a central role in electron-transport chains in many organisms.

Cytochromes can be classified according to the type of haem they contain. The different types of haem produce characteristic optical absorption spectra [4]. a-type cytochromes contain haem a, a substituted form of protohaem IX. b-type cytochromes contain unsubstituted protohaem IX which is not covalently-linked to the protein. In c-type cytochromes, the protohaem IX is attached to the protein by covalent linkages between the two vinyl side-chains on the haem and two cysteine residues on the protein.

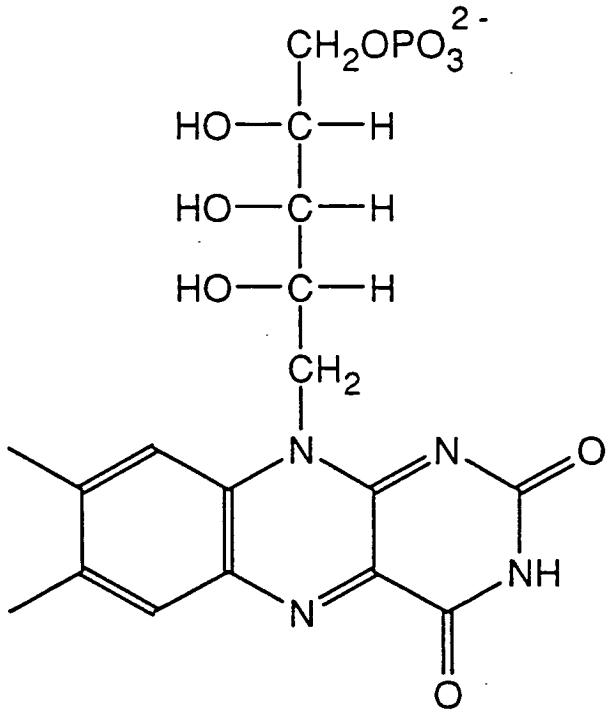

(a) Flavin mononucleotide (FMN)

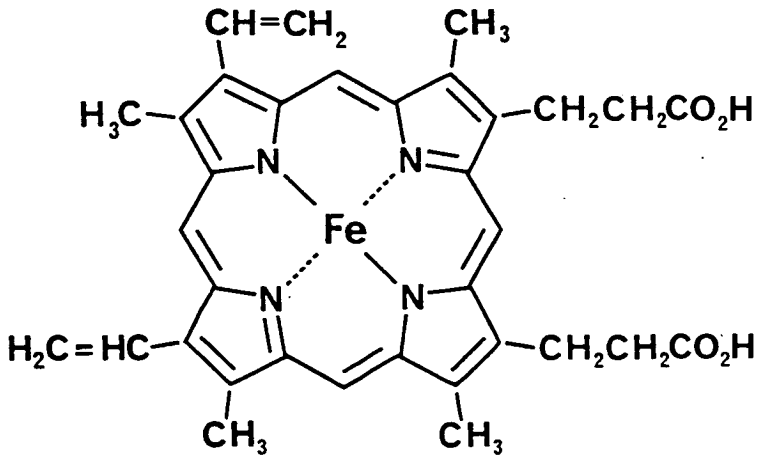

(b) Protohaem IX

FIGURE 1.1 THE PROSTHETIC GROUPS OF FLAVOCYTOCHROME $\underline{b}_2$

1.1.3 FLAVOPROTEINS

Flavoproteins contain either flavin adenine dinucleotide (FAD) or flavin mononucleotide (FMN) (Figure 1.1(b)) which are coenzymatically-active forms of riboflavin (vitamin B12) (Figure 1.2). The catalytically-important part of the flavin is the isoalloxazine ring. The side-chain is important in anchoring the flavin group at the active site but plays no part in catalysis.

Flavins are capable of carrying either one or two electrons by virtue of their ability to exist in a semiquinone form as well as in fully-oxidized and fully-reduced states. These three oxidation states are spectroscopically-distinguishable, the oxidized form being yellow, the reduced (2-electron) state being colourless, and the semiquinone (1-electron) form being either red or blue depending on the location of the radical on the isoalloxazine ring [5]. The ability of flavins to exist in these three states enables flavoproteins to act as transformers in an electron transport chain, linking a 2-electron-carrying system to a 1-electron-carrying system.

1.2 BACKGROUND

1.2.1 HISTORICAL

Flavocytochrome b_2 was first isolated from *Saccharomyces cerevisiae* (baker's yeast) by Bach and co-workers in 1942 [6], who identified an enzyme, responsible for L-lactate dehydrogenase activity, as a *b*-type cytochrome. Later, Appleby and Morton succeeded in purifying and crystallizing the enzyme, and identified a second prosthetic group, FMN, present in an equal ratio to the haem [1].

FIGURE 1.2 RIBOFLAVIN (VITAMIN B2)

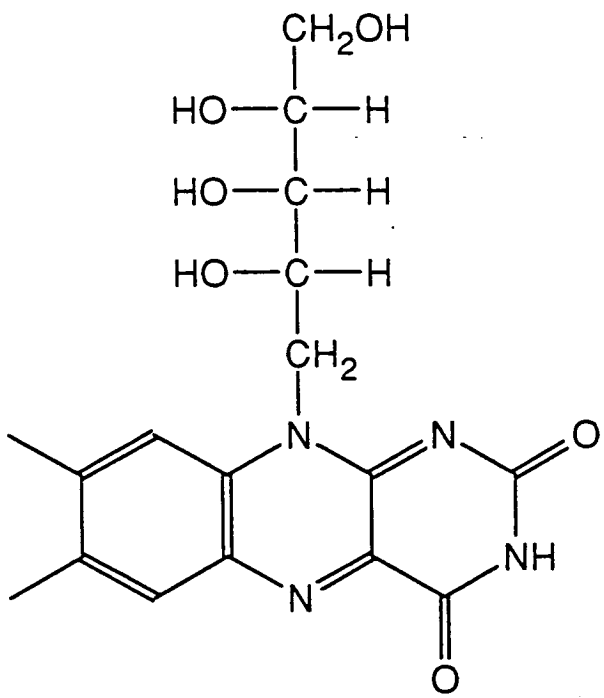

Since then, extensive research has been focussed on flavocytochrome $\underline{b}_2$ (for reviews see [3] and [7]). In recent years, the elucidation of the crystal structure of flavocytochrome $\underline{b}_2$ [8] and the cloning and expression of its gene in E.coli [9] have provided a new means of investigating the relationship between enzyme structure and function. Knowledge of the crystal structure has allowed residues or regions which may have important structural or functional implications to be indentified. Mutant forms of the enzyme in which one or more amino-acids have been specifically replaced, inserted or deleted, have been generated and expressed in E.coli. Such genetically-engineered modifications are enabling the role of single amino-acids, and even of entire structural features, to be deduced.

1.2.2 ISOLATION AND PURIFICATION

Appleby and Morton's first purification of flavocytochrome $\underline{b}_2$ from S.cerevisiae [1] relied on crystallization as a major purification step. The crystallized enzyme thus produced (termed type I) was later found to contain a small proportion of DNA [10] which could be removed by dialysis or chromatography [10-12] to give type II, DNA-free flavocytochrome $\underline{b}_2$ crystals. However, the enzyme prepared in this way was found to be unstable and gave inconsistent kinetic results [10,11,13,14]. It was observed that a "modification" in the enzyme was necessary before crystallization could occur [15]. Electrophoretic studies of the crystallized material revealed that they consisted of two polypeptide chains of M_r 26 000 and M_r 36 000 [16]. It was later shown that the enzyme had undergone selective cleavage by yeast proteases [17]. Purification in the presence of

phenylmethylsulphonyl fluoride (PMSF), a known protease inhibitor, produced a stable enzyme which did not crystallize [17-19]. The purification procedure in the presence of PMSF has since undergone subsequent refinement [17,18,20]. The two forms of flavocytochrome b_2, prepared in the absence and presence of PMSF, are termed "cleaved" and "intact" respectively.

In 1989, Black *et al* succeeded in expressing flavocytochrome b_2 at high levels in *E.coli* [9]. This provided a means of producing large quantities of enzyme quickly and easily, the yield of flavocytochrome b_2 from *E.coli* being estimated to be 500- to 1000-fold higher than the yield from a similar wet weight of yeast [9].

1.2.3 LOCATION AND FUNCTION

Flavocytochrome b_2 is synthesized in the cytoplasm. The pre-protein, which includes an 80-amino acid N-terminal extension,is imported into the mitochondrial intermembrane space where part of the polypeptide penetrates the inner membrane and is proteolytically cleaved, leaving an insoluble membrane-bound intermediate. This intermediate undergoes further cleavage to release the mature enzyme which is found as a soluble component of the intermembrane space [2,21,22], where its function is to oxidize lactate to pyruvate and transfer electrons to cytochrome *c* [23,24]. Flavocytochrome b_2 is thus postulated to take part in a short electron transport chain allowing the yeast to respire on L-lactate even if the main pathway is blocked, for example by antimycin (Figure 1.3) [24].

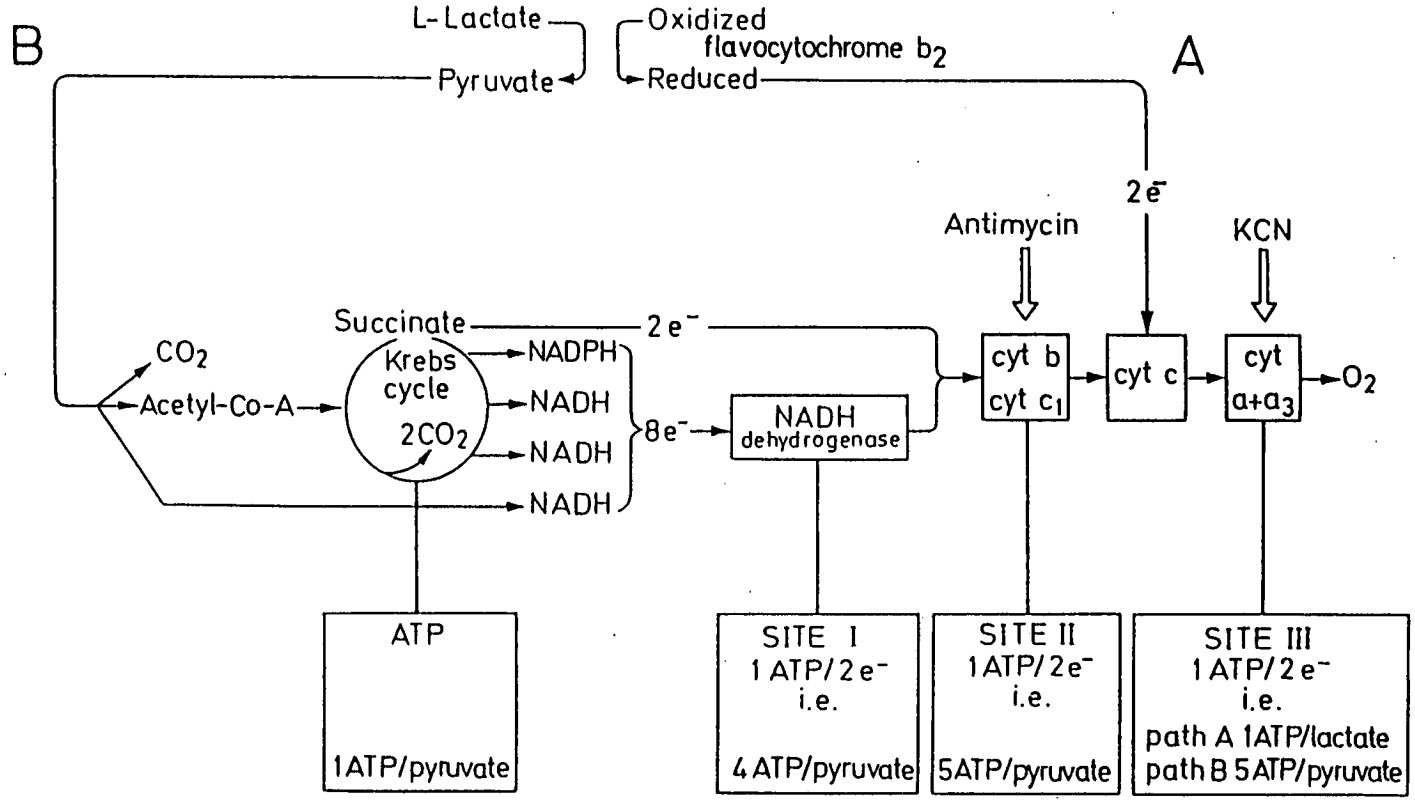

FIGURE 1.3 THE OXIDATION PATHWAYS OF L-LACTATE IN YEAST MITOCHONDRIA [24]

Route A is the shortened respiratory chain involving flavocytochrome $\underline{b}_2$ which allows the yeast to respire if route B should become blocked.

1.3 BIOCHEMICAL AND BIOPHYSICAL PROPERTIES

1.3.1 GENERAL

Biochemical and biophysical properties of flavocytochrome $\underline{b}_2$ have been reviewed in [3] and [7]. The enzyme has been found to be capable of catalyzing the oxidation of a broad range of α-hydroxy-acids [3,7]. From studies on potential substrates of flavocytochrome $\underline{b}_2$ it was concluded that the minimum requirements of a carboxylate group with both a hydrogen and a hydroxyl group next to it must be met [3,7]. L-lactate was found to be the most efficient substrate, as would be expected. The enzyme operates at an optimum pH of between pH 7 and 8 [7].

1.3.2 SPECTROSCOPIC STUDIES

The electronic absorption spectrum of flavocytochrome $\underline{b}_2$ is typical of a $\underline{b}$-type cytochrome. In the reduced state, the absorbances due to the α- and β- bands are seen at 557 and 528nm respectively, with the γ-, or Soret, absorbance at 423nm. In the oxidized state, the sharpest absorbance is the γ-(Soret) band, which appears at 413nm [7]. Molar absorption coefficients have been determined for the enzyme and for proteolytically-isolated cytochrome $\underline{b}_2$ core (Section 1.4.1) [25] and are summarised in Table 1.1.

EPR studies of flavocytochrome $\underline{b}_2$ at 123K, with FMN in the semiquinone form, show a g-value of 2.004 and a bandwidth of around 15G, which is consistent with an anionic, or red, semiquinone [26]. At 28K the FMN signal is largely saturated but a signal typical of low-spin ferric haem is observed [26]. The haem EPR signal is very similar to that observed for cytochrome $\underline{b}_5$ [27].

TABLE 1.1: PEAK POSITIONS AND EXTINCTION COEFFICIENTS IN THE ELECTRONIC ABSORPTION SPECTRA OF FLAVOCYTOCHROME $\underline{b}_2$ [25]

Band	Oxidized		Reduced	
	λ_{max} (nm)	ϵ (mM^{-1} cm^{-1})	λ_{max} (nm)	ϵ (mM^{-1} cm^{-1})
α	560	9.2	557	30.9
β	530	11.3	528	15.6
γ	413	129.5	423	183.0
δ	362	34.4	328	39.0
UV	275	89.0	269	88.0

(Oxidized cytochrome $\underline{b}_2$ core : λ_{max} = 413nm, ϵ = 121.5mM^{-1} cm^{-1})

1.3.3 REDOX POTENTIALS

Redox potentials have been determined for the prosthetic groups in various forms of flavocytochrome $\underline{b}_2$ and are shown in Table 1.2 [3,7]. The difference in potential between the two prosthetic groups is consistent with reversible electron transfer between flavin and haem [3].

1.4 STRUCTURAL STUDIES

Before the crystal structure of flavocytochrome $\underline{b}_2$ had been solved, information about structural features was gained from studies of the enzyme in solution. The amino-acid sequence was determined [28], prosthetic groups identified [1] and the enzyme found to be a tetramer of identical subunits of M_r 57 500 [25,29,30].

1.4.1 PROTEOLYTIC STUDIES

During the preparation of flavocytochrome $\underline{b}_2$ from yeast, it was observed that the enzyme underwent cleavage by yeast proteases (Section 1.2.2), producing two fragments of unequal length [16,17]. Trypsinolysis of the enzyme succeeded in cleaving it into two fragments of M_r 36 000 and 21 000, which became known as fragments α and β respectively [16]. The α-fragment was found to contain the haem-binding site [16] but neither fragment was found to contain FMN.

Further studies of the enzyme revealed a number of proteolytically-sensitive bonds [31]. One haem-containing fraction produced in this way had been isolated as early as 1966, and became known as cytochrome $\underline{b}_2$ core [36]. It was also discovered that a similar fraction could be produced by the action of yeast proteases during the isolation of

TABLE 1.2: SOME PROSTHETIC GROUP REDOX POTENTIALS IN FLAVOCYTOCHROME b_2

Enzyme	Reduction Potentials (mV)				Ref.
	H_{OX}/H_{RED}	F_{OX}/F_{SQ}	F_{SQ}/F_{RED}	F_{OX}/F_{RED}	
S.cerevisiae (cleaved)	6 ± 2	-44 ± 8	-57 ± 9	-51 ± 16	[74]
H.anomala (intact)	-19 ± 5	-23 ± 8	-45 ± 12	-34 ± 10	[74]
S.cerevisiae b_2 core	-28	-	-	-	[33]

Abbreviations: H = haem, F = flavin, OX = oxidized, RED = reduced, SQ = semiquinone

More extensive tables can be found in [3] and [7]

the enzyme from yeast [33]. This fragment was shown, by sequencing and amino-acid analysis, to contain the first 96 amino-acids of the protein sequence [34] forming the N-terminus of the flavocytochrome $\underline{b}_2$ monomer [35].

Proteolytic studies also revealed that FMN binding required the association of both fragments α and β [36]. For this reason, it proved more difficult to isolate a flavin-containing fragment. Further studies using trypsinolysis under very carefully-controlled conditions did succeed in isolating a tetrameric flavin-containing protein from flavocytochrome $\underline{b}_2$ from Hansenula anomala (Section 1.6.2), leading to the conclusion that the prosthetic groups are bound in two domains within the protomer [37]. However, there remained a degree of uncertainty with regard to the structure of the flavin domain. The position of the proteolytically-sensitive region within this domain [38] led to the suggestion of a biglobular flavin domain [36-40]. Such questions were ultimately resolved when the crystal structure of flavocytochrome $\underline{b}_2$ became known [8,41].

1.4.2 X-RAY CRYSTALLOGRAPHY

The x-ray crystal structure of flavocytochrome $\underline{b}_2$ has been solved to 2.4Å resolution [8,41] and confirms that the enzyme is indeed a tetramer (Figure 1.4). Each subunit consists of two domains: a cytochrome domain, comprising residues 1-100 of the amino-acid sequence of the protein, and a single flavin-binding domain (residues 101-511) (Figure 1.5). The four flavin domains pack around the molecular 4-fold axis to form an ellipsoidal disc approximately 100Å across and 60Å deep. The cytochrome domains are situated on the periphery of this disc (Figure 1.4).

FIGURE 1.4 TETRAMERIC FLAVOCYTOCHROME $\underline{b}_2$

Prosthetic groups are shown in dark blue

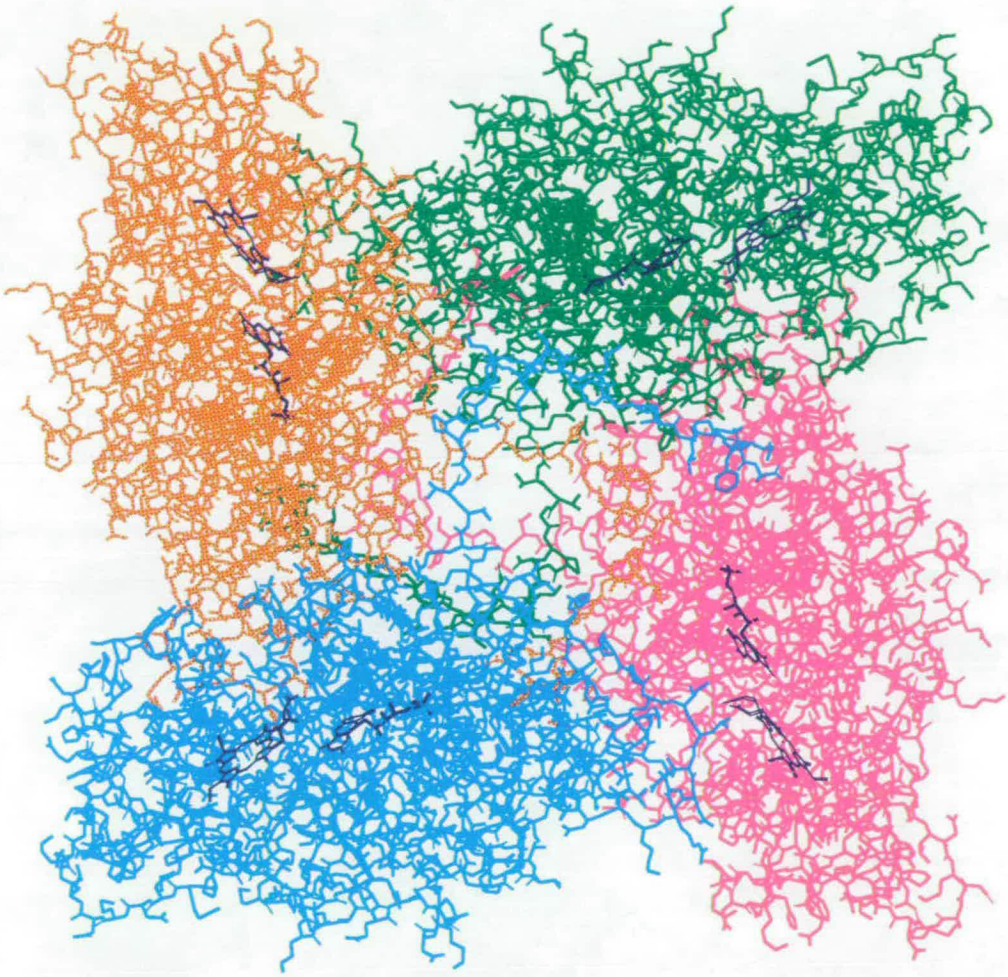

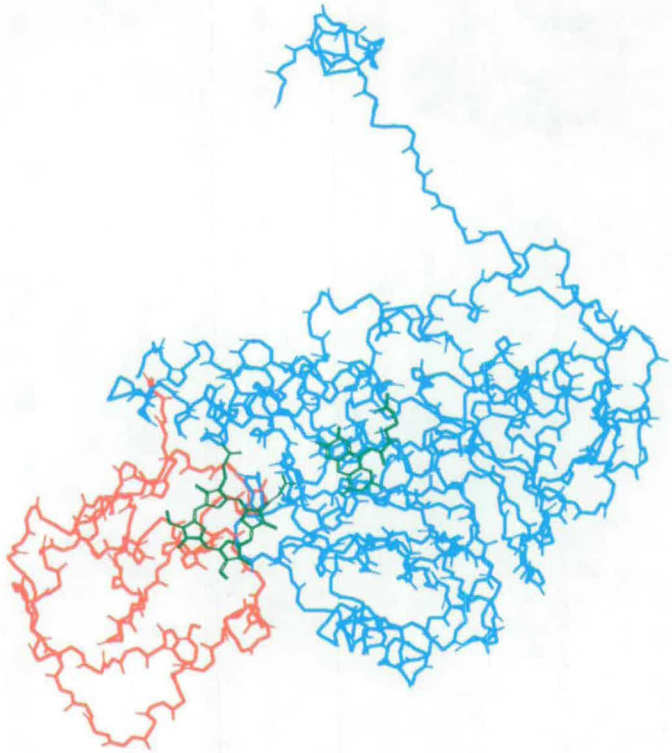

FIGURE 1.5 FLAVOCYTOCHROME $\underline{b}_2$ SUBUNIT

Red = haem domain Blue = flavin domain

The prosthetic groups are shown in green

Although the molecule possesses local 4-fold symmetry, it contains two crystallographically-distinct types of subunit and is therefore located on a crystallographic 2-fold axis. In subunit type 1, the cytochrome domain is resolved. In subunit 2, the haem domain is disordered and a region of electron density is found close to the FMN, identified as pyruvate, the reaction product, bound at the active site. The disordered haem domain is consistent with its being mobile relative to the FMN-binding domain. Such mobility had previously been suggested from NMR observations of flavocytochrome $\underline{b}_2$ and cytochrome $\underline{b}_2$ core [42]. The role of the interdomain hinge has recently been probed by constructing an interspecies hybrid enzyme consisting of the bulk of the enzyme from S.cerevisiae but with the interdomain hinge of H. anomala, which has a dramatically-different amino-acid sequence to the similar region in the S.cerevisiae enzyme [43].

1.4.3 THE HAEM DOMAIN

The haem domain of flavocytochrome $\underline{b}_2$ can be seen, from the 3D crystal structure, to consist of a 6-stranded mixed β-sheet, with a helix on one side and two pairs of antiparallel helices on the other (Figure 1.6) [8,41]. The haem is located at the interface of the two domains and is situated in a hydrophobic pocket formed by the two pairs of antiparallel helices. It is axially-coordinated by two histidine ligands (His 43 and His 66) only, and is not covalently bound to the enzyme. The haem propionates project away from the haem domain, pointing towards the FMN cofactor.

FIGURE 1.6 REPRESENTATION OF THE STRUCTURE OF THE FLAVOCYTOCHROME $\underline{b}_2$ HAEM DOMAIN [41]

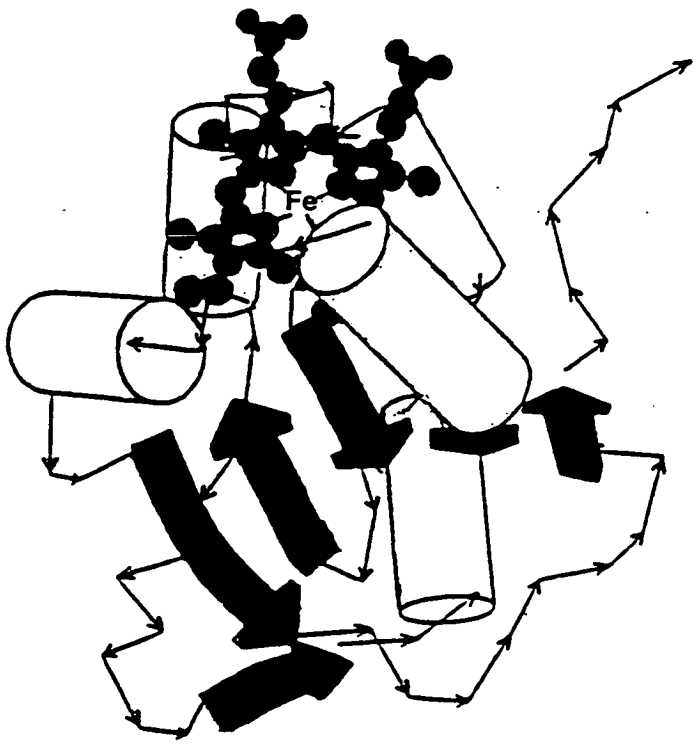

Cylinders represent helices and arrows represent β-pleated sheets

1.4.4 THE FLAVIN DOMAIN

Residues 191-465 of the flavin domain form a parallel $\beta_8\alpha_8$ barrel structure. The remaining amino-acids form four short β-strands and eight helices outwith the barrel, as illustrated in Figure 1.7 [8,41]. The FMN prosthetic group is bound non-covalently at the C-terminal end of the central barrel and, in the tetramer, is only slightly exposed to solvent at atoms C4a, N5 and C5a of the flavin ring. The hydrogen-bonding interactions which bind the prosthetic group to the protein all involve atoms in the main strands of the $\beta_8\alpha_8$ barrel motif. The flavin ring adopts a slightly bent, or "butterfly" conformation, with an angle of 172° between the planes. It is almost coplanar with the haem, with a distance of 9.7Å between the flavin N5 and the edge of the porphyrin ring.

In subunit 2, a region of electron density close to the FMN was attributed to pyruvate. This was believed to originate from lactate in the crystallization buffer by turnover of the crystalline enzyme under aerobic conditions [41]. The active site of the enzyme was thus located and is shown, with pyruvate present, in Figure 1.8. Several catalytically-important amino-acid residues around the active site are labelled in Figure 1.8; their individual roles in the catalytic mechanism will be discussed in Section 1.5.2. The roles of some of these residues have now been probed by site-directed mutagenesis [44-47].

The x-ray crystal structure reveals two other interesting features in the flavin domain itself: a region of disorder corresponding to residues 301-316 in subunit 1 (301-311 in subunit 2), and a C-terminal tail (residues 487-511). The disordered loop

FIGURE 1.7 TOPOLOGICAL REPRESENTATION OF THE FLAVOCYTOCHROME $\underline{b}_2$ FLAVIN DOMAIN [41]

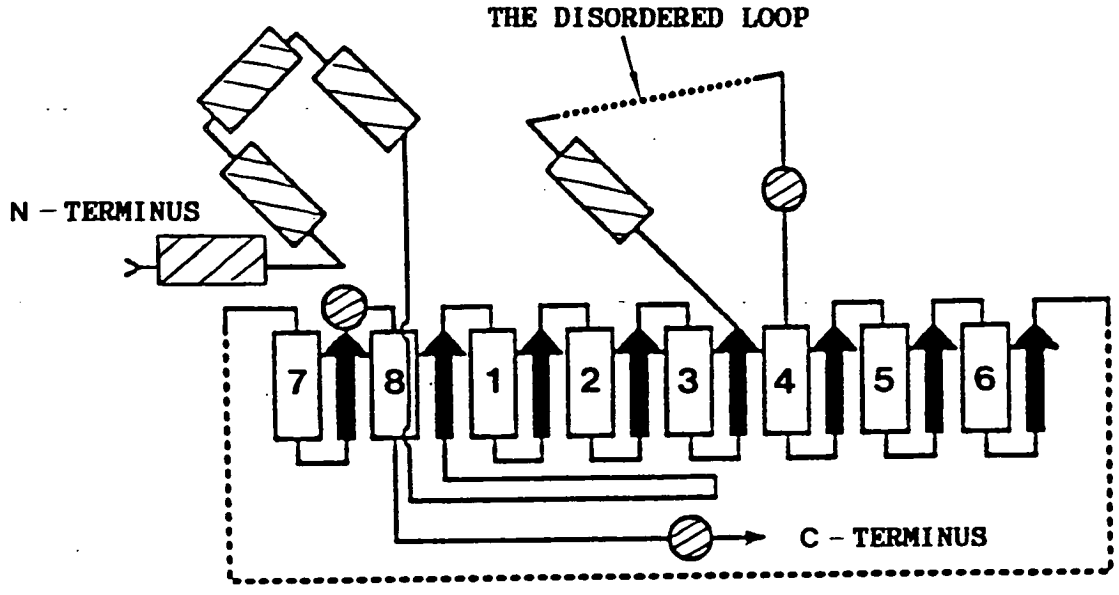

The $\beta_8\alpha_8$ structure is represented by the numbered rectangles (helices) and the arrows (β-sheets), the shaded areas representing the helices outwith the barrel motif.

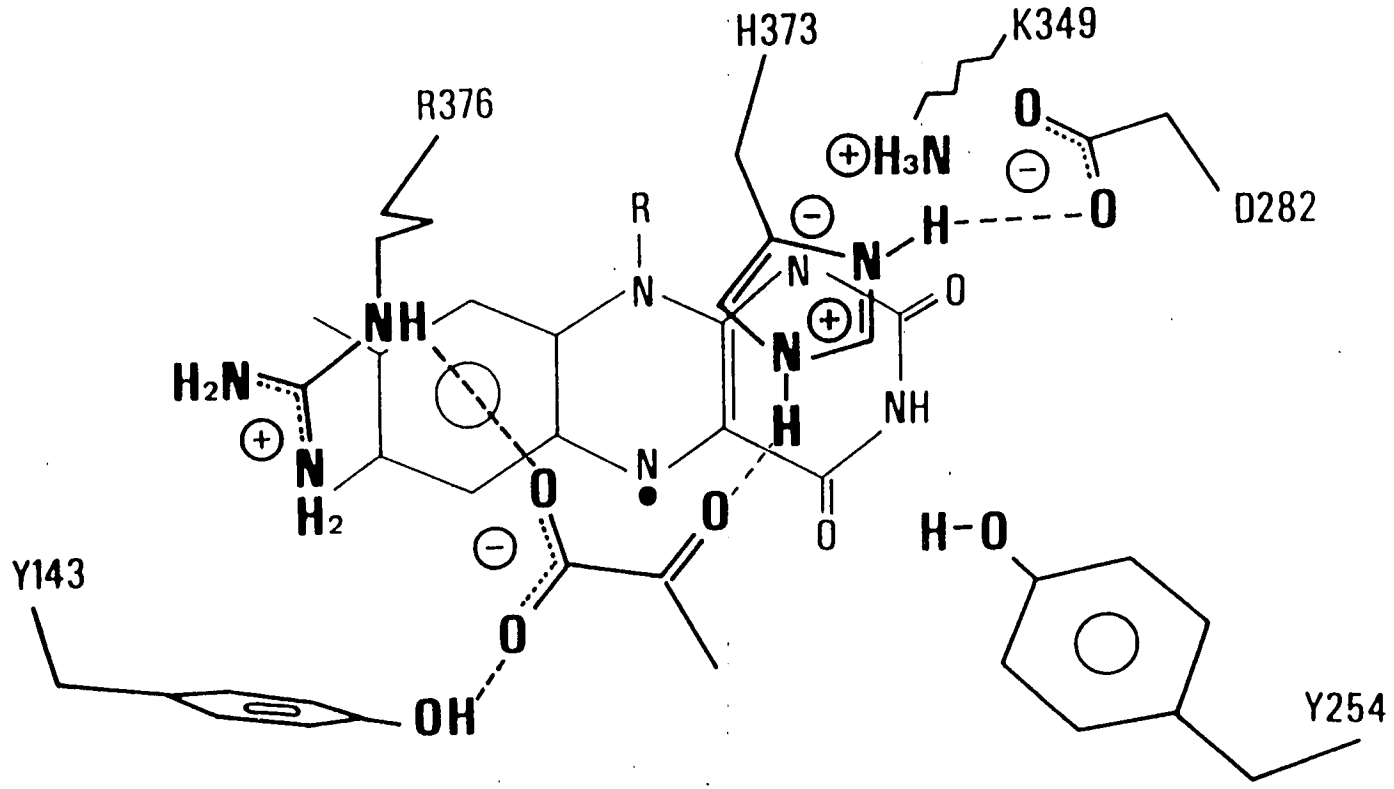

FIGURE 1.8 THE ACTIVE SITE OF FLAVOCYTOCHROME $\underline{b}_2$

Pyruvate is shown bound at the active site. Mechanistically-important amino acid residues are labelled.

corresponds to the proteolytically-sensitive region of the intact enzyme, cleavage at which point produces the two fragments α and β (previously described in Section 1.4.1). The C-terminal tail wraps around the central 4-fold axis, making many intersubunit contacts (Figure 1.4). It was originally thought to play a role in tetramer formation, but a mutant enzyme in which the C-terminal tail had been deleted was still tetrameric. The mutant did, however, lose FMN during turnover; thus the C-terminal tail appears to be important for FMN binding, probably in terms of retaining the necessary structural integrity [48].

1.5 THE CATALYTIC MECHANISM

1.5.1 GENERAL

Extensive research has been carried out into the catalytic mechanism of flavocytochrome $\underline{b}_2$, reviewed in [3] and [7]. The physiological pathway of electron transfer has been shown to be from bound lactate to flavin, flavin to haem and haem to cytochrome $\underline{c}$. The first step, oxidation of L-lactate and electron transfer to FMN, is the slowest step in the enzyme turnover. This was demonstrated by steady-state kinetic isotope effect (KIE) studies using L-lactate deuterated at the C2 position, which revealed the major rate-limiting step to be abstraction of the C2-hydrogen [49]. Stopped-flow studies gave KIE values of 8 for flavin reduction and 6 for haem reduction, indicating that C2-H abstraction is not totally rate-limiting for enzyme turnover [50].

Baudras showed FMN to be essential for lactate dehydrogenase activity from studies on flavocytochrome $\underline{b}_2$ from which FMN had been

removed by ammonium sulphate precipitation under acidic conditions [51]. The rate of reduction of the resulting haemoprotein by lactate, in the presence of small amounts of FMN, was found to be proportional to FMN concentration. In the total absence of FMN, no lactate dehydrogenase activity was observed with ferricyanide or cytochrome c as the electron acceptor.

The necessity of the haem domain for cytochrome c reductase activity was demonstrated by Forrestier and Baudras [52]. They prepared derivatives of flavocytochrome b_2 with varying amounts of bound haem by denaturing the holoenzyme in varying concentrations of guanidine, followed by dialysis against phosphate buffer. This process allowed up to 90% of the bound haem to be removed while retaining up to 65% of the bound FMN. While the relative activity of such samples with cytochrome c extrapolated to zero activity at zero haem content, a finite activity remained when ferricyanide was used as the electron acceptor, albeit at a lower level than in the holoenzyme. Thus it was confirmed that the pathway of electron transfer to cytochrome c proceeds via the haem domain.

The physiological pathway of electron transfer is summarised in Figure 1.9.

1.5.2 LACTATE DEHYDROGENATION/FMN REDUCTION

The oxidation of L-lactate to pyruvate is a two-electron redox process and therefore might be expected to occur in one of two ways: as two one-electron steps (a radical mechanism) or as a single two-electron step. A single two-electron step could take place either as a hydride (H^-) transfer, or as a proton (H^+) abstraction followed by a 2-electron transfer from a carbanion intermediate. In the case

FIGURE 1.9 THE CATALYTIC CYCLE OF FLAVOCYTOCHROME $\underline{b}_2$

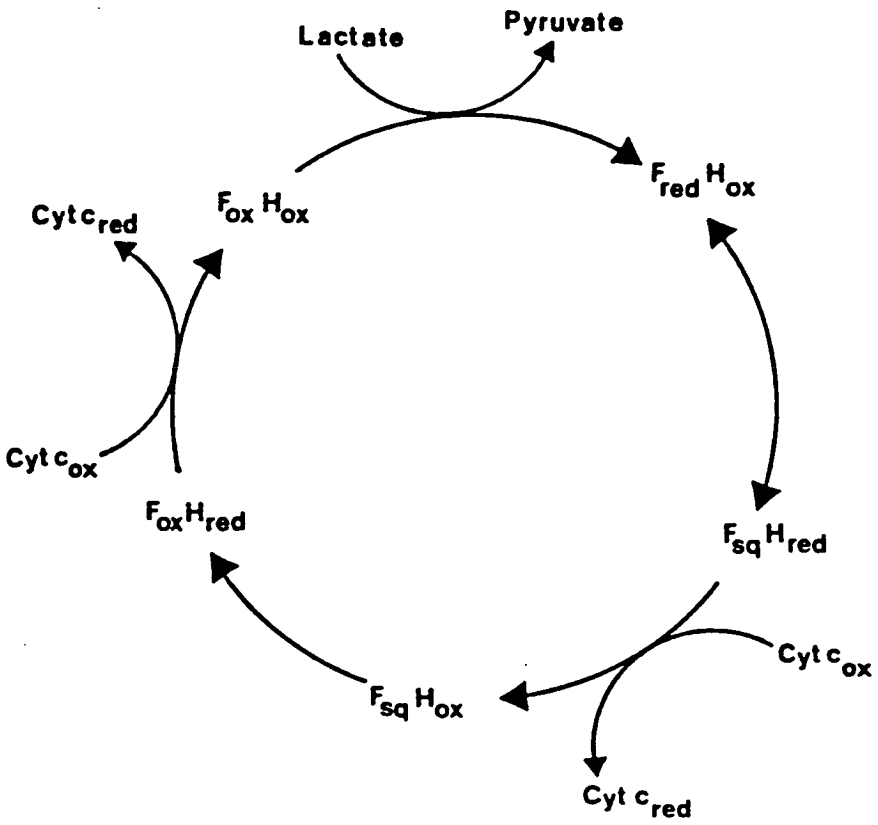

F_{ox}	oxidized FMN	F_{red}	reduced FMN
F_{sq}	flavin semiquinone	H_{ox}	oxidized haem
H_{red}	reduced haem	Cyt c	cytochrome $\underline{c}$

of flavocytochrome b_2, it is now widely accepted, although not conclusively proven, that a carbanion mechanism operates [3,7]. The formation of a carbanion is not, in itself, an oxidation, and therefore must be followed by electron transfer to FMN.

Studies on other flavoproteins thought to operate *via* a carbanion mechanism led to a number of arguments in support of such a hypothesis [3]. Two such observations were: that a number of flavooxidases could catalyse halide ion elimination from halosubstrates; and the suicide inactivation of L-lactate oxidase from *Mycobacterium smegmatis* by 2-hydroxy-3-butynoate. The application of these criteria to flavocytochrome b_2 provides a degree of evidence in favour of a carbanion mechanism for this enzyme, as reviewed in [3] and [7].

Studies of the reverse reaction of flavocytochrome b_2 with halogenated pyruvates demonstrated that dehydrohalogenation occurred with bromo- and chloropyruvate but not with fluoropyruvate [53]. The forward reaction with halogenated lactates proved difficult to observe as the dehydrohalogenation was unable to compete effectively with the usual oxidative reaction. For the forward reaction only one mole of pyruvate was formed per 500 moles of halopyruvate, whereas for the reverse reaction, the ratio of lactate:halolactate was 1:2. The proposed mechanism for this reaction is shown in Figure 1.10. As the rate-limiting step in the forward reaction is abstraction of the substrate C2-H, then, by the principle of microscopic reversibility, the rate-limiting step for the reverse reaction must be C2-H bond formation. A deuterium KIE of 4.4 measured for the reverse reaction is in agreement with this [54]. An inverse isotope effect for bromide elimination of bromopyruvate

was also observed [54]. This provides further evidence for a carbanion mechanism, as the carbanion intermediate can either undergo protonation to form halopyruvate, which is isotope-sensitive (route 1 in Figure 1.10), or halide elimination to form pyruvate, which is isotope-insensitive (route 2). If a hydride mechanism had been operating, an isotope effect would have been expected for halide elimination as well as for protonation [54].

Further evidence for the carbanion mechanism was provided by transhydrogenation reactions carried out with [2-^{3}H] lactate and halogenopyruvate [54]. The enzyme catalyzed an intermolecular tritium transfer from C2 of lactate to C2 of the halogenopyruvate. Tritium was also found in water. If the tritiated halopyruvate then underwent halide elimination, tritium was found at C3 of the resulting pyruvate. The radioactivity of such pyruvate was significantly lower than that of the respective halogenolactate, suggesting that the end intermediate had undergone ketonisation in solution. This observation would be inexplicable if a hydride or radical mechanism were considered [54].

Like lactate oxidase, flavocytochrome $\underline{b}_2$ does undergo inactivation with the suicide inhibitor 2-hydroxy-3-butynoate [49,55] as outlined in Figure 1.11. Abstraction of a proton from 2-hydroxy-3-butynoate forms a carbanion intermediate which is in resonance with an allenic form. This allenic carbanion is capable of forming a covalent adduct with the FMN cofactor by nucleophilic attack at C4a of the flavin, inactivating the enzyme. The observation of inactivated enzyme provides further evidence for a carbanion mechanism: hydride abstraction from 2-hydroxy-3-butynoate would not produce the allenic intermediate necessary for the

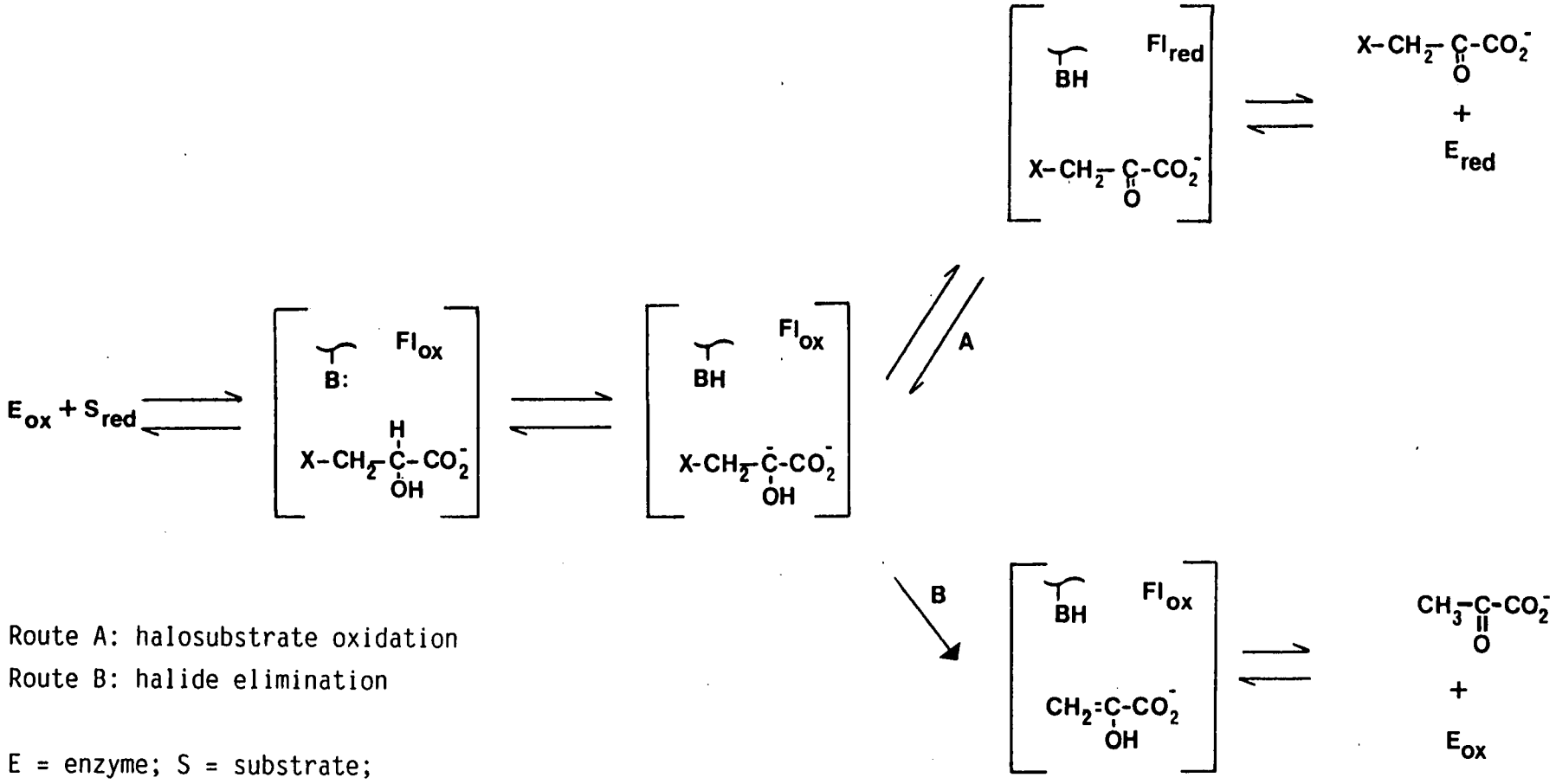

FIGURE 1.10 MECHANISM FOR HALOSUBSTRATE OXIDATION VIA A CARBANION INTERMEDIATE [53,54]

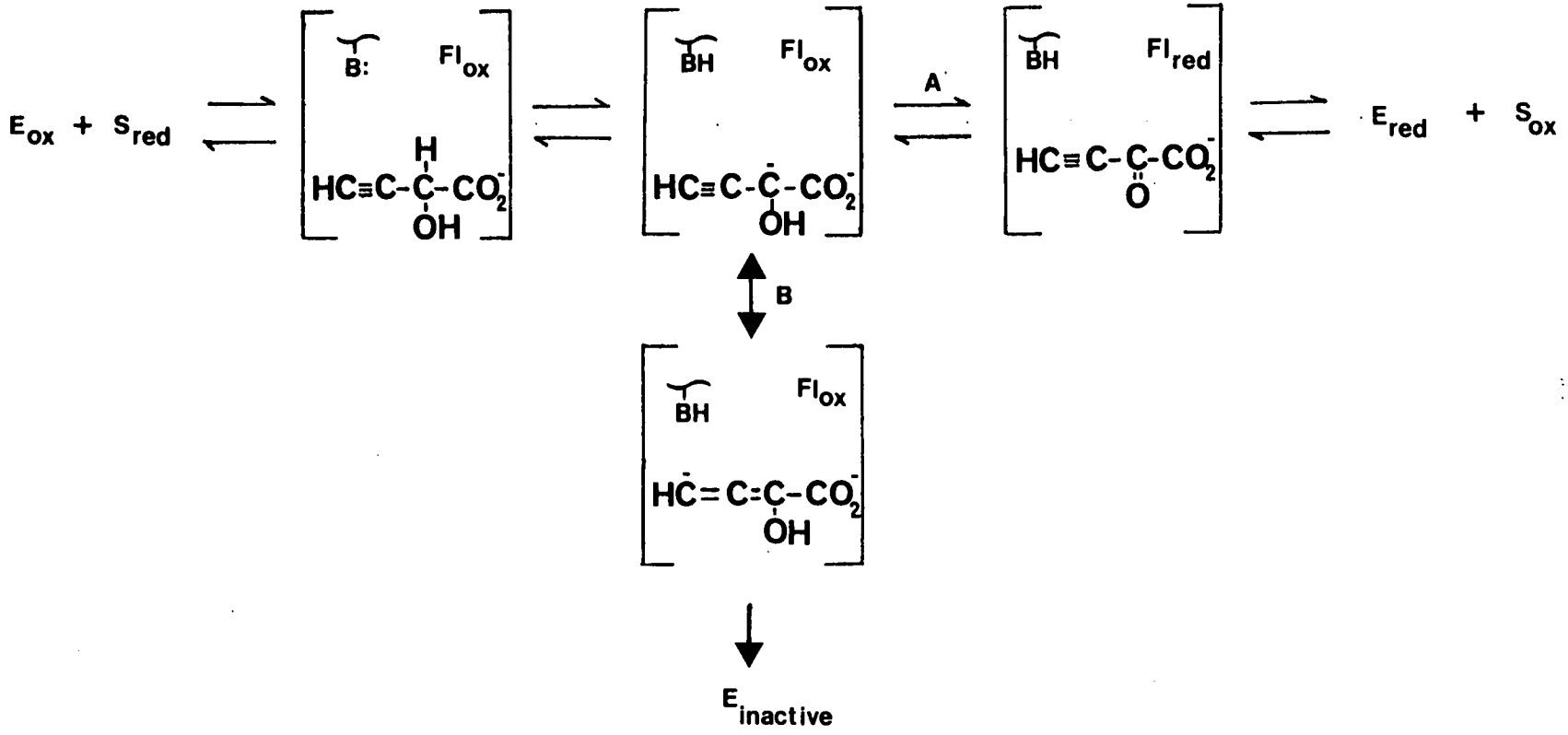

FIGURE 1.11 MECHANISM FOR THE SUICIDE INACTIVATION OF FLAVOCYTOCHROME $\underline{b}_2$ BY 2-HYDROXY-3-BUTYNOATE [49,55]

Inactivation occurs after nucleophilic attack at the FMN by the highly-reactive allenic carbanion, formed by resonance (route B). Route A is the route for substrate oxidation.

E = enzyme; S = substrate; B = active site base; Fl = flavin mononucleotide

formation of a covalent adduct to FMN.

Porter et al found that D-amino acid oxidase, another flavoprotein thought to operate by a carbanion mechanism, recognised ethane nitronate as a substrate [56]. A covalent intermediate was produced, which could be trapped with cyanide. However, ethane nitronate was found to act as an inhibitor of, and not a substrate for, flavocytochrome b_2 [57]. The reason for this is unclear, but as many other flavoenzymes including L-amino acid oxidase, lactate oxidase, glycolate oxidase and long-chain α-hydroxyacid oxidase also fail to react with it [3,7], reaction with ethane nitronate is not a good test for a carbanion mechanism.

Despite the substantial evidence in support of a carbanion mechanism in flavocytochrome b_2, the manner of electron transfer to FMN remains unsolved. The three basic possibilities are: nucleophilic attack at flavin N5, forming a covalent bond which then undergoes cleavage to produce reduced flavin; a radical process comprising two one-electron transfers to flavin, again forming a covalent adduct; and two single-electron transfers to flavin without formation of an adduct. Lederer and Mathews proposed a reaction mechanism for flavocytochrome b_2 by considering the three-dimensional structure of the active site and the evidence for a carbanion mechanism [58]. Their model did not account for electron transfer to FMN, save for excluding the possibility of a covalent intermediate. However, based on observations of covalent substrate-flavin intermediates for lactate oxidase [59,60] and D-amino acid oxidase [56], Ghisla and Massey considered the 3.7Å distance between flavin N5 and pyruvate carbonyl in flavocytochrome b_2 to be too close to preclude formation of a covalent adduct [61]. Taking this

into account, a mechanism has been proposed for substrate oxidation/ FMN reduction in flavocytochrome b_2, based on the mechanism of Lederer and Mathews but allowing for formation of a covalent adduct [7] (Figure 1.12). Substrate is bound and orientated by hydrogen bonds and electrostatic interactions with Arg 376 and hydrogen bonds to Tyr 143. The C2-H of the substrate is abstracted as a proton by the active site base, His 373, forming a carbanion intermediate. Asp 282 stabilises the imidazolium ion thus formed on His 373. The carbanion then collapses to form the covalent adduct (the existence of which is still open to debate), the resulting anion at N1 being stabilised by Lys 349. Tyr 254 was originally assumed to be responsible for the deprotonation of the substrate hydroxyl group, but this has now been disproved by studies of a point mutant in which Tyr 254 has been altered to Phe [3].

The fully-reduced flavin hydroquinone formed in the above mechanism then surrenders its two electrons to the haem by means of two one-electron transfers.

1.5.3 FLAVIN-TO-HAEM ELECTRON TRANSFER

Studies on electron-transfer processes subsequent to the initial flavin reduction were carried out by Capeillere-Blandin *et al* [26], using combined stopped-flow and EPR rapid-freezing experiments on cleaved flavocytochrome b_2, which allowed both flavin and haem reduction to be observed. The accumulation of the different redox forms of flavin and haem were monitored over the course of the reaction. These experiments confirmed that, in the absence of any electron acceptor, the enzyme takes up 3 electrons per protomer (2 by the FMN and 1 by the haem) to become fully reduced.

The mechanism proceeds via a carbanion intermediate. k_2 is the rate-limiting step. The presence of a covalent adduct is at present not proven.

E = enzyme; S = substrate

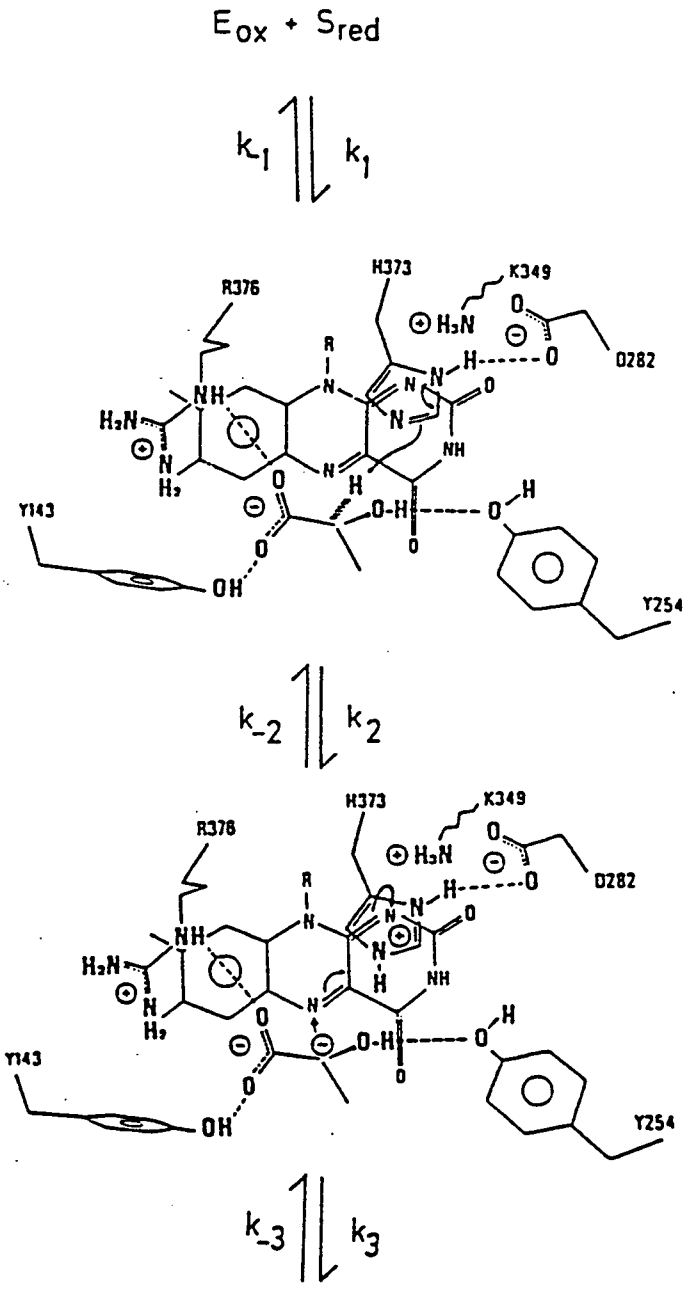

FIGURE 1.12 THE MECHANISM OF L-LACTATE OXIDATION BY FLAVOCYTOCHROME b_2

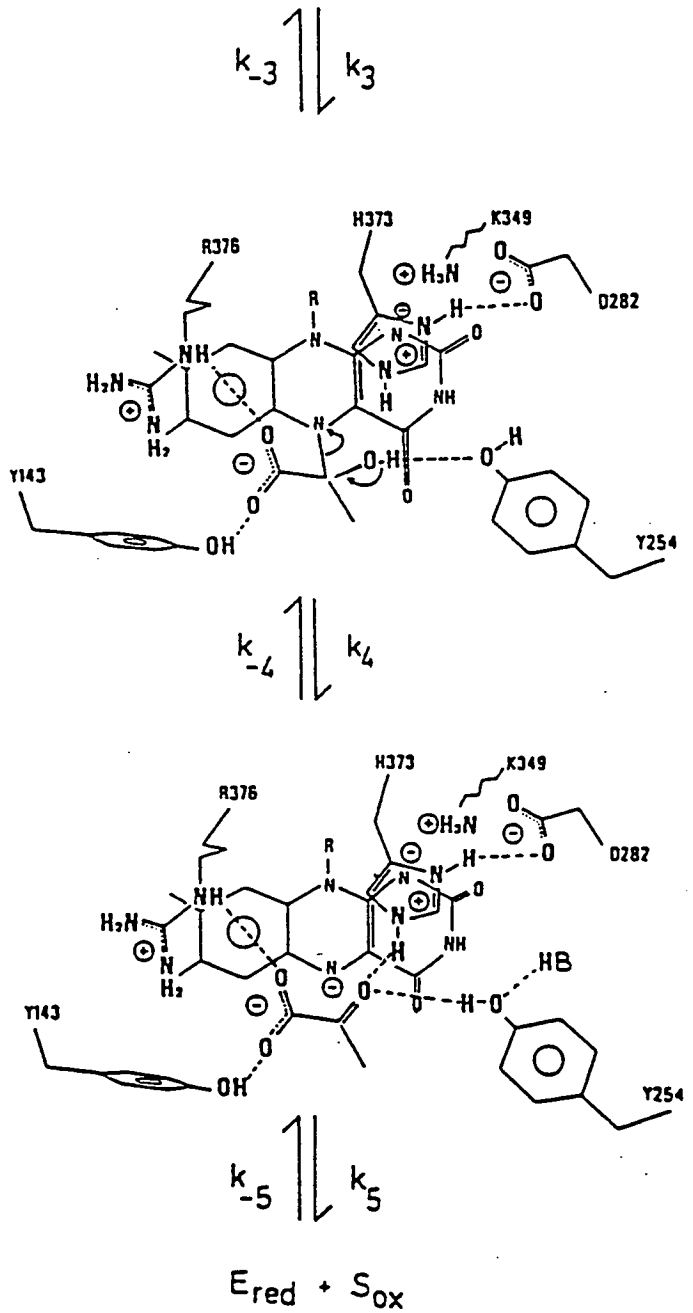

The stopped-flow studies revealed that both flavin and haem reduction followed biphasic time courses, which were superimposable. At the end of the first phase (30-35 msec), EPR studies revealed that up to 80% of the haem was reduced, up to 50% of the FMN was in the semiquinone form and 25-35% was in the hydroquinone (fully-reduced) form. The overall electron distribution at this stage corresponded to two electrons per protomer. The second phase was ascribed to the entry of a third electron per protomer, with a conformational change responsible for rate-determination in this phase. Subsequent laser flash photolysis studies have shown that a conformational change takes place only in the presence of pyruvate [62], suggesting that the conformational changes responsible for intersubunit electron transfer are induced by pyruvate binding.

With the aid of computer simulation studies, an electron transfer scheme based on these results was proposed [63] (Figure 1.13), whereby an interprotomer electron transfer between two flavin semiquinones facilitates the entry of a further two electrons per pair of protomers.

Pompon et al also investigated interprotomer electron transfer at much lower lactate concentrations, giving a low rate of electron entry [50,64]. Pompon proposed a slightly different electron transfer model[64], with several differences to the Capeillere-Blandin model. In the Pompon model, initial reduction of the two FMN groups in a dimer is assumed to be random; in the Capeillere-Blandin model, it is assumed to be synchronized, the two FMNs being reduced simultaneously. The Pompon model includes interprotomer electron transfer between haem groups. This would now seem to be unlikely from the three-dimensional crystal structure of the enzyme, as such

FIGURE 1.13 PROPOSED SCHEME FOR ELECTRON TRANSFER IN FLAVOCYTOCHROME $\underline{b}_2$ [26,63]

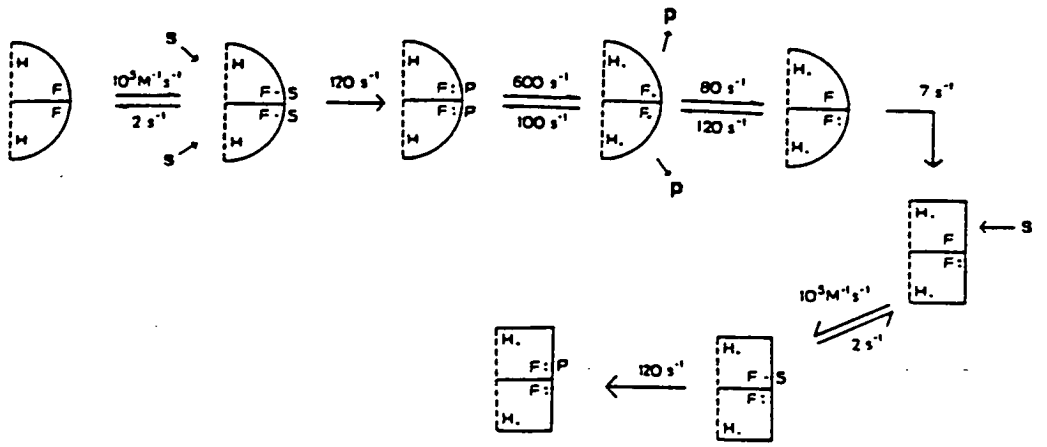

For simplicity, only two subunits of the enzyme are shown. Two electron pairs are transferred to the enzyme, fully reducing the two FMN groups. The haems are then reduced with subsequent formation of flavin semiquinone. Interprotomer electron transfer generates one fully-reduced FMN. The enzyme then undergoes a conformational change to allow the entry of a third pair of electrons.

F = FMN; H = haem; S = substrate; P = product

a transfer would need to take place over a distance of 52.8Å. The rate-limiting step for the slow phase is interprotomer electron transfer in the Pompon model, but a conformational change in the Capeillere-Blandin model. Also, there is an order of magnitude difference between the rates of interprotomer electron transfer in the two models.

To summarise, the two models agree on the general manner of electron transfer involved in enzyme turnover (FMN reduction and some form of interprotomer electron transfer to allow the entry of the third pair of electrons per dimer) but differ in the detailed description of the steps involved in the full reduction of the enzyme.

1.5.4 ELECTRON ACCEPTORS

As previously stated (Section 1.5.1), it is known that haem is essential for cytochrome c reductase activity in flavocytochrome b_2 but not for ferricyanide reductase activity [52,65]. This implies that cytochrome c and ferricyanide are reduced via different electron transfer routes.

Cytochrome c, the physiological electron acceptor of flavocytochrome b_2, was found to interact with the enzyme both in the crystalline state and in solution. Studies on crystalline flavocytochrome b_2 found that cytochrome c allowed to diffuse through the crystals accumulated in a stoichiometric ratio of 1 cytochrome c : 1 flavocytochrome b_2 subunit [66]. Cytochrome c binding was found to be very sensitive to both ionic strength and pH, with maximal complex formation occurring at low ionic strength, around pH 7 [66,67]. The flavocytochrome b_2/cytochrome c complex was still

reducible by L-lactate with a similar time course to the reaction in solution [66], showing that the route by which substrate reaches the active site remained unblocked despite cytochrome *c* binding. In solution, fluorimetric studies of the complex formed by the interaction of *H.anomala* flavocytochrome b_2 and Zn-substituted cytochrome *c* found that the main association area for cytochrome *c* binding was located on the flavin domain [68]. More specifically than this, the binding site for cytochrome *c* on flavocytochrome b_2 has not been located. However, interactions between flavocytochrome b_2 and chemically-modified cytochromes *c* have shown that lysines near the cytochrome *c* haem edge play a major role in the interprotein interaction [69]. One obvious region of negatively-charged residues on flavocytochrome b_2 which could interact with these positively-charged lysines is the C-terminal tail (residues 487-511), which contains six negatively-charged (Glu and Asp) residues, three of which lie in the last 5 residues of the sequence. Removal of the C-terminal tail caused a significant decrease in the rate of cytochrome *c* reduction [48]. It was postulated that, on deletion of the C-terminal tail, either: (a) no stable complex was formed with cytochrome *c*; or (b) a complex, inferior to the holoenzyme/cytochrome *c* complex, was formed with cytochrome *c* less well-orientated for electron transfer, resulting in a decreased rate of cytochrome *c* reduction [70].

Using cytochrome *c* in which the haem iron had been replaced with zinc or tin, Vanderkooi *et al* [71] were able to calculate the interhaem distance in the flavocytochrome b_2/cytochrome *c* complex from the overlap of the fluorescence spectra of the enzyme and the cytochrome *c* derivatives. They found the interhaem distance to be

18Å.

An artificial electron acceptor commonly used in steady-state kinetic experiments on flavocytochrome b_2 is ferricyanide. It was originally suggested that, like cytochrome c, ferricyanide could only accept electrons from the b_2-haem [72]. This was later disproved when it was discovered that dehaemoflavocytochrome b_2 was still capable of reducing ferricyanide [65], implying that ferricyanide can accept electrons from the FMN as well as the haem cofactor. Analysis of the reoxidation of the reduced dehaemoenzyme by ferricyanide in terms of two successive one-electron transfer steps suggested that, while ferricyanide can accept electrons from either the hydroquinone or semiquinone form of the FMN, it reacts at least 20 times faster with the semiquinone than the hydroquinone [65].

1.6 FLAVOCYTOCHROME b_2 FROM *Hansenula anomala*

1.6.1 GENERAL

Flavocytochrome b_2 has also been isolated and purified from another yeast, *Hansenula anomala* [18]. The *H.anomala* enzyme has a subunit molecular weight of 56 200. Its amino-acid sequence shows an overall identity of 60% with the *S.cerevisiae* enzyme, with many regions of the sequence and all the active site residues conserved [73]. However, two regions of the *H.anomala* enzyme sequence are significantly different to that from *S.cerevisiae*. These regions correspond to the crystallographically-disordered surface loop, and the interdomain hinge region (Section 1.4.4). Both of these features carry a charge of -6 in the *H.anomala* enzyme, but carry

charges of +4 for the loop and -2 for the hinge in the S.cerevisiae enzyme.

Flavocytochrome b_2 from H.anomala has a higher specific activity than the S.cerevisiae enzyme ($1000s^{-1}$ compared with $500s^{-1}$ at 30°C [18]). The two enzymes also have different rate-determining steps. In the H.anomala enzyme the rate-limiting step is flavin reduction, but C2-H abstraction is rate-limiting in the S.cerevisiae enzyme [74]. It is thought that these differences in kinetic properties may be due to the differences between the surface loops and hinge regions of the two enzymes. This is now being probed by studying interspecies hybrids comprising various regions of protein from each enzyme [43].

1.6.2 PROTEOLYTIC STUDIES

Flavocytochrome b_2 from H.anomala is much more stable to indigenous yeast proteases than its S.cerevisiae counterpart, and can therefore be isolated from yeast in the intact form without the addition of PMSF [18,75]. This difference between the two enzymes reflects the very different natures of their surface loops.

H.anomala flavocytochrome b_2 can be cleaved by proteases such as trypsin and chlostripain, showing a similar cleavage pattern to the S.cerevisiae enzyme [3,31]. In contrast to the S.cerevisiae enzyme, a tetrameric flavin-containing protein could be isolated after trypsinolysis, in addition to the haem domain [37,40,76], but was isolated in low yields and was sensitive to further proteolysis. A similar flavoprotein was subsequently isolated from the holoenzyme in higher yields using Staphylococcus aureus V8 protease I [77] and also by using a proteinase isolated from H.anomala [78]. The

isolated flavoprotein was tetrameric, with a monomer molecular weitht of 39-43 000 [77,78]. It was found to have lactate dehydrogenase activity when ferricyanide was used as the electron acceptor, but, like dehaemoflavocytochrome $\underline{b}_2$, displayed no cytochrome $\underline{c}$ reductase activity [65,77,78].

1.7 COMPARISON OF FLAVOCYTOCHROME $\underline{b}_2$ WITH ANALOGOUS PROTEINS

1.7.1 HAEM DOMAIN ANALOGUES : THE CYTOCHROME $\underline{b}_5$ SUPERFAMILY

The haem domain of flavocytochrome $\underline{b}_2$ is a member of a group of proteins known as the cytochrome $\underline{b}_5$ superfamily [79]. The members of this family have a number of common characteristics, notably a similar molecular weight and a common folding topography known as the "cytochrome $\underline{b}_5$ fold" [80], which is essentially a hydrophobic haem crevice (composed of 4 helices and a β-pleated sheet), the haem being axially ligated by histidines. Members of this family include the haem domains of cytochrome $\underline{b}_5$, liver sulphite oxidase and assimilatory nitrate reductase [3].

Cytochrome $\underline{b}_5$ could be considered as the founder member of this family of proteins. Cytochrome $\underline{b}_5$ is found in many species, in both microsomes and erythrocytes [81,82].

Microsomal cytochrome $\underline{b}_5$ consists of a single polypeptide chain and has a molecular weight of 12-17 000 per haem [81]. Its crystal structure has been solved [82] and it has also been extensively studied by NMR spectroscopy, a complete sequence-specific assignment being known [83-85].

Liver sulphite oxidase (LSO) is, like flavocytochrome $\underline{b}_2$, a redox enzyme found in the mitochondrial intermembrane space. This

enzyme is a dimer, each sununit of M_r 60 000 containing molybdenum and protohaem IX as prosthetic groups bound in separate domains and linked by a hinge region [86]. The haem domain, which can be isolated by tryptic digestion of the enzyme from rat [86] and by chymotryptic digestion of the enzyme from chicken [87] has M_r 9 500 - 11 000.

All of these proteins (cytochrome $\underline{b}_5$, cytochrome $\underline{b}_2$ core and LSO haem domain) have in common similar molecular weights of around 11 000, similar electronic absorption spectra [79,86] and a high degree of sequence homology [3,79,80]. The three-dimensional crystal structures of beef cytochrome $\underline{b}_5$ [82] and flavocytochrome $\underline{b}_2$ [8] confirm the predictions of a common "$\underline{b}_5$" fold.

Although each of these three enzymes catalyze quite different reactions, they have some similarities in function. Like flavocytochrome $\underline{b}_2$, LSO has been shown to transfer electrons to cytochrome $\underline{c}$ in the mitochondrial intermembrane space and, also like flavocytochrome $\underline{b}_2$, the haem domain of LSO is essential for cytochrome $\underline{c}$ reduction [86]. While cytochrome $\underline{b}_5$ does not use cytochrome $\underline{c}$ as its physiological electron acceptor, it, too, is capable of reducing cytochrome $\underline{c}$ in solution. Taking both the structural and functional similarities of these enzymes into consideration, it has been hypothesized that all three systems developed from the same evolutionary ancestor [79,86].

1.7.2 FLAVIN DOMAIN ANALOGUES

The flavin domain of flavocytochrome $\underline{b}_2$ is structurally homologous with several FMN-containing enzymes, all of which catalyze oxidation of α-hydroxyacids. These are L-lactate oxidase

from Mycobacterium smegmatis, spinach glycolate oxidase and long-chain α-hydroxyacid oxidase from rat kidney [3,88]. Unlike flavocytochrome b_2, in which the flavin moiety is reoxidized by the haem domain, these three enzymes utilise oxygen as the electron acceptor.

The crystal structures of spinach glycolate oxidase and flavocytochrome b_2 (flavin domain) both share a $\beta_8\alpha_8$-barrel motif (Section 1.4.4) [89]. However, the FMN orientation differs significantly in the two structures. It has been suggested that this structural difference is responsible for the functional difference between the two enzymes, spinach glycolate oxidase being a flavooxidase and flavocytochrome b_2 a flavodehydrogenase [89]. It has been suggested that both flavoproteins evolved from a common ancestor, the occurrence of a few mutations during the evolutionary process being sufficient to significantly affect FMN orientation and enzyme function.

Amino-acid sequences are known for L-lactate oxidase and spinach glycolate oxidase [90,91] and a sequence alignment of these two enzymes with flavocytochrome b_2 and long-chain α-hydroxyacid oxidase [92] is shown in Figure 1.14. The four enzymes show a remarkably high degree of sequence homology. All those active-site residues which were previously identified by X-ray crystallography of flavocytochrome b_2 and spinach glycolate oxidase are conserved in all the proteins [89].

The $\beta_8\alpha_8$-barrel motif is also shared by another FMN-containing enzyme, trimethylamine dehydrogenase of bacterium W_3A_1 [89]. However, the recently-published amino-acid sequence of trimethylamine dehydrogenase [93] reveals no obvious sequence homology between the

FIGURE 1.14 ALIGNMENT OF THE AMINO-ACID SEQUENCES OF FLAVOCYTOCHROME b_2 FLAVIN DOMAIN AND ANALAGOUS PROTEINS

```
                                                                  *
Scb2  ETKEDIARKE QLKSLLPPLD NIINLYDFEY LASQTLTKQA WAYYSSGAND EVTHRENHNA
Hab2  LSDEEIDRLE RIER.KPPLS QMINLHDFET IARQILPPPA LAYYCSAADD EVTLRENHNA
 Gox  .......... .........M EITNVNEYEA IAKQKLPKMV YDYYASGAED QWTLAENRNA
 Hao  .......... .......... PLVCLADFKA HAQKQLSKTS WDFIEGEADD GITYSENIAA
 Mdh  .......... .......MSQ NLFNVEDYRK LRQKRLPKMV YDYLEGGAED EYGVKHNRDV
 Lox  NWGDYENEIY GQGLVGVAPT LPMSYADWEA HAQQALPPGV LSYVAGGSGD EHTQRANVEA

Scb2  YHRIFFKPKI LVDVRKVDIS TDMLGSHVDV PFYVSATALC KLGNPLEGEK DVARGCGQGV
Hab2  YHRIFFNPKI LIDVKDVDIS TEFFGEKTSA PFYISATALA KLGHP.EGEV AIAKGAGRE.
 Gox  FSRILFRPRI LIDVTNIDMT TTILGFKISM PIMIAPTAMQ KMAHP.EGEY ATARAASAA.
 Hao  FKRIRLRPRY LRDMSKVDTR TTIQGQEISA PICISPTAFH SIAWP.DGEK STARAAQEA.
 Mdh  FQQWRFKPKR LVDVSRRSLQ AEVLGKRQSM PLLIGPTGLN GALWP.KGDL ALARAATKA.
 Lox  FKHWGLMPRM LMAATERDLS VELWGKTWAA PMFFAPIGVI ALC.AQDGHG DAASAQASAR

                                                  *
Scb2  TKVPQMISTL ASCSPEEIIE AAPSDKQIQW YQLYVNSDRK ITDDLVKNVE KLGVKALFVT
Hab2  .DVVQMISTL ASCSFDEIAD ARIPGQQ.QW YQLYVNADRS ITEKAVRHAE ERGMKGLFIT
 Gox  .GTIMTLSSW ATSSVEEVAS TGPG...IRF FQLYVYKDRN VVAQLVRRAE RAGFKAIALT
 Hao  .NICYVISSY ASYSLEDIVA AAPEG..FRW FQLYMKSDWD FNKQMVQRAE ALGFKALVIT
 Mdh  .GIPFVLSTA SNMSIEDLAR QCDGDL...W FQLYV.IHRE IAQGMVLKAL HTGYTTLVLT
 Lox  TGVPYITSTL AVSSLEDIRK HAGDTPA..Y FQLYYPEDRD LAESFIRRAE EAGYDGLVIT

       *
Scb2  VDAPSLGQRE KDMK...LKF SNTKAGP... .......... .....KAMKK TNVEESQGAS
Hab2  VDAPSLGRRE KDMK...MKF EADSDVQ... .......... .......GDD EDIDRSQGAS
 Gox  VDTPRLGRRE ADIK.NRFVL PPFLTLK... .......... .....NFEGI DLGKMDKAND
 Hao  IDTPVLGNRR RDKR.NQLNL EANILLK... .......... .....DLRAL ...KEEKPTQ
 Mdh  TDVAVNGYRE RDLH.NRFKI PMSYSAKVVL DGCLHPRWSL DFVRHGMPQL ANFVSSQTSS
 Lox  LDTWIFGWRP RDLTISNFPF LRGLCLTNYV TDPVFQKKFK AHSGVEAEGL RD.......N

                                                  *                   *
Scb2  RAL.SKF... .IDPSLTWKD IEELKKKTKL PIVIKGVQRT EDVIKAAEIG VSGVVLSNHG
Hab2  RAL.SSF... .IDPSLSWKD IAFIKSITKM PIVIKGVERK EDVLLAAEHG LQGVVLSNHG
 Gox  SGL.SSYVAG QIDRSLSWKD VAWLQTITSL PILVKGVITA EDARLAVQHG AAGIIVSNHG
 Hao  SVP.VSFPKA ....SFCWND LSLLQSITRL PIILKGILTK EDAELAMKHN VQGIVVSNHG
 Mdh  LEMQAALMSR QMDASFNWEA LRWLRDLWPH KILVKGLLSA EDADRCIAEG ADGVILSNHG
 Lox  PRLAADFWHG LFGHSVTWED IDWVRSITKM PVILKGIQHP DDARRAVDSG VDGIYCSNHG

       *
Scb2  GRQLDFSRAP IEVLAETMPI LEQRNLKDKL EVFVDGGVRR GTDVLKALCL GAKGVGLGRP
Hab2  GRQLDYTRAP VEVLAEVMPI LKERGLDQKI DTFVDGGVRR GTDVLKLLCL AAKGVGLGRP
 Gox  ARQLDYVPAT IMALEEVVK. ....AAQGRI PVFLDGGVRR GTDVFKALAL GAAGVFIGRP
 Hao  GRQLDEVSAS IDALREVVA. ....AVKGKI EVYMDGGVRT GTDVLKALAL GARCIFLGRP
 Mdh  GRQLDCAISP MEVLAQSVA. ......KTGK PVLIDSGFRR GSDIVKALAL GAEAVLLGRA
 Lox  GRQANGGLPA LDCLPEVVK. .....ASGDT PVLFDSGIRT GADVVKALAM GASAVGIGRP

Scb2  FLYANSCYGR NGVEKAIEIL RDEIEMSMRL LGVTSIAELK PDLLDLSTLK ARTVGVPNDV
Hab2  FLYAMSSYGD KGVTKAIQLL KDEIEMNMRL LGVNKIEELT PELLDTRSIH TRAVPVAKDY
 Gox  VVFSLAAEGE AGVKKVLQMM RDEFELTMAL SGCRSLKEIS RSHIAADWDG PSSRAVARL.
 Hao  ILWGLACKGE DGVKEVLDIL TAELHRCMTL SGCQSVAEIS PDLIQFSRL. ..........
 Mdh  TLYGLAARGE TGVDEVLTLL KADIDRTLAQ IGCPDITSLS PDYLQNEGVT NTAPVDHLIG
 Lox  YAWGAALGGS KGIEHVARSL LAEADLIMAV DGYRNLKELT IDALRPTR.. ..........

Scb2  LYNEVYEGPT LTEFEDA...
Hab2  LYEQNYQRMS GAEFRPGIED
 Gox  .......... ..........
 Hao  .......... ..........
 Mdh  KGTHA..... ..........
 Lox  .......... ..........
```

Scb2: flavocytochrome b_2 from S.cerevisiae

Hab2: flavocytochrome b_2 from H.anomala

Gox : glycolate oxidase Hao: hydroxyacid oxidase

Mdh : mandelate dehydrogenase Lox: lactate oxidase

Active site residues are marked *.

two enzymes. No sequence similarity was, in any case, anticipated because trimethylamine dehydrogenase contains covalently-bound FMN and does not show extensive structural similarity to flavocytochrome $\underline{b}_2$ and spinach glycolate oxidase further than the basic folding framework [89].

1.8 CONCLUSION

Flavocytochrome $\underline{b}_2$, a yeast respiratory enzyme which oxidizes L-lactate to pyruvate, has been extensively researched. It contains two prosthetic groups, protohaem IX and FMN, which are bound in two functionally-distinct domains playing separate well-characterized roles in enzyme turnover.

The haem-containing domain is essential for electron transfer to cytochrome $\underline{c}$, the physiological electron acceptor for the enzyme. It can be isolated from the holoenzyme by proteolytic methods, and is a member of the cytochrome $\underline{b}_5$ superfamily.

The flavin domain contains the active site and is essential for lactate dehydrogenase activity. It contains a region of protein highly sensitive to proteases, making isolation more difficult than for the haem domain. It is analogous to several other FMN-containing proteins.

The two domains of flavocytochrome $\underline{b}_2$ have now been expressed independently in *E.coli*. The following chapters will describe the isolation, purification and characterization of the individually-expressed domains, and the characterization of one point mutant of the isolated flavin domain.

1.9 REFERENCES

[1] Appleby, C.A. & Morton, R.K., Nature **173**, 749-752 (1954)

[2] Daum, G., Bohni, P.C. & Schatz, G., J. Biol. Chem **257**, 13028-13033 (1982)

[3] Lederer, F., in "Chemistry and Biochemistry of Flavoenzymes", (Muller, F., ed), CRC Press Inc., Boca Raton, 153-242 (1991)

[4] Keilin, D., Proc. Roy. Soc. **B**, 312 (1925)

[5] Massey, V. & Palmer, G., Biochemistry **5**, 3181-3189 (1966)

[6] Morton, R.K., Soc. Biol. Chem. India, 177-187 (1955)

[7] Chapman, S.K., White, S.A. & Reid, G.A., Adv. Inorg. Chem. **36**, 257-301 (1991)

[8] Xia, Z.-x. & Mathews, F.S., J. Mol. Biol. **212**, 837-863 (1990)

[9] Black, M.T., White, S.A., Reid, G.A. & Chapman, S.K., Biochem. J. **258**, 255-259 (1989)

[10] Appleby, C.A. & Morton, R. K., Biochem. J. **75**, 258-269 (1960)

[11] Morton, R.K. & Shepley, K., Nature **192**, 639-641 (1961)

[12] Symons, R.H., Biochim. Biophys. Acta **103**, 298-310 (1965)

[13] Symons, R.H. & Burgoyne, L.A., Methods. Enzymol. **9**, 314-321 (1966)

[14] Morton, R.K., Nature **192**, 727-731 (1961)

[15] Somlo, M. & Slonimski, P.P., Bull. Soc. Chim. Biol. **48**, 1221-1249 (1966)

[16] Lederer, F. & Simon, A.M., Eur. J. Biochem. **20**, 469-474 (1971)

[17] Jacq, C. & Lederer, F., Eur. J. Biochem. **25**, 41-48 (1972)

[18] Jacq, C. & Lederer, F., Eur. J. Biochem. **41**, 311-320 (1974)

[19] Labeyrie, F. & Baudras, A., Eur. J. Biochem. **25**, 33-40 (1972)

[20] Labeyrie, F., Baudras, A. & Lederer, F., Methods. Enzymol. **53**, 238-256 (1978)

[21] Reid, G.A., Yonetani, T. & Schatz, G., J. Biol. Chem. **257**, 13068-13074 (1982)

[22] Daum, G., Gasser, S.M. & Schatz, G., J. Biol. Chem. **257**, 13075-13080 (1982)

[23] Ohnishi, T., Kawaguchi, K. & Hagihara, B., J. Biol. Chem. **241**, 1797-1806 (1966)

[24] Pajot, A.P. & Claisse, M.L., Eur. J. Biochem. **49**, 275-285 (1974)

[25] Pajot, P. & Groudinsky, O., Eur. J. Biochem. **12**, 158-164 (1970)

[26] Capeillere-Blandin, C., Bray, R.C., Iwatsubo, M. & Labeyrie, F. Eur. J. Biochem. **54**, 549-566 (1975)

[27] Watari, H., Groudinsky, O. & Labeyrie, F., Biochim. Biophys. Acta **131**, 592-594 (1967)

[28] Lederer, F., Cortial, S., Becam, A.M., Haumont, P.Y. & Perez, L., Eur. J. Biochem. **152**, 419-428 (1985)

[29] Jacq, C. & Lederer, F., Eur. J. Biochem. **12**, 154-157 (1970)

[30] Monteilheit, C. & Risler, Y., Eur. J. Biochem. **12**, 165-169 (1970)

[31] Naslin, L., Spyridakis, A. & Labeyrie, F., Eur. J. Biochem. **34**, 268-283 (1973)

[32] Labeyrie, F., Groudinsky, O., Jacquot-Armand, Y. & Naslin, L., Biochim. Biophys. Acta **128**, 492-503 (1966)

[33] Labeyrie, F., di Franco, A., Iwatsubo, M. & Baudras, A., Biochemistry **6**, 1791-1797 (1967)

[34] Guiard, B. & Lederer, F., Biochimie **58**, 305-316 (1976)

[35] Guiard, B., Groudinsky, O. & Lederer, F., Eur. J. Biochem. **34**, 241-247 (1973)

[36] Mevel-Ninio, M., Risler, Y. & Labeyrie, F., Eur. J. Biochem. **73**, 131-140 (1977)

[37] Gervais, M., Groudinsky, O., Risler, Y. & Labeyrie, F., Biochem. Biophys. Res. Commun. **77**, 1543-1551 (1977)

[38] Ghrir, H. & Lederer, F., Eur. J. Biochem. **120**, 279-287 (1981)

[39] Gervais, M., Labeyrie, F., Risler, Y. & Vergnes, O., Eur. J. Biochem. **111**, 17-31 (1980)

[40] Gervais, M., Risler, Y., Capeillere-Blandin, C., Vergnes, O. & Labeyrie, F., in "Limited Proteolysis in Microorganisms" (Cohen, G.N. & Holzer, H., eds), US. Government Printing Office, Washington DC 277-234 (1979)

[41] Mathews, F.S. & Xia, Z-x., in "Flavins and Flavoproteins 1987" (McCormick, D.B. & Edmonson, D.E., eds), Walter de Gruyter & Co., Berlin, New York, 123-132 (1987)

[42] Labeyrie, F., Beloeil, J.C. & Thomas, M.A., Biochim. Biophys. Acta **953**, 131-141 (1988)

[43] White, P., **et al** (in press)

[44] Reid, G.A., White, S.A., Black, M.T., Lederer, F., Mathews, F.S. & Chapman, S.K., Eur. J. Biochem. **178**, 329-333 (1988)

[45] Dubois, J., Chapman, S.K., Mathews, F.S., Reid, G.A. & Lederer, F., Biochemistry **29**, 6393-6400 (1990)

[46] Miles, C.S., Rouviere-Fourmy, N., Lederer, F., Mathews, F.S., Reid, G.A. & Chapman, S.K., Biochem. J. **285**, 187-192 (1992)

[47] Miles, C.S., PhD Thesis, University of Edinburgh (1992)

[48] White, S.A., Black, M.T., Reid, G.A. & Chapman, S.K., Biochem. J. **263**, 849-853 (1989)

[49] Lederer, F., Eur. J. Biochem. **46**, 393-399 (1974)

[50] Pompon, D., Iwatsubo, M. & Lederer, F., Eur. J. Biochem. **104**, 479-488 (1980)

[51] Baudras, A., Bull. Soc. Chim. Biol. **47**, 1143-1175 (1965)

[52] Forrestier, J.P. & Baudras, A., in "Flavins and Flavoproteins" (Kamin, H., ed) 599-605 (1971)

[53] Urban, P. & Lederer, F., Eur. J. Biochem. **144**, 345-357 (1984)

[54] Urban, P. & Lederer, F., J. Biol. Chem. **260**, 11115-11122 (1985)

[55] Pompon, D. & Lederer, F., Eur. J. Biochem. **148**, 145-154 (1985)

[56] Porter, D.J.T., Voet, J.G. & Bright, H.J., J. Biol. Chem. **248**, 4400-4416 (1973)

[57] Genet, R. & Lederer, F., Biochem. J. **266**, 301-304 (1990)

[58] Lederer, F. & Mathews, F.S., in "Flavins and Flavoproteins 1987" (McCormick, D.B. & Edmonson, D.E., eds) Walter de Gruyter & Co., Berlin 133-142 (1987)

[59] Ghisla, S. & Massey, V., J. Biol. Chem. **255**, 5688-5696 (1980)

[60] Lockridge, O., Massey, V. & Sullivan, P.A., J. Biol. Chem. **247**, 8097-8106 (1972)

[61] Ghisla, S. & Massey, V., Eur. J. Biochem. **181**, 1-17 (1989)

[62] Walker, M.C. & Tollin, G., Biochemistry **30**, 5546-5555 (1991)

[63] Capeillere-Blandin, C., Eur. J. Biochem. **56**, 91-101 (1975)

[64] Pompon, D., Eur. J. Biochem. **106**, 151-159 (1980)

[65] Iwatsubo, M., Mevel-Ninio, M. & Labeyrie, F., Biochemistry **16**, 3558-3566 (1977)

[66] Tegoni, M., Mozzarelli, A., Rossi, G.L. & Labeyrie, F., J. Biol. Chem. **258**, 5424-5427 (1983)

[67] Baudras, A., Krupa, M. & Labeyrie, F., Eur. J. Biochem. **20**, 58-74 (1971)

[68] Thomas, M.A., Gervais, M., Favaudon, V. & Valat, P., Eur. J. Biochem. **135**, 577-581 (1983)

[69] Matsushima, A., Yoshimura, T. & Aki, K., J. Biochem. **100**, 543-551 (1986)

[70] White, S.A., PhD Thesis, University of Edinburgh (1989)

[71] Vanderkooi, J., Glatz, P., Casadel, J. & Woodrow, G.V., Eur. J. Biochem. **110**, 189-196 (1980)

[72] Ogura, Y. & Nakamura, T., J. Biochem. **60**, 77-86 (1966)

[73] Black, M.T., Gunn, F.J., Chapman, S.K. & Reid, G.A., Biochem. J. **263**, 745-756 (1986)

[74] Capeillere-Blandin, C., Barber, M.J. & Bray, R.C., Biochem. J. **238**, 745-756 (1986)

[75] Baudras, A., Biochimie **53**, 929-963 (1971)

[76] Gervais, M. & Tegoni, M., Eur. J. Biochem. **111**, 357-367 (1980)

[77] Gervais, M., Risler, Y. & Corazzin, S., Eur. J. Biochem. **130**, 253-259 (1983)

[78] Celerier, J., Risler, Y., Schwenke, J., Janot, J.M. & Gervais, M., Eur. J. Biochem. **182**, 67-75 (1989)

[79] Lederer, F. & Guiard, B., in "Methods in Peptide and Protein Sequence Analysis" (Birr, C., ed), Elsevier North Holland Biomedical Press, 433-438 (1980)

[80] Guiard, B. & Lederer, F., J. Mol. Biol. **135**, 639-650 (1979)

[81] Cramer, W.A., Whitmarsh, J. & Horton, P., in "The Porphyrins" **VII**, (D. Dolphin, ed.), Academic Press Inc., London, 71-106 (1979)

[82] Mathews, F.S., Czerwinski, E.W. & Argos, P., in "The Porphyrins" **VII**, (D. Dolphin, ed.), Academic Press Inc., London, 71-106 (1979)

[83] Keller, R.M. & Wuthrich, K., Biochim. Biophys. Acta. **621**, 204-217 (1980)

[84] McLachlan, S.J., La Mar, G.N. & Sletten, E., J. Am. Chem. Soc. **108**, 1285-1291 (1986)

[85] Guiles, R.D., Altman, J., Kuntz, D. & Waskell, L. Biochemistry **29**, 1276-1289 (1990)

[86] Johnson, J.L. & Rajagopalan, K.V., J. Biol. Chem **252**, 2017-2025 (1977)

[87] Guiard, B. & Lederer, F., Eur. J. Biochem. **74**, 181-190 (1977)

[88] Ghisla, S. & Massey, V., in "Chemistry and Biochemistry of Flavoenzymes", (Muller, F. ed.), CRC Press Inc., Boca Raton, 1-58 (1991)

[89] Lindqvist, Y., Branden, C.I., Mathews, F.S. & Lederer, F., J. Biol. Chem. **266**, 3198-3207 (1991)

[90] Giegel, D.A., Williams, C.H., Jr., & Massey, V., J. Biol. Chem. **265**, 6626-6632 (1990)

[91] Cederlund, E., Lindqvist, Y., Soderland, G., Branden, C.I. & Jornvall, H., Eur. J. Biochem. **173**, 523-530 (1988)

[92] Urban, P., Chirat, I. & Lederer, F., Biochemistry **27**, 7365-7371 (1988)

[93] Boyd, G., Mathews, F.S., Packman, L.C. & Scrutton, N.S., FEBS Lett. **308**, 271-276 (1992)

CHAPTER 2

ISOLATION AND PURIFICATION OF THE b_2-HAEM DOMAIN EXPRESSED IN *E.coli*

2.1 INTRODUCTION

2.1.1 BACKGROUND

In 1966, Labeyrie and co-workers found that tryptic hydrolysis of flavocytochrome $\underline{b}_2$ liberated a polypeptide fragment with a molecular weight of around 11 000, containing one haem group [1]. The isolated polypeptide had a very similar electronic absorption spectrum to the native enzyme from yeast. It had a redox potential of -28mV [1], which compares with a value close to neutral for the haem in the holoenzyme [2] and a value of +273mV for cytochrome $\underline{c}$, the physiological electron acceptor of flavocytochrome $\underline{b}_2$ [3]. It was also discovered that a similar fragment could be formed by the action of yeast proteases during the preparation of flavocytochrome $\underline{b}_2$ from yeast [4]. This isolated fragment came to be known as cytochrome $\underline{b}_2$ core, designated "tryptic" or "spontaneous" depending on whether it was produced by tryptic hydrolysis or the action of yeast proteases. Sequencing studies showed that cytochrome $\underline{b}_2$ core had a high level of identity with cytochrome $\underline{b}_5$ and two histidines were identified as probable haem ligands [5]. In contrast to the enzyme from *S. cerevisiae*, flavocytochrome $\underline{b}_2$ from *H. anomala* showed different stability with respect to yeast proteases, but nevertheless shared a number of protease-sensitive bonds. This confirmed that the two flavocytochromes $\underline{b}_2$ were similar in terms of tertiary folding, having a polyglobular structure [6].

Sequencing and amino-acid analysis showed that the cytochrome $\underline{b}_2$ core formed the N-terminal part of the flavocytochrome $\underline{b}_2$ protomer [7] and comprised the first 96 residues of the amino-acid sequence [8].

2.1.2 STRUCTURE OF THE HAEM DOMAIN

The crystal structure of flavocytochrome b_2 [9,10] reveals that the four haem domains in the tetramer are located at the periphery of an ellipsoid disc formed by the flavin domains. Two of the monomers, in which pyruvate is present at the active site, have haem domains which are positionally disordered in the crystal structure. This gives an indication that the haem domain is mobile relative to the rest of the protomer. In the ordered monomer, the haem group is located at the interface between the haem domain and the flavin-binding domain. The haem is situated inside a hydrophobic crevice within the haem domain, axially ligated by the imidazoles of His 43 and His 66 (Figure 2.1). The haem propionate groups extend away from the haem domain towards the FMN group and the centre of the molecule.

2.1.3 CATALYTIC ROLE OF THE HAEM DOMAIN

Appleby and Morton [11] were the first to link the haem with electron transfer to acceptors. It was later shown that the pathway of electron transfer within the enzyme was from substrate to FMN and from FMN to haem (Section 1.5) [12,13].

Studies on haem-free preparations of flavocytochrome b_2 and dehaemoenzyme reconstituted with different amounts of haem showed haem to be essential for electron transfer to the physiological electron acceptor, cytochrome *c*, but not for transfer to ferricyanide, a widely-used electron acceptor *in vitro* [14,15].

2.1.4 EXPRESSION OF THE b_2-HAEM DOMAIN IN *E. coli*

Although cytochrome b_2 core can be isolated from the wild-type

FIGURE 2.1 THE STRUCTURE OF THE HAEM DOMAIN OF FLAVOCYTOCHROME $\underline{b}_2$ SHOWING THE AXIALLY-COORDINATED HAEM

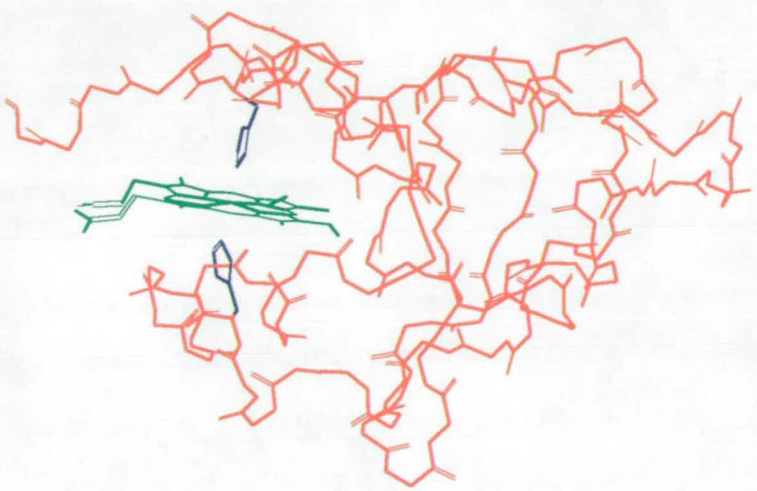

The axial histidines are shown in blue

enzyme by proteolytic methods, it is only produced in low yields, rendering detailed investigation difficult. It was therefore desirable to express the haem domain independently in *E. coli*.

The flavocytochrome b_2 haem domain was expressed in *E. coli* by Dr. G.A. Reid using essentially the same method as previously used to express wild-type flavocytochrome b_2 [16,17]. Site-directed mutagenesis was used to introduce a stop codon (TGA) immediately after residue Gly 100 in the gene for flavocytochrome b_2. An *Eco*RI-cleavage site was also introduced overlapping the stop codon to allow the DNA encoding the haem domain to be excised from a mutant clone using *Eco*RI, a restriction endonuclease which cleaves duplex DNA at GAATTC sites on each strand. This results in a staggered cut, with a short protruding single strand on each piece of cleaved DNA. A synthetic oligonucleotide containing the desired sequence mutation (CTCCTGGTTG AATTCATGGAAACTAAG) was used to perform mutagenesis. Resulting clones were screened for the introduction of the *Eco*RI cleavage site and the DNA of a positive clone was sequenced to confirm that the TGA stop codon had been introduced and that no other unwanted mutations had taken place. The fragment of DNA was then inserted into the *Eco*RI site of a plasmid, pDS6, which was then transferred to *E. coli* MM294. The TGA stop codon has the effect of terminating expression of the enzyme at that point, resulting in the expression of residues 6 to 100 only, which constitute the haem domain. A schematic representation comparing the proteolytically-produced b_2 core and the b_2-haem domain expressed in *E. coli* appears in Figure 2.2. Further detailed descriptions of the expression technique can be found in [16,17] and references therein.

The isolation and purification of the b_2-haem domain expressed in *E. coli* is described in the following section.

FIGURE 2.2 SCHEMATIC STRUCTURAL REPRESENTATION OF THE AMINO ACID SEQUENCE OF FLAVOCYTOCHROME $\underline{b_2}$ FROM PROTEOLYTIC AND X-RAY CRYSTALLOGRAPHIC STUDIES

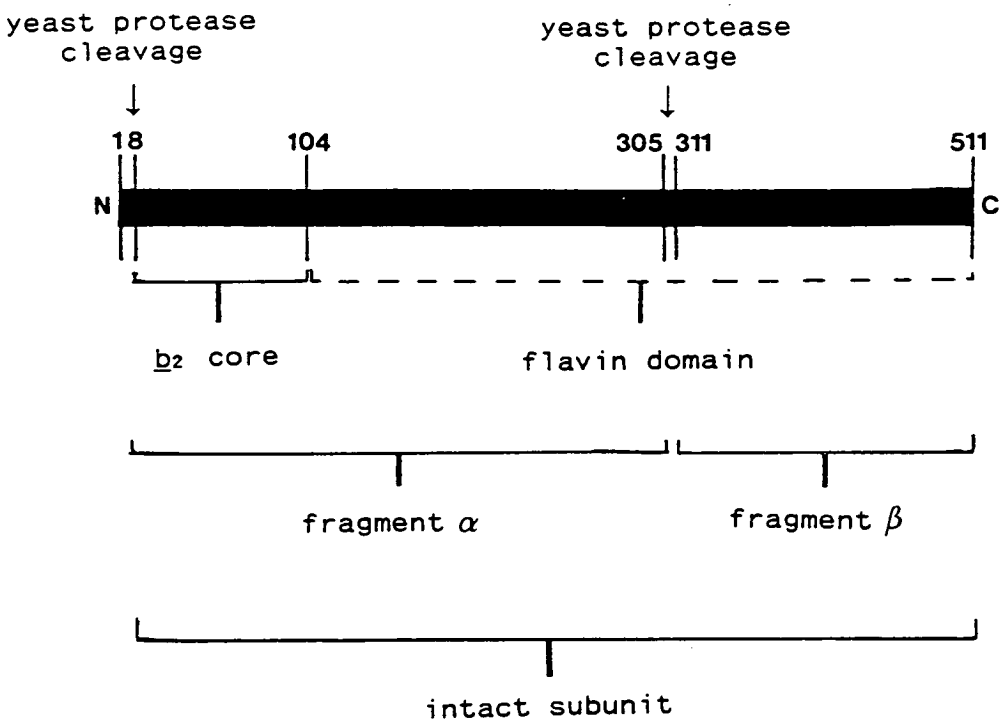

(a) Proteolytic cleavage sites, fragment compositions and domain structure elucidated from proteolysis studies (after [10])

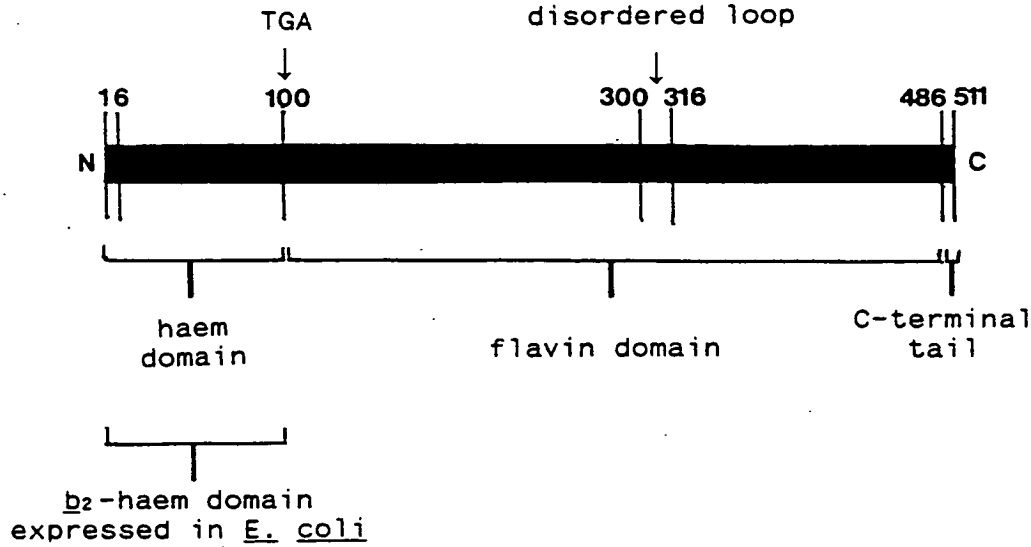

(b) Composition from X-ray results, showing the region expressed as the $\underline{b_2}$-haem domain in E. coli

2.2 RESULTS: EXTRACTION AND PURIFICATION

2.2.1 EXTRACTION OF b_2-HAEM DOMAIN FROM *E. coli*

Frozen *E. coli* cells containing the b_2-haem domain were suspended in 100mM-sodium phosphate buffer, pH 7.0, containing 10mM-EDTA. (Full descriptions of all buffers used can be found in Chapter 8). Lysozyme (Sigma) was added to approximately 0.2mg/ml and the mixture was incubated with stirring at 0-4°C for 20 minutes. The solution was then centrifuged (39 000g, 20 min) yielding a red supernatant and a brownish-red pellet. The supernatant was retained and the pellet, consisting of cell debris and unlysed cells, was subjected to a second lysis and centrifugation. This second lysis was found to greatly improve yield. The red supernatant from the second lysis was combined with that from the first lysis and the solution adjusted to 30% $(NH_4)_2SO_4$ saturation, stirring until all the $(NH_4)_2SO_4$ had dissolved (*ca.* 5 min). The solution was centrifuged (39 000g, 10 min) and the pellet discarded. The supernatant was adjusted to 70% $(NH_4)_2SO_4$ saturation to precipitate the impure cytochrome, stirring for 5-10 minutes to ensure dissolution of $(NH_4)_2SO_4$. The precipitated protein was collected by centrifugation (39 000g, 10 min) and was stored under nitrogen at 0-4°C prior to further purification.

2.2.2 PURIFICATION

Precipitated b_2-haem domain, prepared as descrbed in 2.2.1, was redissolved in a minimum volume of 10mM-sodium phosphate buffer, pH 7.0, and dialysed overnight against the same buffer at 0-4°C. The dialysed protein solution was centrifuged (39 000g, 2 min) to

remove any insoluble debris and loaded onto a hydroxyapatite (Fluka, fast-flow) column (8cm x 2.5cm) previously equilibrated in 10mM-sodium phosphate buffer, pH 7.0. The column was washed with two column volumes of the 10mM-phosphate buffer before elution using a gradient of 0-5% saturation $(NH_4)_2SO_4$ in the 10mM-phosphate buffer. Fractions were collected and monitored for purity by measuring the ratio of absorbances at 275nm and 413nm. Wild-type flavocytochrome $\underline{b}_2$ has a UV absorbance of 89.0 $mM^{-1}cm^{-1}$ at 275nm [18] but the $\underline{b}_2$-haem domain has a much lower molecular weight (approx. 10 000 compared to approx. 230 000 for wild-type flavocytochrome $\underline{b}_2$) and would therefore have a smaller UV absorbance. An extinction coefficient of 121.5 $mM^{-1}cm^{-1}$ had previously been determined for cytochrome $\underline{b}_2$ core [18]. Thus samples with $A_{275}/A_{413} < 89.0/121.5$, i.e. $A_{275}/A_{413} < 0.7$, can be assumed to be quite pure. Those fractions with $A_{275}/A_{413} < 1.0$ were pooled, precipitated at 70% $(NH_4)_2SO_4$ and centrifuged (39 000g, 10 min).

The precipitated protein was redissolved in a minimum volume of 2mM-sodium phosphate buffer, pH 8.5, and dialysed overnight against this buffer at 0-4°C. The dialysed solution was centrifuged as before (39 000g, 2 min) and loaded onto a DE-52 (Whatman) column (21.5cm x 2.5cm) equilibrated in the 2mM-phosphate buffer. After washing with two column volumes of this buffer the $\underline{b}_2$-haem domain was eluted with a gradient of 2-20mM-sodium phosphate buffer, pH 8.5. Fractions were collected and those with $A_{275}/A_{413} < 0.3$ were pooled and $(NH_4)_2SO_4$-precipitated as before.

SDS-PAGE of the $\underline{b}_2$-haem domain purified on hydroxyapatite and DE-52 columns showed one main band of M_r $\underline{ca.}$ 10 000 but also revealed a faint band of higher molecular weight. This contaminant

was removed by gel filtration using Sephadex G-75, a gel with an exclusion limit of 80 000.

Precipitated $\underline{b}_2$-haem domain was redissolved in a minimum volume of 20mM-sodium phosphate buffer, pH 7.0, and passed through a Sephadex G-75 column (130cm x 2.5cm) equilibrated in the same buffer. Fractions were collected and those with $A_{275}/A_{413} = 0.2 \pm 0.01$ were pooled. SDS-PAGE of the cytochrome after gel filtration showed a single band of M_r 10 500.

The purification procedure, yields and purification achieved is summarised in Table 2.1.

2.3 DISCUSSION

Introduction of a termination codon immediately after the codon for the hundredth residue of flavocytochrome $\underline{b}_2$ from S. cerevisiae enabled the haem domain to be expressed in E. coli using the same vector previously employed to express the holoenzyme [17,18]. N-terminal amino-acid sequencing found that the $\underline{b}_2$-haem domain expressed in E. coli commences at the amino-acid position equivalent to Met 6 of the mature enzyme from yeast [17], consistent with the holoenzyme when expressed in E. coli [16,17].

An effective purification procedure for the $\underline{b}_2$-haem domain expressed in E. coli has been developed as outlined in Section 2.2.2. This enables large quantities of the isolated $\underline{b}_2$-haem domain to be prepared without recourse to proteolytic methods. The advantages of this method of preparing the isolated domain are twofold. Firstly, expression and purification of the $\underline{b}_2$-haem domain from E. coli is simpler than proteolytic treatment of holoenzyme, which not only requires that the holoenzyme be isolated but also needs incubation

TABLE 2.1: PURIFICATION DATA FOR b_2-HAEM DOMAIN EXPRESSED IN *E. coli*

Purification step	Total protein (mg)	b_2-haem domain (mg)	Recovery (%)	A_{275}/A_{413} ratio	Purification fold
Supernatant after cell lysis	500	8	100	>6	1
After $(NH_4)_2SO_4$ and dialysis	160	7.1	89	1.9	3
After hydroxyapatite column chromatography	28	4.3	54	0.6	10
After DE-52 column chromatography	3.2	2.2	27	0.27	43
After Sephadex G-75 column chromatography	2.0	2.0	25	0.19	63

Based on a preparation of 10g wet weight *E. coli* cells

of the enzyme with the selected proteases under controlled conditions and a method of halting proteolysis at the required stage. The mixture of proteolysis products then requires separation. However, when isolated from *E. coli*, a simple extraction and purification procedure is sufficient to produce b_2-haem domain to a very high degree of purity. Secondly, the yield of b_2-haem domain is much higher than the yield of flavocytochrome b_2 from yeast (typically no more than 0.05mg per g. dried yeast [20], compared to 0.2mg of b_2-haem domain per g. wet weight of *E. coli* cells). Expression and isolation of b_2-haem domain from *E. coli* is vastly more productive than the isolation of spontaneously-formed cytochrome b_2 core from yeast [4].

The availability of large quantities of very pure b_2-haem domain afforded by its expression in *E. coli* allows many opportunities for further investigation of the structural and functional properties of the haem domain. Characterization of the isolated b_2-haem domain will be discussed in the next chapter.

2.4 REFERENCES

[1] Labeyrie, F., Groudinsky, O., Jacquot-Armand, Y. & Naslin, L., Biochim. Biophys. Acta **128**, 492-503 (1966)

[2] Chapman, S.K., White, S.A. & Reid, G.A., Adv. Inorg. Chem. **36**, 257-301 (1991)

[3] Augustin, M.A., Chapman, S.K., Davies, D.M., Watson, A.D. & Sykes, A.G., J. Inorg. Biochem. **20**, 281-289 (1984)

[4] Labeyrie, F., di Franco, A.M., Iwatsubo, M. & Baudras, A., Biochemistry **6**, 1791-1797 (1967)

[5] Guiard, B., Groudinsky, O. & Lederer, F., Proc. Nat. Acad. Sci. USA **71**, 2539-2543 (1974)

[6] Naslin, L., Spyridakis, A. & Labeyrie, F., Eur. J. Biochem. **34**, 268-283 (1973)

[7] Guiard, B., Groudinsky, O. & Lederer, F., Eur. J. Biochem. **34**, 241-247 (1973)

[8] Guiard, B. & Lederer, F., Biochimie **58**, 305-316 (1976)

[9] Mathews, F.S. & Xia, Z.-x., in "Flavins and Flavoproteins 1987" (Edmondson, D.E. & McCormick, D.B., eds), Walter de Gruyter & Co., New York, 123-132 (1987)

[10] Xia,Z.-x. & Mathews, F.S., J. Mol. Biol. **212**, 837-863 (1990)

[11] Appleby, C.A. & Morton, R.K., Nature **173**, 749-752 (1954)

[12] Suzuki, H. & Ogura, Y., J. Biochem. **67**, 277-289 (1970)

[13] Morton, R.K. & Sturtevant, J.M., J. Biol. Chem. **239**, 1614-1624 (1964)

[14] Forrestier, J.P. & Baudras, A., in "Flavins and Flavoproteins" (Kamin, H., ed), University Park Press, Baltimore, 599-605 (1971)

[15] Iwatsubo, M., Mevel-Ninio, M. & Labeyrie, F., Biochemistry **16**, 3558-3566 (1977)

[16] Black, M.T., White, S.A., Reid, G.A. & Chapman, S.K., Biochem. J. **258**, 255-259 (1989)

[17] Brunt, C.E., Cox, M.C., Thurgood, A.G.P., Moore, G.R., Reid, G.A. & Chapman, S.K., Biochem. J. **283**, 87-90 (1992)

[18] Pajot, P. & Groudinsky, O., Eur. J. Biochem. **12**, 158-164 (1970)

[19] Strueber, D., Ibrahimi, I., Cutler, D., Dobberstein, B. & Bujard, H., EMBO J. **3**, 255-259 (1984)

[20] Labeyrie, F., Baudras, A. & Lederer, F., Methods Enzymol. **53**, 238-256 (1978)

CHAPTER 3

HAEM DOMAIN: CHARACTERIZATION

3.1 INTRODUCTION

In Chapter 2 the expression of the haem domain of flavocytochrome $\underline{b}_2$ was described. In this chapter, the characterization of the isolated $\underline{b}_2$-haem domain will be discussed. The $\underline{b}_2$-haem domain can be characterized in a number of ways. Techniques including electronic absorption spectroscopy, nuclear magnetic resonance spectroscopy (NMR), gel electrophoresis and redox titration can be used to determine biochemical and biophysical properties of this novel cytochrome. In the case of the isolated $\underline{b}_2$-haem domain, these can then be compared with the known properties of the proteolytically-cleaved cytochrome $\underline{b}_2$ core, and of the haem domain when bound to the flavodehydrogenase function in the holoenzyme. Comparisons can also be made between the isolated $\underline{b}_2$-haem domain and other members of the cytochrome $\underline{b}_5$ superfamily.

3.2 EXPERIMENTAL

3.2.1 ELECTRONIC ABSORPTION SPECTROSCOPY

Electronic absorption spectra were recorded using either a Pye Unicam SP8-400 or Beckman DU-62 UV/visible spectrometer, thermostatted at 25°C. Assays to detect any enzyme activity were carried out at 550nm.

3.2.2 REDOX POTENTIAL DETERMINATION

The mid-point potentials of the haem in the isolated $\underline{b}_2$-haem domain and in the wild-type holoenzyme expressed in E.coli were determined by potentiometric titration as described in Section 8.11. The reaction was carried out under anaerobic conditions in 0.1M

Tris.HCl buffer, pH 7.5.

3.2.3 THERMAL STABILITY

Microcalorimetry (Alan Cooper, University of Glasgow) was used to investigate the thermal stability of the isolated $\underline{b}_2$-haem domain. This technique involves observing the optical density of a protein solution as it is heated. A thermally-stable protein will show no increase in optical density until it reaches a characteristic temperature at which it denatures. At this point a sharp increase in absorbance is observed.

3.2.4 NMR STUDIES

NMR studies were carried out in collaboration with G.R. Moore, M.C. Cox and A.G.P. Thurgood (University of East Anglia). Spectra were recorded using a JEOL GX-400 spectrometer operating at 400 MHz and a Varian VXR 600S spectrometer operating at 600 MHz. Samples were exchanged into ^2H_2O for NMR experiments as described in Section 8.13.2. 1,4-Dioxan was used as an internal standard but chemical shifts are reported in p.p.m. downfield from the methyl resonance of 4,4-dimethyl-4-silapentane-1-sulphonate. Other conditions are as described in figure legends.

3.3 RESULTS AND DISCUSSION

3.3.1 ELECTRONIC ABSORPTION SPECTRUM

Cytochromes have very characteristic electronic absorption spectra due to the presence of the haem, which gives rise to intense bands arising from π-π^* transitions. All porphyrins exhibit three

main bands in their electronic absorption spectra, which are dependent on the nature of the substituents of the pyrrole carbon atoms. These are: a very intense band at around 400nm, known as the Soret, or γ, band; and two closely-spaced bands of lower intensity, known as the α and β bands. The wavelength of the α-band can be used to classify cytochromes. Cytochromes containing low-spin iron can be classified into types a (α-band above 570nm) b (α in range 550-560nm) and c (α in range 548-552nm).

The electronic absorption spectrum of the isolated haem domain of flavocytochrome b_2 expressed in E.coli appears in Figure 3.1. The spectrum has peaks at 557, 528 and 423nm in the reduced form and 560, 530 and 413nm in the oxidized form. These wavelengths are identical to those observed for the cytochrome b_2 core isolated by proteolysis [1] and the holoenzyme [2]. This, along with other data (Section 3.3.3), suggests that the isolated b_2-haem domain expressed in E.coli (residues 6 - 100 of the holoenzyme) is essentially the same as the cytochrome b_2 core isolated by proteolysis of the holoenzyme from yeast (residues 8 - 103) [3].

3.3.2 KINETIC CHARACTERISATION

The haem domain of flavocytochrome b_2 is essential for electron transfer to cytochrome c [4, 5] as electrons are transferred to the physiological electron acceptor directly from the haem cofactor [4]. It was therefore postulated that the isolated haem domain might act as an external electron acceptor for the isolated flavin domain of flavocytochrome b_2, itself an efficient L-lactate dehydrogenase (Chapters 4 & 5). However, when assayed under steady-state conditions no reduction of the b_2-haem domain was detected when it was used as the electron acceptor with the isolated flavin domain.

FIGURE 3.1 ELECTRONIC ABSORPTION SPECTRUM OF ISOLATED b_2-HAEM DOMAIN

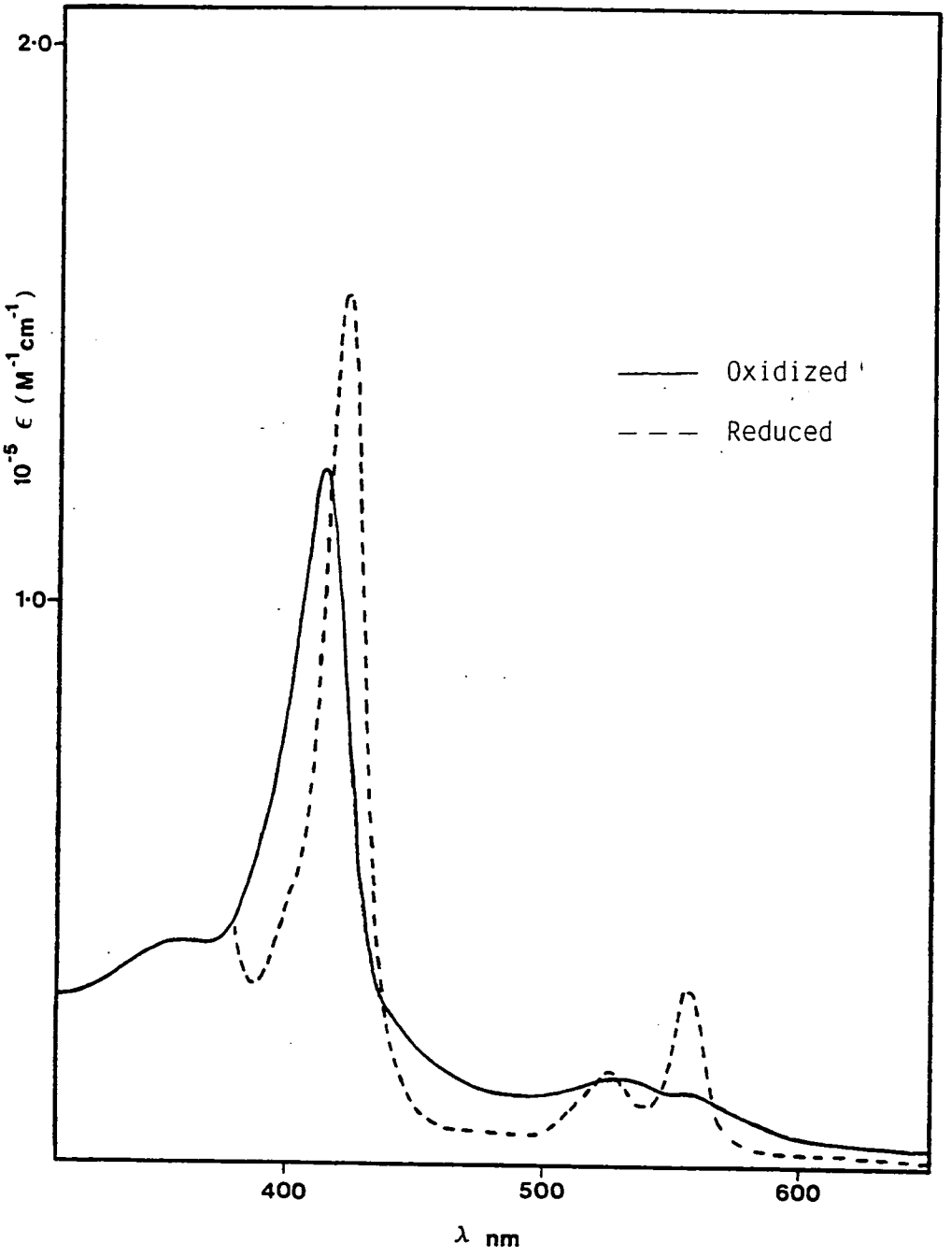

Electronic absorption spectra of 10 μM b_2-haem domain in Tris.HCl buffer, I = 0.10M, pH 7.5, 25 °C.

For further details see Section 8.12.

Why should it be that these two entities, which function so efficiently together when part of the same holoenzyme, totally fail to communicate when expressed independently? It must be remembered that although the actual physical manner of electron transfer from the active site to the haem domain is still unknown, it has been shown that amino-acid side-chains in the interdomain contact region dramatically affect interdomain electron transfer [6]. When the two domains are isolated these contacts are disrupted, preventing flavin to haem electron transfer.

3.3.3. REDOX POTENTIAL

The oxidative titration of the isolated $\underline{b}_2$-haem domain expressed in *E.coli* is shown in Figure 3.2 and Nernst plots for the oxidation and reduction of the isolated $\underline{b}_2$-haem domain and holoenzyme are shown in Figures 3.3 and 3.4. The absence of hysteresis between the oxidative and reductive plots confirms that the redox process under observation is reversible.

The redox potential determined by this method for the isolated $\underline{b}_2$-haem domain and the holoenzyme, along with previously reported values, are summarised in Table 3.1. The redox potential of the isolated $\underline{b}_2$-haem domain was found to be very close to the value determined for proteolytically-produced cytochrome $\underline{b}_2$ core [1]. The value determined for the haem in the holoenzyme by this method is not consistent with the value recorded for the haem couple in intact flavocytochrome $\underline{b}_2$ isolated from *S.cerevisiae* [7], but does compare well with the value determined for intact flavocytochrome $\underline{b}_2$ from *H.anomala* [8].

FIGURE 3.2 REDOX TITRATION OF $\underline{b}_2$-HAEM DOMAIN, OBSERVING ABSORBANCE CHANGES AT 557nm

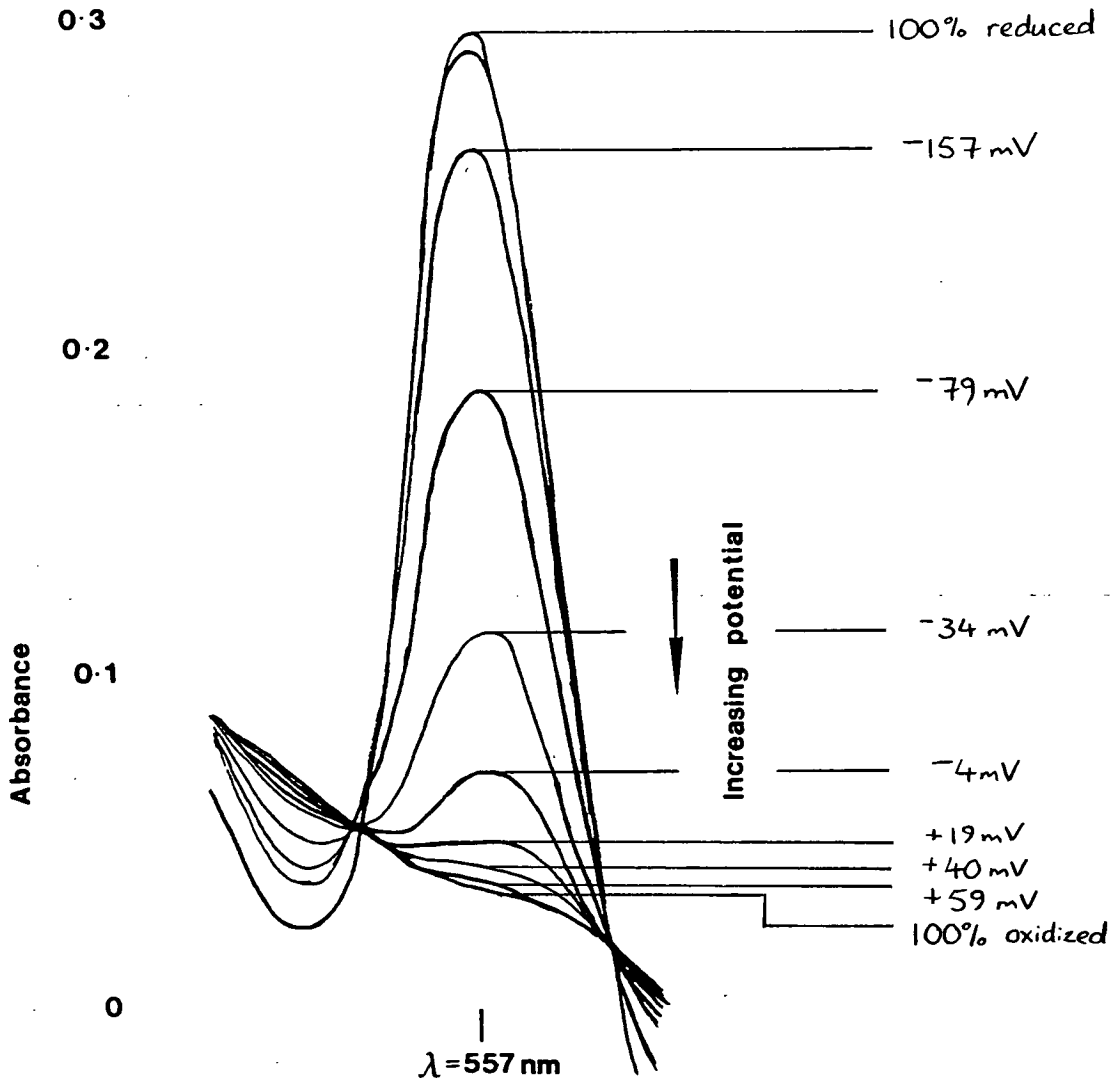

Spectra used to generate Nernst plot (Figure 3.3) are labelled

FIGURE 3.3 NERNST PLOT FROM THE REDOX TITRATION OF $\underline{b}_2$-HAEM DOMAIN

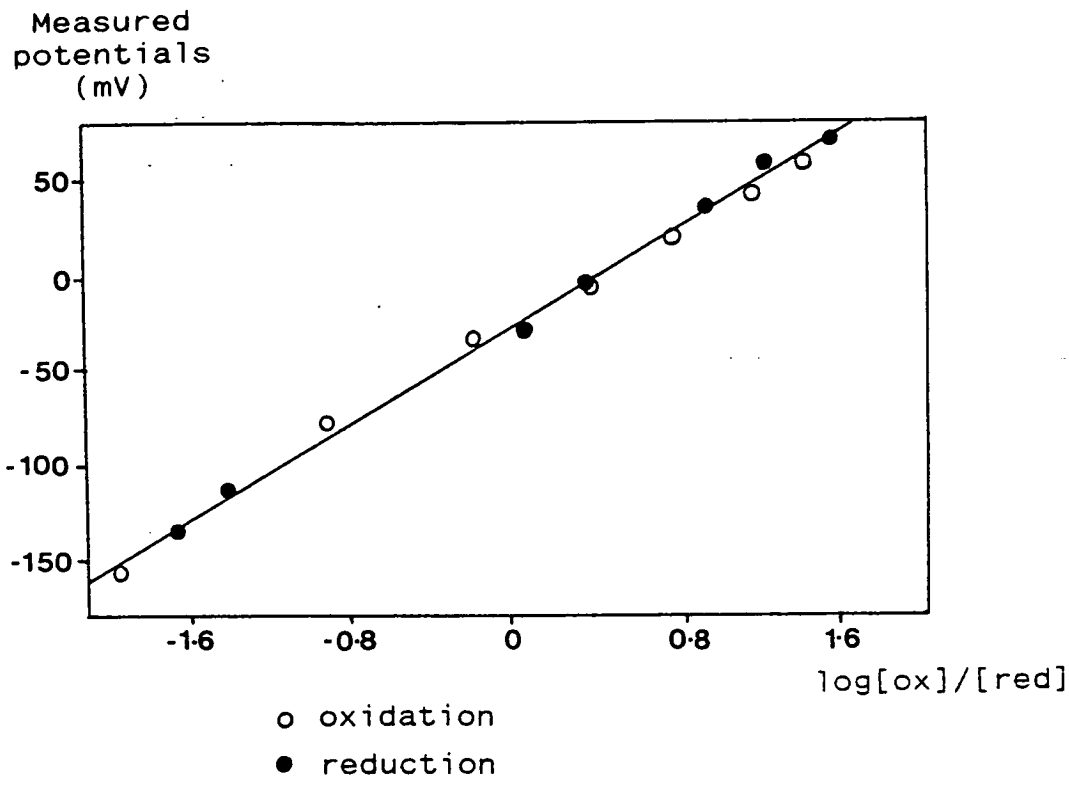

Line shown is for a 1-electron process.

Gradient = 51.0 mV

FIGURE 3.4 NERNST PLOT FROM THE REDOX TITRATION OF HOLO-FLAVOCYTOCHROME $\underline{b}_2$

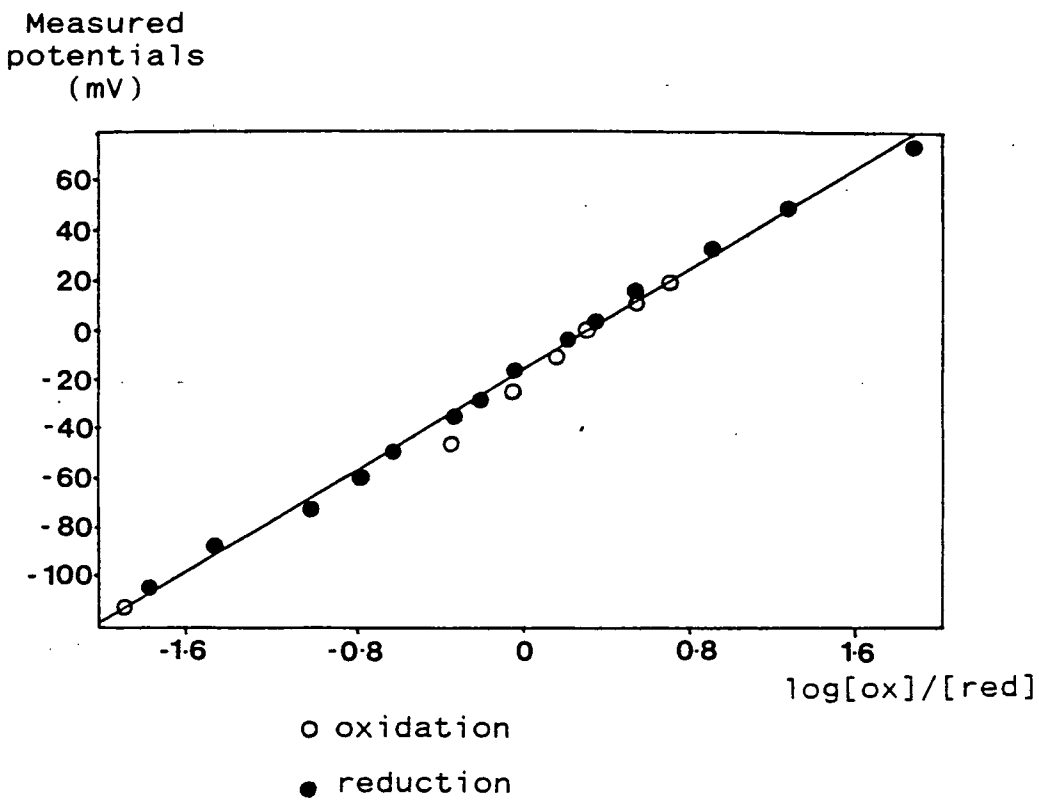

Line shown is for a 1-electron process.

Gradient = 51.2 mV

TABLE 3.1: REDOX POTENTIALS FOR HAEM IN VARIOUS TYPES OF FLAVOCYTOCHROME $\underline{b}_2$

Enzyme	H_{ox}/H_{red} (mV)	Conditions	Ref.
S_I	+10		(4)
S_I	-19	See Chapter 7	
$\underline{b}_2$ core	-28		(9)
$\underline{b}_2$-haem domain	-31 ± 2	See Chapter 7	
H_I	-16 ± 5		(15)

Abbreviations:

S_I = flavocytochrome $\underline{b}_2$ from S.cerevisiae, intact form

H_I = flavocytochrome $\underline{b}_2$ from H.anomala, intact form

$\underline{b}_2$ core = cytochrome $\underline{b}_2$ core prepared by proteolysis

$\underline{b}_2$-haem domain = isolated haem domain of flavocytochrome $\underline{b}_2$ expressed in E.coli

3.3.4 THERMAL STABILITY

The results obtained for the isolated $\underline{b}_2$-haem domain and wild-type flavocytochrome $\underline{b}_2$ are shown in Figure 3.5. The gradual increase in absorbance with temperature recorded for the wild-type enzyme indicates that it denatures gradually until at around 55°C it coagulates, as indicated by the dip in absorbance. In contrast, the absorbance of the isolated $\underline{b}_2$-haem domain shows no significant change up to 89°C, at which a small peak is observed as the protein begins to denature. This is followed immediately by a decrease in absorbance below the previous level. Examination of the sample showed that the protein had coagulated. Thus the isolated haem domain of flavocytochrome $\underline{b}_2$ appears to be stable up to a temperature close to 90°C.

3.3.5 pH STABILITY

In order to ascertain the effect of changing pH on the stability of the isolated $\underline{b}_2$-haem domain, the electronic absorption spectrum of the protein was monitored with decreasing pH. As pH decreased, the absorbance at 413nm decreased in intensity. At pH 2.5, a shoulder appeared on the 413nm peak. At pH 2.1, the absorbance peak at 413nm had disappeared entirely and the haem peak at 380nm had increased in intensity. Two peaks had also appeared at around 540 and 570nm (Figure 3.6). These peaks are consistent with the presence of free haem [9]. On neutralising the solution to pH 7.5 the free haem absorbance had disappeared and the absorbance at 413nm had reappeared to 70% of the original intensity. This suggests that some reincorporation of haem has taken place. This pH stability, especially in the range pH 3 to pH 7.5, is especially

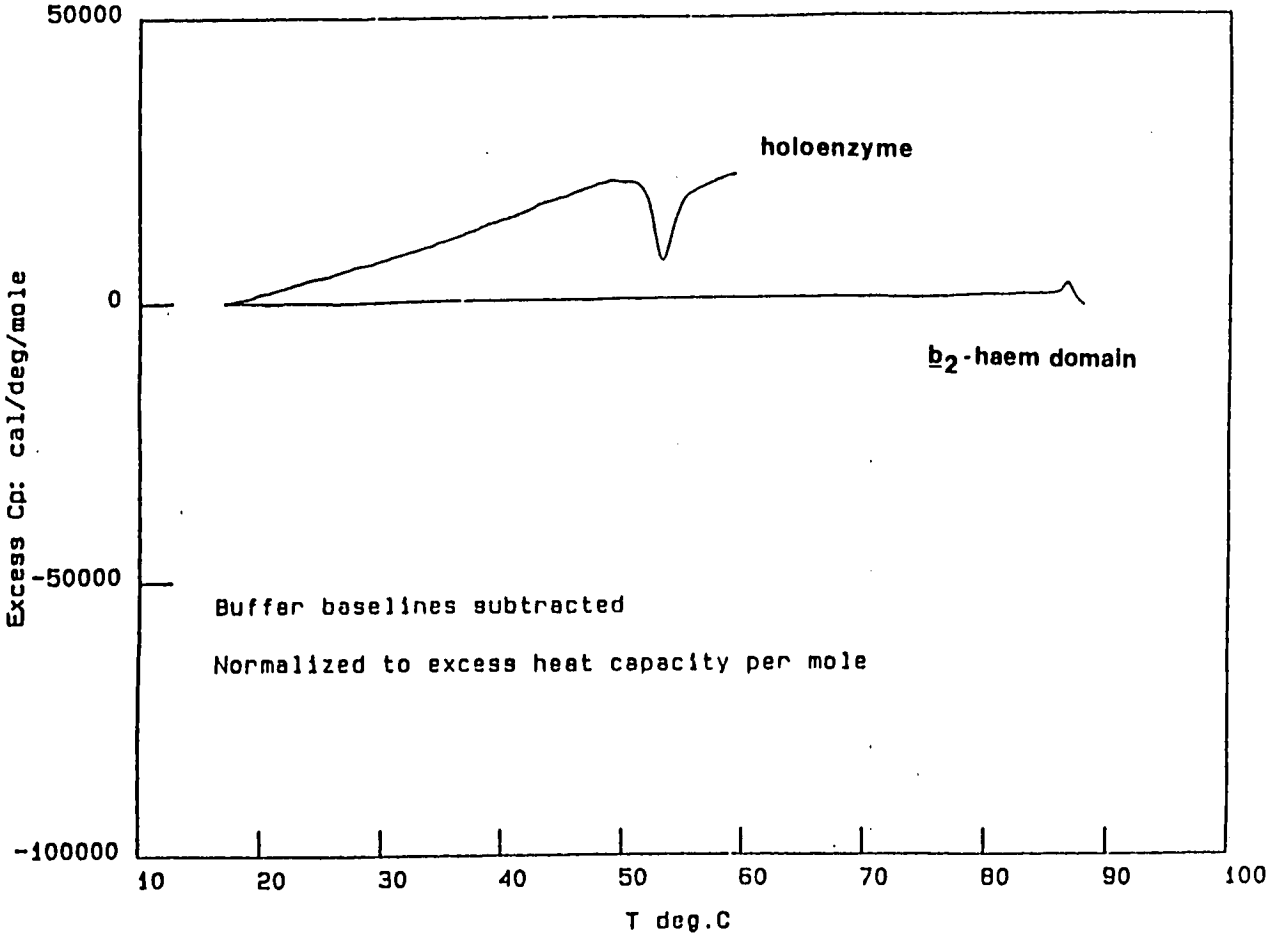

FIGURE 3.5 MICROCALORIMETRY OF FLAVOCYTOCHROME $\underline{b}_2$ AND $\underline{b}_2$-HAEM DOMAIN

FIGURE 3.6 pH TITRATION OF $\underline{b}_2$-HAEM DOMAIN

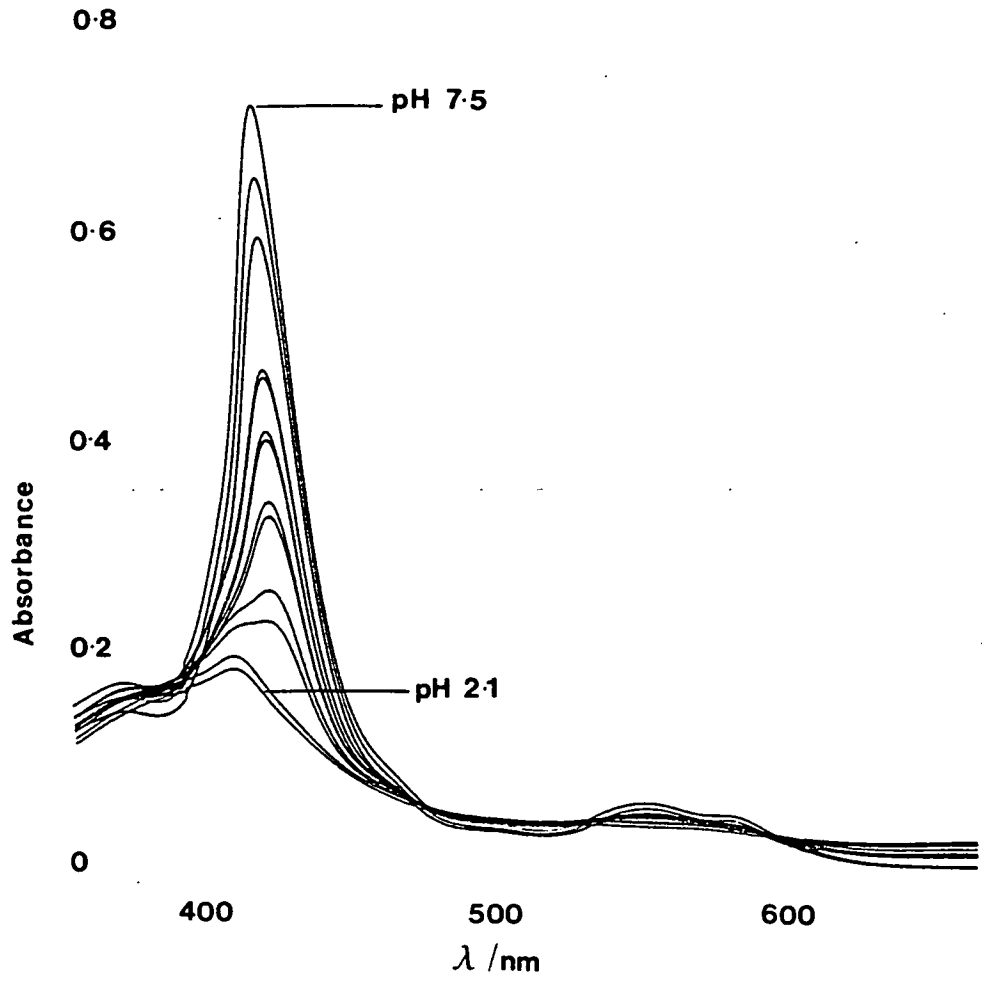

pH was adjusted by titration with HCl (0.5M) with stirring.

useful for NMR studies (Section 3.4.4.)

3.4 NUCLEAR MAGNETIC RESONANCE STUDIES

3.4.1 INTRODUCTION

Solution structures of proteins can be markedly different from their crystal structures, which may be distorted by crystal packing forces. Nuclear magnetic resonance (NMR) spectroscopy is a useful technique for investigating solution structures, and has been widely used to study cytochrome $\underline{b}_5$ [10 - 13].

Despite its effectiveness in determining solution structures, it has limitations when applied to proteins [14]. NMR sensitivity is lowered for proteins with molecular weights much higher than 10 000, as larger molecules have slower tumbling rates leading to increased linewidths. This usually requires, therefore, that the protein should be in a monomeric form. Usually, a protein concentration of at least 1mM (0.5ml) is required to obtain NMR spectra of sufficient quality for structural studies. These concentrations can be hard to achieve, especially if the protein concerned has to be isolated from its natural source.

In addition, the protein should be stable at or near room temperature for at least 24 hours.

By these criteria, the isolated haem domain of flavocytochrome $\underline{b}_2$ would appear to be ideal for investigation by NMR. It has a molecular weight close to 10 000, is a monomer, and is thermally stable. Prior to the expression of the $\underline{b}_2$-haem domain in *E.coli* some NMR studies were carried out using proteolytically-isolated cytochrome $\underline{b}_2$ core from both *S. cerevisiae* and *H. anomala* [15,16],

and similarities with the NMR spectra of cytochrome $\underline{b}_5$ were noticed [15]. More sensitive experiments, notably two-dimensional (2D) NMR, were not performed as they require more protein than can easily be isolated from the natural sources alone. Consequently, the haem domain of flavocytochrome $\underline{b}_2$ had not been as thoroughly studied by NMR as had cytochrome $\underline{b}_5$. The expression of isolated $\underline{b}_2$-haem domain in E. coli enabled isolation of sufficient protein for more searching NMR experiments to be carried out.

3.4.2 PROTON NMR OF PROTEINS

The resonances in the proton NMR spectrum of a protein can, by and large, be divided into two categories. The first category comprises the resonances due to protons in aromatic amino-acid side chains (tyrosines, phenylalanines and tryptophans). When subjected to a magnetic field the π-electrons of the aromatic ring circulate, inducing a magnetic field in opposition to the applied field. This induced field decreases the effects of the applied magnetic field on the aromatic protons, resulting in a shift of their resonances to between 5 and 10ppm. The second, and major, category of resonances are those arising from the aliphatic protons in the protein, of which there are considerably more than the aromatic protons. The resonances due to the aliphatic protons are not shifted by aromatic ring currents and occur in the region 0 - 5ppm. As there are so many aliphatic protons this region of the NMR spectrum tends to be very crowded, leading to problems in interpretation of protein NMR spectra.

Several features and techniques can be exploited to clarify the information buried in the crowded regions of the NMR spectra.

Firstly, NMR peaks show fine structure due to spin-spin coupling between neighbouring protons. This is a through-bond effect, giving information about protons which are within three bonds of each other. Amino-acid side-chains will therefore have characteristic splitting patterns, which can in some cases be used to assign resonances in the spectrum.

A second very useful technique in assigning proton resonances in the NMR spectrum relies on the Nuclear Overhauser Effect (NOE) used in NOE spectroscopy (NOESY) experiments. This involves selectively irradiating and saturating the sample at the resonant frequency of one proton, which may result in the resonances of protons which are spatially close to the selected proton being observed with an increased intensity. As well as being useful in the assignment of proton resonances, this technique is useful in elucidating protein structure. As the NOE relies on through-space interactions, it identifies protons which are spatially close, even though they may be far apart in the amino-acid sequence, providing information on protein folding.

These effects aid the interpretation of one-dimensional (1D) NMR spectra but can also be useful in two-dimensional (2D) NMR experiments to further simplify assignment of the proton resonances of a protein. 2D techniques utilising these features are correlated spectroscopy (COSY), which relies on spin-spin coupling effects, and 2D NOESY experiments. In 2D NMR experiments a second radiofrequency pulse is applied at an interval after the first pulse, and spectra are collected. The individual resonances of the proton depend on the interval between the two radiofrequency pulses. By repeating the experiment with a number of different intervals between the

pulses and using Fourier transformation on the results, a 2D spectrum can be obtained. In the 2D spectrum the overlapping resonances of the 1D NMR spectrum are spread into two orthogonal dimensions showing all the spin-spin couplings between connected protons, with an appearance rather like a contour map. This is the basis of the COSY experiment. In the 2D NOESY experiment, a third radiofrequency pulse at the appropriate frequency for irradiation of the selected resonance is applied at a constant time interval after the second pulse. Spectra are then collected after the third pulse. The pulse schemes for these experiments are summarised in Figure 3.7.

3.4.3 ASSIGNMENT OF HAEM PROTONS

The 1D NMR spectrum of the isolated $\underline{b}_2$-haem domain in the oxidized state is shown in Figure 3.8. The oxidized cytochrome contains low spin iron III and is therefore paramagnetic [17,18]. In the NMR spectra of cytochromes the presence of paramagnetic iron causes the resonances of the protons around it to shift by significant amounts to regions above 10ppm and below 0ppm [19]. This effect is reinforced by the large ring current of the aromatic porphyrin. In the 1D NMR spectrum of oxidized $\underline{b}_2$-haem domain a number of resonances are indeed seen to undergo such a shift. These shifted resonances must therefore arise either from protons on groups directly attached to the porphyrin ring, or from amino-acid side-chains close to the prosthetic group, most notably the axially-coordinating histidine ligands.

Although the resonances occurring in the highly-shifted regions of the 1D NMR spectrum of isolated $\underline{b}_2$-haem domain are known to be due to protons close to the haem, the 1D spectrum alone does not

FIGURE 3.7 PULSE SCHEMES FOR 2D NMR EXPERIMENTS

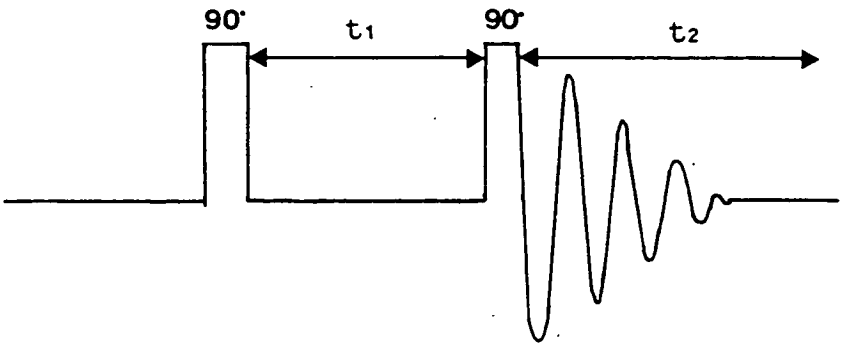

(a) The COSY experiment

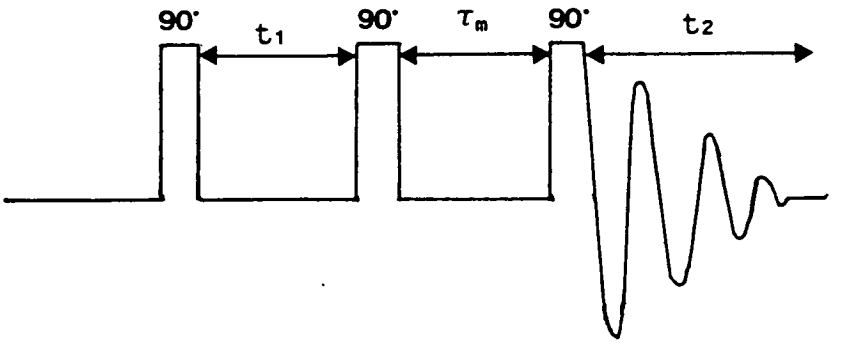

(b) The 2D NOESY experiment

t_1 = variable time interval between the two pulses giving rise to 2D spectra

τ_m = fixed time interval between 2nd and 3rd pulse in NOESY experiment

t_2 = data acquisition time

FIGURE 3.8 1D NMR SPECTRUM OF OXIDIZED b_2-HAEM DOMAIN

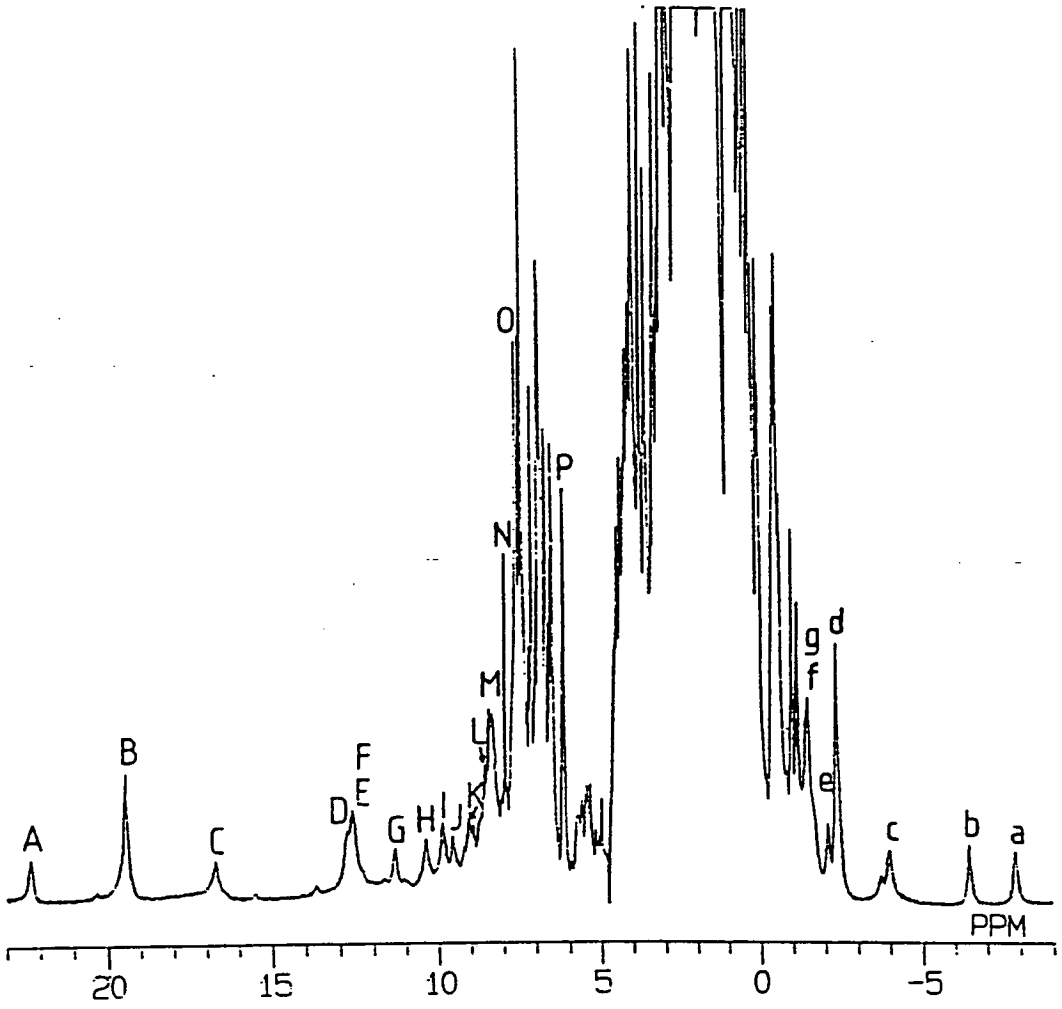

400 MHz spectrum in 50mM phosphate buffer, pH 7, 25°C

TABLE 3.2: ASSIGNMENT OF HAEM PROTONS IN THE NMR SPECTRUM OF OXIDIZED $\underline{b}_2$-HAEM DOMAIN

Label in Figure 3.8	δ ppm	Assignment
A	22.2	Vinyl 2α
B	19.4	Methyl 3
E	12.6	Propionate 7α
F	12.5	Propionate 7α
G	11.4	Propionate 6α
J	9.6	Propionate 6α
M	8.3	Methyl 8
O	7.5	Methyl 5
P	6.1	Methyl 1
a	-7.2	Vinyl 2β
b	-6.5	Vinyl 2β
d	-2.3	Propionate 6β
e	-2.0	Propionate 6β
f	-1.3	Propionate 7β
g	-1.2	Propionate 7β

provide sufficient data to assign each peak to a certain proton. A useful first step in assignment of these peaks is to consult the COSY spectrum of the cytochrome. Figure 3.9 shows the 1D and COSY spectra of isolated $\underline{b}_2$-haem domain. As previously noted (3.4.2) the COSY spectrum is the contour plot resulting from a 2D NMR experiment. The two axes of the COSY plot represent the chemical shifts of the individual resonances and the diagonal represents an "aerial view" of the 1D NMR spectrum. The peaks lying away from the diagonal, or cross-peaks, occur between protons which are spin-spin coupled in the 1D NMR spectrum and can therefore be used to identify the resonances arising from various groups of haem protons. Groups giving rise to such cross-peaks are the haem propionates and haem vinyls. These groups have different, very characteristic, cross-peak patterns due to the arrangement of their protons. For example, the four protons of a propionate group are all spin-spin coupled (figure 3.10(a)),which would give rise to four resonances in the 1D spectrum (figure 3.10(b)). (For haem propionates, the presence of the paramagnetic iron has the effect of broadening any fine structure so no other peaks arising from the propionate group would be seen in the 1D spectrum). In the COSY spectrum these four peaks would be seen on the diagonal with a cross-peak pattern as shown in figure 3.10(c). Coupling between the two α-protons and between the two β-protons, which are only separated from each other by two bonds, is much stronger than coupling between an α- and a β-proton. Hence stronger cross peaks are observed for coupling between the two similar protons (both α or both β) than for coupling between two different types of proton (one α and one β). Figure 3.10 also shows the characteristic cross-peak pattern arising from a haem

vinyl group. The COSY spectrum of the vinyl shows cross-peaks between the α-proton and each of the β-protons but not between the two β-protons themselves. This reflects the dependence of spin-spin coupling on the angle between two protons. In the case of the vinyl β-protons the angle between them (120°) is sufficient to reduce the coupling constant, or distance between the two coupled resonances, to zero, and no cross-peak is seen.

Returning to the COSY spectrum of isolated $\underline{b}_2$-haem domain (figure 3.9), a number of cross-peak patterns can be seen in the highly-shifted regions. One cross-peak pattern arises from resonances at approximately 21, -4 and -7ppm on the diagonal, and is typical of a haem vinyl group. Two other sets of four resonances (approximately 11, 10, -0.7 and -1.0ppm and 13, 12, -1.5 and -1.8ppm) have cross-peaks which, although not quite identical to the theoretical pattern, have been assigned to haem propionate groups. Further confirmation of these assignments is given in Section 3.4.4.

Although these resonances were assigned to propionate groups, the individual peaks in the NMR spectrum could not be specifically assigned to α- or β-protons, nor could the groups of resonances be firmly attributed to one or other of the two propionate groups. By comparison with previously-assigned spectra of cytochrome $\underline{c}$ [20,21] and cytochrome $\underline{b}_5$ [10,13] it was deduced that the low-field resonances of each group were likely to arise from the propionate α-protons and the high-field resonances from the propionate β-protons.

After the assignment of the two haem propionates and one of the vinyls, the resonances of the haem methyls were sought. A haem methyl group is expected to have a resonance of three-proton intensity appearing in the highly-shifted region of the NMR spectrum.

FIGURE 3.9 COSY SPECTRUM (CONTOUR PLOT) OF $\underline{b}_2$-HAEM DOMAIN

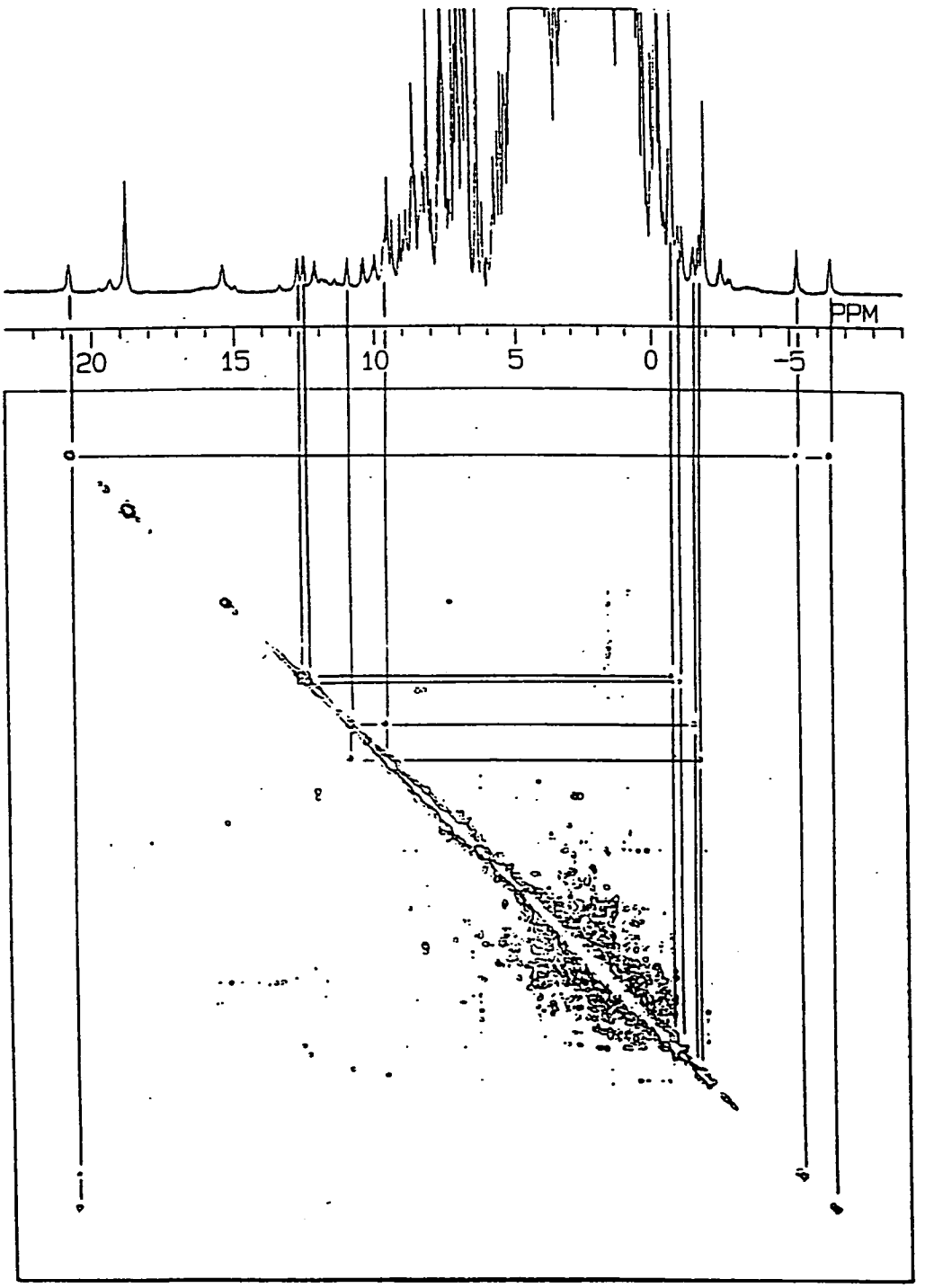

500mM phosphate buffer, pH 7.5, 45°C

The 1D NMR spectrum is shown above the contour plot

FIGURE 3.10 CHARACTERISTIC 1D AND 2D NMR SPLITTING PATTERNS FOR HAEM PROPIONATES AND VINYLS

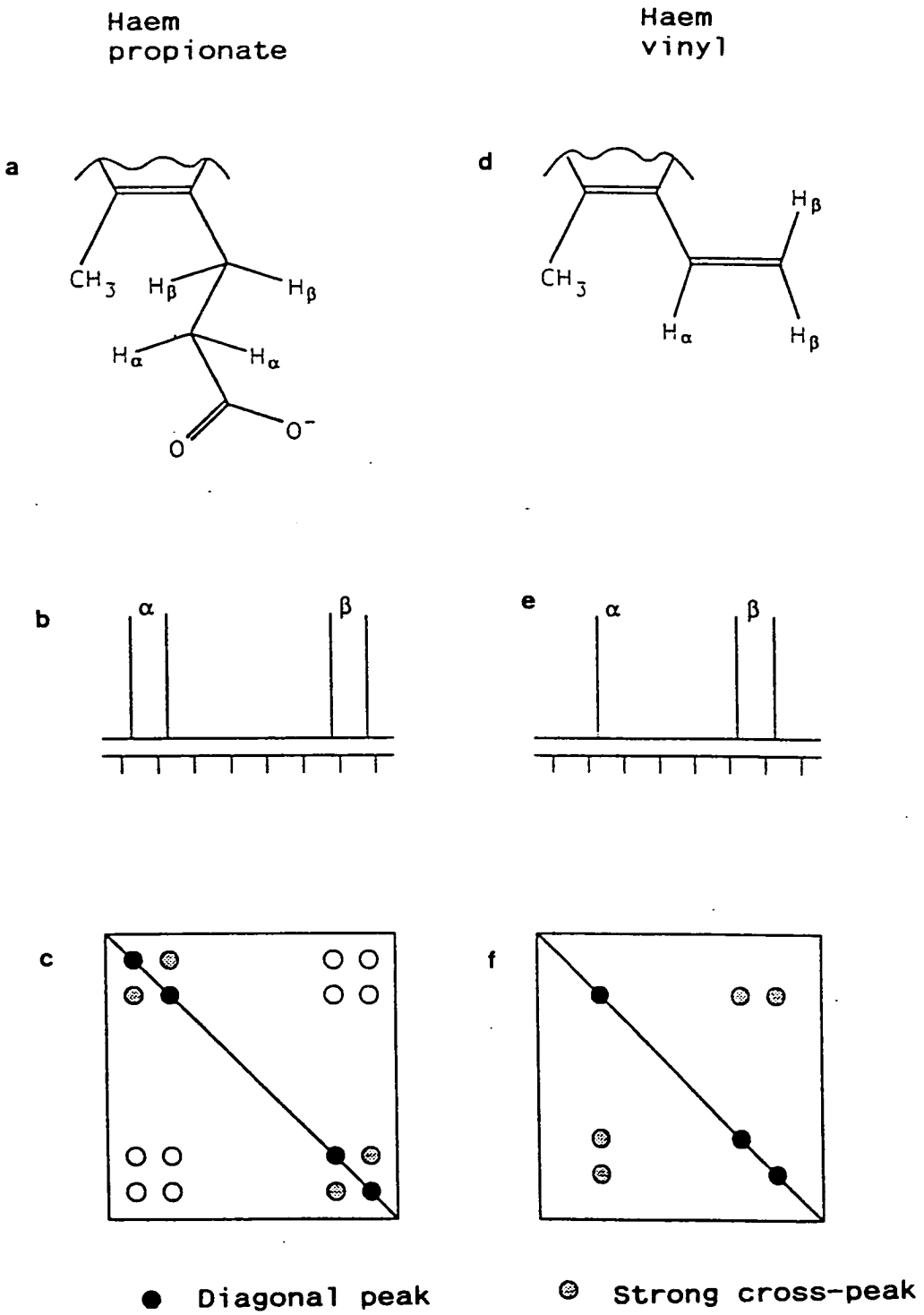

a,d propionate and vinyl groups
b,e 1D NMR splitting patterns
c,f 2D NMR cross-peak patterns

Examination of the 1D NMR spectrum of isolated b_2-haem domain revealed only one such resonance, at approximately 19.4ppm. It was suspected that, although the remaining haem methyls had been shifted by the paramagnetic iron and the porphyrin ring current, they nevertheless remained buried amongst the aromatic resonances in the region immediately below 10ppm.

In an attempt to find those resonances due to hidden haem methyls, the thermal stability of the isolated b_2-haem domain was exploited by recording NMR spectra at a range of temperatures. Paramagnetic centres are sensitive to changes in temperature, and consequently the resonances in the NMR spectrum will also be affected by temperature change. Thus a haem proton resonance which is masked by other resonances may exhibit considerable changes in chemical shift at different temperatures. This property was employed to discover any peaks of 3-proton intensity which were sensitive to temperature variation (Figure 3.11). One resonance of three proton intensity was found to be resolved in both the 45°C and 40°C spectra. By plotting chemical shift against temperature, its position in the 20°C spectrum was found by extrapolation to be 9.5ppm. The intensity of this peak, and its large temperature shift, confirmed its assignment as a haem methyl resonance.

The resonances of the remaining haem methyls were still unapparent. In order to locate them, temperature vs. chemical shift plots were made for a number of peaks in the region 7-11ppm. Two haem methyls at 9.1 and 8.6ppm in the 20°C spectrum were identified by their highly temperature-sensitive shifts. A temperature dependence was also seen for a resonance at 7.7ppm in the 30°C spectrum.

FIGURE 3.11 THE HIGHLY-SHIFTED REGION OF THE NMR SPECTRUM OF OXIDIZED $\underline{b}_2$-HAEM DOMAIN AT TEMPERATURES FROM 20°C TO 45°C

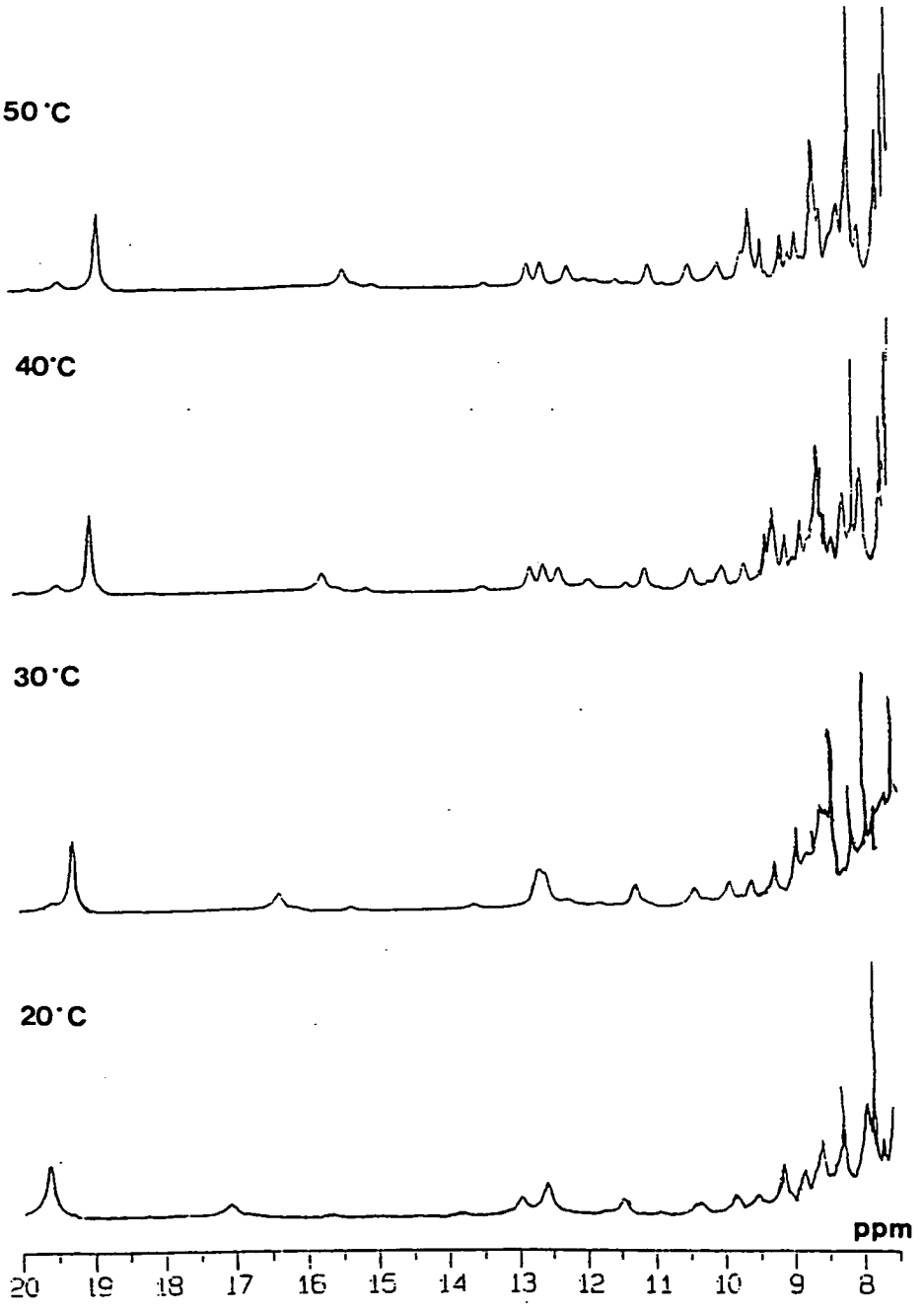

50mM phosphate buffer, pH 7

1D NOE experiments were used to assign the resonances of all the types of protons so far identified to specific groups of protons on the haem. The various different sets of haem proton are labelled in Figure 3.12. On irradiating the resonances of a known haem group, the resonances of neighbouring protons will be affected. This can sometimes be used to identify the specific groups involved. For example, if a methyl resonance is irradiated and effects are seen at the resonances known to be due to vinyl group and a propionate group, the methyl can be identified as methyl 5 as this is the only methyl which could show NOE's to such groups. The Nuclear Overhauser effect can also confirm assignments made from COSY spectra, for example, confirming the assignment of a propionate group by checking for NOE's between α- and β- propionate protons.

In order to resolve the buried methyl peaks sufficiently for unambiguous NOE's to be observed, difference NOE spectra were run at 45°C as well as at 25°C. At 25°C a NOE was observed between the vinyl group (assigned to vinyl 2 by comparison with previously-determined data on cytochrome $\underline{b}_5$ [10]) and the haem methyl resonance at 19.4ppm. This effect means that the methyl group at 19.4ppm is a neighbour of vinyl group 2 and is therefore due to either haem methyl 1 or 3 (Figure 3.12). To differentiate between the two possible assignments the intensities of the NOE's between the methyl and the peaks due to the α- and β- protons of vinyl 2 were examined. A weak NOE was discovered between the vinyl α- proton and the methyl peak in question, while no NOE was observed between one of the vinyl β- protons and the methyl. This is consistent with the methyl being quite distant from the vinyl, confirming that the resonance at 19.4ppm is due to methyl 3.

FIGURE 3.12 PROTOHAEM IX AND AXIAL HISTIDINES, SHOWING HAEM PROTONS

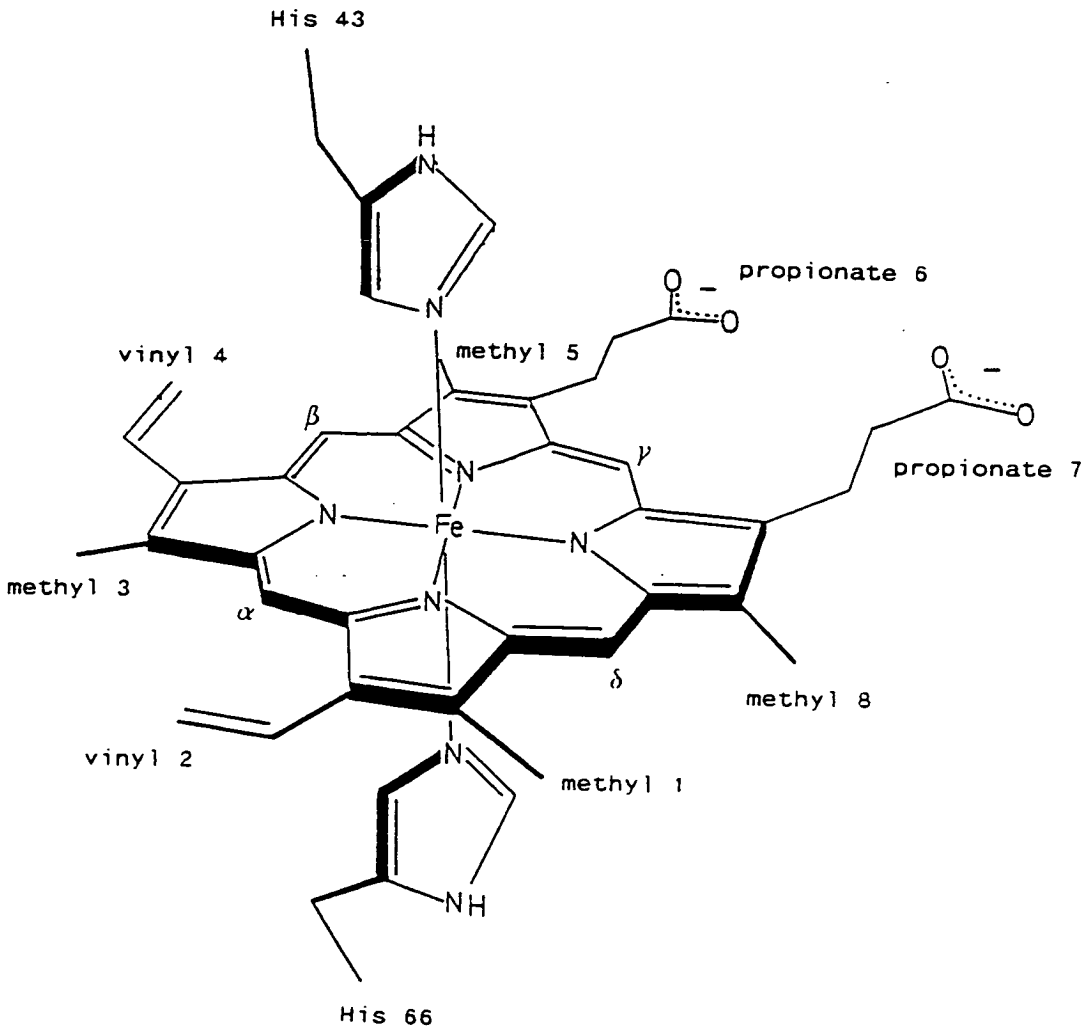

Irradiation of the vinyl also revealed a NOE to a peak at around 6ppm, in the crowded region of the spectrum. Although this peak has an intensity which in inconsistent with that of a methyl group alone, the peak could also reflect the contribution of other protons with the same chemical shift. Thus this peak was tentatively assigned to haem methyl 1.

Other NOE experiments were performed at 45°C in order to resolve some of the overlapping haem resonances. Irradiation at the various propionate resonances and at the resolved haem methyl resonances confirmed the assignments of the buried resonances at 8.3 and 7.5ppm in the 25°C spectrum to be haem methyls 5 and 8, but did not provide sufficient data to assign the individual peaks to their respective methyl sources.

Further assignments were not possible using 1D NOE experiments due to the inability to selectively irradiate buried resonances. Although this problem can be overcome to an extent by running spectra at high temperatures this can be very time-consuming. 2D NOE, or NOESY, is a less time-consuming technique which can be of use in resolving overlapping resonances. A portion of the NOESY spectrum of isolated $\underline{b}_2$-haem domain between 5 and 10ppm is shown in Figure 3.13. This spectrum, as well as showing many NOE's between aromatic groups, reveals a cross-peak between resonances at 8.5ppm (assigned to either methyl 5 or 8 in the 1D NOE experiment) and 6.2ppm (tentatively assigned to methyl 1 in the 1D experiment). The only pair of haem methyl groups capable of showing interaction by NOE's are methyls 1 and 8 (Figure 3.12). Thus the assignment of methyl 1 at 6.2ppm is confirmed and the 8.5ppm resonance is assigned to methyl 8. By deduction, the methyl resonance at 7.5ppm must arise

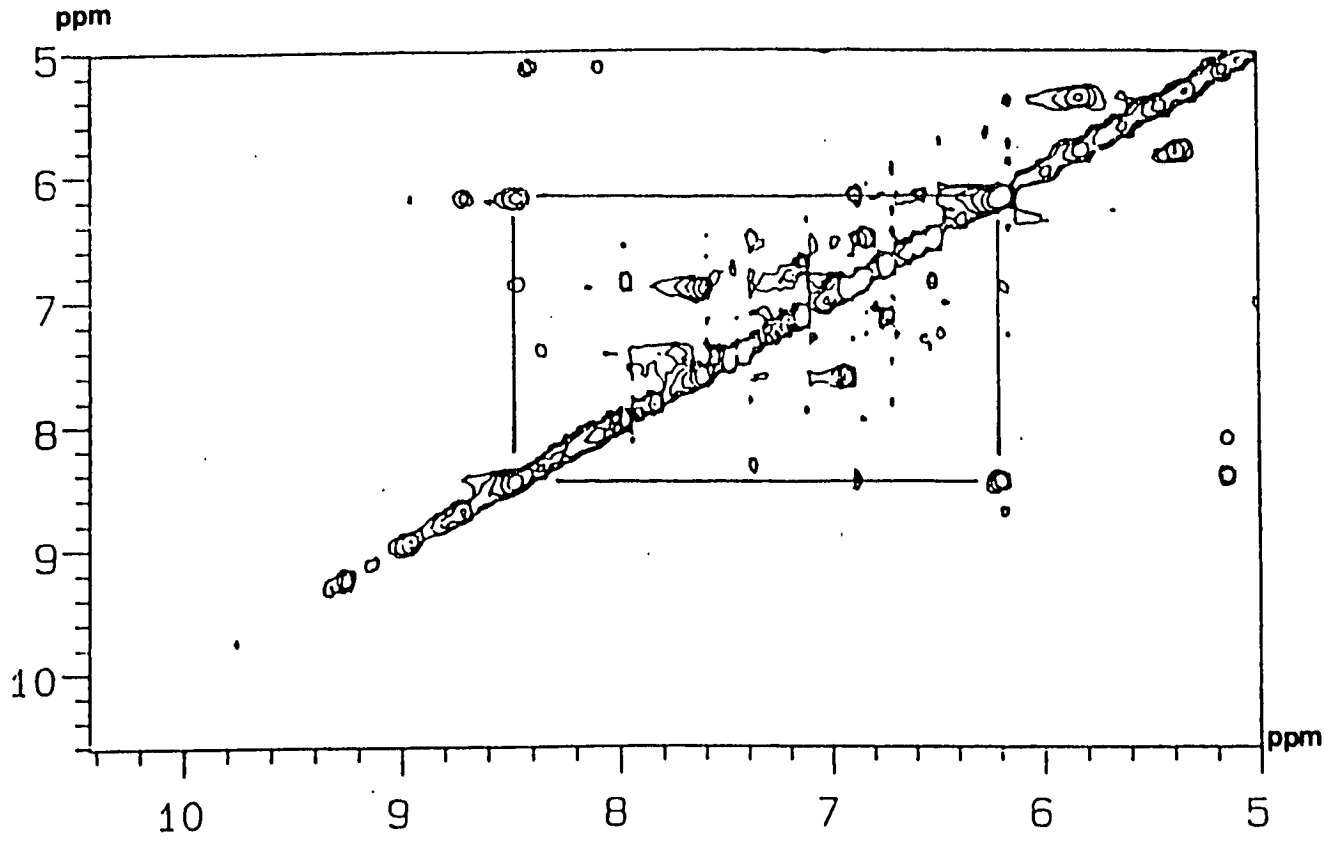

FIGURE 3.13 NOESY SPECTRUM OF $\underline{b}_2$-HAEM DOMAIN BETWEEN 5 AND 10 ppm

50mM phosphate buffer, pH 7, 25°C

from methyl 5..

As all the haem methyl resonances have now been assigned, further studies of NOE interactions between the methyls and the haem propionates also allow the groups of resonances arising from each propionate to be identified.

Having assigned all the groups of protons on the haem (with the exception of one vinyl) there remained the haem meso protons (α, β, γ and δ in Figure 3.12) to assign. These resonances were identified by 1D NOE experiments using the isolated $\underline{b}_2$-haem domain in the reduced form. When reduced, the cytochrome contains low-spin Fe^{2+} and is therefore no longer paramagnetic. As a result, the haem proton resonances are no longer shifted to the extreme regions seen in the oxidized spectrum, but the resonances in the reduced spectrum are much sharper due to the loss of paramagnetic broadening (Figure 3.14). It was postulated that in the reduced spectrum, the meso proton resonances lay in the region 9-10ppm. The assignments were confirmed by 1D NOE experiments observing interactions between the postulated meso resonances and the haem methyls, which were located in the reduced spectrum by observing the shift of the methyl resonances on reduction of the oxidized protein using dithionite. An example of the NOE experiment appears in Figure 3.15.

The assigned resonances are summarised in Table 3.2.

3.4.4 DETERMINATION OF HAEM PROPIONATE pK_A VALUES

In section 3.4.3, two sets of four resonances in the NMR spectrum of isolated $\underline{b}_2$-haem domain were assigned to the haem propionates. The pH stability of the isolated haem domain, which shows no significant change in the electronic absorption spectrum

FIGURE 3.14 1D NMR SPECTRUM OF REDUCED $\underline{b}_2$-HAEM DOMAIN

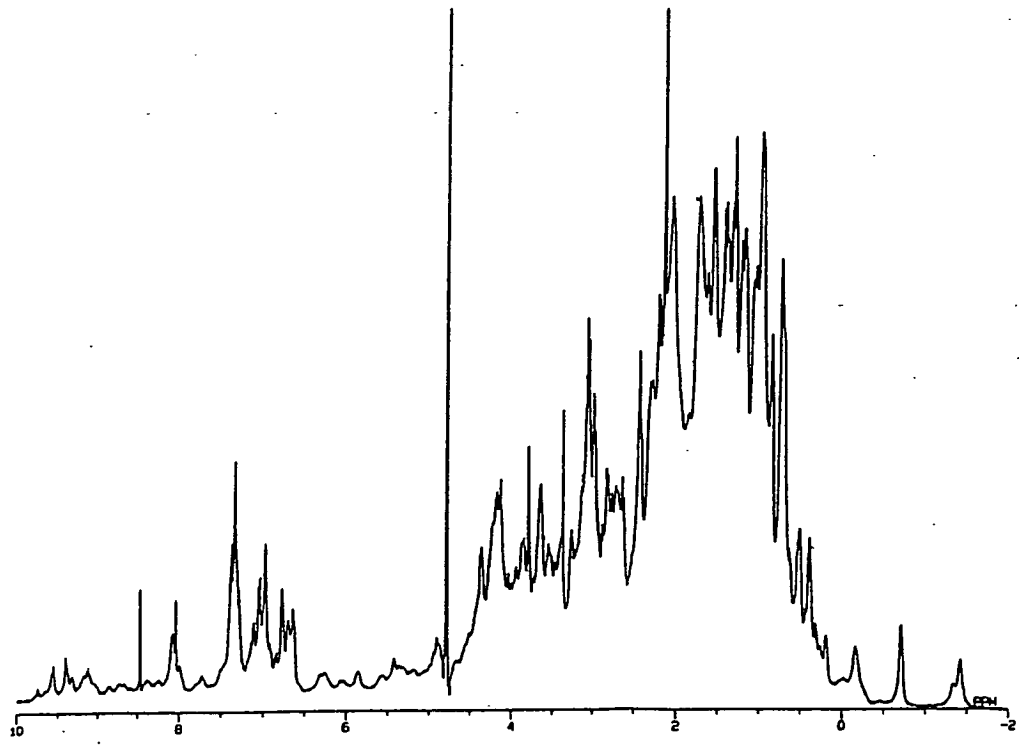

50mM phosphate buffer, pH 7, 25°C

The isolated $\underline{b}_2$-haem domain was reduced by the addition of solid sodium dithionite and was kept under anaerobic conditions by gently passing argon over the surface of the solution before being sealed with a rubber septum.

FIGURE 3.15 USE OF THE NUCLEAR OVERHAUSER EFFECT (NOE) IN ASSIGNING NMR RESONANCES OF HAEM MESO PROTONS

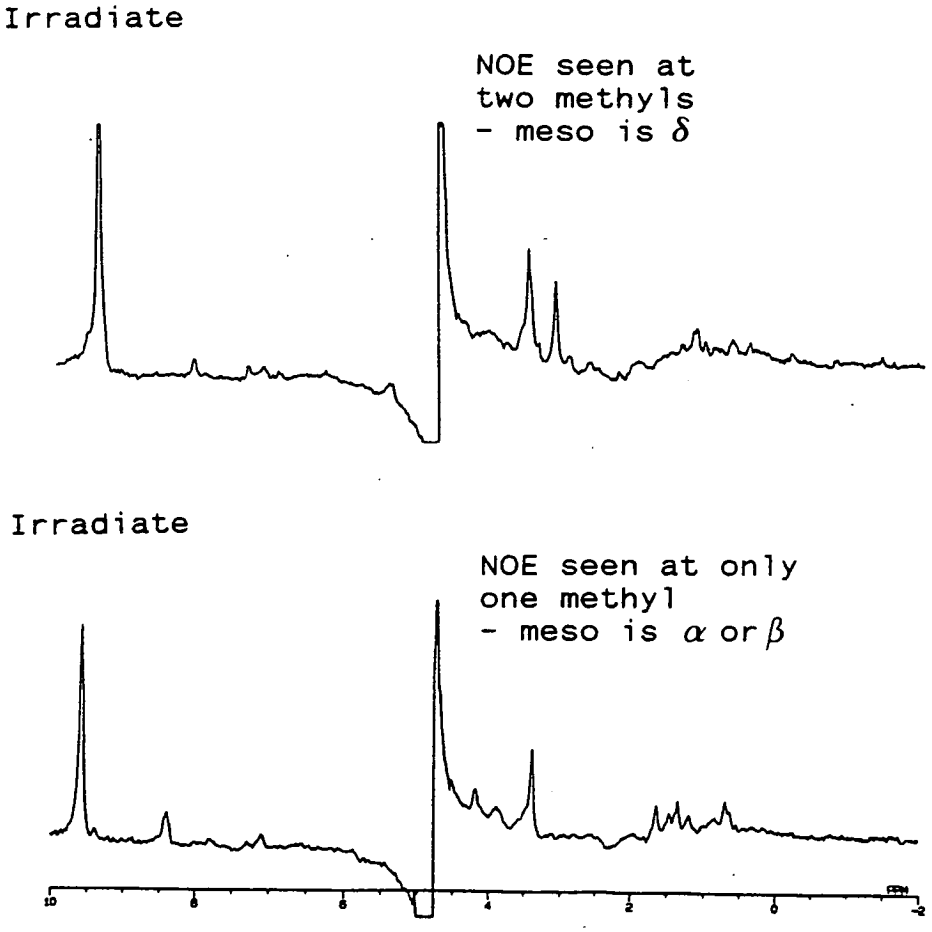

between pH 4.0 and pH 7.0 (Section 3.3.5) made NMR studies at various pH values feasible. This property can be used to determine the pK_A values of the two haem propionate groups using high-field proton NMR.

NMR spectra were recorded at a range of pH's between pH 4 and pH 7. At low pHs the propionates become protonated, causing their resonances to shift. The assigned propionate resonances can be tracked as they move with decreasing pH (Figure 3.16). Although some new peaks appear in the spectrum, the major peaks remain largely unaltered even at the lower pH values, suggesting that the protein remains overall in its native state during the titration.

Plots of chemical shift vs. pH for the resonances tracked are sigmoidal in shape (Figure 3.17) which is typical of a proton undergoing ionisation. This confirms tha assignment of these resonances as arising from the haem propionates. The pK_A of the propionate in question can be determined from a Hill plot (Figure 3.18).

The Hill plots for both propionates are linear with a slope of approximately 1, consistent with a single ionisation. The pK_A is given by the intercept with the x-axis and is found to be 4.80 for the resonance of the α-proton of haem propionate 7 and 4.56 for the resonance of the α- proton of haem propionate 6. These values are both close to the observed values for the propionates of free porphyrin c in water, which both have pK_As of 5.6 [19]. This suggests that the propionates of the isolated b_2-haem domain are exposed to solvent and not buried within the protein. In the X-ray crystal structure of flavocytochrome b_2 the haem propionates point directly into the flavin-binding domain [22]. Therefore the isolated b_2-haem domain would indeed by expected to have exposed propionate groups, as shown in Figure 3.19.

FIGURE 3.16 NMR pH TITRATION OF $\underline{b}_2$-HAEM DOMAIN

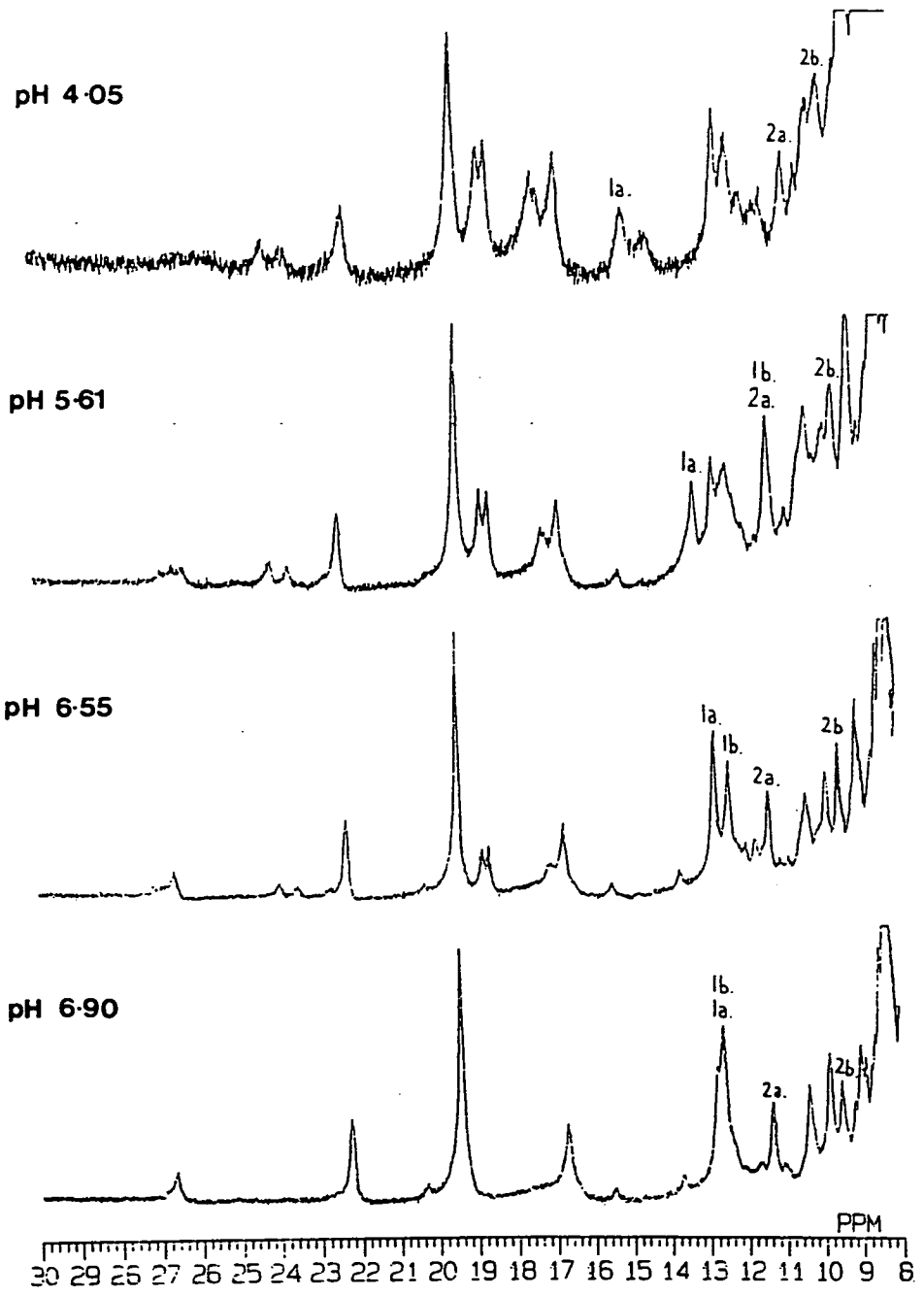

5mM phosphate buffer, 25°C

1a, 1b, 2a & 2b are the resonances of the haem propionate α-protons

FIGURE 3.17 CHEMICAL SHIFT VS pH PLOTS FOR NMR RESONANCES OF THE HAEM PROPIONATES OF b_2-HAEM DOMAIN

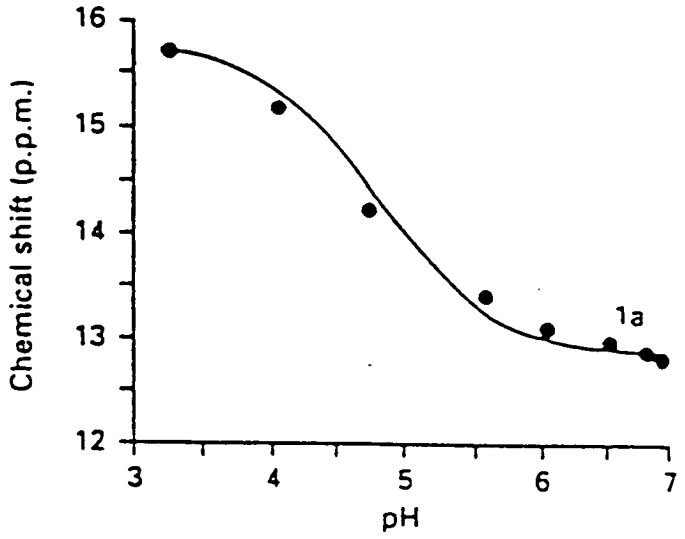

(a) pH titration of resonance 1a in Figure 3.16

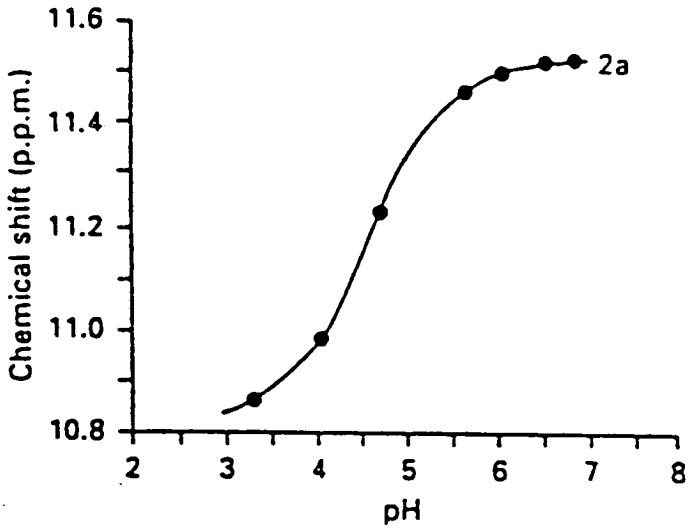

(b) pH titration of resonance 2a in Figure 3.16

FIGURE 3.18 DETERMINATION OF HAEM PROPIONATE pK_A VALUES (HILL PLOT)

Hill plots are shown for the pH titration of resonances 1a and 2a in Figure 3.16

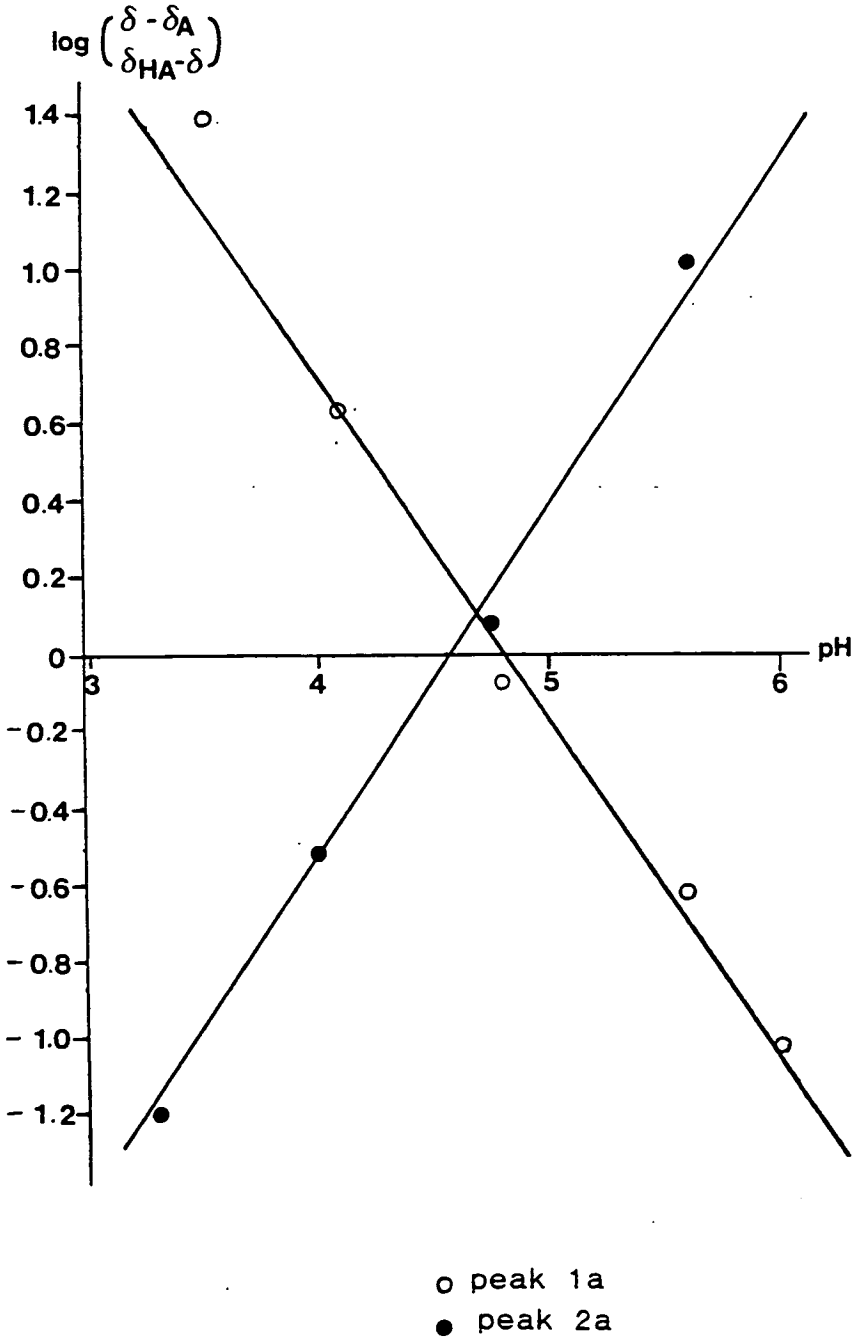

FIGURE 3.19 COMPARISON OF THE CRYSTAL STRUCTURES OF THE HAEM DOMAINS OF FLAVOCYTOCHROME b_2 AND CYTOCHROME b_5 [22]

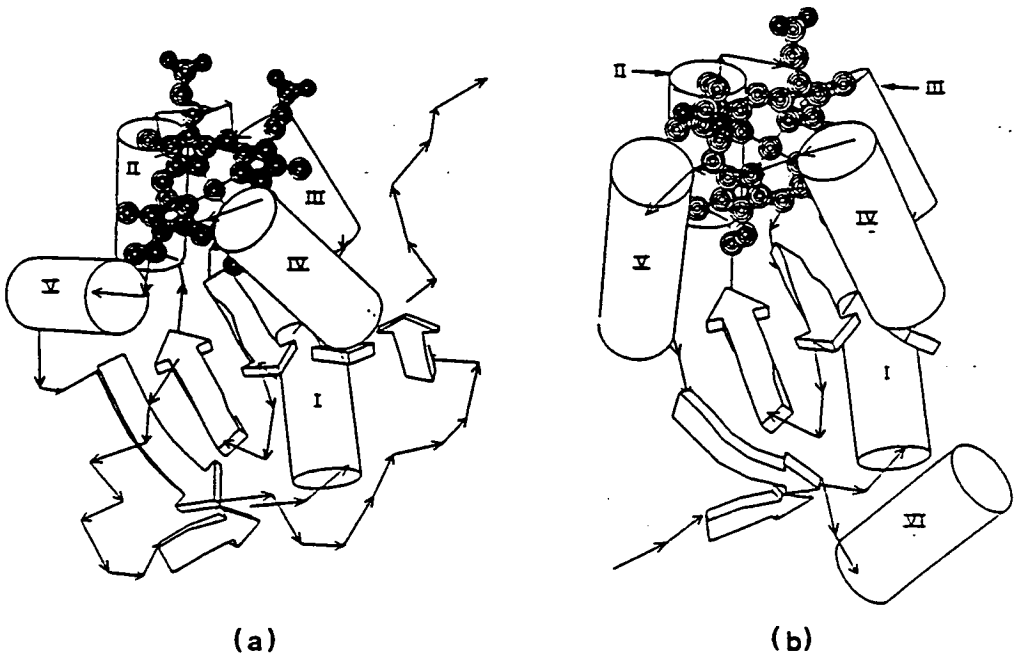

(a) flavocytochrome b_2

(b) cytochrome b_5

Cylinders I-VI represent α-helices.
Broad arrows represent β-sheets.

3.4.5 ELECTRON SELF-EXCHANGE RATE CONSTANTS

Electron self-exchange rate constants are the rate constants observed for electron exchange between two identical molecules, giving a measure of their efficiency at electron transfer. The self-exchange rate constants for two different molecules can then be used to calculate the theoretical rate constant for the cross-reaction between them (Figure 3.20).

High-field NMR experiments were used to determine the electron self-exchange rate constant for the isolated $\underline{b}_2$-haem domain. The fully-oxidized cytochrome was reduced by titrating with sodium dithionite. NMR spectra were recorded after each addition, in order to achieve a spectrum at the half-way point of the reduction, with 50% of the cytochrome in the oxidized state and 50% in the reduced state (Figure 3.21). The self-exchange rate constant was then calculated from the 50% oxidized : 50% reduced spectrum using the equation shown in Figure 3.21.

By this method the electron self-exchange rate constant for the isolated $\underline{b}_2$-haem domain at relatively low ionic strength (5mM - phosphate) was found to be 2.3×10^6 M^{-1} s^{-1} (25°C, pH 7.4). This value is compared with the self-exchange rate constants of other cytochromes in Table 3.3.

The electron self-exchange rate constant for the isolated $\underline{b}_2$-haem domain is around 600 times larger than that observed for cytochrome $\underline{b}_5$ under similar conditions. This vast difference between the inherent electron-transfer properties of the two proteins may arise from the difference in their overall charges. Although cytochrome $\underline{b}_5$ and isolated $\underline{b}_2$-haem domain have a high degree of sequence similarity with a number of invariant amino-acid

FIGURE 3.20 USE OF ELECTRON SELF-EXCHANGE RATE CONSTANTS TO PREDICT RATE CONSTANTS

For a group of reactions of molecules 1 & 2:

$$Ox_1 + Red_1 \longrightarrow Red_1 + Ox_1 \qquad (k_{11})$$

$$Ox_2 + Red_2 \longrightarrow Red_2 + Ox_2 \qquad (k_{22})$$

$$Ox_1 + Red_2 \longrightarrow Red_1 + Ox_2 \qquad (k_{12})$$

$$k_{12} = (k_{11} k_{22} K_{12} f)^{1/2}$$

where k_{11} = electron self-exchange rate constant for molecule 1
k_{22} = electron self-exchange rate constant for molecule 2
k_{12} = rate constant for the cross-reaction
K_{12} = equilibrium constant for the cross-reaction
f = factor relating the above values to the frquency of collision of the reactants (significant only when K_{12} is large)

Example:

cyt $\underline{b}_{2(ox)}$ + cyt $\underline{b}_{2(red)} \longrightarrow$ cyt $\underline{b}_{2(red)}$ + cyt $\underline{b}_{2(ox)}$

$E_m = -31$ mV, $k_{11} = 2.3 \times 10^6$ $M^{-1}s^{-1}$

cyt $\underline{c}_{(ox)}$ + cyt $\underline{c}_{(red)}$ cyt $\underline{c}_{(red)}$ + cyt $\underline{c}_{(ox)}$

$E_m = 260$ mV, $k_{22} = 10^3$ $M^{-1}s^{-1}$

cyt $\underline{b}_{2(ox)}$ + cyt $\underline{c}_{(red)}$ cyt $\underline{b}_{2(red)}$ + cyt $\underline{c}_{(ox)}$

$k_{12} = ?$

Using $k_{12} = (k_{11} k_{22} K_{12} f)^{1/2}$

and taking logs

$\log k_{12} = 1/2(\log k_{11} + \log k_{22} + \log K_{12} + \log f)$

K_{12} can be calculated from $\Delta E_o = -RT \log K$, and f can be disregarded, giving

$$k_{12} = 1.40 \times 10^7 \ M^{-1}s^{-1}$$

FIGURE 3.21 NMR OXIDATION-REDUCTION TITRATION OF $\underline{b}_2$-HAEM DOMAIN

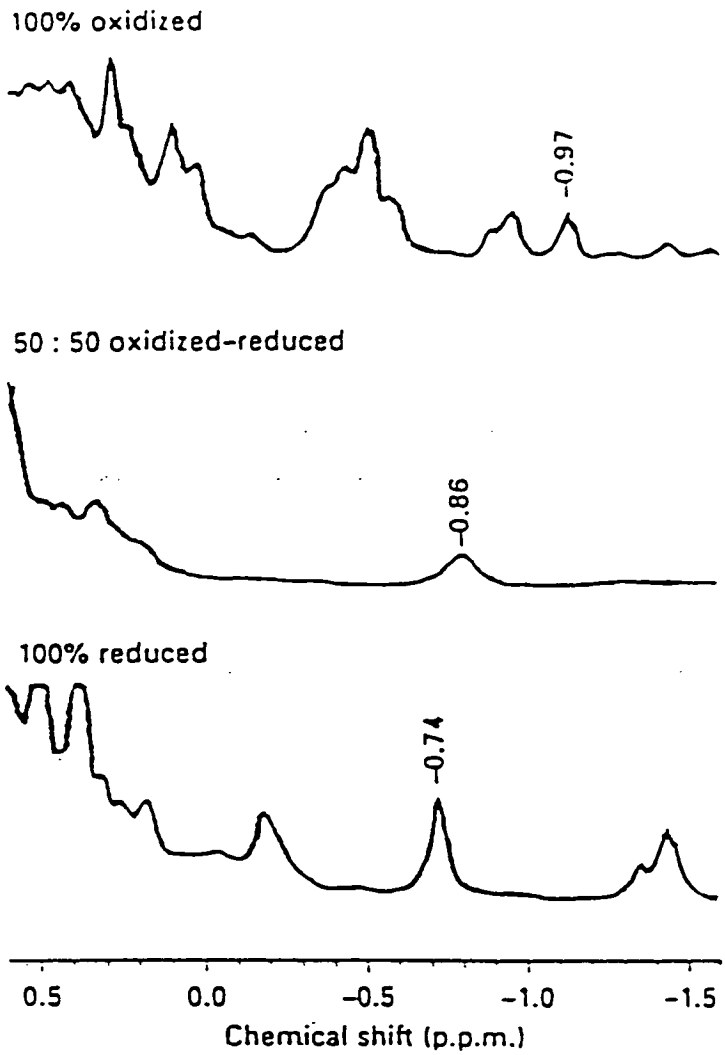

A solution of oxidized $\underline{b}_2$-haem domain in 5mM-phosphate buffer, pH 7, was reduced by titrating with a solution of $Na_2S_2O_4$ (3% w/v) in ^2H_2O. The electron self-exchange rate constant was calculated using the equation

$$\Delta\upsilon_{\frac{1}{2}}^{e} = \frac{2\pi(\upsilon_A - \upsilon_B)}{k_e}$$

where υ_A = chemical shift in the oxidized spectrum
υ_B = chemical shift in the reduced spectrum
$\Delta\upsilon_{\frac{1}{2}}^{e}$ = excess linewidth at half-height in the 50:50 oxidized-reduced spectrum
k_e = first-order electron self-exchange rate constant

TABLE 3.3: SELF-EXCHANGE RATES OF SOME CYTOCHROMES

Cytochrome	k_{11} (M^{-1} s^{-1})	Conditions	Ref.
Cytochrome *c* (horse)	10^3 -10^4	25°C, ph7 I = 0.1M	26
Cytochrome *c* (*C.krusei*)	10^2	25°C, ph7 I = 0.1M	26
Isolated b_2-haem domain	2.3×10^6	25°C, pH7.4 I = 0.005M	29
Cytochrome b_5	4.6×10^{-3}	25°C, 0.3M	19

residues, cytochrome $\underline{b}_5$ has an overall charge of around -8 whereas the isolated $\underline{b}_2$-haem domain has an overall charge close to zero. This means that a larger coulombic barrier has to be overcome for electron transfer to take place between two molecules of cytochrome $\underline{b}_5$ than for two molecules of the isolated $\underline{b}_2$-haem domain. This effect would result in a slower electron self-exchange rate in cytochrome $\underline{b}_5$ than in the isolated $\underline{b}_2$-haem domain, as reflected in the measured rate constants.

3.4.6 PROTEIN-PROTEIN INTERACTIONS

Cytochrome $\underline{c}$, the physiological electron acceptor of flavocytochrome $\underline{b}_2$, is known to accept electrons via the haem domain [23] but the actual binding site for cytochrome $\underline{c}$ on flavocytochrome $\underline{b}_2$ remains unknown. NMR studies were used to investigate the binding of cytochrome $\underline{c}$ to both the isolated $\underline{b}_2$-haem domain and the intact holoenzyme.

Spectra (a) and (b) in Figure 3.22 show the highly-shifted region of the 1D NMR spectra of cytochrome $\underline{c}$ and isolated $\underline{b}_2$-haem domain respectively. Each of these cytochromes has a very characteristic pattern of sharp NMR resonances in this region. Figure 3.22(c) shows the same region of the spectrum of a 1:1 mixture of cytochrome $\underline{c}$ and isolated $\underline{b}_2$-haem domain, and Figure 3.22 (d) shows the composite spectrum achieved by adding spectrum (a) to spectrum (b). It can be seen almost at a glance that the chemical shifts of the resonances in spectrum (c) (the 1:1 mixture of cytochrome $\underline{c}$ and isolated $\underline{b}_2$-haem domain) are identical to those in spectrum (d) (the addition of the spectra of the individual proteins). Had cytochrome $\underline{c}$ formed a complex with the $\underline{b}_2$-haem

FIGURE 3.22 NMR STUDY OF THE INTERACTION OF $\underline{b}_2$-HAEM DOMAIN AND CYTOCHROME $\underline{c}$

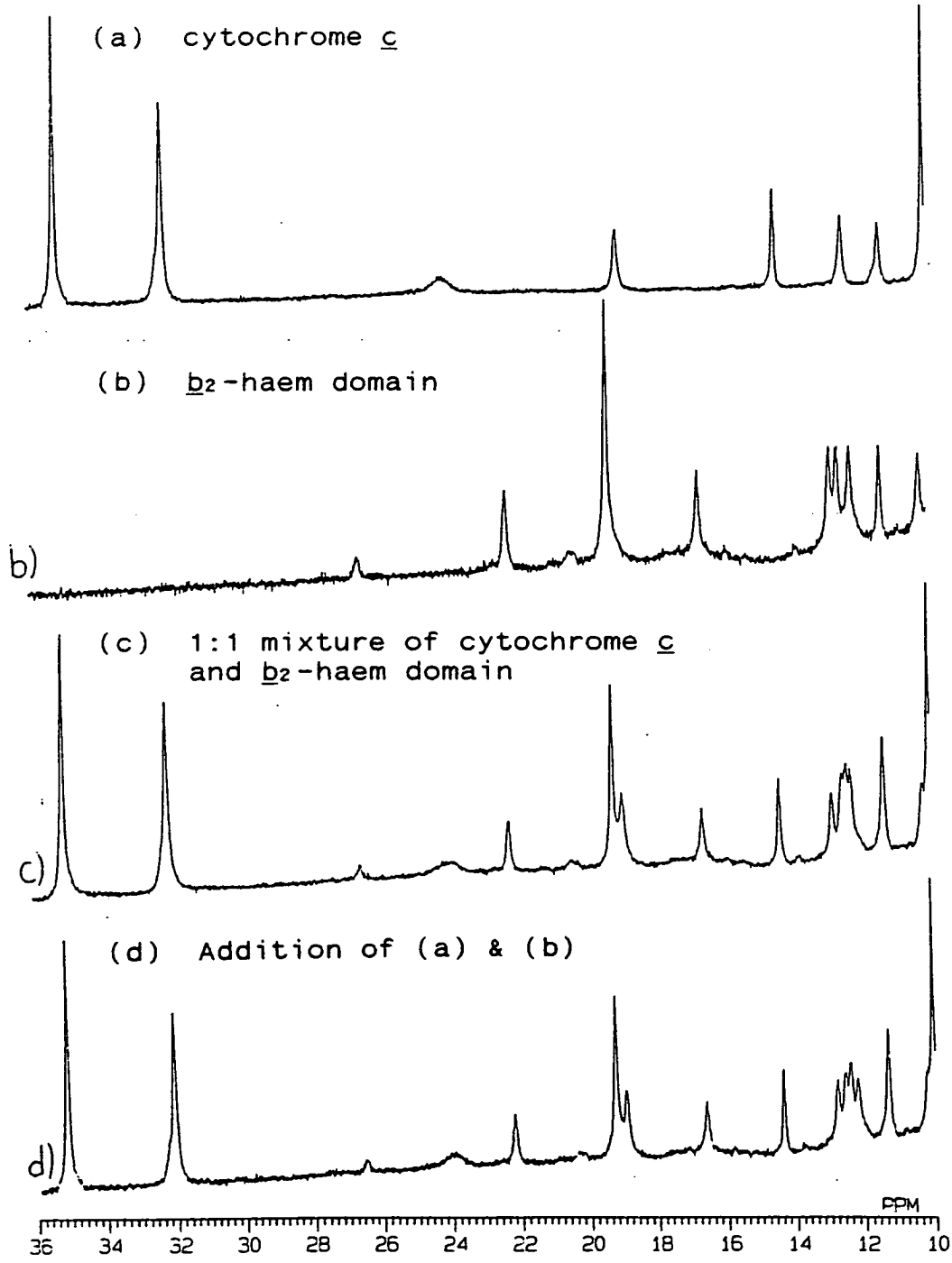

All solutions are in 20mM phosphate buffer, pH 7, 25°C

domain, the resonances of the mixture might be expected to be shifted, and should certainly be broadened, producing a spectrum which would therefore have been appreciably different to spectrum (d). As it is, the similarity of spectra (c) and (d) indicate that cytochrome *c* does not form a complex with the isolated haem domain of flavocytochrome b_2 under these conditions.

Flavocytochrome b_2, the intact, tetrameric enzyme of which b_2-haem domain is only a part, has a molecular weight of around 230 000. While this is normally too large to allow a protein to be studied by NMR [14], the presence of the paramagnetic haem in the oxidized enzyme causes shifting of the haem resonances, enabling them to be resolved. Resolution of the haem proton resonances is further enhanced by the mobility of the haem domain within the holoenzyme [16], resulting in more efficient relaxation of the resonances of the haem domain relative to the rest of the protein.

The highly-shifted regions of the 1D NMR spectra of holo-flavocytochrome b_2 and the isolated b_2-haem domain are shown in Figure 3.23. Although the shifted haem resonances of the holoenzyme are very broad owing to the size of the protein, they can be clearly seen, and lie at similar chemical shifts to the haem protons of the isolated b_2-haem domain.

A similar interaction study to that carried out on cytochrome *c* and isolated b_2-haem domain was performed using cytochrome *c* and holo-flavocytochrome b_2. The results are shown in Figure 3.24. Spectrum (a) is the shifted region of the cytochrome *c* 1D NMR spectrum. Spectrum (b) shows the similar region of the spectrum of holo-flavocytochrome b_2. The spectrum of a 1:1 mixture of cytochrome *c* and holo-flavocytochrome b_2 is shown in (c), contrasted

FIGURE 3.23 COMPARISON OF THE HIGHLY-SHIFTED REGIONS OF THE NMR SPECTRA OF FLAVOCYTOCHROME $\underline{b}_2$ AND $\underline{b}_2$-HAEM DOMAIN

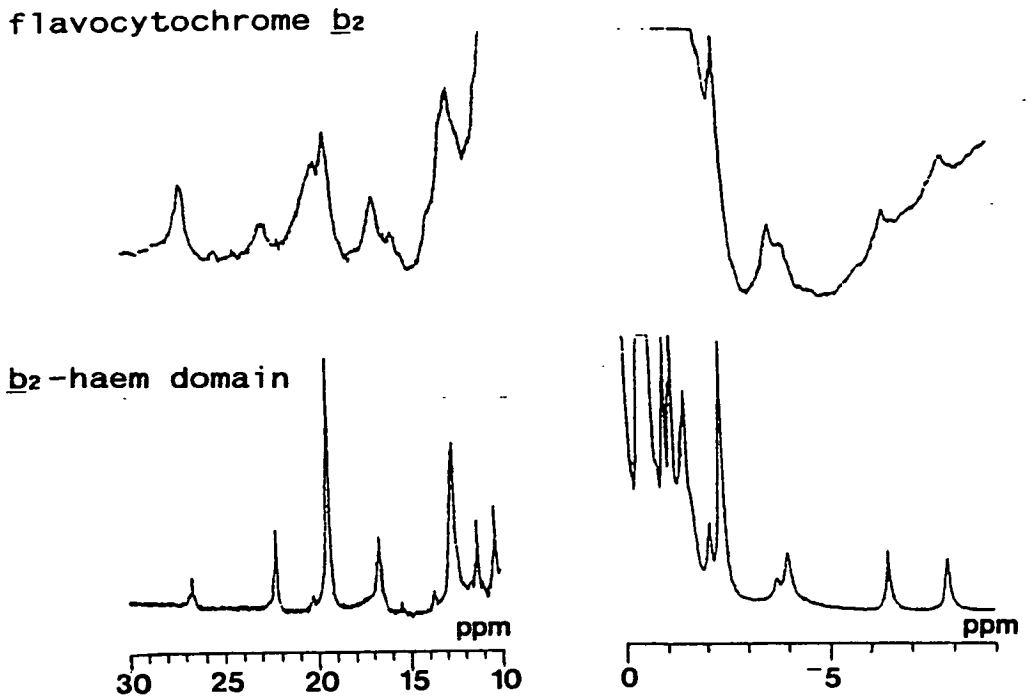

Both spectra are recorded in 5mM phosphate buffer, pH 7, 25°C

with the composite spectrum of the two individual proteins (d). Although spectrum (c) is noisy, it is immediately obvious that it is not superimposable on spectrum (d). Many of the peaks in the spectrum of the mixture are considerably broadened compared to the peaks in the addition spectrum, especially the cytochrome c resonances at approximately 32 and 35ppm. These resonances, while sharp and intense in the addition spectrum, are so broadened in the spectrum of the mixture as to be almost non-existant. The broadening and shifting of resonances on the mixing of these two proteins confirm that a complex is being formed between them.

NMR studies of the interaction of cytochrome c with isolated b_2-haem domain and tetrameric holo-flavocytochrome b_2 showed that, while cytochrome c binds to the holoenzyme, it does not form a complex with the isolated b_2-haem domain. This observation raises the question of the location of the binding site of the physiological electron acceptor, cytochrome c, on flavocytochrome b_2. It is known that haem is essential for electron transfer to cytochrome c [4,5] and that electrons proceed to the physiological electron acceptor via the haem domain [23]. It would therefore appear to be necessary for the electron acceptor to bind fairly close to the haem. However, these NMR studies have shown that cytochrome c does not bind to the monomeric isolated b_2-haem domain even though it complexes with the tetrameric holoenzyme. This suggests that the cytochrome c binding site is not located exclusively on the haem domain. It must, at least partially, lie on the flavin domain, and may involve more than one subunit of the holoenzyme.

The nature of the cytochrome c binding site on flavocytochrome b_2 has long been a puzzle to researchers. A model for cytochrome c

FIGURE 3.24 NMR STUDY OF THE INTERACTION OF FLAVOCYTOCHROME $\underline{b}_2$ AND CYTOCHROME $\underline{c}$

All solutions are in 20mM phosphate buffer, pH 7, 25°C

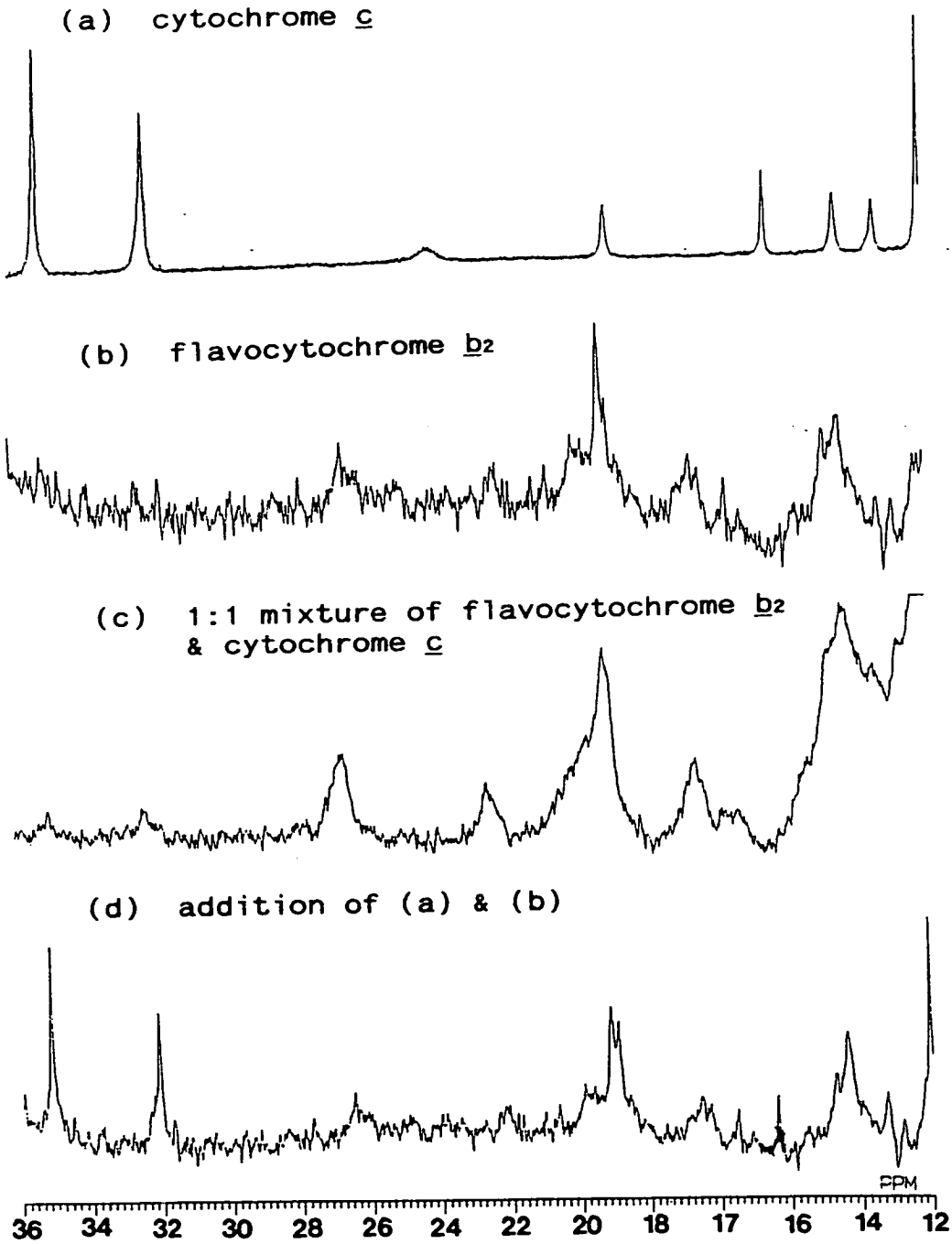

binding to cytochrome $\underline{b}_5$ [24] led to suggestions that a similar model might also describe cytochrome $\underline{c}$ binding to the haem domain of flavocytochrome $\underline{b}_2$, in the light of the evolutionary relationship between cytochrome $\underline{b}_5$ and the $\underline{b}_2$-haem domain [25]. This model shows positively-charged residues on cytochrome $\underline{c}$ interacting with the negatively-charged residues on cytochrome $\underline{b}_5$ in such a way that the edges of the haems in both molecules are brought together (Figure 3.25). This model is inappropriate for flavocytochrome $\underline{b}_2$ for two main reasons. Firstly, the area of the $\underline{b}_2$-haem domain corresponding to the cytochrome $\underline{c}$-binding region of cytochrome $\underline{b}_5$ in the model does not contain the negatively-charged residues essential for cytochrome $\underline{c}$ interaction. In fact, the only negative charges in this region of the $\underline{b}_2$-haem domain are the haem propionates [25]. Secondly, the face of the haem domain at which cytochrome $\underline{c}$ is hypothesised to bind is in fact obscured by the flavin domain in the tetrameric holo-flavocytochrome $\underline{b}_2$ molecule [22].

These observations, coupled with studies of cytochrome $\underline{c}$ binding to the haem domain of flavocytochrome $\underline{b}_2$ from *H.anomala* [26-28] bear out the findings from the NMR studies that cytochrome $\underline{c}$ is unable to bind to the haem domain alone and that binding must also involve interactions with the flavin domain. Molecular modelling studies [29] have located some regions of negative charge on the flavin domain, proteolytically-sensitive loop and the C-terminal tail which lie close enough in the crystal structure of flavocytochrome $\underline{b}_2$ to form a possible binding site for cytochrome $\underline{c}$. If these regions do indeed constitute the binding site, cytochrome $\underline{c}$ would be held in an orientation which would enable electron transfer between the haem of flavocytochrome $\underline{b}_2$ and the haem of cytochrome $\underline{c}$,

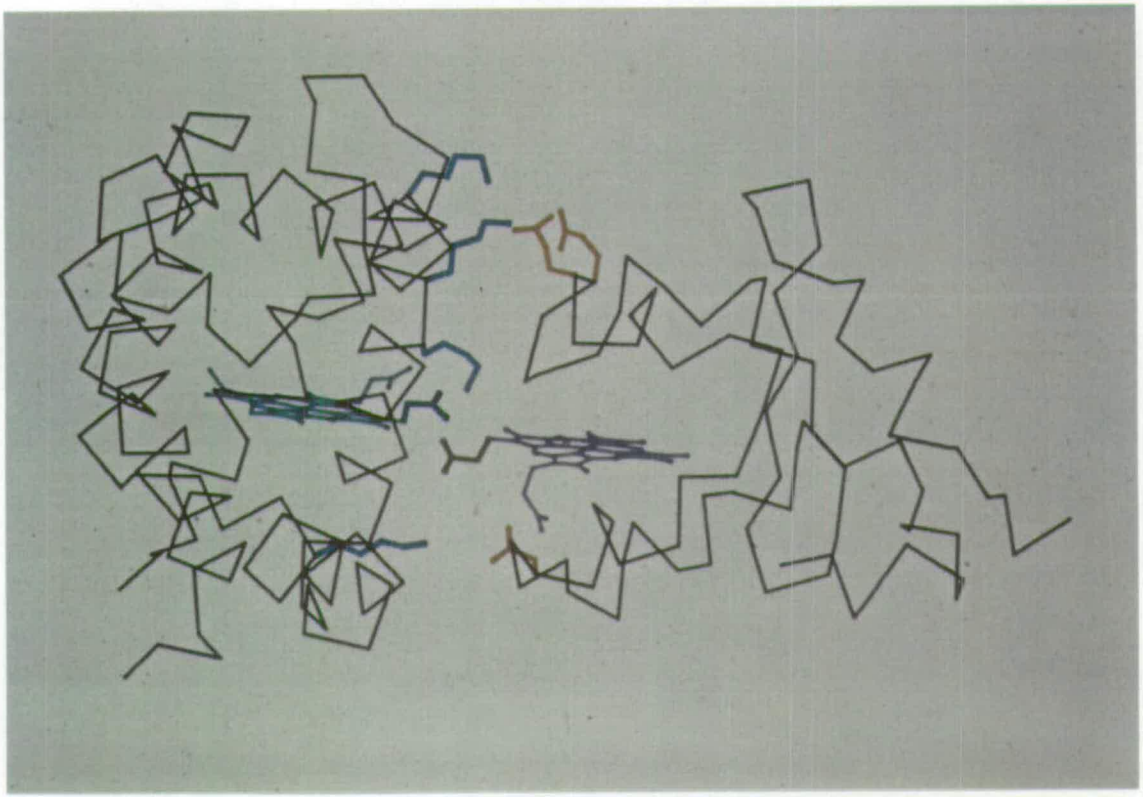

FIGURE 3.25 MODEL OF INTERACTIONS BETWEEN CYTOCHROME c AND CYTOCHROME b_5 BASED ON SALEMME'S MODEL [24]

This model shows positively-charged residues on cytochrome c (blue) interacting with negatively-charged residues on cytochrome b_5 (red).

in a manner which would be consistent with the observations from NMR studies.

3.5 NMR SPECTRUM OF ISOLATED $\underline{b}_2$-HAEM DOMAIN: FURTHER DISCUSSION

Prior to this work the only NMR studies of flavocytochrome $\underline{b}_2$ had been performed at relatively low magnetic fields (up to 400 MHz), mainly using cytochrome $\underline{b}_2$ core isolated from the holoenzyme by proteolysis [15,16]. These studies had discovered that the haem domain displayed a high degree of mobility relative to the rest of the holoenzyme [16] and also found some similarities between the NMR spectra of cytochrome $\underline{b}_2$ core and cytochrome $\underline{b}_5$ [15]. Some studies had also been carried out on cytochrome $\underline{c}$ binding [26-28]. However, all these early experiments were hampered by the lack of highly-purified, concentrated protein, and the relatively low magnetic field strengths then available. With the advent of more powerful NMR spectrometers and the expression of flavocytochrome $\underline{b}_2$ and $\underline{b}_2$-haem domain in *E.coli* [30,31] it has been possible to carry out more detailed NMR studies on flavocytochrome $\underline{b}_2$.

The haem proton resonance assignments of the isolated $\underline{b}_2$-haem domain are listed in Table 3.2. However, when the 1D NMR spectrum is studied (Figure 3.8) it can be seen that a number of highly-shifted haem peaks remain unassigned. Some of these resonances have been attributed to the axial histidine ligands coordinating the porphyrin [32].

The only group of haem protons to remain unassigned in the NMR spectrum of $\underline{b}_2$-haem domain is vinyl group 4 (Figure 3.12). It is probable that the resonances of this group of protons are obscured by the resonances of amino-acid side-chains in the crowded region of

the spectrum, from 0-9ppm. As the resonances of the vinyl 4 protons are not shifted to the high and low field regions they are difficult to locate by COSY experiments, because many of the amino acid resonances which occur in the same area have similar splitting patterns.

3.5.1 COMPARISON OF $\underline{b}_2$-HAEM DOMAIN WITH CYTOCHROME $\underline{b}_5$

As previously stated (Section 1.7.1) the haem domain of flavocytochrome $\underline{b}_2$ had long been considered to be a possible member of the cytochrome $\underline{b}_5$ superfamily [33,34] and some comparisons had been made between the NMR spectra of cytochrome $\underline{b}_5$ and proteolytically-produced cytochrome $\underline{b}_2$ core which seemed to confirm this [15]. The more detailed NMR studies of isolated $\underline{b}_2$-haem domain can now be compared with the NMR spectrum of cytochrome $\underline{b}_5$ [10,11,13], in the light of the solved crystal structures of cytochrome $\underline{b}_5$ [35] and intact holo-flavocytochrome $\underline{b}_2$ [22,36].

The 1D NMR spectra of the isolated $\underline{b}_2$-haem domain and cytochrome $\underline{b}_5$ are compared in Figure 3.26. The two spectra share many similar resonances, most notably the resonances of haem vinyl 2 and haem propionate 6. One of the resonances of propionate 7 does, however, differ for the two cytochromes. In the cytochrome $\underline{b}_5$ spectrum, one of the α- protons of haem propionate 7 occurs at -1.8ppm, whereas both the α- proton resonances of propionate 7 occur between 12 and 13ppm in the $\underline{b}_2$-haem domain NMR spectrum. This implies a difference between the propionate environment of the two cytochromes which is further borne out by the pK_A values determined for the two propionates of the $\underline{b}_2$-haem domain. For the isolated $\underline{b}_2$-haem domain the two propionates have pK_A values close to that of

FIGURE 3.26 COMPARISON OF THE NMR SPECTRA OF OXIDIZED CYTOCHROME $\underline{b}_5$ AND $\underline{b}_2$-HAEM DOMAIN

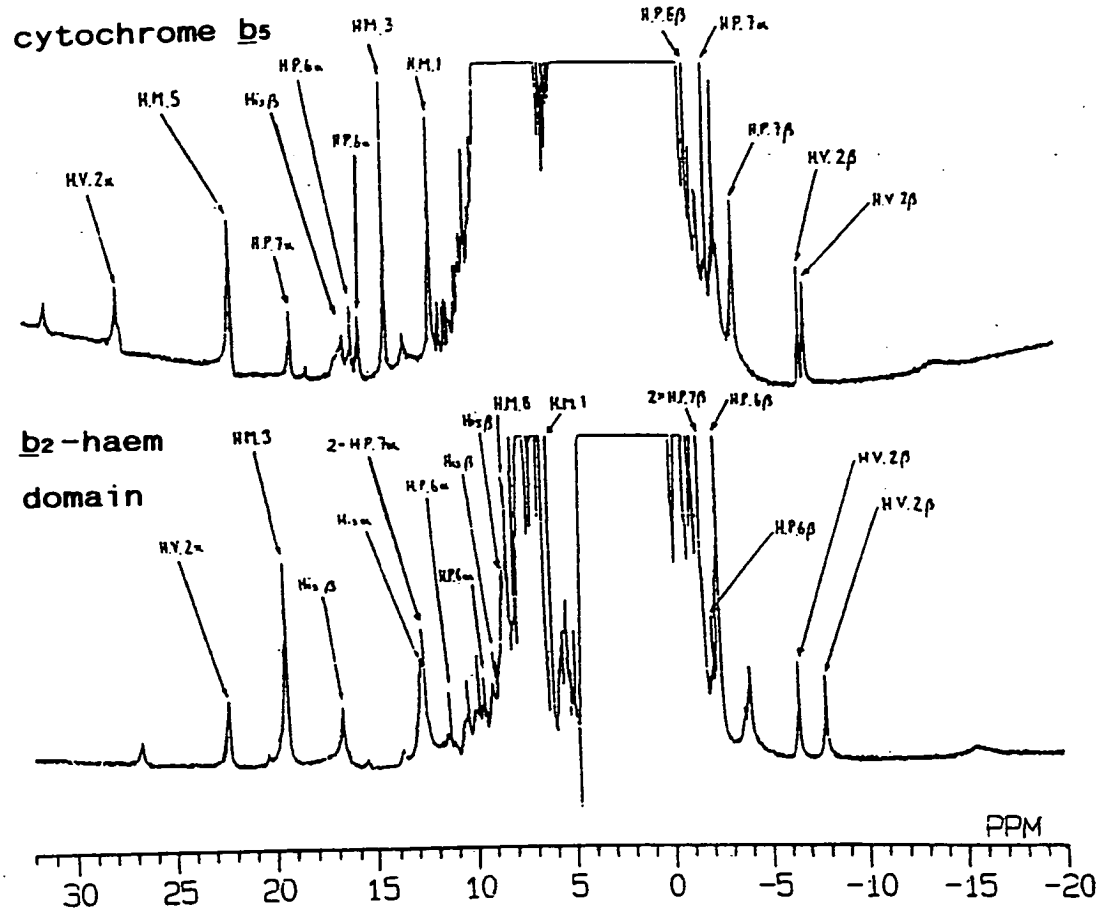

H.V.: haem vinyl
H.M.: haem methyl
H.P.: haem propionate
His : axially-coordinating histidine ligand

free haem propionates (Section 3.4.4) indicating that the $\underline{b}_2$-haem domain propionates are exposed to solvent and not buried within the protein. In the X-ray crystal structure of flavocytochrome $\underline{b}_2$, the haem propionates extend away from the haem domain, pointing directly into the flavin-binding domain [22], whereas in cytochrome $\underline{b}_5$, the X-ray crystal structure reveals only one exposed propionate [35], the other being folded back into the protein, as shown in Figure 3.19.

3.6 REFERENCES

[1] Labeyrie, F., Groudinsky, O., Jacquot-Armand, Y. & Naslin, L., Biochim. Biophys. Acta **128**, 492-503 (1966)

[2] Chapman, S.K., White, S.A. & Reid, G.A., Adv. Inorg. Chem. **36**, 257-301 (1991)

[3] Guiard, B. & Lederer, F., Biochimie **58**, 305-316 (1966)

[4] Forestier, J.P. & Baudras, A., in "Flavins and Flavoproteins" (Kamin, H., ed), University Park Press, Baltimore, 599-605 (1971)

[5] Iwatsubo, M., Mevel-Ninio, M. & Labeyrie, F., Biochemistry **16**, 3558-3566 (1977)

[6] Miles, C.S., Rouviere-Fourmy, N., Lederer, F., Mathews, F.S., Reid, G.A., & Chapman, S.K., Biochem. J. **285**, 187-192 (1992)

[7] Walker, F.A., Emrick, D., Rivera, J.E., Hanquet, B.J. & Buttlaire, D.H., J. Am. Chem. Soc. **110**, 6234-6240 (1988)

[8] Tegoni, M., Janot, J.M. & Laveyrie, F., Eur. J. Biochem. **155**, 491-503 (1986)

[9] Dawson, R.M.C., Elliot, D.C., Elliot, W.H. & Jones, K.M., "Data for Biochemical Research" (Third Edition), Oxford Science Publications (1986)

[10] Keller, R.M. & Wuthrich, K., Biochim. Biophys. Acta **621**, 204-217 (1980)

[11] McLachlan, S.J., La Mar, G.N. & Sletten, E., J. Am. Chem. Soc. **108**, 1285-1291 (1986)

[12] Dixon, D.W., Hong, X., Woehler, S.E., Mauk, A.G. & Shista, B.P., J. Am. Chem. Soc. **112**, 1082-1088 (1990)

[13] Guiles, R.D., Altman, J., Kuntz, D. & Waskell, L., Biochemistry **29**, 1276-1289 (1990)

[14] Bax, A., Annu. Rev. Biochem. **58**, 223-256 (1989)

[15] Keller, R., Groudinsky, O. & Wuthrich, K., Biochem. Biophys. Acta **328**, 233-238 (1973)

[16] Labeyrie, F., Beloeil, J.C., & Thomas, M.A., Biochim. Biophys. Acta **953**, 134-141 (1988)

[17] Watari, H., Groudinsky, O. & Labeyrie, F., Biochim. Biophys. Acta **131**, 592-594 (1967)

[18] Capeillere-Blandin, C., Bray, R.C., Iwatsubo, M. & Labeyrie, F. Eur. J. Biochem. **54**, 549-566 (1975)

[19] Moore, G.R. & Pettigrew, G.W., "Cytochrome c : Evolutionary, Structural and Physicochemical Aspects", Springer-Verlag, Berlin, Heidelberg (1990)

[20] Moore, G.R. & Williams, G., Biochim. Biophys. Acta **788**, 147-150 (1984)

[21] Santos, H. & Turner, D.L., FEBS Letters **286**, 179-185 (1987)

[22] Xia, Z.-x. & Mathews, F.S., J. Mol. Biol. **212**, 837-863 (1990)

[23] Suzuki, H. & Ogura, Y., J. Biochem. **67**, 277-289 (1970)

[24] Salemme, F.R., J. Mol. Biol. **102**, 563-568 (1976)

[25] Lederer, F. in "Chemistry and Biochemistry of Flavoenzymes" (Muller, F. ed) CRC Press, Inc., Boca Raton, 153-242 (1991)

[26] Thomas, M.A., Favaudon, V. & Pochon, F., Eur. J. Biochem. **135**, 569-576 (1983)

[27] Thomas, M.A., Gervais, M., Favaudon, V. & Valat, P., Eur. J. Biochem. **135**, 577-581 (1983)

[28] Thomas, M.A., Delsuc, M.A., Beloeil, J.C. & Lallemand, J.Y., Biochem. Biophys. Res. Commun., **145**, 1098-1104 (1987)

[29] Tegoni, M., unpublished results

[30] Black, M.T., White, S.A., Reid, G.A. & Chapman, S.K., Biochem. J. **258**, 255-259 (1989)

[31] Brunt, C.E., Cox, M.C., Thurgood, A.G.P., Moore, G.R., Reid, G.A. & Chapman, S.K., Biochem. J. **283**, 87-90 (1992)

[32] Cox, M.C., unpublished results

[33] Guiard, B. & Lederer, F., J. Mol. Biol. **135**, 639-650 (1979)

[34] Lederer, F. & Guiard, B., in "Methods in Peptide and Protein Sequence Analysis" (C. Birr., ed), Elsevier North-Holland Biomedical Press, 433-438 (1980)

[35] Mathews, F.S., Czerwinski, E.W. & Argos, P. in "The Porphyrins" Volume VII (D. Dophin, ed) Academic Press, Inc., London, 107-147 (1979)

[36] Mathews, F.S. & Xia, Z.-x., in "Flavins and Flavoproteins 1987" (D.E. Edmondson & D.B. McCormick, eds), Walter de Gruyter, Berlin, 123-132 (1987)

CHAPTER 4

ISOLATION AND PURIFICATION OF THE b_2-FLAVIN DOMAIN EXPRESSED IN *E.coli*

4.1 INTRODUCTION

4.1.1 BACKGROUND

Although the haem domain of flavocytochrome b_2 could be isolated by proteolysis of the holoenzyme from yeast [1], separation of a flavin-binding fragment proved to be more difficult. Treatment with proteases caused the flavin-binding region to cleave into two fragments, and it was therefore speculated that the FMN prosthetic group was bound in a biglobular region of protein rather than in a single domain [2-5]. The cleavage was later found to be due to a region of protein highly sensitive to proteases, located within a single flavin-binding domain [6]. Elucidation of the crystal structure of flavocytochrome b_2 eventually proved that the FMN was indeed bound in a single, monoglobular domain [7,8]. The proteolytically-sensitive area was found to be a disordered loop of around 40 residues, lying on the surface of the flavin domain. This explained why the flavin domain itself had not been isolated by proteolysis.

Gervais and co-workers finally succeeded in isolating a tetrameric flavoprotein by proteolysis of flavocytochrome b_2 from *H.anomala* under carefully-controlled conditions [2,5,9,10]. This flavoprotein had lactate dehydrogenase activity but failed to transfer electrons to cytochrome *c*, and could only be isolated in small amounts.

4.1.2 STRUCTURE OF THE FLAVIN DOMAIN

From the crystal structure [8] it was found that the flavin domain of flavocytochrome b_2 comprises residues 101-486 of the

amino-acid sequence, with residues 487-511 forming the C-terminal tail. The flavin domains pack around the molecular four-fold axis of symmetry to form an oblate disc (Figure 4.1). Each flavin domain is essentially composed of a $\beta_8\alpha_8$- barrel structure formed by residues 192-465. This structural motif consists of eight parallel strands and eight helices connected by loops of peptide (Figure 4.2). In addition to the $\beta_8\alpha_8$- barrel structure, residues 101-191 form four helices and three β-sheets, which, along with the C-terminal tail, make many intersubunit contacts [8,11].

The $\underline{b}_2$-flavin domain is structurally-related to the flavin domains of other FMN-containing enzymes which both have parallel $\beta_8\alpha_8$ structures [12]. One of these enzymes, spinach glycollate oxidase (SGO) has an almost identical three-dimensional structure and 37% of the same amino acid sequence as flavocytochrome $\underline{b}_2$ [13]. Another structurally-homologous enzyme is trimethylamine dehydrogenase of bacterium W_3A_1. While it, too, has a $\beta_8\alpha_8$ barrel conformation [13], its amino acid sequence does not share a high degree of homology with flavocytochrome $\underline{b}_2$ or spinach glycollate oxidase [14] (Section 1.7.2).

The crystal structure of flavocytochrome $\underline{b}_2$ revealed a region of electron density at the site of the FMN in two of the four subunits, which was attributed to pyruvate, the reaction product, bound at the active site of the enzyme [7,8]. This enabled the active site of flavocytochrome $\underline{b}_2$ to be located in each of the crystallographically-distinguishable types of subunit (Figure 4.3). Several amino-acid residues around the active site interact with either the substrate or FMN and are important in the reaction mechanism (Section 1.5.2).

FIGURE 4.1 THE TETRAMERIC STRUCTURE OF FLAVOCYTOCHROME $\underline{b}_2$ [7,8]

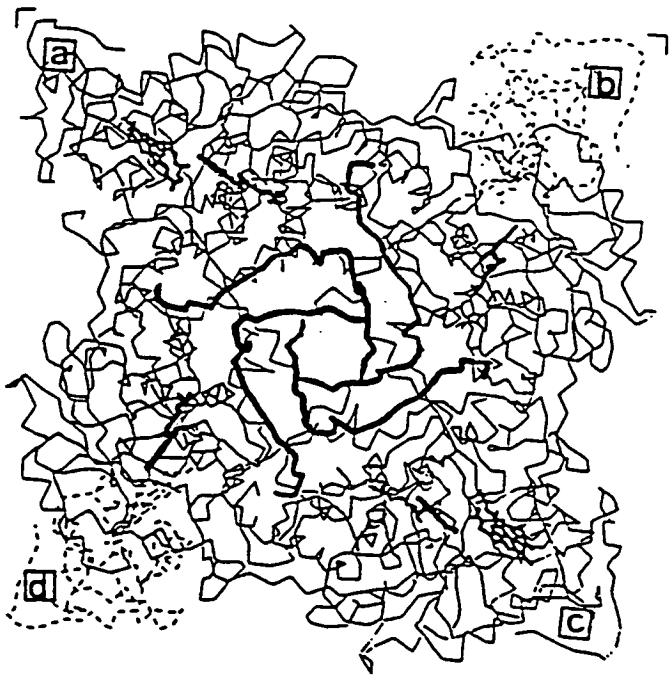

The tetramer is shown looking along the molecular 4-fold axis of symmetry. Subunits are marked [a]-[d]. The dashed lines in subunits [b] and [d] represent the two cytochrome domains that are positionally disordered in the crystal structure.

FIGURE 4.2 SCHEMATIC REPRESENTATION OF THE STRUCTURE OF THE FLAVIN DOMAIN OF FLAVOCYTOCHROME $\underline{b}_2$

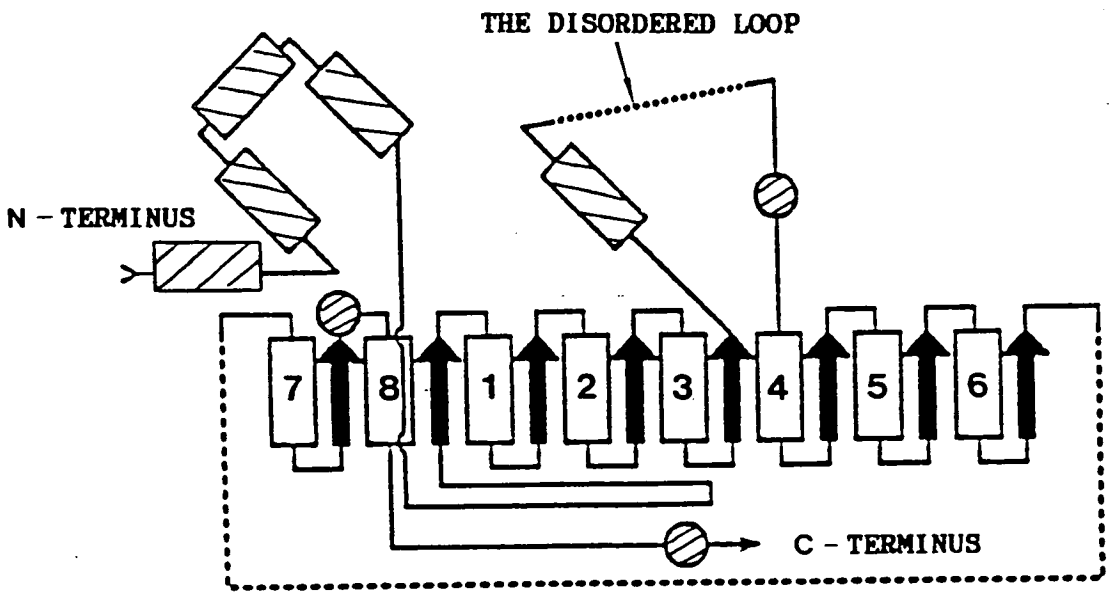

For legend, see Figure 1.7

FIGURE 4.3 RELATIVE POSITIONS OF THE PROSTHETIC GROUPS IN THE TWO CRYSTALLOGRAPHICALLY-DISTINCT SUBUNITS OF FLAVOCYTOCHROME b_2

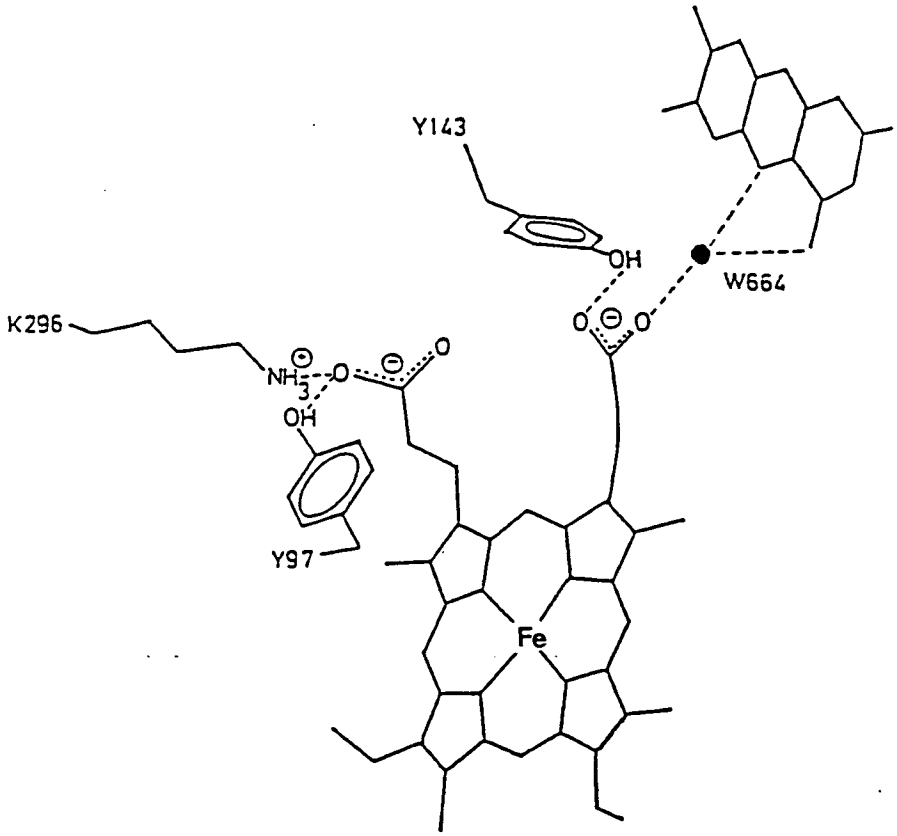

SUBUNIT 1 (PYRUVATE ABSENT)

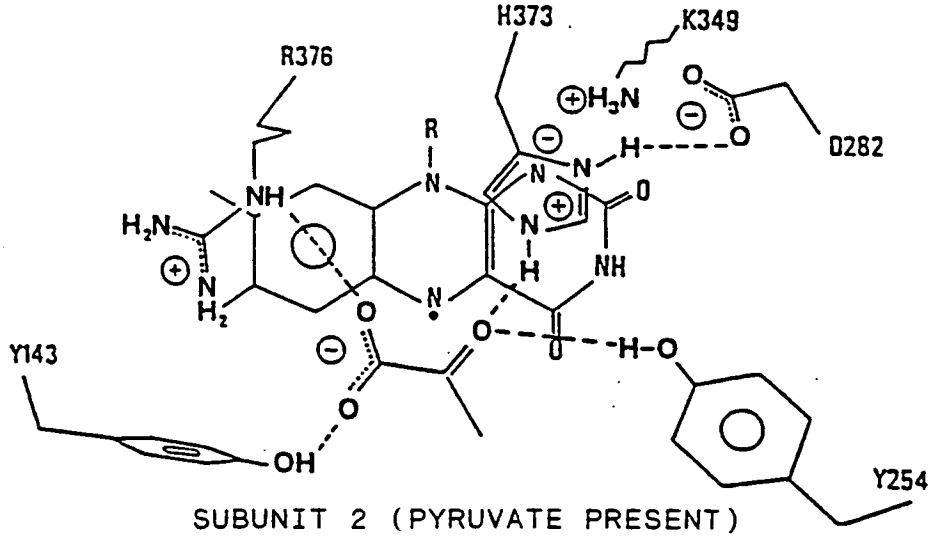

SUBUNIT 2 (PYRUVATE PRESENT)

4.1.3 CATALYTIC ROLE OF THE FLAVIN DOMAIN

Studies of flavin-free and haem-free preparations of flavocytochrome $\underline{b}_2$ have shown that FMN is essential for lactate dehydrogenase activity [15], while haem is essential for cytochrome $\underline{c}$ reductase activity [16]. The first step of the electron transfer pathway is from bound lactate to FMN, oxidising lactate to pyruvate and fully-reducing FMN (a two-electron step). The reduced FMN then undergoes two reversible one-electron transfers to the haem, from which electrons are transferred to cytochrome $\underline{c}$. This is summarised in Figure 4.4. The role of the FMN cofactor, then, can be envisaged as that of a transformer, converting the enzyme from a system dealing with pairs of electrons to one dealing with single electrons. FMN can only play such a part because it can be stabilised in the semiquinone state, midway between full oxidation and full reduction.

Mechanistically, the FMN accepts electrons from the carbanion intermediate formed by the abstraction of the α-proton from lactate. The unique nature of the isoalloxazine ring subsequently allows it to undergo the necessary single-electron transfers to complete the catalytic cycle. Full details of the reaction mechanism of flavocytochrome $\underline{b}_2$ are given in Chapter 1 and references [11] & [12].

Expression of the $\underline{b}_2$-flavin binding domain independently of the haem domain would provide an effective way of producing the isolated flavin domain in large amounts. This would, in turn, enable the flavin domain to be studied both biochemically and biophysically without interference from the haem domain and might therefore be useful in investigating more fully the role of the flavin domain, its mode of action, and the importance of interdomain contacts in the catalytic cycle of flavocytochrome $\underline{b}_2$.

FIGURE 4.4 ELECTRON TRANSFER SCHEME IN HOLO-FLAVOCYTOCHROME $\underline{b}_2$

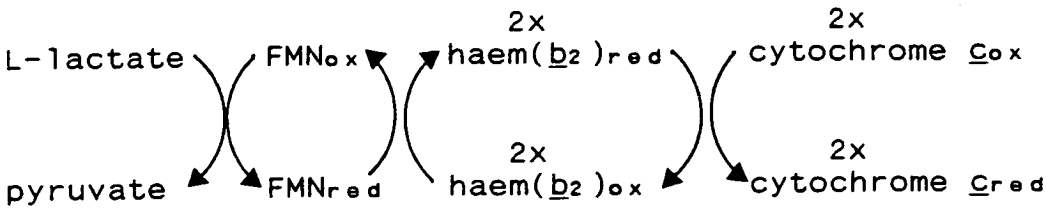

Overall:

$$\text{L-lactate} \xrightarrow{2e} \text{FMN} \underset{}{\overset{1e}{\rightleftharpoons}} 2 \text{ haem} \xrightarrow{1e} 2 \text{ cytochrome } \underline{c}$$

Two electrons are transferred from L-lactate to the FMN of flavocytochrome $\underline{b}_2$; this is then followed by two reversible one-electron transfers from FMN to $\underline{b}_2$ haem and two irreversible one-electron transfers from $\underline{b}_2$ haem to cytochrome $\underline{c}$.

FMN : flavin mononucleotide
haem($\underline{b}_2$) : bound haem of flavocytochrome $\underline{b}_2$
ox : oxidized
red : reduced

FIGURE 4.5 GENE MODIFICATION USED IN THE EXPRESSION OF THE FLAVIN DOMAIN OF FLAVOCYTOCHROME $\underline{b_2}$ IN E.coli

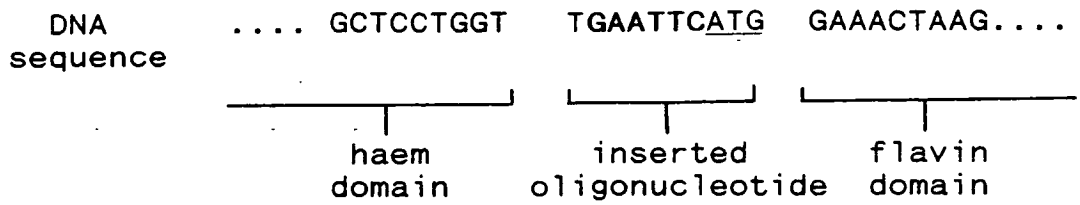

The EcoRI site is shown in bold and the ATG initiation codon is underlined

4.2 EXPRESSION OF THE b_2-FLAVIN DOMAIN IN *E.coli*

Residues 101-511 of the amino acid sequence of flavocytochrome b_2, comprising the flavin domain and the C-terminal tail, hereafter referred to as b_2-flavin domain, were expressed in *E.coli* by G.A. Reid and R.L. Pallister [17]. An ATG codon was introduced before the sequence encoding the flavin domain, allowing expression to commence at residue 101. At the same time, a cleavage site for the endonuclease *EcoRI* was also incorporated, as shown in Figure 4.5. This allows the region of DNA encoding the flavin domain only to be excised from the mutated flavocytochrome b_2 gene and inserted into an expression vector (in this case, pRC23). The expression vector can then be incorporated into a host. The host used for the b_2-flavin domain was *E.coli* NF1. This strain of *E.coli*, when used in conjunction with the pRC expression vector, allows expression to be induced by a shift in temperature. Growth conditions used to express the b_2-flavin domain are described in Section 8.1.4.

4.3 RESULTS: EXTRACTION AND PURIFICATION

4.3.1 EXTRACTION OF THE b_2-FLAVIN DOMAIN FROM *E.coli*

Frozen *E.coli* cells were suspended in 100mM-sodium phosphate buffer, pH 7.0, containing 10mM L(+)-lactate (in the form of lithium L(+)-lactate) and 10mM EDTA. (Full descriptions of all buffers can be found in Chapter 8). L(+)-lactate was kept present throughout the extraction and purification of the b_2-flavin domain in order to keep the enzyme in the reduced state. The cells were lysed by adding lysozyme (approx. 0.2mg/ml) and incubating at 0-4°C, with stirring, for 30 minutes. The solution was centrifuged (39 000g,

10 mins.) to remove insoluble cell debris and unlysed cells. The supernatant, a pale brownish-yellow solution, was retained and the pellet was subjected to a second lysis and centrifugation. The supernatants from both lyses were combined and the solution was adjusted to 30% $(NH_4)_2SO_4$ saturation, stirring at 0-4°C for at least 10 minutes to ensure dissolution of $(NH_4)_2SO_4$. After centrifugation (39 000g, 10 mins.) to remove impurities precipitated at this salt concentration, the $\underline{b}_2$-flavin domain was precipitated from the supernatant by adjusting to 70% $(NH_4)_2SO_4$ saturation, again stirring at 0-4°C for at least 10 minutes. The precipitated protein was removed by centrifugation (39 000g, 10 min). The pale yellowish precipitate was stored under nitrogen at 0-4°C, prior to further purification.

4.3.2 PURIFICATION

The isolated $\underline{b}_2$-flavin domain was purified by column chromatography using DE-52 (Whatman), the same microgranular cellulose anion exchange material used during the purification of the $\underline{b}_2$-haem domain expressed in *E.coli* (Section 2.3.2).

Impure $\underline{b}_2$-flavin domain, which had been stored as a $(NH_4)_2SO_4$ - precipitate as described in Section 4.3.1, was dissolved in a minimum volume of 10mM - sodium phosphate buffer, pH 7.0, containing 10mM L(+)-lactate, and dialysed against this same buffer overnight, at 0-4°C and under nitrogen. After dialysis the solution was centrifuged (39 000g, 10 min) to remove any insoluble debris, and loaded onto a DE-52 column (10cm x 2.5cm), previously equilibrated in the 10mM - phosphate, 10mM L(+)-lactate, pH 7.0 buffer. The column was washed with two column volumes of the 10mM phosphate/10mM

L(+)-lactate buffer, and eluted using a gradient of 50 - 200mM - sodium phosphate buffer, pH 7.0, with L(+)-lactate present at 10mM concentration throughout. All washings were retained and fractions were collected immediately the gradient was commenced. Fractions and washings were monitored for the presence of $\underline{b}_2$-flavin domain by assaying for lactate dehydrogenase : ferricyanide reductase activity (Section 8.7). Some activity was usually detected in the column washings due to overloaded $\underline{b}_2$-flavin domain which had not bound to the column material. On commencement of the elution gradient, no further lactate dehydrogenase : ferricyanide reductase activity was detected until several fractions had been collected, when a number of fractions of high activity were eluted. The active fractions were pooled and the $\underline{b}_2$-flavin domain precipitated by adjusting to 70% $(NH_4)_2SO_4$ saturation and centrifuging (39 000g, 10 min). The pellet was stored under nitrogen at 0-4°C.

Protein thus purified exhibited a major band of M_r 47 000 on SDS/PAGE, with several less intense bands of lower and higher molecular weights. Further purification was achieved by dissolving the precipitated protein in a minimum volume of 100mM-sodium phosphate buffer, pH 7.0, containing 10mM L(+)-lactate, and passing through a Sepharose S300 (Pharmacia LKB) gel filtration column (150cm x 3cm) in the same buffer. Active fractions were pooled, precipitated at 70% $(NH_4)_2SO_4$ saturation, and stored under nitrogen at 0-4°C. After gel filtration, the protein showed a single band of M_r 47 000 on SDS/PAGE. The purification procedure, yields and degree of purification achieved are summarised in Table 4.1.

The $\underline{b}_2$-flavin domain expressed in *E.coli* has also been purified by FPLC (U. Muh & coworkers, University of Michigan, Ann Arbor). A

TABLE 4.1: DATA FOR THE ISOLATION OF THE b_2-FLAVIN DOMAIN PURIFIED BY DE-52 COLUMN CHROMATOGRAPHY

Purification step	Total protein (mg)	b_2-flavin domain (mg)	Recovery %
Supernatant after cell lysis	327	36	100
After $(NH_4)_2SO_4$ and dialysis	225	25	69
After DE-52 column	148	12	33

Based on a preparation from 10g wet weight *E.coli* cells

Q-sepharose column (approx. 20ml) equilibrated in 10mM-sodium phosphate buffer, pH 7.0, containing 10mM L(+)-lactate, was used to purify protein prepared as for column chromatography on DE-52. The enzyme was eluted using a gradient of 0-0.3M NaCl in the 10mM phosphate/10mM lactate buffer at a rate of 20mM salt per column volume. Protein content of fractions was monitored by measuring their absorbance at 280nm. Those fractions with high absorbances at 280nm were assayed for activity. Active fractions were pooled and $(NH_4)_2SO_4$-precipitated as before. SDS/PAGE of protein purified by FPLC showed a similar degree of purity to that purified by column chromatography using DE-52.

4.3.3 NATIVE MOLECULAR WEIGHT DETERMINATION

From SDS/PAGE, the monomer molecular weight of the $\underline{b}_2$-flavin domain expressed in E.coli was found to be 47 000. However, this did not resolve the question of whether the isolated $\underline{b}_2$-flavin domain is monomeric, like the $\underline{b}_2$-haem domain expressed in E.coli, or tetrameric, like the intact holoenzyme. Determination of the molecular weight of native $\underline{b}_2$-flavin domain (i.e. not denatured as in SDS/PAGE) was estimated using the same S300 column used in the purification procedure (Section 4.3.2). By dissolving some ferricyanide (M_r 329) and blue dextran (average M_r 2 000 000) in the protein solution before loading onto the column, both the void volume of the column, V_o, and the elution volume of the protein, V_e (the volume at which the most active fraction is eluted), could be determined. A calibration graph of V_e/V_o versus log (molecular weight) had previously been determined for the same column using several molecules of known molecular weight [18] (Section 8.5.4).

This linear calibration graph was used to estimate the native molecular weight of the protein.

Using the above method, the native molecular weight of $\underline{b}_2$-flavin domain expressed in E.coli was found to be 175 000 $\pm$ 30 000. A tetramer formed of monomers with M_r 47 000 would be expected to have M_r 188 000, which is within experimental error of the native molecular weight of the $\underline{b}_2$-flavin domain determined by gel filtration chromatography. Thus the $\underline{b}_2$-flavin domain expressed in E.coli is indeed a tetramer.

4.4 DISCUSSION

The region of flavocytochrome $\underline{b}_2$ corresponding to the flavin domain and the C-terminal tail (residues 101-511) has been successfully expressed in E.coli. A purification procedure for the $\underline{b}_2$-flavin domain has been developed (Section 4.3.2) enabling the isolated domain to be prepared with ease. The resulting protein is a tetramer made up of four identical protomers, each having M_r 47 000.

Prior to the expression of the $\underline{b}_2$-flavin domain in E.coli, studies of its function in the absence of the haem domain were only possible using preparations of the holoenzyme from which both prosthetic groups had been removed by denaturation and which was then reconstituted with FMN [16]. However, it is possible that conformational differences exist between native and reconstituted flavocytochrome $\underline{b}_2$ [11], bringing into question the true value of studies on the dehaemoenzyme. The isolated $\underline{b}_2$-flavin domain expressed in E.coli provides a means of investigating the role and function of the flavin domain without the necessity for denaturing and reconstituting the protein.

Isolation of the $\underline{b}_2$-flavin domain also provides an opportunity to study spectroscopic properties of the flavin which were previously impossible to monitor directly. In the holoenzyme, UV-visible absorbances due to flavin are swamped by the much stronger absorbances of the haem. With the haem domain removed, the spectroscopic properties of the flavin can be investigated and exploited in experimental techniques such as stopped-flow kinetics to study changes at the FMN.

Characterization of the isolated $\underline{b}_2$-flavin domain in terms of both its biophysical and biochemical properties will be discussed in Chapter 5.

4.5 REFERENCES

[1] Labeyrie, F., Groudinsky, O., Jacquot-Armand, Y. & Naslin, L., Biochem. Biophys. Acta **128**, 492-503 (1966)

[2] Gervais, M., Groudinsky, O., Risler, Y. & Labeyrie, F., Biochem. Biophys. Res. Commun. **77**, 1543-1551 (1977)

[3] Mevel-Ninio, M., Risler, Y. & Labeyrie, F., Eur. J. Biochem. **73**, 131-140 (1977)

[4] Gervais, M., Labeyrie, F., Risler, Y. & Vergnes, O., Eur. J. Biochem. **111**, 17-31 (1980)

[5] Gervais, M., Risler, Y., Capeillere-Blandin, C. Vergnes, O., & Labeyrie, F., in "Limited Proteolysis in Microorganisms" (G.N. Cohen & H. Holzer, eds), US Government Printing Office, Washington DC, 277-234 (1979)

[6] Ghrir, H. & Lederer, F., Eur. J. Biochem. **120**, 279-287 (1981)

[7] Mathews, F.S. & Xia, Z.-x., in "Flavins and Flavoproteins 1987" (D.E. Edmonson & D.B. McCormick, eds), Walter de Gruyter & Co., New York, 123-132 (1987)

[8] Xia, Z.-x. & Mathews, F.S., J. Mol. Biol. **212**, 837-863 (1990)

[9] Gervais, M., Risler, Y. & Corazzin, S., Eur. J. Biochem. **130**, 253-259 (1983)

[10] Celerier, J., Risler, Y., Schwenke, J., Janot, J-M. & Gervais, M., Eur. J. Biochem. **182**, 67-75 (1989)

[11] Lederer, F., in "Chemistry and Biochemistry of Flavoenzymes" (Muller, F., ed) CRC Press Inc., Boca Raton, 153-242 (1991)

[12] Chapman, S.K., White, S.A. & Reid, G.A., Adv. Inorg. Chem. **36**, 257-301 (1991)

[13] Lindqvist, Y., Branden, C.I., Mathews, F.S. & Lederer, F., J. Biol. Chem. **266**, 3198-3207 (1991)

[14] Boyd, G., Mathews, F.S., Packman, L.C., Scrutton, N.S., FEBS Lett., **308**, 271-276 (1992)

[15] Baudras, A., Bull. Soc. Chim. Biol. **47**, 1143-1175 (1965)

[16] Iwatsubo, M., Mevel-Ninio, M. & Labeyrie, F., Biochemistry **16**, 3558-3566 (1977)

[17] Pallister, R.L., Reid, G.A., Brunt, C.E., Miles, C.S. & Chapman, S.K., in "Flavins and Flavoproteins 1990", (Curti, B., Ronchi, S. & Zanetti, G., eds), Walter de Gruyter & Co., Berlin, 787-790 (1991)

[18] Wallis, M.G., PhD Thesis, University of Edinburgh (1990)

CHAPTER 5

FLAVIN DOMAIN: CHARACTERIZATION

5.1 INTRODUCTION

In Chapter 1 and Chapter 4, the role of FMN in the catalytic cycle of flavocytochrome $\underline{b}_2$ was discussed. Essential for lactate dehydrogenase activity [1], FMN is found at the active site of the emzyme and is bound into a protein domain which is functionally-distinct from the haem-containing domain [2,3]. Isolation of the $\underline{b}_2$-flavin domain, described in Chapter 4, provides a means of investigating the role of the flavin domain independently from the haem domain, which had not hitherto been possible.

The isolated domain can be studied using both steady-state and stopped-flow kinetics. It is particularly suitable for investigation under stopped-flow conditions enabling closer observation of FMN than had been possible with the holoenzyme. Stopped-flow studies of the flavin in the holoenzyme rely on monitoring the changes in absorbance of the flavin at a haem isosbestic point [4], at which absorbance changes due to flavin itself are not optimal. However, the absence of any haem in the $\underline{b}_2$-flavin domain expressed in *E.coli* enables observation at 452nm, the wavelength where the maximum change in FMN absorbance takes place (Figure 5.1).

In this chapter, the characterization of the isolated $\underline{b}_2$-flavin domain by both steady-state and stopped-flow kinetic methods will be discussed.

5.2 EXPERIMENTAL

5.2.1 GENERAL

Kinetics experiments were carried out on isolated $\underline{b}_2$-flavin domain purified by DE-52 column chromatography (Section 4.3.2).

FIGURE 5.1 ELECTRONIC ABSORPTION SPECTRUM OF ISOLATED $\underline{b}_2$-FLAVIN DOMAIN

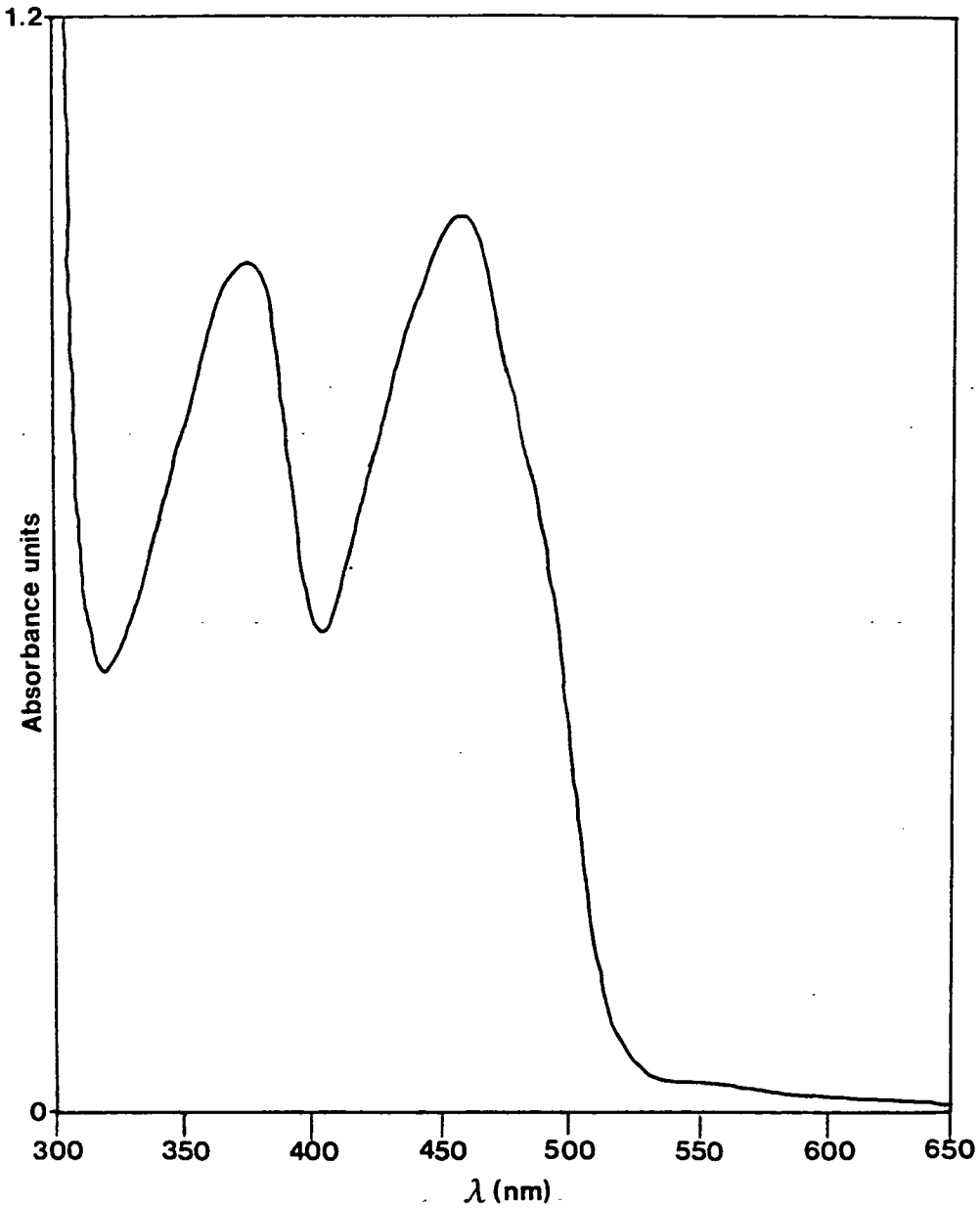

Electronic absorption spectrum of 90μM oxidized $\underline{b}_2$-flavin domain in Tris.HCl buffer, I = 0.10M, pH 7.5, 25 °C.

For further details see Section 8.12.

TABLE 5.1: EXTINCTION COEFFICIENTS OF BOUND FLAVIN IN DEHAEMO-FLAVOCYTOCHROME $\underline{b}_2$ [5]

Wavelength nm	ϵ_{OX} $mM^{-1}\ cm^{-1}$	ϵ_{HQ} $mM^{-1}\ cm^{-1}$
453	11.1 ± 0.5	1.1 ± 0.2
375	10.6 ± 0.5	5.9 ± 0.5
470	9.8 ± 0.5	1.08 ± 0.2
490	7.2 ± 0.4	0.9 ± 0.2

ϵ_{OX} = extinction coefficient for fully-oxidized FMN

ϵ_{HQ} = extinction coefficient for fully-reduced FMN (flavin hydroquinone)

Concentrations of $\underline{b}_2$-flavin domain were calculated using the previously-published extinction coefficient at 452nm for dehaemoflavocytochrome $\underline{b}_2$ in the oxidized state ([5], and Table 5.1). All buffers and solutions were prepared as described in Sections 8.2 and 8.8.

Electronic absorption spectra were recorded as described in Section 3.2.1.

5.2.2 STEADY-STATE KINETICS

Steady-state kinetic experiments were performed using a Beckman DU-62 spectrophotometer, thermostatted at 25 $\pm$ 0.1°C. All experiments were carried out in Tris.HCl buffer, pH 7.5, I=0.10M, using either L-[2-^{1}H] lactate or L-[2-^{2}H] lactate as substrates. Enzyme activity was measured using ferricyanide (2mM) as the electron acceptor, monitoring decrease in absorbance at 420nm, (ϵ_{420} (ferricyanide) = 1010M^{-1} cm^{-1}). Dependence on electron acceptor concentration was measured in the same way, at a constant substrate concentration of 6mM L-[2-^{1}H] lactate. Owing to the high concentrations of electron acceptor used, all assays were performed using spectrophotometer cuvettes of 0.2cm path length.

5.2.3 STOPPED-FLOW KINETICS

Stopped-flow studies were performed using purified $\underline{b}_2$-flavin domain which had been oxidized by passing through a Sephadex G-25 column (18x0.8cm) equilibrated in Tris.HCl buffer, pH 7.5, I=0.10M. Experiments were carried out in this same buffer at 25 $\pm$ 0.1°C, using an Applied Photophysics SF.17MV stopped-flow spectrofluorimeter in the absorbance mode to monitor flavin reduction at

452nm, using varying concentrations of L-[2-^{1}H] and L-[2-^{2}H] lactate.

Experimental data were analysed using non-linear regression analysis performed with the SF.17 MV spectrofluorimeter software.

5.3 RESULTS AND DISCUSSION

5.3.1 ELECTRONIC ABSORPTION SPECTRUM

Spectroscopic properties of the FMN in holo-flavocytochrome $\underline{b}_2$ had been difficult to observe before expression of the $\underline{b}_2$-flavin domain in *E.coli* due to the domination of the visible spectrum by the haem absorbance. Various attempts to deduce the flavin contribution were made using methods to subtract the haem absorbance [6], or by the sulphite-induced difference spectroscopy method of Lederer [7]. Expression of the $\underline{b}_2$-flavin domain in *E.coli* allowed the spectrum to be recorded directly.

The electronic absorption spectrum of the $\underline{b}_2$-flavin domain oxidized by G-25 column chromatography, is shown in Figure 5.1. The bright yellow oxidized enzyme has absorbance maxima at 375 and 452nm. In the visible region, the spectrum is identical to that observed for dehaemoflavocytochrome $\underline{b}_2$ [5], for which extinction coefficients have been published (Table 5.1).

5.3.2 STEADY-STATE KINETICS

Isolated $\underline{b}_2$-flavin domain expressed in *E.coli* has L-lactate dehydrogenase activity when ferricyanide is used as the electron acceptor but not when cytochrome *c* is used. This is in accordance with results obtained from previous studies using haem-free preparations of flavocytochrome $\underline{b}_2$ [5] and the tetrameric flavoprotein

isolated from H.anomala flavocytochrome b_2 by proteolytic methods [8 - 10].

The isolated b_2-flavin domain exhibits typical saturation kinetics with both L-[2-^{1}H] lactate and L-[2-^{2}H] lactate (L-lactate deuterated at the C-2 position) as substrates (Figures 5.2 and 5.3). The results of such experiments are shown in Table 5.2, where they are compared with previously-determined values for the holoenzyme.

The observed steady-state parameters for b_2-flavin domain and holo-flavocytochrome b_2 appear, at first glance, to differ both in terms of k_{cat} and K_m. The value of k_{cat} observed for the b_2-flavin domain with L-[2-^{1}H] lactate is only about 59% of that recorded for the holoenzyme. A similar decrease in activity is observed for both dehaemoflavocytochrome b_2 and the proteolytically-produced flavin domain of flavocytochrome b_2 from H.anomala when compared to the respective holoenzymes from which they were isolated [5,11]. This loss of activity was explained, in the case of the dehaemoenzyme, by the fact that electron transfer from flavin to ferricyanide via the b_2-haem is much more efficient than direct electron transfer to ferricyanide from either the hydroquinone or the semiquinone form of FMN [5]. For this reason the observed rates of reaction for the haem-containing holoenzymes are faster, in each case, than those observed for their respective haem-free derivatives (dehaemoenzyme or isolated flavin domain).

The K_m for the holoenzyme also differs from that for the b_2-flavin domain with both [2-^{1}H] and [2-^{2}H] lactate. As the kinetic schemes for the catalytic cycles of flavocytochrome b_2 and the b_2-flavin domain consist of more than one step these K_m values are difficult to interpret in their own right, since they are not

FIGURE 5.2 MICHAELIS-MENTEN AND DOUBLE RECIPROCAL PLOTS FOR THE OXIDATION OF L-[2-^{1}H] LACTATE CATALSYED BY $\underline{b}_2$-FLAVIN DOMAIN UNDER STEADY-STATE CONDITIONS

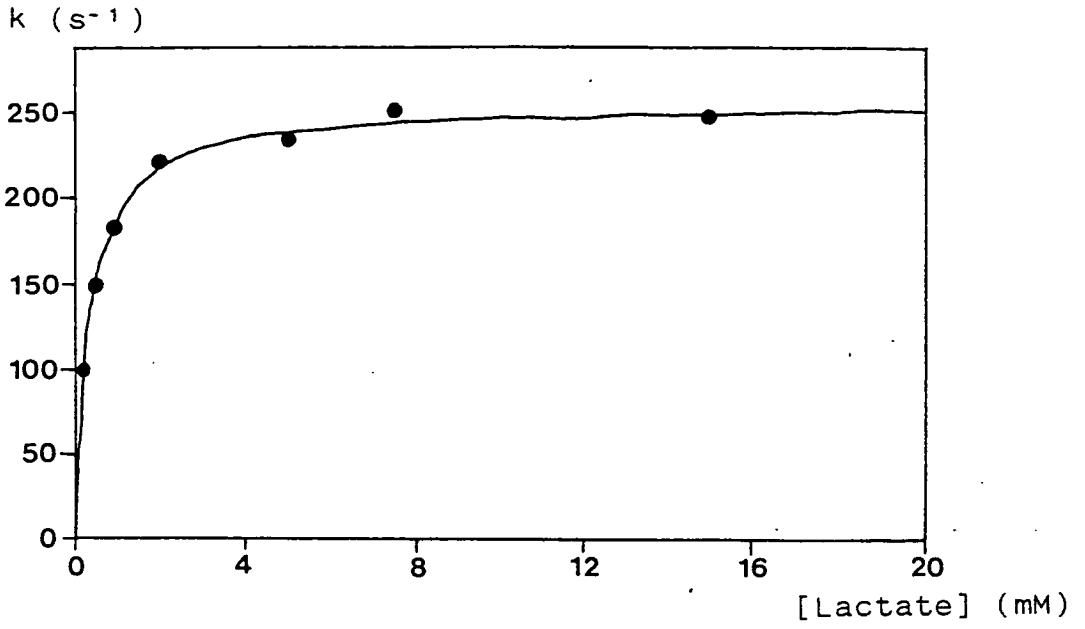

(a) MICHAELIS-MENTEN PLOT

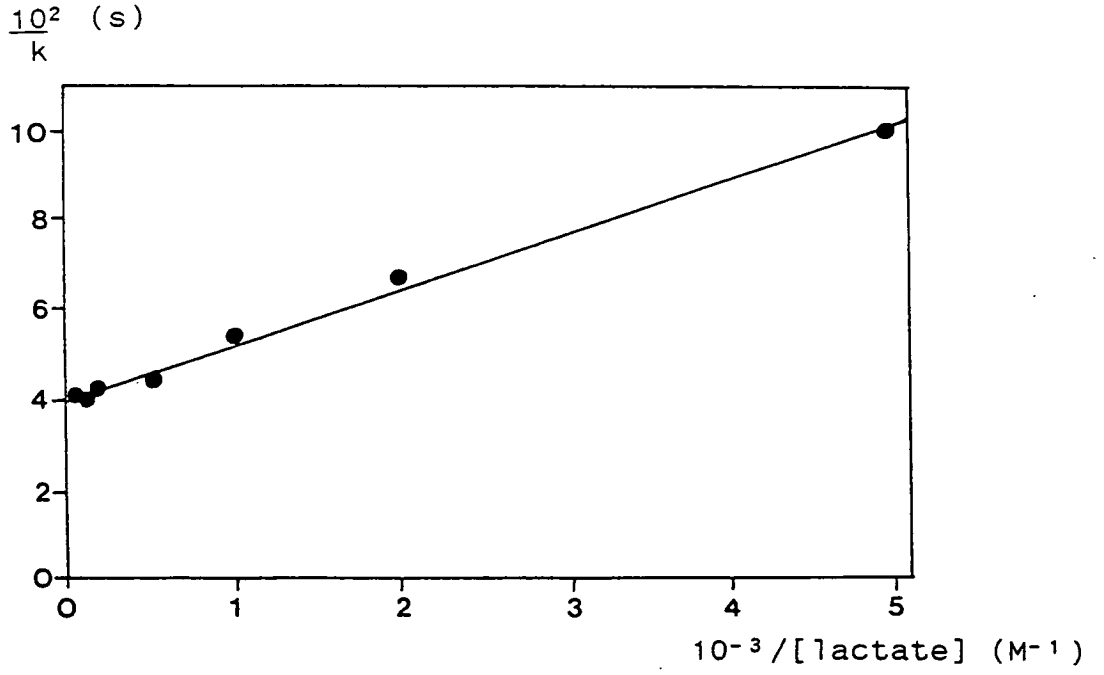

(b) DOUBLE-RECIPROCAL PLOT

Experimental conditions are described in Section 5.2

FIGURE 5.3 MICHAELIS-MENTEN AND DOUBLE RECIPROCAL PLOTS FOR THE OXIDATION OF L-[2-^{2}H] LACTATE CATALYSED BY $\underline{b}_2$-FLAVIN DOMAIN UNDER STEADY-STATE CONDITIONS

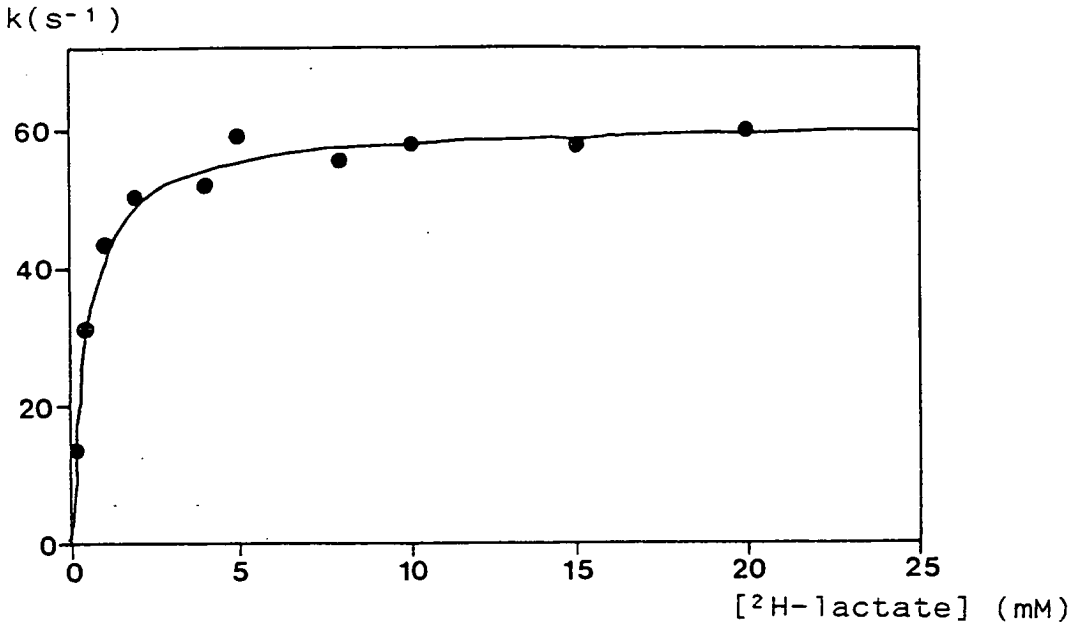

(a) MICHAELIS-MENTEN PLOT

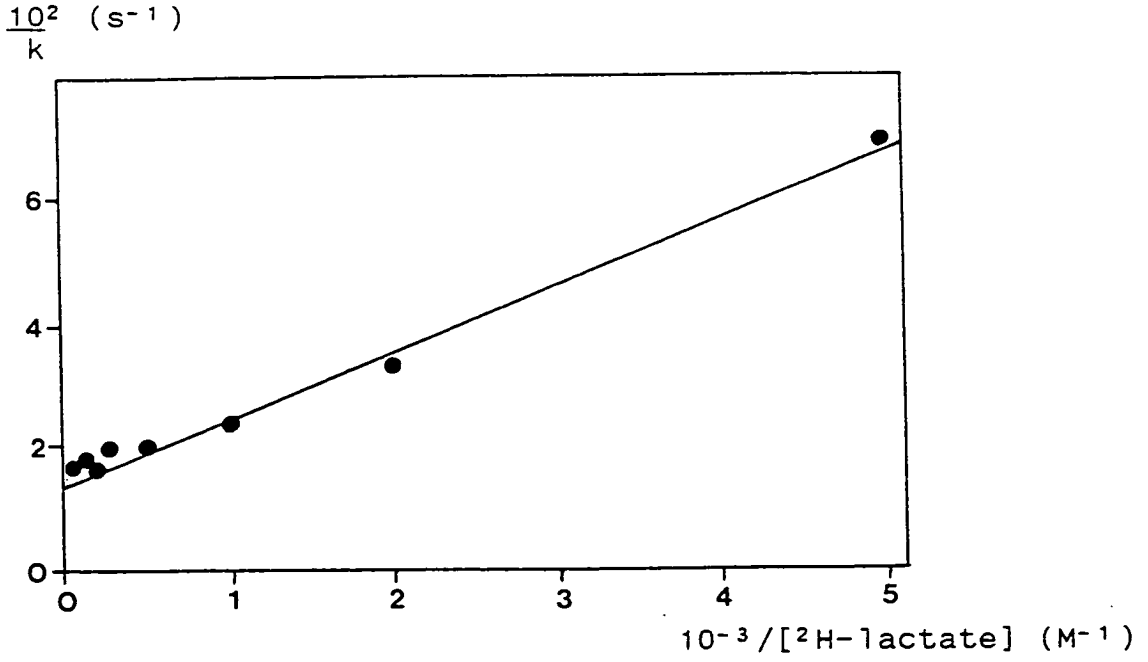

(b) DOUBLE-RECIPROCAL PLOT

Experimental conditions are described in Section 5.2

TABLE 5.2: STEADY-STATE KINETIC PARAMETERS FOR HOLO-FLAVOCYTOCHROME $\underline{b}_2$ AND ISOLATED $\underline{b}_2$-FLAVIN DOMAIN

Enzyme	k_{cat} (s^{-1})		K_m (mM)		k_{cat}/K_m		Ref.
	[^{1}H]lac	[^{2}H]lac	[^{1}H]lac	[^{2}H]lac	[^{1}H]lac	[^{2}H]lac	
Holoenzyme	400 ± 10	86 ± 5	0.49 ± 0.05	0.76 ± 0.06	8.2×10^5	1.1×10^5	[4]
$\underline{b}_2$-flavin domain	235 ± 35	62 ± 2	0.27 ± 0.04	0.51 ± 0.06	8.7×10^5	1.8×10^5	This work

All experiments were carried out at 25°C in Tris.HCl buffer, pH 7.5, I=0.10M, using ferricyanide as the electron acceptor. Results are reported at 1mM ferricyanide for the holoenzyme and 2mM ferricyanide for the $\underline{b}_2$-flavin domain. k_{cat} is expressed as mol. electrons transferred per second.

Abbreviations: [^{1}H]lac = L-[2-^{1}H] lactate

[^{2}H]lac = L-[2-^{2}H] lactate

All parameters given for $\underline{b}_2$-flavin domain are averages of the data from at least five experiments giving concordant results. Errors are standard deviations from the average.

simply dissociation constants. However, the ratio k_{cat}/K_m can be used as an indication of catalytic efficiency. It can be seen from Table 5.2 that despite differences between their individual k_{cat} and K_m values, both the holoenzyme and the $\underline{b}_2$-flavin domain are, overall, almost equally efficient L-lactate dehydrogenases.

The ^{2}H-kinetic isotope effect (KIE) has been measured for $\underline{b}_2$-flavin domain and is compared with previously-determined values for the holoenzyme in Table 5.3. The value of the KIE observed for the holoenzyme showed the major rate-limiting step of the catalytic cycle to be proton abstraction at C-2 of lactate [12]. A substantial KIE, similar to that observed for the holoenzyme, is observed for $\underline{b}_2$-flavin domain. This confirms that the major rate-limiting step in the isolated $\underline{b}_2$-flavin domain has not been significantly altered and is still abstraction of the C-2 hydrogen as a proton.

The apparent K_m values for ferricyanide, the electron acceptor, are summarised for the holoenzyme and $\underline{b}_2$-flavin domain in Table 5.4. Unlike the holoenzyme, the rate of reaction of the $\underline{b}_2$-flavin domain depends on electron acceptor concentration. For this reason, steady-state kinetics experiments on the $\underline{b}_2$-flavin domain were carried out at 2mM ferricyanide concentration (Section 5.2.2), which is approximately 86% saturating. Results for the holoenzyme, which does not show a similar dependence on ferricyanide concentration, are reported at 1mM ferricyanide [4]. The observation of a similar dependence on ferricyanide concentration for dehaemoflavocytochrome $\underline{b}_2$ [5] led to the development of a reaction scheme as outlined in Figure 5.4. With the help of simulation studies it was discovered that ferricyanide reacts 20 times faster with flavin in the semiquinone form than in the hydroquinone form [5]. Thus the rate

TABLE 5.3: DEUTERIUM KINETIC ISOTOPE EFFECTS (KIEs) FOR HOLO-FLAVOCYTOCHROME $\underline{b}_2$ AND $\underline{b}_2$-FLAVIN DOMAIN

Enzyme	k_{cat} (s^{-1})		KIE	Ref.
	[^{1}H]lac	[^{2}H]lac		
Holoenzyme	400 ± 10	86 ± 5	4.7 ±0.4	[4]
$\underline{b}_2$-flavin domain	235 ± 35	62 ± 2	3.4 ±0.3	This work

For conditions and abbreviations, see legend for Table 5.2.

TABLE 5.4: VALUES OF K_m FOR FERRICYANIDE

Enzyme	K_m (mM)	Reference
Holoenzyme	<<0.1	[4]
$\underline{b}_2$-flavin domain	>0.5	This work
Dehaemoenzyme	0.5	[5]

Experiments on $\underline{b}_2$-flavin domain were carried out at 25°C in Tris. HCl buffer, pH 7.5, I=0.10M, at 6mm L-[2-^{1}H]lactate.

FIGURE 5.4 PROPOSED REACTION SCHEME FOR ENZYME TURNOVER BY $\underline{b_2}$-FLAVIN DOMAIN

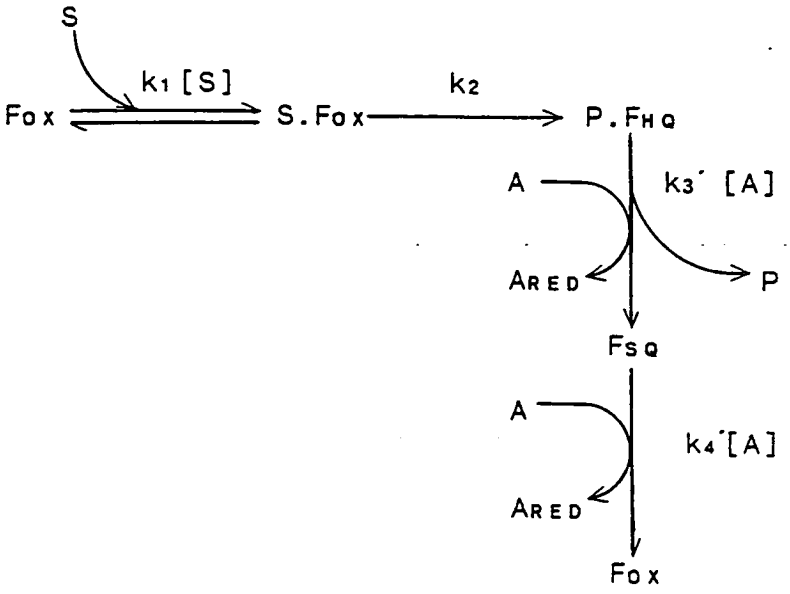

where Fox = oxidized FMN
FSQ = flavin semiquinone
FHQ = flavin hydroquinone (reduced FMN)
S = substrate
P = product
A = electron acceptor

of turnover of the flavoprotein is not only limited by lactate to flavin electron transfer but also by the rate of oxidation of the flavin hydroquinone by ferricyanide. The ferricyanide K_m determined for the isolated $\underline{b}_2$-flavin domain is of a similar magnitude to that observed for the dehaemoenzyme (Table 5.4). It would therefore seem likely that the $\underline{b}_2$-flavin domain, which is totally devoid of haem, should show similar characteristics to the dehaemoenzyme with respect to ferricyanide.

5.3.3 STOPPED-FLOW KINETICS

The reduction of FMN in the $\underline{b}_2$-flavin domain expressed in *E.coli* was investigated by stopped-flow kinetics using both L-[2-^{1}H] and L-[2-^{2}H] lactate as substrates. At all lactate concentrations used, monophasic traces were observed for FMN reduction (Figure 5.5). This is in agreement with observations for dehaemoflavocytochrome $\underline{b}_2$ [5] but contrasts dramatically with the results obtained for holo-flavocytochrome $\underline{b}_2$, which displays biphasic kinetics for FMN reduction [4,12,13]. In the wild-type enzyme the two phases can be accounted for by the initial reduction of FMN (and subsequently of the haem group) by two electrons from one molecule of L-lactate (fast phase) followed by the entry of a third electron into the protomer [12,13]. One scheme proposed to account for this observation is represented in Figure 5.6(a). After oxidation of one molecule of lactate at each protomer, intramolecular rearrangement of electrons within the tetramer generates two fully-reduced and two fully-oxidized FMN centres. This facilitates oxidation of a further two molecules of lactate by the tetramer, effectively constituting the entry of a third electron per protomer. Unlike the holoenzyme,

FIGURE 5.5 MONOPHASIC TRACE OBSERVED FOR FMN REDUCTION IN b_5-FLAVIN DOMAIN UNDER STOPPED-FLOW CONDITIONS

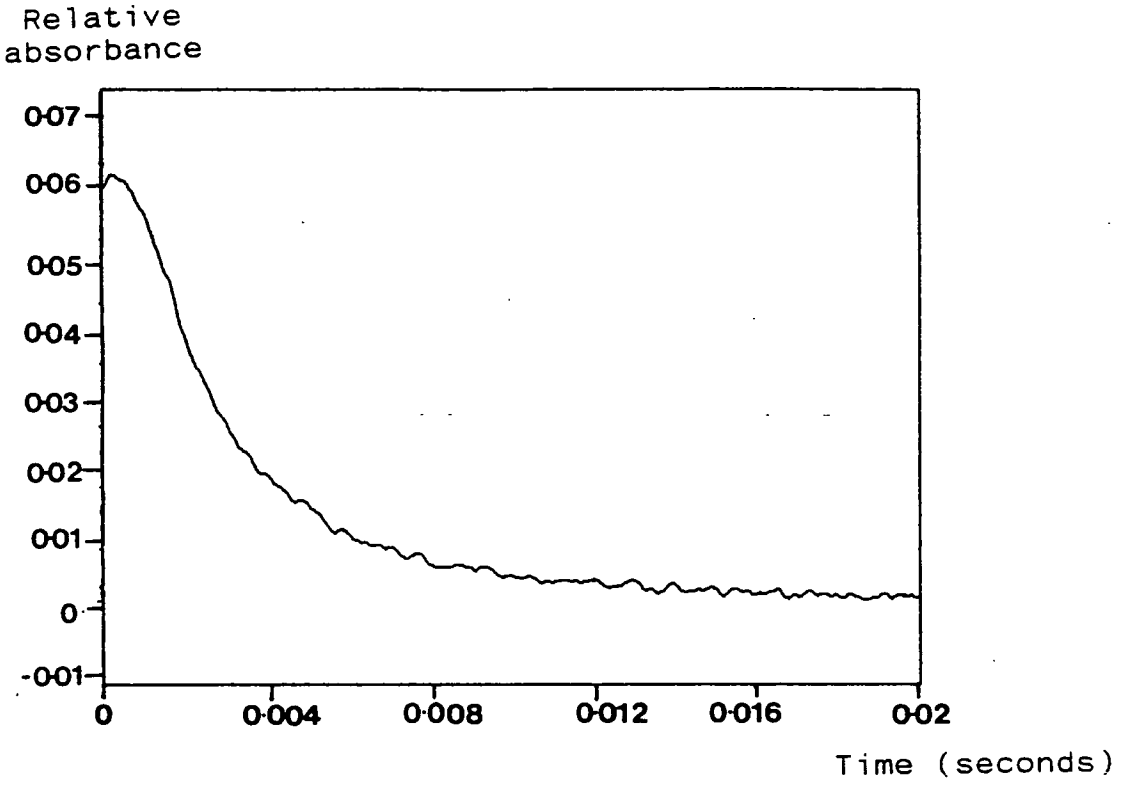

FIGURE 5.6 PROPOSED SCHEME FOR ELECTRON TRANSFER IN HOLO-FLAVOCYTOCHROME $\underline{b}_2$ AND ISOLATED $\underline{b}_2$-FLAVIN DOMAIN

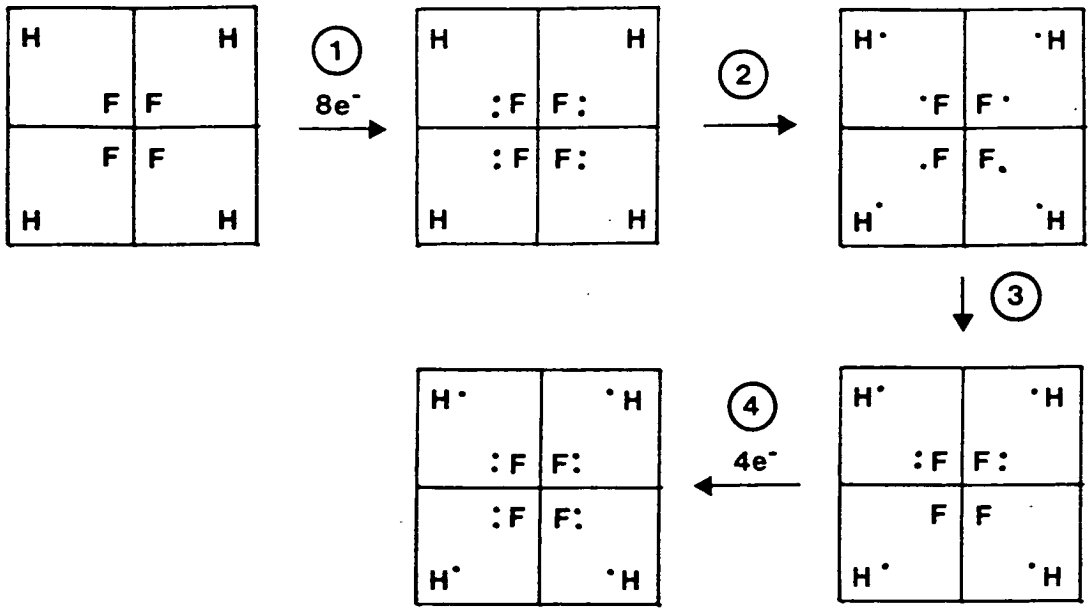

(a) REDUCTION OF FLAVOCYTOCHROME $\underline{b}_2$ TETRAMER

1 Reduction of 4xFMN by 8 electrons
2 Reduction of haems
3 Intramolecular electron rearrangement
4 Full reduction of tetramer by a further 4 electrons

Steps 1-3 form the fast phase, step 4 the slow phase

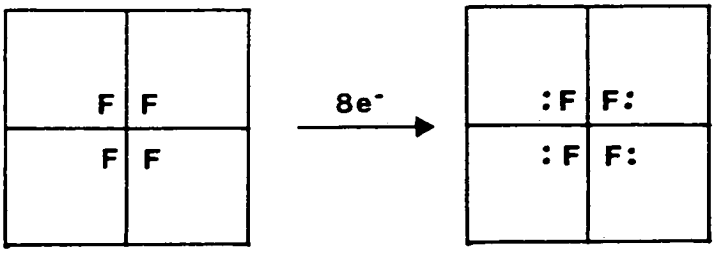

(b) REDUCTION OF $\underline{b}_2$-FLAVIN DOMAIN TETRAMER

Full reduction of tetramer by 8 electrons; one phase

Abbreviations: F = flavin mononucleotide
H = haem
e^- = electron
· = electron

$\underline{b}_2$-flavin domain has no prosthetic haem to accept electrons from the oxidized FMN, and therefore such an intramolecular rearrangement is impossible in the isolated domain. Thus by this model, only a single phase would be expected for flavin reduction in the isolated $\underline{b}_2$-flavin domain (Figure 5.6(b)). Wild-type flavocytochrome $\underline{b}_2$, on the other hand, requires three electrons per protomer or twelve per tetramer (two electrons each from six molecules of lactate) for complete reduction [12], the isolated $\underline{b}_2$-flavin domain requires only two electrons per protomer or eight electrons per tetramer (two each from four molecules of lactate).

A Michaelis-Menten plot of some of the kinetic data obtained for $\underline{b}_2$-flavin domain from stopped-flow studies is shown in Figure 5.7, and kinetic parameters determined for the $\underline{b}_2$-flavin domain with [2-^{1}H] and [2-^{2}H] lactate are compared with values for the holoenzyme in Table 5.5. The observed value of k_{cat} ($\sim 400 s^{-1}$) for FMN reduction by ^{1}H-lactate in the $\underline{b}_2$-flavin domain is only a little lower than that observed for the holoenzyme ($\sim 600 s^{-1}$). The KIEs observed for FMN reduction in both the $\underline{b}_2$-flavin domain and the holoenzyme are the same, within experimental error, further illustrating their similarity in terms of the reduction of flavin by lactate. However, the K_m value for the isolated $\underline{b}_2$-flavin domain is lower than that observed for the holoenzyme with both [2-^{1}H] and [2-^{2}H] lactate, suggesting that lactate binding is more effective in the isolated $\underline{b}_2$-flavin domain than in the holoenzyme. Nevertheless, the rate-determining step is the same in the isolated $\underline{b}_2$-flavin domain as in the holoenzyme (proton abstraction at C-2 of lactate) as illustrated by the agreement in KIE values for the two enzymes.

FIGURE 5.7 MICHAELIS-MENTEN PLOT FOR THE REDUCTION OF b_2-FLAVIN DOMAIN BY L-[2-^{1}H] LACTATE UNDER STOPPED-FLOW CONDITIONS

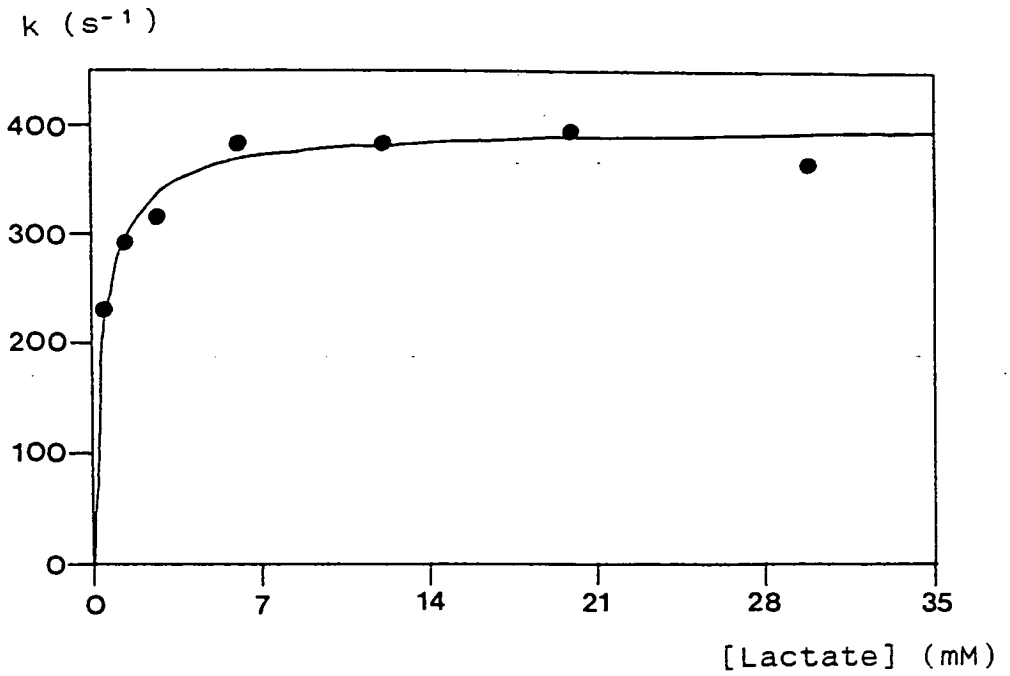

Experimental conditions are described in Section 5.2

TABLE 5.5: STOPPED-FLOW KINETIC PARAMETERS AND ^{2}H-KINETIC ISOTOPE EFFECTS (KIEs) FOR HOLO-FLAVOCYTOCHROME $\underline{b}_2$ AND ISOLATED $\underline{b}_2$-FLAVIN DOMAIN

Enzyme	k_{cat} (s^{-1})		Km (mM)		KIE	Ref.
	[^{1}H]lac	[^{2}H]lac	[^{1}H]lac	[^{2}H]lac		
Holoenzyme*	604 ± 60	75 ± 5	0.84 ± 0.2	1.33 ± 0.28	6.3 ± 0.7	[4]
$\underline{b}_2$-flavin domain	390 ± 10	69 ± 3	0.26 ± 0.07	0.38 ± 0.09	5.8 ± 0.3	This work

*Flavin mononucleotide reduction, fast phase

For conditions and abbreviations, see legend for Table 5.2

5.3.4 FURTHER DISCUSSION OF COMBINED KINETICS RESULTS

Prior to the expression of the $\underline{b}_2$-flavin domain in *E.coli*, attempts to study its function in isolation had focussed on studies of dehaemoenzyme - holoenzyme from which both prosthetic groups were removed by denaturation, which was then reconstituted with FMN only [5]. The true value of such studies was brought into question when it was suggested that conformational differences may exist between native and reconstituted flavocytochrome $\underline{b}_2$ [6]. However, many similarities have been found between the kinetic characteristics of the dehaemoenzyme and the isolated $\underline{b}_2$-flavin domain. Both have L-lactate dehydrogenase activity when ferricyanide is used as the electron acceptor but not when cytochrome $\underline{c}$ is used; their reaction rates both show a dependence on ferricyanide concentration; and FMN reduction is monophasic in both enzymes, when studied under stopped-flow conditions. Although the kinetic parameters recorded for the $\underline{b}_2$-flavin domain and the dehaemoenzyme are not in close agreement it should be remembered that the dehaemoenzyme was prepared from the "cleaved" form of flavocytochrome $\underline{b}_2$, which does show some kinetic differences to the intact form [6]. Also, slightly different experimental conditions were used.

From steady-state kinetic studies the $\underline{b}_2$-flavin domain appears to be an efficient L-lactate dehydrogenase with the same rate-determining step as the holoenzyme. The proposed catalytic cycle for the isolated $\underline{b}_2$-flavin domain is shown in Figures 5.8 and 5.9. The first step in the cycle, FMN reduction, is slower in the isolated $\underline{b}_2$-flavin domain than in the holoenzyme (Figure 5.9) even though all of the catalytically-important active site residues [14] have been conserved. Computer modelling studies of the crystal

FIGURE 5.8 PROPOSED PATHWAY OF ELECTRON TRANSFER IN ISOLATED $\underline{b}_2$-FLAVIN DOMAIN

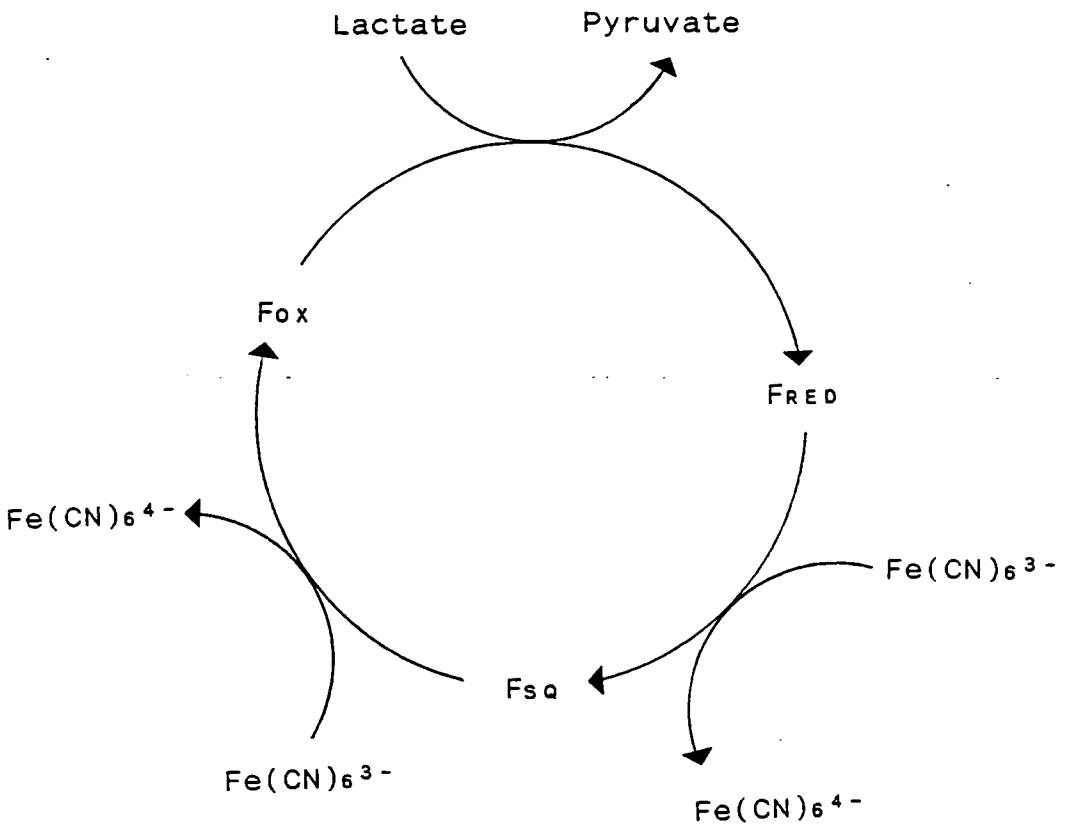

Abbreviations: FOX = oxidized FMN
FRED = reduced FMN
FSQ = flavin semiquinone

FIGURE 5.9 PATHWAY OF ELECTRON TRANSFER IN $\underline{b}_2$-FLAVIN DOMAIN, COMPARING RATE CONSTANTS FOR $\underline{b}_2$-FLAVIN DOMAIN AND HOLO-FLAVOCYTOCHROME $\underline{b}_2$

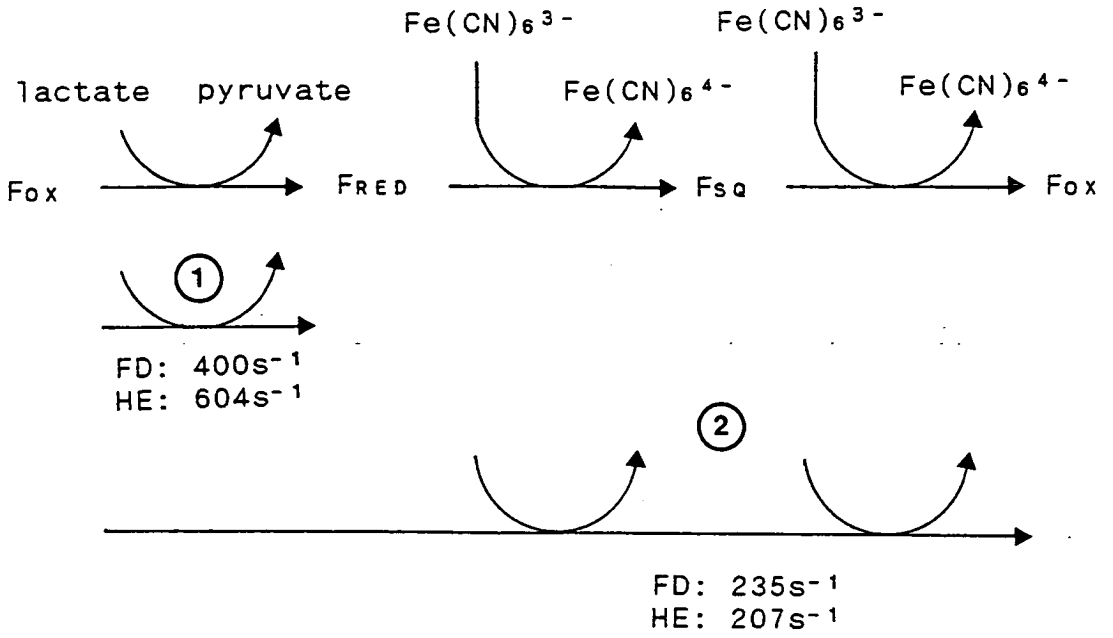

Rate constants are reported at 25°C for holo-flavocytochrome $\underline{b}_2$ [4] and $\underline{b}_2$-flavin domain.

(1) L-lactate ⟶ FMN electron transfer
(2) L-lactate ⟶ ferricyanide electron transfer

Abbreviations: F_{OX} = oxidized flavin
F_{SQ} = flavin semiquinone
F_{HQ} = flavin hydroquinone
FD = $\underline{b}_2$-flavin domain
HE = holo-flavocytochrome $\underline{b}_2$

structure of flavocytochrome $\underline{b}_2$ have found a solvent-accessible channel lying between the two domains, which has been hypothesised as a possible route via which substrate reaches the active site [15]. Removal of the haem domain would disrupt this channel, increasing the accessibility of the active site to solvent. This would vastly alter the dielectric nature of the active site, thus affecting catalyis, and could account for the slower FMN reduction observed in the isolated $\underline{b}_2$-flavin domain.

5.4 CONCLUSIONS

Expression of the $\underline{b}_2$-flavin domain in *E.coli* has provided a means of directly observing both spectroscopic and kinetic properties of the flavodehydrogenase moiety of flavocytochrome $\underline{b}_2$. The isolated $\underline{b}_2$-flavin domain has an electronic absorption spectrum which is typical of an FMN-containing flavoprotein and is in agreement with observations of the dehaemoenzyme [5].

The isolated $\underline{b}_2$-flavin domain is an efficient L-lactate dehydrogenase but is incapable of reducing cytochrome $\underline{c}$.

Steady-state kinetic studies have been carried out using ferricyanide as the electron acceptor, and in conjunction with stopped-flow techniques, these experiments reveal that $\underline{b}_2$-flavin domain shares the same overall rate-determining step as the holoenzyme.

In marked contrast to the holoenzyme, which displays biphasic reduction, FMN reduction in the isolated $\underline{b}_2$ flavin domain is monophasic. This is a result of the removal of the haem domain, which precludes any interprotomer electron transfer after initial reduction of FMN.

5.5 REFERENCES

[1] Boudras, A., Bull. Soc. Chim. Biol. **47**, 1143-1175 (1965)

[2] Mathews, F.S. & Xia, Z.-x., in "Flavins and Flavoproteins 1987" (D.E. Edmondson & D.B. McCormick, eds)., Walter de Gruyter & Co., New York, 123-132 (1987)

[3] Xia, Z-x. & Mathews, F.S., J. Mol. Biol. **212**, 837-863 (1990)

[4] Miles, C.S., Rouviere-Fourmy, N., Lederer, F., Mathews, F.S., Reid, G.A., Black, M.T. & Chapman, S.K., Biochem. J. **285**, 187-192 (1992)

[5] Iwatsubo, M., Mevel-Ninio, M. & Labeyrie, F., Biochemistry **16**, 3558-3566 (1977)

[6] Lederer, F., in "Chemistry and Biochemistry of Flavoenzymes" (Muller, F., ed) CRC Press Inc., Boca Raton, 153-242 (1991)

[7] Lederer, F., Eur. J. Biochem **88**, 425-431 (1978)

[8] Gervais, M., Groudinsky, O., Risler, Y. & Labeyrie, F., Biochem. Biophys. Res. Commun. **77**, 1543-1551 (1977)

[9] Gervais, M., Risler, Y., Capeillere-Blandin, C., Vergnes, O. & Labeyrie, F., in "Limited Proteolysis in Microorganisms" (Cohen, G.N. & Holzer, H., eds), US Government Printing Office, Washington DC, 227-234 (1979)

[10] Gervais, M., Risler, Y. & Corrazzin, S., Eur. J. Biochem. **130**, 253-259 (1983)

[11] Celerier, J., Risler, Y., Schwenke, J., Janot, J-M. & Gervais, M., Eur. J. Biochem. **182**, 67-75 (1989)

[12] Pompon, D., Iwatsubo, M. & Lederer, F., Eur. J. Biochem. **104**, 479-488 (1980)

[13] Capeillere-Blandin, C., Bray, R.C., Iwatsubo, M. & Labeyrie, F., Eur. J. Biochem. **54**, 549-566 (1975)

[14] Chapman, S.K., White, S.A. & Reid, G.A., Adv. Inorg. Chem. **36**, 257-301 (1991)

[15] Tegoni, M., unpublished results

CHAPTER 6

b_2-FLAVIN DOMAIN:

INHIBITION STUDIES

6.1 INTRODUCTION

An inhibitor is a substance which causes the rate of an enzyme-catalysed reaction to decrease, by binding either reversibly or irreversibly to the enzyme or enzyme-substrate complex. The four major modes of reversible inhibition [1,2] are: (i) competitive, in which the inhibitor competes with the substrate for one binding site (the active site), affecting K_m but not k_{cat} (Figure 6.1 (a)); (ii) uncompetitive, in which the inhibitor binds at a different site to the substrate. Both inhibitor and substrate bind simultaneously but do not compete for the same site, decreasing k_{cat} but leaving K_m unaffected (Figure 6.1 (b)); (iii) non-competitive, when the inhibitor binds only to the enzyme-substrate complex, altering both K_m and k_{cat} (Figure 6.1 (c)); (iv) mixed, when substrate-binding and inhibitor-binding are not independent but arise from a mixture of two of the other types of inhibition (i)-(iii). Again both k_{cat} and K_m are affected (Figure 6.1 (d)).

Figure 6.1 (e) shows the Lineweaver-Burk and double reciprocal plots for substrate inhibition. This occurs when, at increasing substrate concentrations, the rate of reaction decreases below V_{max} In general this type of inhibition occurs when one molecule of substrate binds at the active site, after which another molecule of substrate binds to a separate site to form a dead-end complex. Substrate inhibition is therefore a form of uncompetitive inhibition, the second substrate molecule acting as the inhibitor.

Various inhibitors of flavocytochrome $\underline{b}_2$ have been studied [3], the most notable being pyruvate and oxalate. The inhibitory effects of excess substrate and of these molecules on the isolated $\underline{b}_2$-flavin domain have been investigated. The results of inhibition studies

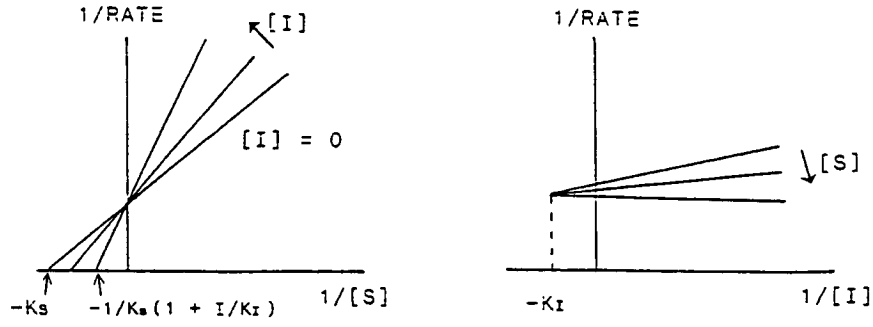

(a) Competitive

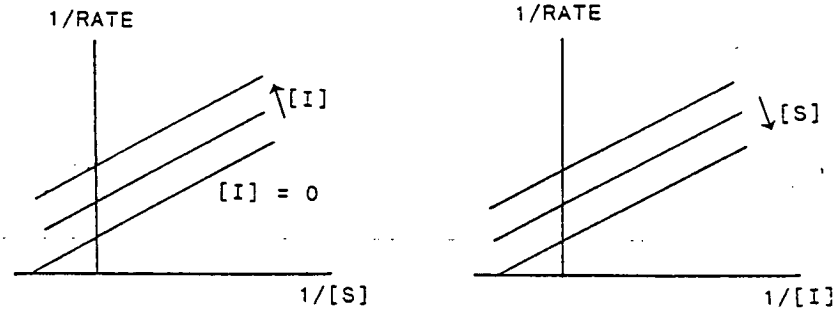

(b) Uncompetitive

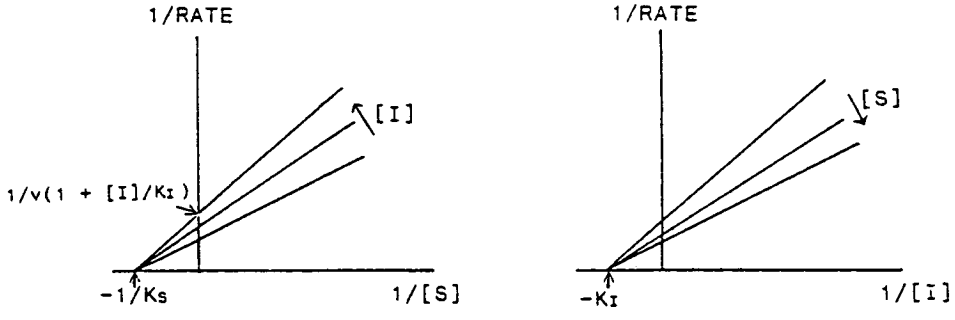

(c) Non-competitive

FIGURE 6.1 TYPICAL PLOTS FOR ENZYME INHIBITION

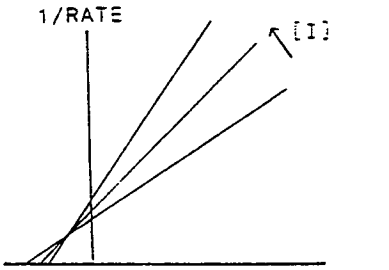

(d) Mixed

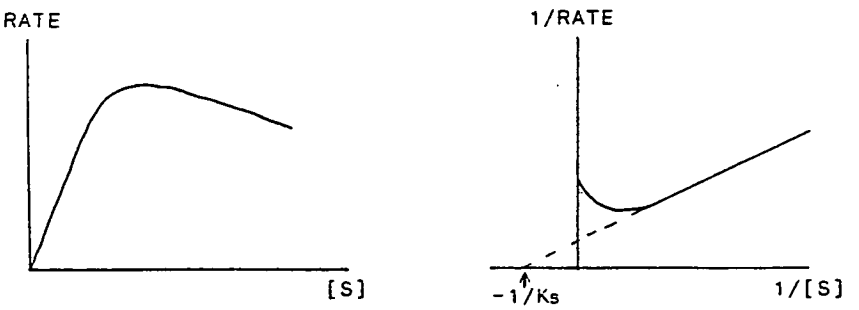

(e) Inhibition by excess substrate

S = substrate
I = inhibitor

are summarised in Table 6.1.

6.2 EXPERIMENTAL

6.2.1 PREPARATION OF INHIBITORS

Inhibitors were prepared as solutions in Tris.HCl buffer, pH 7.5, I=0.10M. The inhibitors used were L(+)-lactic acid (sodium salt) (Sigma), pyruvic acid (sodium salt) (Fluka) and sodium oxalate (Fisons).

6.2.2 KINETIC STUDIES

Kinetic studies were carried out under steady-state conditions as described in Section 5.2.2. All experiments were performed at 2mM ferricyanide except for those using L(+)-lactate, which were performed at both 1mM and 2mM ferricyanide. Kinetic parameters were evaluated graphically or by fitting to a linear least mean squares program.

6.3 RESULTS AND DISCUSSION

6.3.1 INHIBITION BY EXCESS L(+)-LACTATE

The results obtained from substrate inhibition studies of the $\underline{b}_2$-flavin domain at subsaturating ferricyanide concentrations are represented graphically in Figure 6.2. The isolated $\underline{b}_2$-flavin domain, unlike the holoenzyme, does not show any appreciable inhibition by excess substrate at lactate concentrations up to 20mM when the electron acceptor (ferricyanide) is saturating. However, at subsaturating ferricyanide concentrations a typical

TABLE 6.1: A COMPARISON OF KINETIC PARAMETERS FOR THE INHIBITION OF $\underline{b}_2$-FLAVIN DOMAIN AND HOLOFLAVOCYTOCHROME $\underline{b}_2$

Inhibitor	$\underline{b}_2$-flavin domain				Holoflavocytochrome $\underline{b}_2$		
	Type of inhibition		K_I (mM)	S_{opt} (mM)	Type of inhibition	K_I (mM)	S_{opt} (mM)
L-lactate	Excess substrate	Saturating $Fe(CN)_6^{3-}$	73 ± 4	5	Excess substrate [4]	174 ± 8	10
		Subsaturating $Fe(CN)_6^{3-}$	186 ± 32	7			
Pyruvate	Non-competitive		10 ± 5		Competitive (low concentrations)	3	
					Non-competitive (high concentrations) [10]	30	

Oxalate	Uncompetitive (low lactate)	1.92 ± 0.4	Mixed [4,10]
	Mixed (high lactate)	0.16 ± 0.07	

K_I values are the eoncentration of inhibitor at which the observed rate is half the maximum.

s_{opt} is the substrate concentration at which the maximum rate is observed.

FIGURE 6.2 INHIBITION OF b_2-FLAVIN DOMAIN BY EXCESS SUBSTRATE AT SUBSATURATING FERRICYANIDE CONCENTRATION

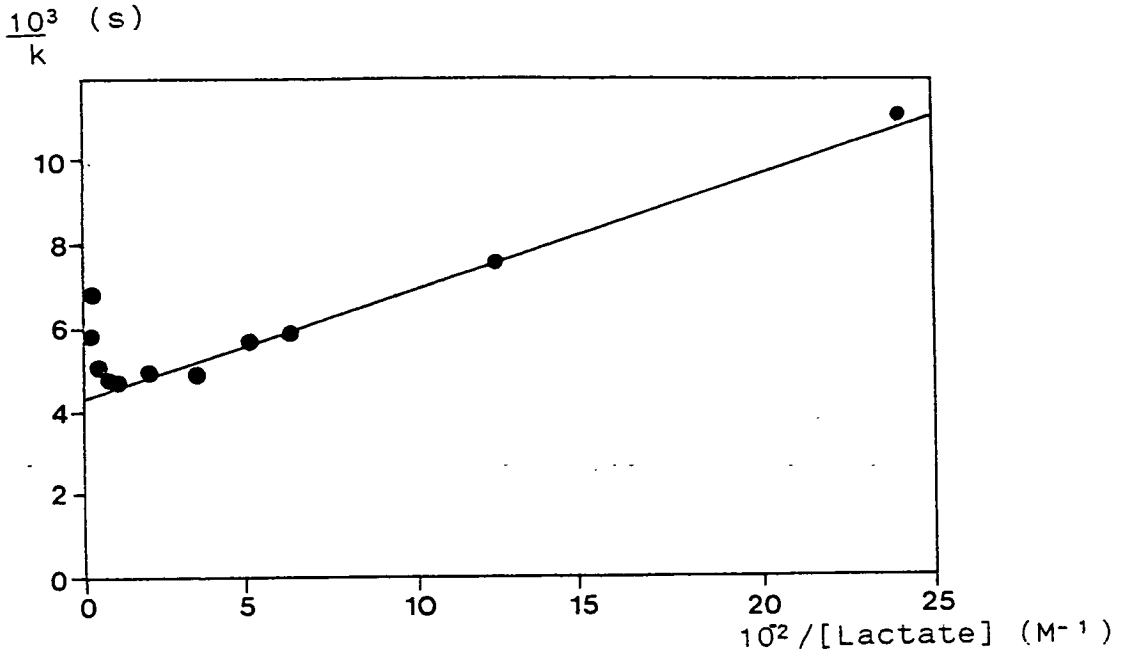

(a) DOUBLE-RECIPROCAL PLOT

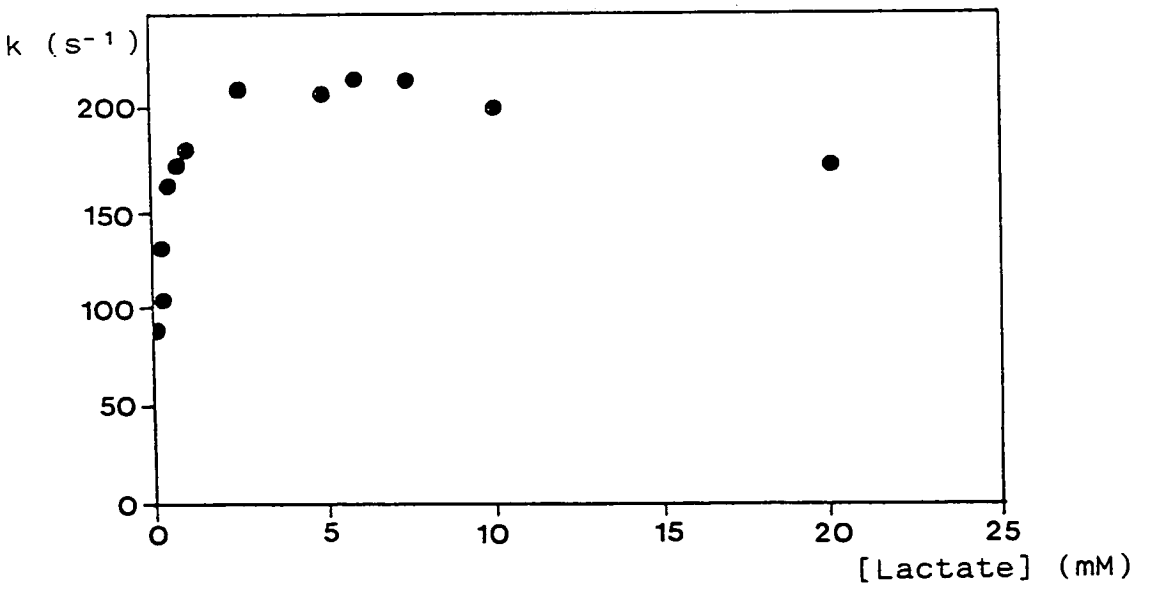

(b) MICHAELIS-MENTEN PLOT

Experimental conditions are described in Section 6.2

curve for substrate inhibition is observed (Figure 6.2(b)).

From Table 6.1 it can be seen that the parameters observed for $\underline{b}_2$-flavin domain at subsaturating ferricyanide concentrations are close to those observed for the holoenzyme. One theory advanced for substrate inhibition is that there are two binding modes at the active site [4]. In the isolated $\underline{b}_2$-flavin domain, electrons are donated to ferricyanide from either the flavin hydroquinone or semiquinone, electron transfer from the semiquinone to ferricyanide being the more rapid of the two [5]. When ferricyanide is saturating, electron transfer would be efficient with both the hydroquinone and semiquinone forms of the FMN being rapidly reoxidized. However, under subsaturating conditions, it may be that reoxidation is delayed sufficiently to allow a build-up of semiquinone to occur, which could then complex with excess substrate, resulting in inhibition. In the case where ferricyanide is saturating, no such build-up of semiquinone would occur and thus no inhibition would be seen.

6.3.2 INHIBITION BY PYRUVATE

Pyruvate, the reaction product of lactate dehydrogenation, is an inhibitor of flavocytochrome $\underline{b}_2$, showing competitive inhibition at low concentrations and non-competitive inhibition at high concentrations (Table 6.1). Initial studies of the inhibition of $\underline{b}_2$-flavin domain by pyruvate appear to indicate that inhibition is non-competitive (Figure 6.3), with a K_I close to that observed for the non-competitive inhibition of the holoenzyme. There is no obvious difference between inhibition of the isolated $\underline{b}_2$-flavin domain at low and high pyruvate concentrations.

FIGURE 6.3 INHIBITION OF b_2-FLAVIN DOMAIN BY PYRUVATE

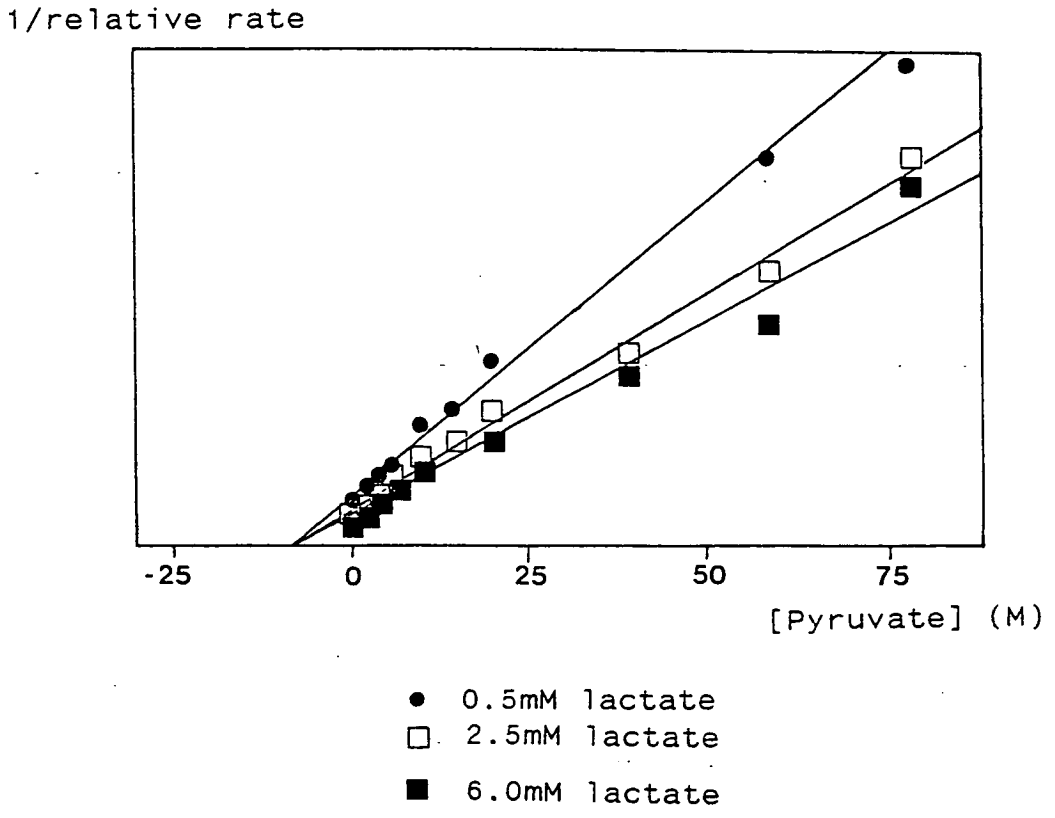

Experimental conditions are described in Section 6.2

Studies on flavocytochrome $\underline{b}_2$ from H.anomala have shown that the complex formed between pyruvate and flavin semiquinone is much more stable than the complexes of pyruvate with the fully-reduced and fully-oxidized forms of the flavin [6]. The same study concluded that the non-competitive inhibition observed at high pyruvate concentrations was the result of the sum of a competitive effect arising from pyruvate binding at fully-oxidized FMN and an uncompetitive effect due to the formation of a "dead-end" complex between the flavin semiquinone and pyruvate, incapable of undergoing further reaction. The non-competitive inhibition observed for $\underline{b}_2$-flavin domain in the presence of pyruvate can be attributed to a similar process.

6.3.3 INHIBITION BY OXALATE

Oxalate has long been known to be a strong inhibitor of flavocytochrome $\underline{b}_2$, showing mixed competitive-noncompetitive inhibition with the holoenzyme ([3], and references therein). It is also well known as an inhibitor of other enzymes which oxidize lactate [7], notably lactate oxidase [8], the active site of which is analogous to that of flavocytochrome $\underline{b}_2$ [5,7]. Oxalate has been suggested to be a transition state analogue for the carbanion intermediate formed during catalysis by flavocytochrome $\underline{b}_2$ (Figure 6.4) [9].

The double-reciprocal plots obtained for the inhibition of $\underline{b}_2$-flavin domain by oxalate are shown in Figure 6.5, and the values of K_I from these graphs appear in Table 6.1. At saturating concentrations of L(+)-lactate, mixed (competitive and non-competitive) inhibition is observed, as for the holoenzyme [4,10]. However at

FIGURE 6.4 OXALATE AS AN ANALOGUE FOR THE TRANSIENT CARBANION INTERMEDIATE

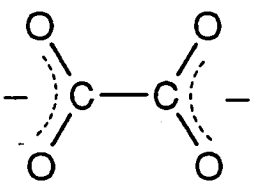

Oxalate

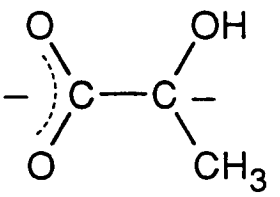

Proposed intermediate

FIGURE 6.5 INHIBITION OF $\underline{b}_2$-FLAVIN DOMAIN BY OXALATE

(a) [Lactate] $\leqslant$ 2mM: uncompetitive inhibition

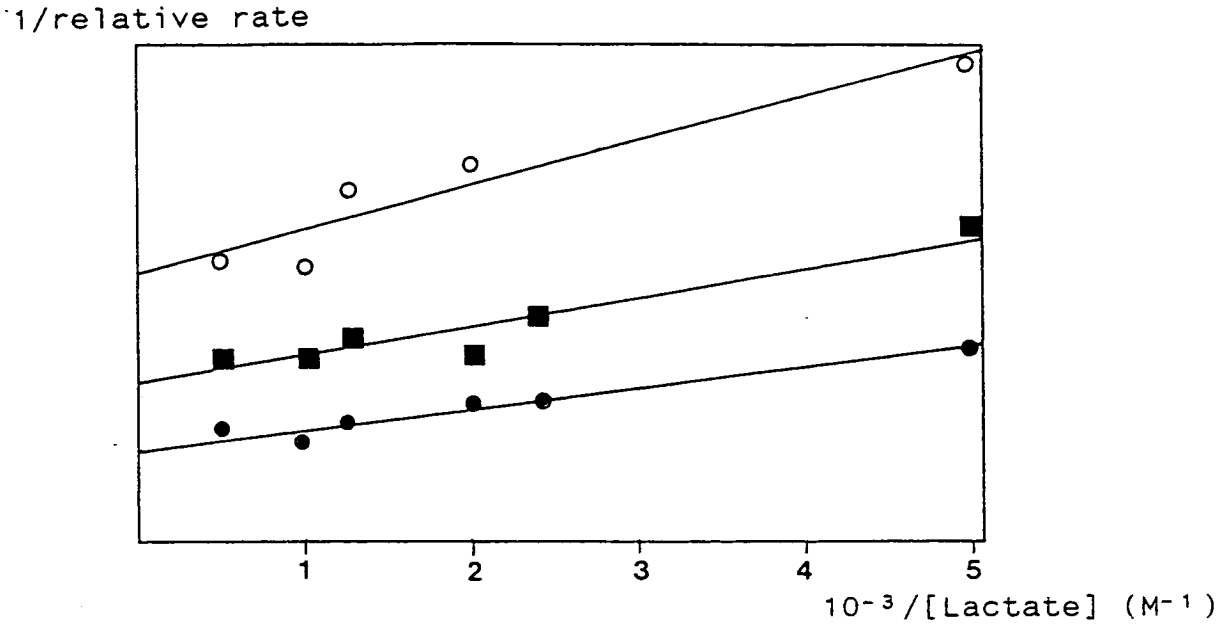

(b) [Lactate] $\geqslant$ 2mM: mixed inhibition

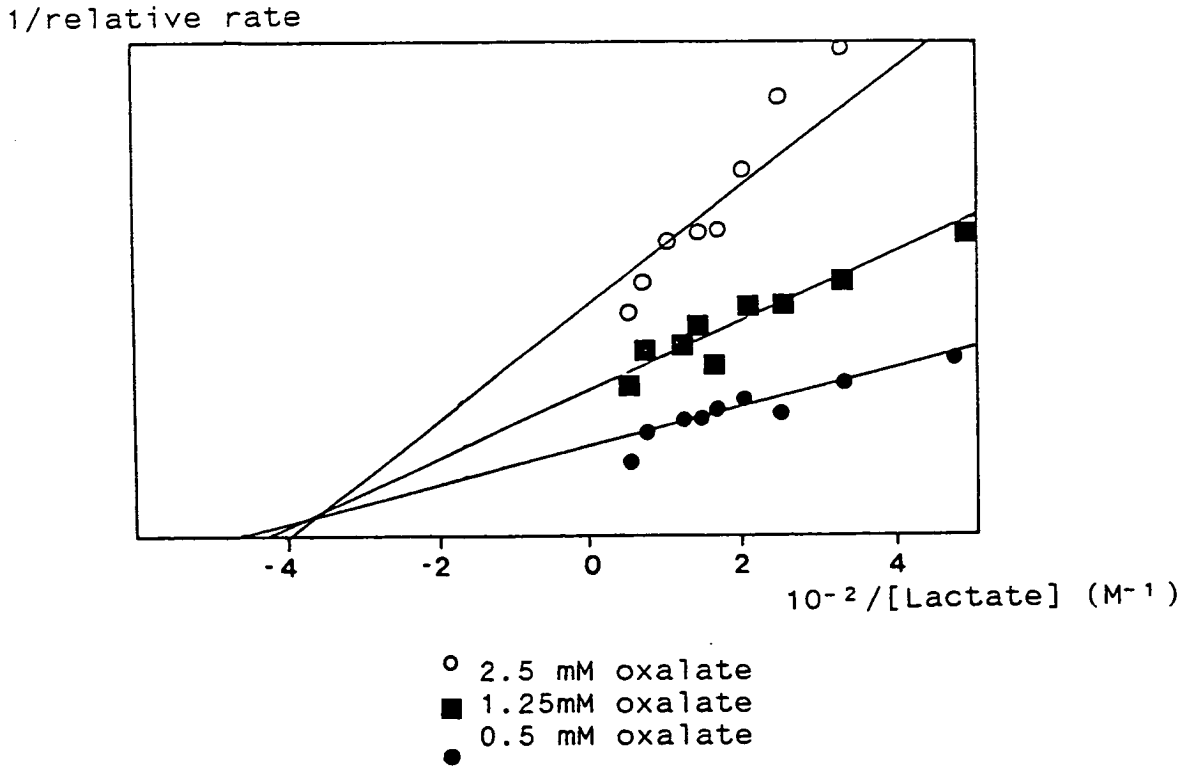

Experimental conditions are described in Section 6.2

lower, subsaturating, substrate concentrations, inhibition of the $\underline{b}_2$-flavin domain by oxalate is clearly uncompetitive. The K_I values show that the inhibitory effect of oxalate is much stronger at high concentrations of substrate.

The mixed inhibition of holo-flavocytochrome $\underline{b}_2$ was explained in terms of a ternary complex between the Michaelis complex formed during enzyme turnover and oxalate [11]. This leaves the uncompetitive inhibition observed for the $\underline{b}_2$-flavin domain at low substrate concentrations unexplained. Uncompetitive inhibitors bind only to the enzyme-substrate complex and not to the free enzyme [2]. It must be remembered that by removing the entire haem domain from the holoenzyme many regions of protein which are normally inaccessible to solvent and to substrate become exposed. Such exposed residues in the $\underline{b}_2$-flavin domain, especially close to the active site, could well provide alternative modes of substrate or inhibitor binding to those seen in the holoenzyme. It is therefore possible that the $\underline{b}_2$-flavin domain-substrate complex is capable of binding oxalate in a different manner to the holoenzyme, resulting in the uncompetitive inhibition seen at low substrate concentrations.

6.4 CONCLUSIONS

Isolated $\underline{b}_2$-flavin domain fails to show any appreciable inhibition by excess substrate at saturating concentrations of the electron acceptor but does exhibit typical substrate inhibition at subsaturating electron acceptor concentrations. This is in marked contrast to the holoenzyme, which exhibits substrate inhibition at saturating ferricyanide concentrations.

Like the holoenzyme, $\underline{b}_2$-flavin domain shows non-competitive

inhibition with pyruvate.

With oxalate, $\underline{b}_2$-flavin domain undergoes mixed inhibition at high substrate concentrations and uncompetitive inhibition at low substrate concentrations. This is unlike the holoenzyme which displays mixed inhibition only.

The observations with excess substrate and oxalate demonstrate the changes in inhibitor binding characteristics introduced on removal of the haem domain from flavocytochrome $\underline{b}_2$.

6.5 REFERENCES

[1] Mahler, H.R. & Cordes, E.H., "Biological Chemistry" (2nd Edition), Harper & Row, 267-234 (1971)

[2] Palmer, T., "Understanding Enzymes" (2nd Edition), Ellis Horwood, 142-164 (1985)

[3] Lederer, F., in "Chemistry and Biochemistry of Flavoenzymes" (Muller, F., ed) CRC Press Inc., Boca Raton, 153-242 (1991)

[4] Miles, C.S., PhD Thesis, University of Edinburgh (1992)

[5] Iwatsubo, M., Mevel-Ninio, M. & Labeyrie, F., Biochemistry **16**, 3558-3566 (1977)

[6] Tegoni, M., Janot, J.-M. & Labeyrie, F., Eur. J. Biochem. **190**, 329-342 (1990)

[7] Ghisla, S. & Massey, V., in "Chemistry and Biochemistry of Flavoenzymes" (Muller, F., ed), CRC Press Inc., Boca Raton, 153-242 (1991)

[8] Ghisla, S. & Massey, V., J. Biol. Chem. **250**, 577-584 (1975)

[9] Ghisla, S. & Massey, V., J. Biol. Chem. **252**, 6729-6735 (1977)

[10] Lederer, F., Eur. J. Biochem. **88**, 425-431 (1978)

[11] Blàzy, B., Thusius, D. & Baudras, A., Biochemistry **15**, 257-261 (1976)

CHAPTER 7

CHARACTERIZATION OF A b_2-FLAVIN DOMAIN POINT MUTANT

7.1 INTRODUCTION

Site-directed mutagenesis has been used in the past to probe the roles of active site amino-acid residues in flavocytochrome b_2 expressed in both yeast and *E.coli* [1-3]. This technique allows a specific amino-acid to be replaced by another amino-acid of choice, introducing a desired modification. For example, mutation of a tyrosine to a phenylalanine retains the steric bulk and aromatic character of the side chain, but, by removing the hydroxyl function, removes the capability of that residue to form hydrogen bonds. In a similar manner, mutant forms of the isolated b_2-flavin domain can be utilised to probe the roles of specific amino-acids in electron transfer to FMN, without interference from the haem. This also provides a means of investigating whether the functions of certain residues differ in the isolated b_2-flavin domain compared to the holoenzyme.

One amino-acid residue of particular interest with respect to interdomain electron transfer is Tyrosine 143. This residue lies at the interface of the flavin and haem domains (Figure 7.1) and is involved in a different interaction in each of the crystallographically-distinguishable types of subunit [4]. In subunit 1, with no pyruvate at the active site, Tyr 143 is hydrogen-bonded to a haem propionate. In subunit 2, with pyruvate present at the active site, it is hydrogen-bonded to the carboxylate group of pyruvate (Figure 7.1).

The role of Tyr 143 in the holoenzyme was probed by replacing it with a phenylalanine, in the mutant enzyme Y143F [3]. Kinetic characterisation of Y143F revealed that the rate-determining step was no longer C-2 proton abstraction but interdomain electron transfer. It was concluded that Tyr 143 plays a key role in flavin

FIGURE 7.1 THE ROLE OF TYR 143 IN THE TWO CRYSTALLOGRAPHICALLY-DISTINCT SUBUNITS OF FLAVOCYTOCHROME $\underline{b}_2$

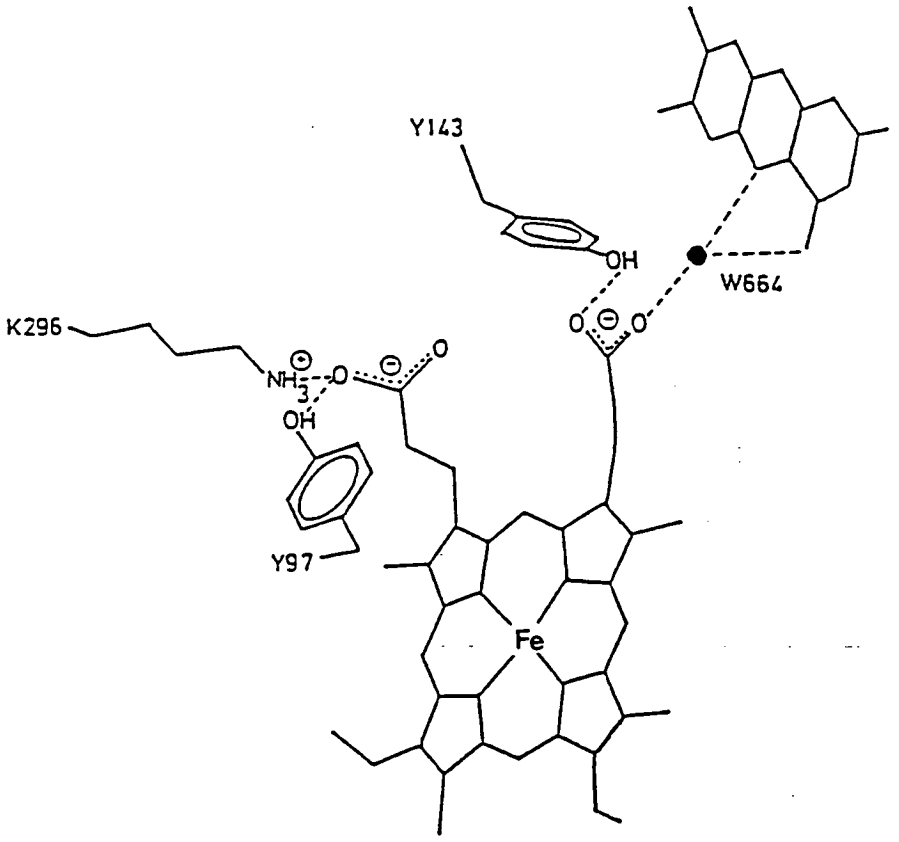

SUBUNIT 1 (PYRUVATE ABSENT)

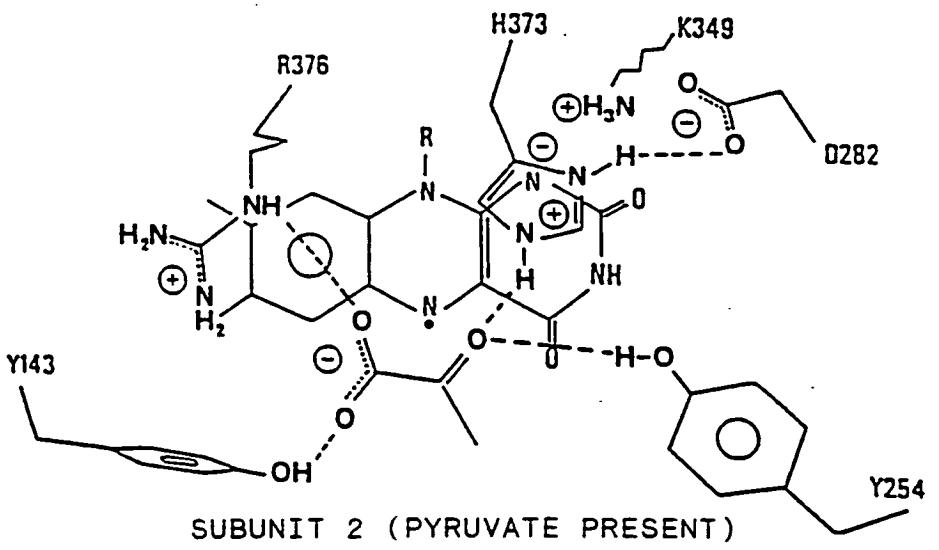

SUBUNIT 2 (PYRUVATE PRESENT)

to haem electron transfer.

In the isolated b_2-flavin domain there can be no interdomain electron transfer and so the role of Tyr 143 is not obvious. A mutant form of isolated b_2-flavin domain with Tyr 143 replaced by Phe has been generated (F.D.C. Manson), enabling the role of Tyr 143 in the dehydrogenation of lactate to be further investigated. The mutant is referred to as FD/Y143F, to distinguish it from the same mutation in the holoenzyme.

7.2 EXPERIMENTAL

7.2.1 CONSTRUCTION OF FD/Y143F (Dr. F.D.C. MANSON)

FD/Y143F was generated by site-directed mutagenesis using the oligonucleotide GTGGGCCTTCTATTCCT, synthesised on an Applied Biosystems model 380B DNA synthesizer. FD/Y143F was expressed in E.coli in the same way as the b_2-flavin domain (Section 4.2). Growth conditions were as described in Section 8.1.4.

7.2.2 ENZYME PREPARATION

FD/Y143F was isolated from E.coli and purified by DE-52 column chromatography as described for b_2-flavin domain (Sections 4.3.1 & 4.3.2).

7.2.3 ENZYME CHARACTERIZATION

FD/Y143F was characterized by steady-state and stopped-flow kinetics under conditions and using procedures described in Section 5.2. Inhibitor studies were carried out as described in Section 6.2.

7.3 RESULTS AND DISCUSSION

7.3.1 STEADY-STATE KINETICS

Results obtained for FD/Y143F under steady-state conditions are summarised in Table 7.1, where they are compared with values for the native $\underline{b}_2$-flavin domain, holoenzyme and Y143F mutation in the holoenzyme (referred to as HE/Y143F). Like HE/Y143F, FD/Y143F has a high K_m for L-lactate and shows a substantial dependence on electron acceptor (ferricyanide) concentration at saturating lactate concentrations. The two mutants also have identical steady-state KIE values, indicating that the rate-determining step is no longer C2 proton abstraction. In HE/Y143F, the rate-determining step is flavin to haem electron transfer [3]. However, FD/Y143F does not contain a haem group and so could not possibly have the same rate-determining step as the holoenzyme mutant.

A striking difference in the steady-state kinetic parameters can be seen in k_{cat} values. For example, k_{cat} for FD/Y143F is almost 8 times smaller than that observed for the isolated $\underline{b}_2$-flavin domain, although k_{cat} for HE/Y143F is the same as for native flavocytochrome $\underline{b}_2$ when ferricyanide is used as the electron acceptor [3]. The overall catalytic efficiency of FD/Y143F is also greatly reduced compared to the isolated $\underline{b}_2$-flavin domain and HE/Y143F (Table 7.1). These observations show that the substitution of Tyr 143 by Phe substantially affects lactate dehydrogenase properties, suggesting that the role of Tyr 143 is important in catalysis in the isolated $\underline{b}_2$-flavin domain. Indeed, the role of Tyr 143 in this context appears, at first glance, to be of greater importance in the isolated $\underline{b}_2$-flavin domain than in the holoenzyme.

TABLE 7.1: STEADY-STATE KINETIC PARAMETERS FOR FD/Y143F COMPARED WITH VALUES FOR HOLO-FLAVOCYTOCHROME $\underline{b}_2$, $\underline{b}_2$-FLAVIN DOMAIN AND HOLO-Y143F

	Holo-$\underline{b}_2$	HE/Y143F	$\underline{b}_2$-flavin domain	FD/Y143F
K_m (lactate) (mM)	0.49 ± 0.05	2.90 ± 0.23	0.27 ± 0.04	1.42 ± 0.45
k_{cat} (s^{-1})	400 ± 10	400 ± 30	235 ± 35	29.5 ± 2.1
KIE	4.7 ± 0.4	2.0 ± 0.4	3.4 ± 0.3	1.9 ± 0.3
k_{cat}/K_m ($m^{-1}s^{-1}$)	8.2×10^5	1.4×10^5	8.7×10^5	2.08×10^4
K_m (ferricyanide) (mM)	<<0.1	3.3 ± 0.6	>0.5	1.2 ± 0.3
Reference	(3)	(3)	This work	This work

All experiments carried out under conditions described in Section 7.2.3

In the isolated $\underline{b}_2$-flavin domain, the active site is exposed to solvent and it can easily be imagined that substrate is more difficult to stabilise in this exposed environment than in the holoenzyme, in which the active site occupies a vacuole which can be closed to solvent by the haem domain. In the isolated $\underline{b}_2$-flavin domain, where there is no haem domain to close the vacuole, the role of Tyr 143 might be more important for lactate dehydrogenase activity.

The behaviour of FD/Y143F with inhibitors (L-lactate, oxalate and pyruvate) is illustrated in Figure 7.2 and compared with the behaviour seen for isolated $\underline{b}_2$-flavin domain in Table 7.2. The behaviour of the FD/Y143F mutant is different to that of the isolated $\underline{b}_2$-flavin domain but is similar to HE/Y143F with respect to L-lactate and oxalate. The value of K_I observed for FD/Y143F with oxalate is greater than that observed for $\underline{b}_2$-flavin domain, showing that oxalate binding to FD/Y143F is weaker than to $\underline{b}_2$-flavin domain. This is consistent with the observation for HE/Y143F in comparison with the holoenzyme [10]. The higher K_I for oxalate in HE/Y143F, along with previous results from circular dichroism (CD) spectroscopy, also showed Tyr 143 to be involved in oxalate binding [10].

Oxalate is considered to be analogous to the transient carbanion formed during catalysis (Figure 7.3)[12], and hence to the structure of the intermediate species formed during the reaction. The above observations would therefore suggest that, according to the Hammond postulate which states that the transition state and intermediate are similar in structure, Tyr 143 plays an important role in transition state stabilisation. Further confirmation of this can be obtained from the difference in free energy for oxalate

FIGURE 7.2 THE BEHAVIOUR OF FD/Y143F WITH INHIBITORS

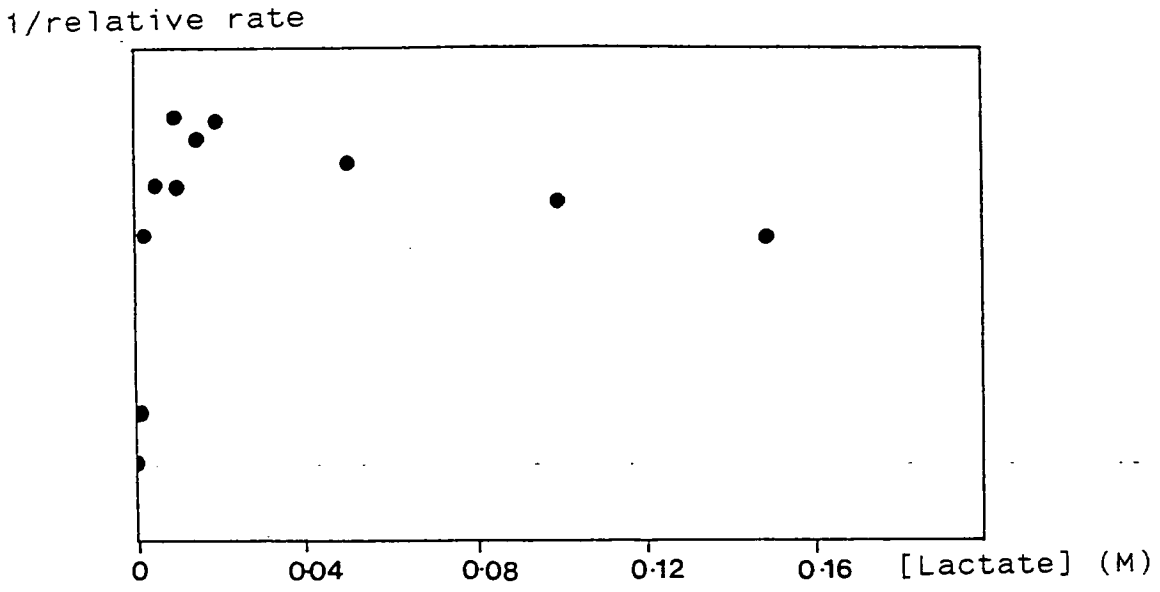

(a) Excess substrate

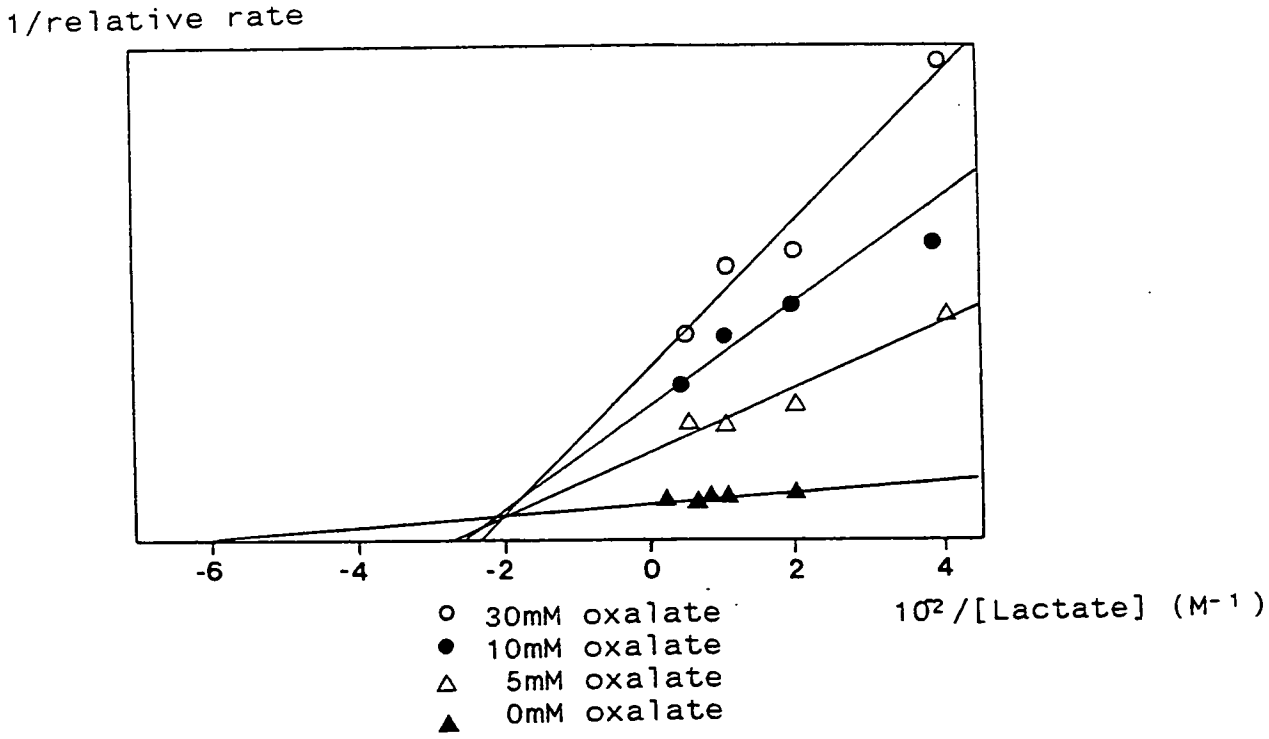

(b) Oxalate

FIGURE 7.2 (CONTINUED)

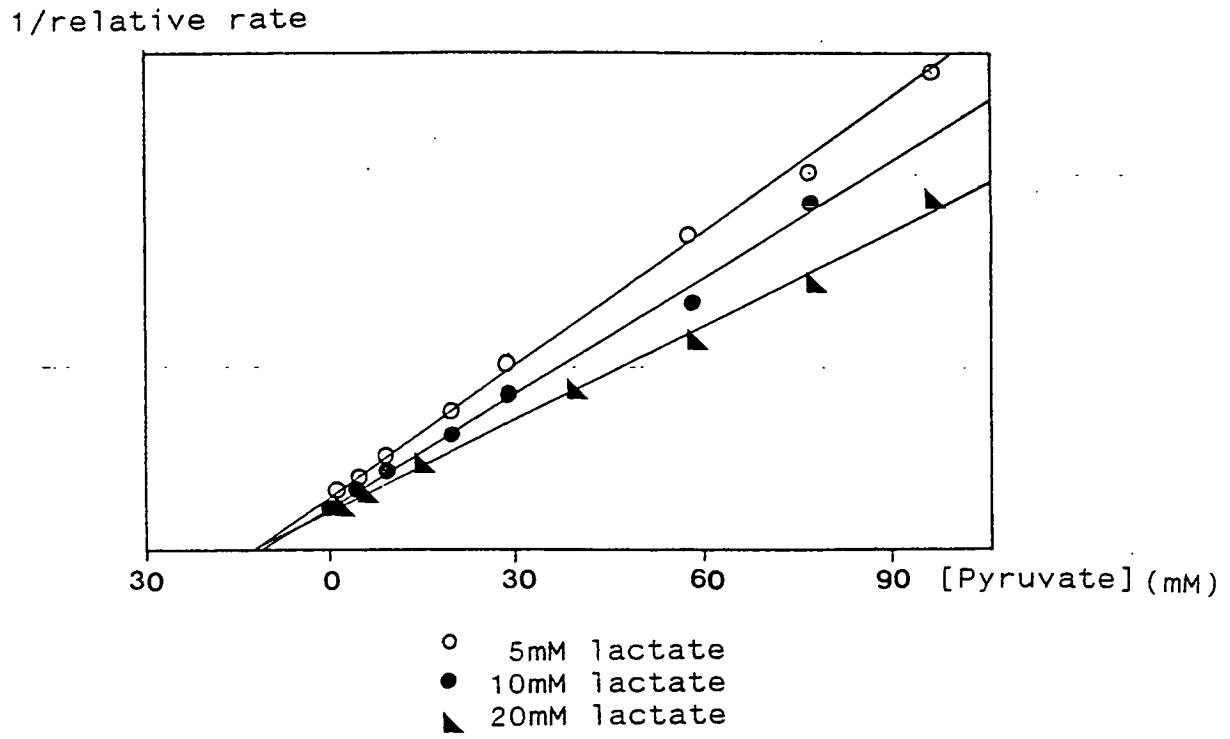

(c) Pyruvate

Experimental conditions are described in Section 7.2

INHIBITOR	holo-$\underline{b}_2$	HE/Y143F [10]
L-lactate	Excess substrate inhibition $K_I = 174 \pm 8$ [10]	Excess substrate inhibition $K_I = 324 \pm 15$ [10]
Oxalate	Mixed [11,10]	Mixed [10]
Pyruvate	High conc.: Competitive $K_I = 3mM$ Low conc.: Non-competitive $K_I = 30mM$ [11]	-

TABLE 7.2: BEHAVIOUR OF FD/Y143F, $\underline{b}_2$-FLAVIN DOMAIN, HOLO-FLAVOCYTOCHROME $\underline{b}_2$ AND HOLO-Y143F WITH INHIBITORS

$\underline{b}_2$-flavin domain	FD/Y143F
At saturating $[Fe(CN)_6^{3-}]$	Excess substrate inhibition
$K_I = 73 \pm 4$mM	$K_I \sim 700$mM
Low lactate conc.: Uncompetitive	Mixed
$K_I = 1.92 \pm 0.4$mM	$K_I = 4.4 \pm 0.8$mM
High lactate conc.: Mixed	
$K_I = 0.16 \pm 0.07$mM	
Non-competitive	Competitive
$K_I = 10 \pm 5$mM	K_I 2.5mM

FIGURE 7.3 ENERGY PROFILE OF AN ENZYME-CATALYSED REACTION

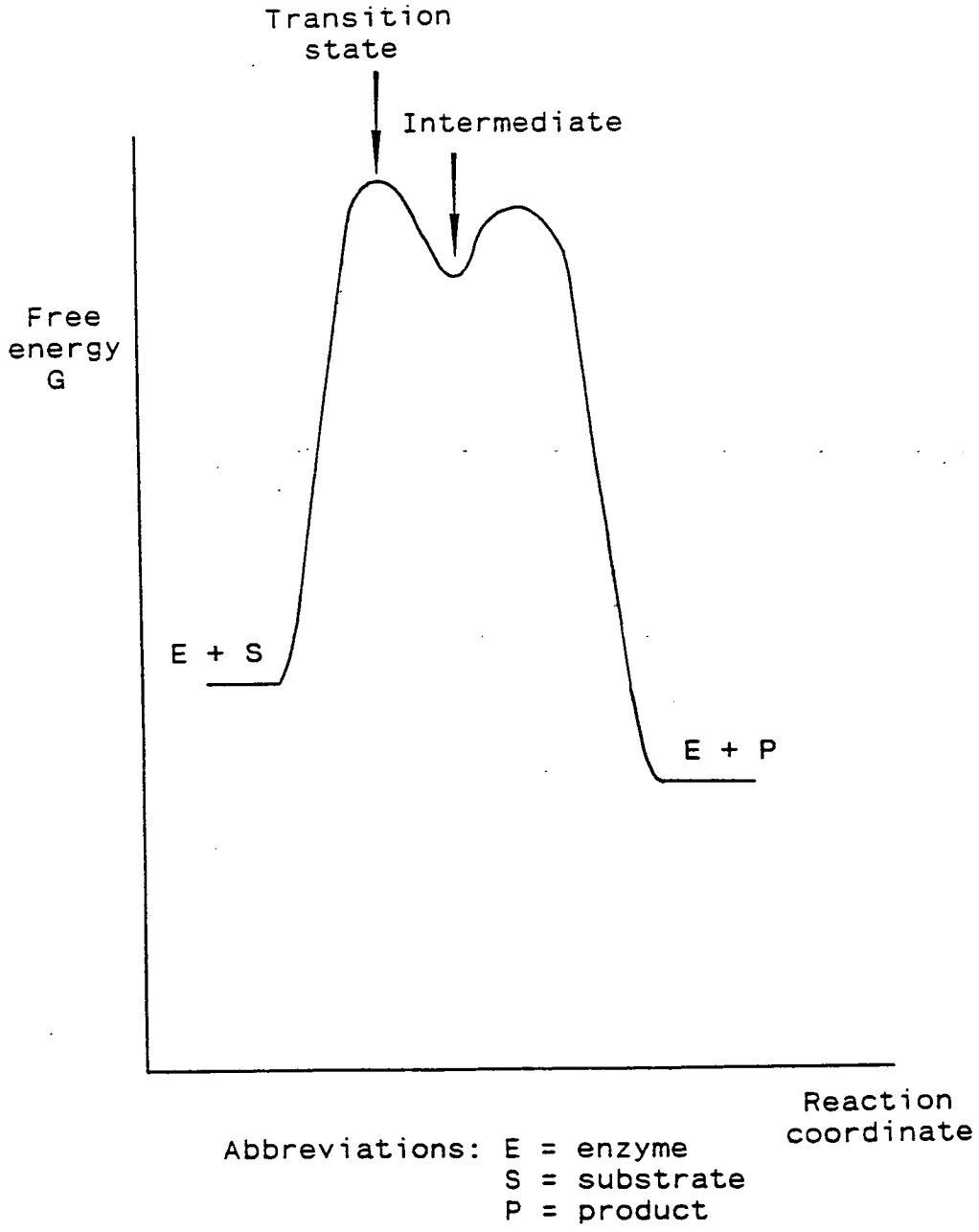

Oxalate is an analogue for the transition state formed during the oxidation of lactate by flavocytochrome $\underline{b}_2$.

binding between $\underline{b}_2$-flavin domain and FD/Y143F, which, at 8.3kJM^{-1} is close to the expected difference for removal of a hydrogen bond [13].

7.3.2 STOPPED-FLOW KINETICS

The reduction of FMN by L-lactate in FD/Y143F is biphasic (Figure 7.4) in sharp contrast with the monophasic process seen in the $\underline{b}_2$-flavin domain (Section 5.3.3). The biphasic nature of this reaction and its implications will be discussed presently.

Parameters obtained from stopped-flow kinetics for FD/Y143F (Table 7.3) show that there are several differences between FMN reduction in the FD/Y143F mutant and the isolated $\underline{b}_2$-flavin domain. k_{cat} for FD/Y143F is more than 2-fold greater than for the $\underline{b}_2$-flavin domain. K_m for L-lactate is also increased in FD/Y143F relative to $\underline{b}_2$-flavin domain. Similar differences were observed between the k_{cat} and K_m values of HE/Y143F and the holoenzyme (Table 7.3) [3,10].

Perhaps the most striking difference between the kinetic parameters of $\underline{b}_2$-flavin domain and FD/Y143F is in their KIE values. The KIE value observed for the fast (initial reduction) phase in FD/Y143F is larger than that observed for the isolated $\underline{b}_2$-flavin domain. Such a difference is not seen for HE/Y143F, which has a KIE for FMN reduction lower than that of the holoenzyme [3].

The implications of biphasic FMN reduction and an increased KIE value are not clear. One possible explanation for the biphasic reduction could be that, in FD/Y143F, substrate binding might be anti-cooperative. Cooperativity and anti-cooperativity occur in proteins having more than one binding site for a given ligand which may interact during the binding process. Thus the affinity of the enzyme for substrate increases or decreases with saturation giving

FIGURE 7.4 BIPHASIC TRACE OBSERVED FOR FMN REDUCTION IN FD/Y143F UNDER STOPPED-FLOW CONDITIONS

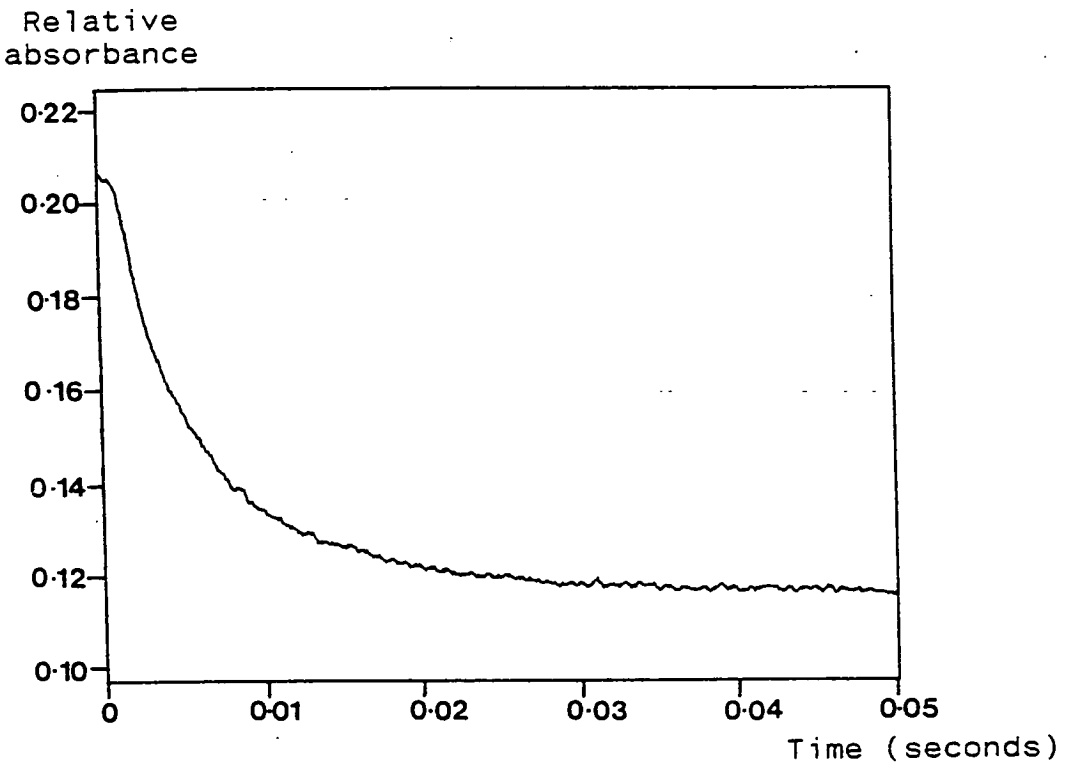

TABLE 7.3: STOPPED-FLOW KINETIC PARAMETERS FOR FMN REDUCTION IN FD/Y143F COMPARED WITH VALUES FOR HOLO-FLAVOCYTOCHROME $\underline{b}_2$, $\underline{b}_2$-FLAVIN DOMAIN AND HOLO-Y143F

	Holo-$\underline{b}_2$	HE/Y143F	$\underline{b}_2$-flavin domain	FE/Y143F	
				Fast phase	Slow phase
K_m lactate (mM)	0.84 ± 0.20	2.81 ± 0.3	0.26 ± 0.07	1.33 ± 0.41	1.8 ± 0.7
k_{cat} (s^{-1})	604 ± 60	735 ± 80	390 ± 10	885 ± 74	173 ± 22
KIE	8.1 ± 1.4	4.3 ± 0.8	5.8 ± 0.3	~10	~20
Reference	(3)	(3)	(This work)	(This work)	(This work)

Experimental conditions are described in Section 7.2.3

characteristic plots of rate vs. substrate concentration (Figure 7.5). A plot of the ratio of amplitude of fast phase:amplitude of slow phase against substrate concentration is linear for FD/Y143F (Figure 7.6). This suggests that there could be a degree of anti-cooperativity between the four substrate binding sites, because the amplitude of the fast phase increases and that of the slow phase decreases with increasing lactate concentration. For example, it could be that once one or more of the substrate binding sites in the tetrameric enzyme are occupied, the remaining sites become less accessible to substrate. The outcome of this scenario would be that, at low lactate concentrations, binding at the remaining sites would be less favourable and two phases would clearly be seen (reduction of the first binding sites by substrate, followed by reduction of the remaining sites). At higher lactate concentrations, binding at the remaining sites would become more likely, making FMN reduction tend further towards monophasicity. However, although this is a tempting explanation for the observed trends, the Michaelis-Menten plots obtained for FD/Y143F are not noticeably sigmoidal and provide no other evidence for cooperativity (Figure 7.7).

7.4 CONCLUSIONS

FD/Y143F, while still active as a L-lactate:ferricyanide oxidoreductase, shows considerable kinetic differences to isolated $\underline{b}_2$-flavin domain. Studies with oxalate, a transition state analogue, show that Tyr 143 plays an important role in transition state stabilisation in the native $\underline{b}_2$-flavin domain.

FIGURE 7.5 THE EFFECTS OF POSITIVE AND NEGATIVE COOPERATIVITY

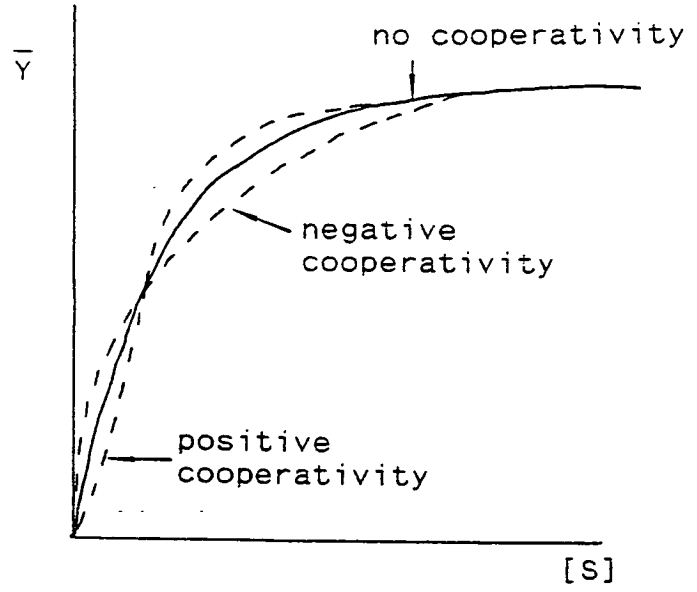

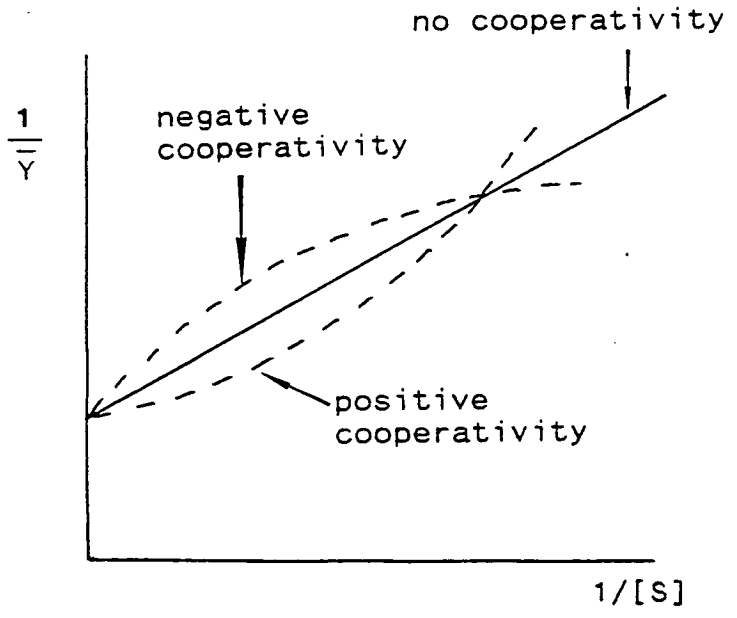

[S] = concentration of substrate

$\bar{Y}$ = fractional saturation

If the Michaelis-Menten assumption is valid, then

$$\bar{Y} = \frac{v}{V_{max}}$$

FIGURE 7.6 PLOT OF AMPLITUDE RATIO VS LACTATE CONCENTRATION FOR FD/Y143F STUDIED UNDER STOPPED FLOW CONDITIONS

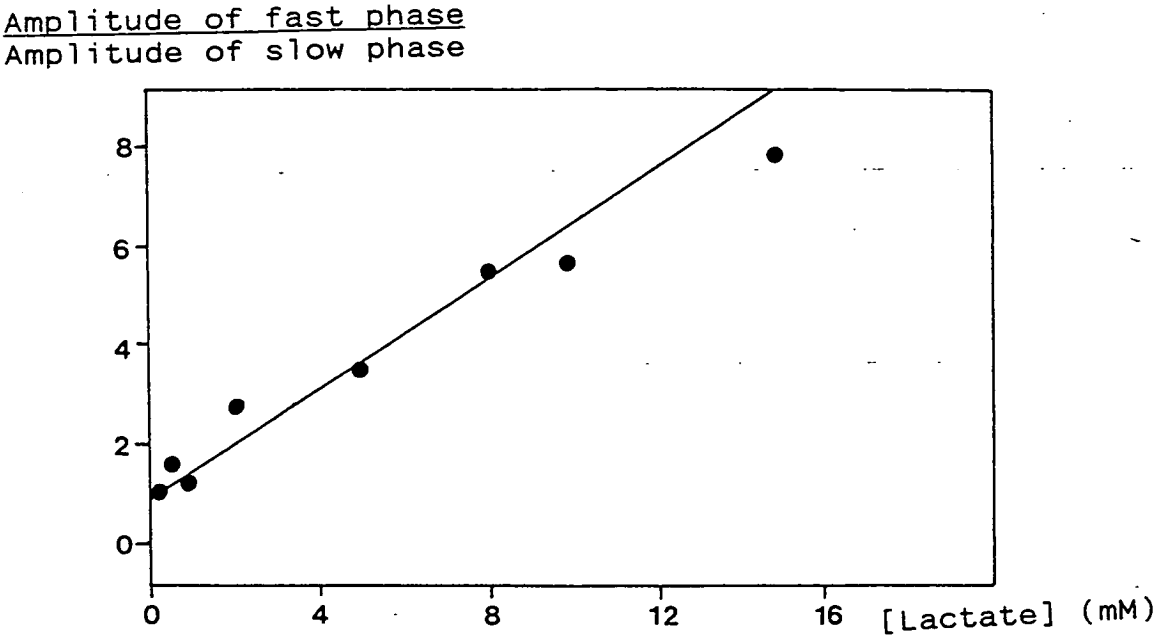

Experimental conditions are described in Section 7.2

FIGURE 7.7 MICHAELIS-MENTEN PLOTS FOR FMN REDUCTION IN FD/Y143F UNDER STOPPED-FLOW CONDITIONS

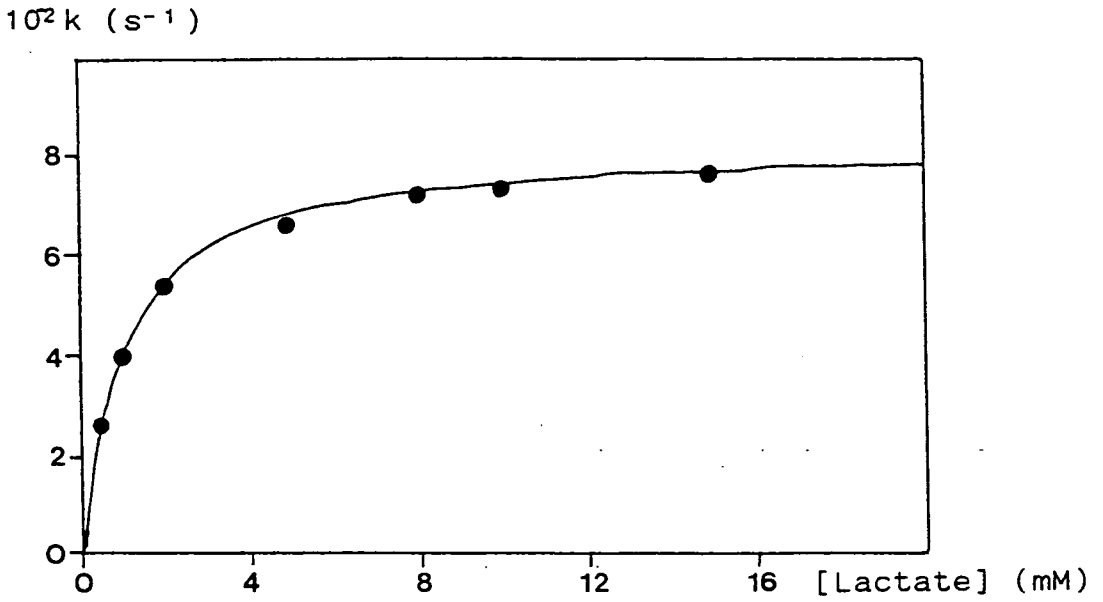

(a) Fast phase

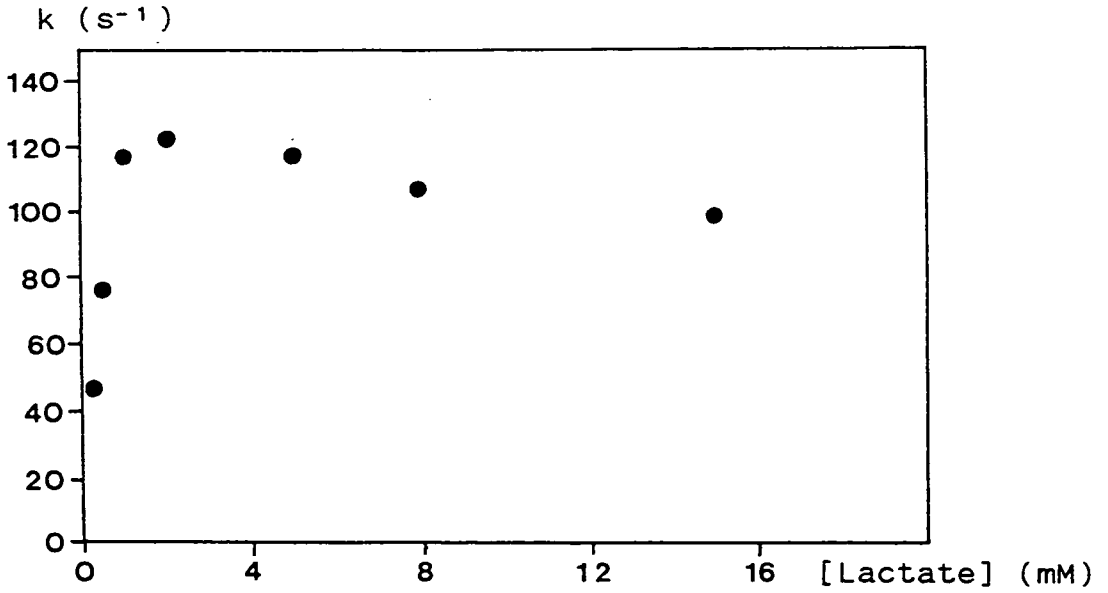

(b) Slow phase

Experimental conditions are described in Section 7.2

7.5 REFERENCES

[1] Chapman, S.K., White, S.A. & Reid, G.A., Adv. Inorg. Chem. **36**, 257-301 (1991)

[2] Reid, G.A., White, S.A., Black, M.T., Lederer, F., Mathews, F.S. & Chapman, S.K., Eur. J. Biochem. **178**, 329-333 (1988)

[3] Miles, C.S., Rouviere-Fourmy, N., Lederer, F., Mathews, F.S., Reid, G.A., Black, M.T. and Chapman, S.K., Biochem. J. **285**, 187-192 (1992)

[4] Xia, Z,-x. & Mathews, F.S., J. Mol. Biol. **212**, 837-863 (1990)

[5] Lederer, F., in "Chemistry and Biochemistry of Flavoenzymes", (Muller, F., ed), CRC Press Inc., Boca Raton, 153-242 (1991)

[6] Black, M.T., Gunn, F.J., Chapman, S.K. & Reid, G.A., Biochem. J. **263**, 973-976 (1989)

[7] Labeyrie, F., Beloeil, J.C. & Thomas, M.-A., Biochim. Biophys. Acta **953**, 134-141 (1988)

[8] White, P., Manson, F.D.C., Brunt, C.E., Chapman, S.K. & Reid, G.A. (in press)

[9] Black, M.T., White, S.A., Reid, G.A. & Chapman, S.K., Biochem. J. **258**, 255-259 (1989)

[10] Miles, C.S., PhD Thesis, University of Edinburgh (1992)

[11] Lederer, F., Eur. J. Biochem. **88**, 425-431 (1978)

[12] Ghisla, S. & Massey, V., J. Biol. Chem. **252**, 6729-6735 (1977)

[13] Fersht, A., "Enzyme Structure and Mechanism" (2nd Edition), W.H. Freeman, & Co., New York, 297-299 (1985)

CHAPTER 8

METHODS AND MATERIALS

8.1 GROWTH OF *E.coli*

8.1.1 GENERAL

The strains of *E.coli* used for plasmid propagation and expression of the isolated domains of flavocytochrome b_2 and FD/Y143F as described in 2.1.4 and 4.2 were grown in Luria broth as described below.

8.1.2 PREPARATION OF GROWTH MEDIA

Luria Broth (LB) :	Tryptone (Difco)	10g per litre
	Yeast extract (Difco)	5g per litre
	Sodium chloride (Fisons SLR)	5g per litre

The broth was made up in deionised water and autoclaved (20 min, 122°C, 16psi).

Before inoculation with *E.coli* LB was supplemented with carbenicillin or ampicillin to prevent the growth of contaminating organisms and to select for transformed cells. Carbenicillin (50μg/ml, Sigma) or ampicillin (100μg/ml, Sigma) was first dissolved in a small volume of water and sterilised by filtration through a Millex-GS 0.22μm filter unit (Millipore) before being added to autoclaved LB.

Culture plates and stabs for the propagation of *E.coli* strains were prepared by autoclaving separately double-strength LB and agar (Difco) solution (3%). The autoclaved solutions were mixed while still warm to give a final agar concentration of 1.5%. Carbenicillin was added as before and the mixture poured into sterile plates or stab bottles.

8.1.3 GROWTH CONDITIONS : b_2-HAEM DOMAIN

Starter cultures were prepared by inoculating LB containing carbenicillin or ampicillin with single colonies of E.coli containing the plasmid expressing b_2-haem domain. Growth took place aerobically at 37°C on an orbital incubator shaking at 250 r.p.h. for approximately 12 hours. Starter cultures producing red cells were then used to inoculate larger volumes of media (1ml starter culture per litre of media) and grown under similar conditions.

8.1.4 GROWTH CONDITIONS : b_2-FLAVIN DOMAIN AND FD/Y143F

The plasmid used for expression of the b_2-flavin domain and FD/Y143F is temperature sensitive (Section 4.2). This means that expression of the enzyme can be induced by a shift in growth temperature.

Starter cultures were grown from single colonies of E.coli as described in Section 8.1.3. A portion of approximately 40ml of the culture was then harvested (Section 8.1.5) and tested for enzyme activity. The harvested cells were frozen at -20°C for approximately 2 hours or plunged into liquid nitrogen for several minutes. The frozen cells were resuspended in 2-3ml of 100mM phosphate buffer, pH 7.0, containing 10mM EDTA and 10mM L-lactate. Lysozyme was added (0.2mg/ml) and the mixture incubated at 0-4°C for approximately 20 minutes. The crude lysate was then assayed for activity as described in Section 7.7.

Active starter cultures were used to inoculate larger volumes of media (1ml culture per litre of media) and grown aerobically at 40°C on an orbital shaker (250 r.p.h., 12 hours). This temperature was found to be effective at inducing enzyme expression by the

temperature-sensitive promoter (Section 4.2).

8.1.5 HARVESTING OF CELLS

Cells were harvested by centrifuging for 6 minutes at 15 000g, 0-4°C (Sorvall RC-5B refrigerated superspeed centrifuge). Cells were stored frozen at -20°C until required.

8.2 PREPARATION OF BUFFERS

8.2.1 GENERAL

All buffers were prepared using deionised water purified by reverse osmosis and ion-exchange to a resistivity of 18.3MΩ (Millipore Milli-QSP reagent water system). Buffer pH was measured using a WPA CD620 digital pH meter and WPA glass electrode, calibrated at pH 7.00 and either pH 4.00 or pH 10.00 using standard Colourkey buffer solutions (BDH).

8.2.2 PHOSPHATE BUFFERS

Phosphate buffers were prepared using monobasic (NaH_2PO_4) and dibasic (Na_2HPO_4) sodium phosphate (Sigma, reagent grade). Phosphate buffers of a required concentration and pH were prepared by titrating a solution of the relevant concentration of monobasic sodium phosphate against the same concentration of dibasic phosphate at 25°C to the required pH (in the range pH 5.8 to 8.0) [1].

8.2.3 TRIS.HCl BUFFER

Tris.HCl buffer was prepared using Trizma base (tris(hydroxymethyl) aminoethane) (Sigma, reagent grade) and HCl

(Fisons, SLR). 10ml of 1M HCl was added to 500ml deionised water containing 5.265g of NaCl (Fisons, SLR). The solution was then titrated to pH 7.50 with Trizma base and the volume adjusted to 1 litre, to yield Tris.HCl buffer pH 7.50, I=0.10M. Tris.HCl buffers were used within two to three weeks of preparation.

8.3 AMMONIUM SULPHATE FRACTIONATION

Ammonium sulphate fractionation was used as a purification step for both $\underline{b}_2$-haem and flavin domains. In polar solvents, proteins become solvated. Addition of a high concentration of an electrolyte such as ammonium sulphate causes the solvent molecules to bind tightly to the electrolyte with the result that the protein comes out of solution and can be collected by centrifugation.

By using different saturations of $(NH_4)_2SO_4$, this phenomenon can be useful as a step in protein purification. $(NH_4)_2SO_4$ (Fisons, SLR) was used in the purification of $\underline{b}_2$-haem and flavin domains at 30% saturation to salt out contaminating proteins and at 70% saturation to salt out the enzymes themselves (Sections 2.2.2 and 4.3.2)

8.4 DIALYSIS

Seamless, semi-permeable dialysis tubing (Sigma) was soaked in deionised water to remove glycerol (added to the tubing as a humectant) and was then rinsed with the appropriate buffer solution. The enzyme solution was then pipetted into a dialysis sack made by knotting the tubing at one end. The free end of the filled sack was knotted and the sack was then placed in a large volume of buffer (at least 100 times the volume of buffer in the sack) at 0-4°C. The

protein was then dialysed overnight, with at least one change of dialysis buffer, to ensure complete exchange of the enzyme into the buffer.

8.5 COLUMN CHROMATOGRAPHY

8.5.1 COLUMN PREPARATION

A small plug of glass wool was placed in the bottom of a vertically-mounted glass column. A slurry of the column material prepared according to the manufacturer's directions was poured into the column, with the tap fully open, until the desired column height was achieved. The column was then equilibrated by washing with several volumes of the relevant buffer. All columns were used and stored at 0-4°C. When required, fractions were collected using a Biorad 2110 fraction collector.

8.5.2 HYDROXYAPATITE COLUMN CHROMATOGRAPHY

Hydroxyapatite chromatography was used in the purification of b_2-haem domain as described in Section 2.2.2. Hydroxyapatite is a crystalline form of $Ca_{10}(PO_4)_6(OH)_2$. The actual method of action of hydroxyapatite is uncertain, but it is thought to bind proteins by interaction with the phosphate groups [3].

Hydroxyapatite was prepared for use by suspending in the relevant buffer to form a slurry. After use it was recovered by washing with 1M NaCl and stored as a slurry at 0-4°C, with 0.02% azide added.

8.5.3 ION EXCHANGE CHROMATOGRAPHY

Ion exchange chromatography using DE-52 (Whatman) was used in the purification of $\underline{b}_2$-haem domain, $\underline{b}_2$-flavin domain and FD/Y143F. DE-52 is a microgranular cellulose anion exchange material with diethylaminoethyl (DEAE) groups. The positively-charged amino group binds to negatively-charged regions of protein. Protein can then be displaced using a salt solution.

DE-52 was obtained pre-swollen and required no preliminary treatment except equilibration with the desired buffer. The dry cellulose was stirred with a concentrated solution (0.1-0.2M) of the buffer to be used (15-30ml buffer per g dry cellulose) and allowed to settle. The supernatant was decanted and the cellulose resuspended in fresh buffer, allowed to settle and decanted again. The cellulose was then stirred with a third volume of buffer and the pH adjusted to the desired value by adding the acidic or basic component of the buffer as necessary. The supernatant was then decanted, the cellulose resuspended in fresh buffer and poured into the column. The column was then washed with at least three volumes of the column buffer before use.

DE-52 columns were regenerated by washing with one column volume of 0.5M HCl, several column volumes of deionised water, one column volume of 0.5M NaOH and finally with several column volumes of deionised water.

8.5.4 GEL FILTRATION COLUMN CHROMATOGRAPHY

A gel is an inert 3D random network containing pores. When a solution of different sized molecules is passed through the column molecules which are larger than the pore size move through the

column quickly. Those molecules which are smaller than the pore size are slowed down by diffusion in and out of the pores, the smallest molecules being retarded the most. Thus gel filtration is an effective method of separating molecules on the basis of molecular weight. Gel filtration chromatography was used in purification of the $\underline{b}_2$-haem and flavin domain, to remove lactate from enzyme solutions, and to determine the native molecular weight of the $\underline{b}_2$-flavin domain.

Sephadex G-75-120 gel filtration beads (Sigma) were used to remove high molecular weight impurities from $\underline{b}_2$-haem domain (Section 2.2.2). This gel has an exclusion limit of M_r 80 000, i.e. proteins of higher molecular weight than this are excluded from the inner volume of the gel particles. The gel filtration beads were prepared by swelling in excess buffer (7.5 $\pm$ 0.5g of water is taken up per gram of dry gel) and the column was poured and equilibrated as described in Section 8.5.1.

Sephadex G-25 (Sigma) was used to remove lactate from enzyme solutions. This gel has a fractionation range of M_r 1000 - 5000 for proteins; thus an enzyme such as flavocytochrome $\underline{b}_2$ (M_r 230 000) or $\underline{b}_2$-flavin domain (M_r 184 000) passes through the column quickly while lactate is retained in the pore spaces. Like G-75-120, G-25 was prepared by swelling in buffer (2.5 $\pm$ 0.2g water taken up per gram of dry gel) before being poured and equilibrated.

Gel filtration using Sephacryl S-300 beads (Sigma) was used both as the final purification step for the $\underline{b}_2$-flavin domain and to determine its native molecular weight. For a variety of gels, including S-300, a plot of V_e/V_o versus log(molecular weight), where V_e is the elution volume (volume at which the most active fraction

is eluted) and V_0 is the void volume, is linear. V_0 can be calculated by passing Blue Dextran (Sigma, average M_r 2 000 000) through the column. The column can then be calibrated using molecules of known M_r to plot a graph of V_e/V_0 vs. log (M_r) from which the M_r of an unknown may be interpolated.

Sephacryl S-300 beads were suspended in buffer and the column was poured as described in Section 8.5.1. The column was calibrated using Sigma molecular weight markers as follows: β-amylase (M_r 200 000), alcohol dehydrogenase (M_r 150 000), bovine serum albumin (M_r 66 000), carbonic anhydrase (M_r 29 000), myoglobin (M_r 17 500) and cytochrome $\underline{c}$ (M_r 12 500).

S-300 has a fractionation range of M_r 10 000 to 1.5 x 10^6. It is therefore also used to remove impurities from $\underline{b}_2$-flavin domain purified by DE-52 column chromatography (Section 4.3.2).

8.6 SODIUM DODECYL SULPHATE - POLYACRYLAMIDE GEL ELECTROPHORESIS (SDS - PAGE)

8.6.1 GENERAL

Most biological polymers such as proteins are electrically charged and will therefore move in an electric field. Such mobility of proteins in polyacrylamide gels containing sodium dodecyl sulphate (SDS) can be used to determine their molecular weights [4] and also to separate proteins of different molecular weights. Thus SDS-PAGE is useful not only in determining molecular weights but also for monitoring the composition of a mixture of proteins.

SDS is a powerful protein denaturant. At neutral pH in 1% SDS and 0.1M mercaptoethanol, most proteins bind SDS and dissociate.

The mercaptoethanol breaks disulphide bridges and protein secondary structure is lost, and the resulting complexes of protein subunits and SDS assume a random-coil configuration, behaving as though they have uniform shape and an identical charge-to-mass ratio. The charge of the complex is determined solely by the SDS, which is bound at a constant proportion of 1.4g SDS per gram of protein. Thus, when proteins which have been treated in this way are electrophoresed, their mobility is related only to molecular weight and not to the intrinsic charge of the amino acids forming the protein [5]. A calibration graph of log (molecular weight) against distance moved along the gel can be plotted for a number of proteins of known molecular weight, which can then be used to estimate the molecular weight of the unknown protein. The molecular weight determined by this method will be that of the protein subunit, due to the denaturing effect of SDS.

SDS-PAGE was carried out using a vertical gel box system (BRL), the applied potential being controlled by a Biorad 200/2.0 power supply.

8.6.2 ELECTROPHORESIS BUFFERS

Resolving buffer : stored as a 2-fold concentrate.

Tris.HCl pH 8.8	0.375M
SDS (Sigma)	0.1%

Stacking buffer : stored as a 2-fold concentrate.

Tris.HCl pH 6.8	0.125M
SDS	0.1%

Reservoir buffer : stored as a 5-fold concentrate and diluted immediately before use with deionised water.

Tris.HCl pH 8.8	0.025M
Glycine (Sigma)	0.19M
SDS	0.1%

8.6.3 STAIN AND DESTAINS

Stain

Isopropanol (v/v)	25%
Acetic acid (v/v)	10%
Coomassie Brilliant Blue (Sigma)	0.1%

Destains

(1)	Isopropanol	25%
	Acetic acid	10%
(2)	Isopropanol	10%
	Acetic acid	10%
(3)	Acetic acid	10%

8.6.4 PREPARATION OF GELS

Resolving gel

The resolving gel was prepared with resolving buffer (Section 8.6.2), an appropriate amount of acrylamide (Acrylogel 5 premix (BDH), stored as a 36% (w/v) solution or as a solid), 10% ammonium persulphate solution (2.5 μl/ml) and deionised water. The mixture was filtered and degassed before being polymerised by the addition of N,N,N^1,N^1 - tetramethyl ethylenediamine (TEMED) (Sigma) (1 μl/ml).

Typical acrylamide concentrations used were 12% for $\underline{b}_2$-haem domain and 18% for $\underline{b}_2$-flavin domain.

Stacking gel

The stacking gel was prepared as for the resolving gel, using stacking buffer (Section 8.6.2) instead of resolving buffer and at half the acrylamide concentration of the resolving gel.

8.6.5 SAMPLE PREPARATION

Sample buffer

Tris.HCl pH 6.8	0.125M
SDS	2%
Glycerol (Fisons AR Grade)	10%
β-mercaptoethanol (Sigma)	10%
Bromophenol blue (BDH)	0.01%

Protein samples were prepared by mixing the sample with sample buffer in a 1:1 ratio and heated in a boiling water bath for 2 minutes. The samples were mixed on a vortex mixer before returning to the water bath for a further minute. The samples were mixed again before being loaded onto the gel.

8.6.6 MOLECULAR WEIGHT MARKERS

Molecular weight marker kits for SDS-PAGE (BDH) were used to calibrate the gel. The mixture of markers was prepared with sample buffer as described in Section 8.6.5. Molecular weight markers were run on the same gel alongside protein samples. The contents of the molecular weight marker kits are as described below.

M_r range 12 300 - 78 000

	M_r
Cytochrome c (equine)	12 300
Myoglobin (equine)	17 200
Carbonic anhydrase	30 000
Ovalbumin (hen egg)	42 700
Albumin (bovine serum)	66 200
Ovotransferrin (hen egg)	76-78 000

M_r range 2 512 - 16 949

This kit contains a series of peptides formed by cleavage of myoglobin. Molecular weights are 2 512, 6 214, 8 519, 14 404 and 16 949.

8.6.7 RUNNING THE GEL

The gel was run in reservoir buffer (Section 8.6.2). A current of 0.02A was applied across the gel until the dye front reached the foot of the gel (approximately 5 hours). The gel was removed and placed in stain solution (Section 8.6.3) overnight. The gel was destained by washing with three changes each of destains (1)-(3) (Section 8.6.3), allowing the gel to soak in the destain for an hour between changes.

8.7 MONITORING ENZYME ACTIVITY

Because b_2-flavin domain is not coloured and has no distinctive electronic absorption spectrum in the reduced state, its presence can be detected by assaying for enzyme activity. An appropriate volume of the enzyme sample is injected into a spectrophotometer cuvette containing 1mM ferricyanide and 10mM L-lactate in Tris.HCl

buffer, pH 7.5, I=0.10M. After mixing, the decrease in ferricyanide absorbance at 420nm is monitored.

8.8 PREPARATION OF SOLUTIONS FOR KINETIC STUDIES

8.8.1 GENERAL

Substrate, inhibitor and electron acceptor solutions of appropriate concentrations were prepared in Tris.HCl buffer, pH 7.5, I=0.10M (Section 8.2.3).

8.8.2 SUBSTRATES

L-[1-^{1}H]lactate solutions were prepared using L(+)-lactic acid (lithium salt, 98-100%)(Sigma).

L-[2-^{2}H]lactate was synthesised by a coupled enzyme procedure as described in [6]. Yeast alcohol dehydrogenase (2mg)(Sigma) and beef heart lactate dehydrogenase (12mg)(Sigma) were added to 50ml of 90mM hexadeuteroethanol (Sigma), 70mM pyruvate (pyruvic acid, sodium salt, Sigma), 1.8mM nicotinamide adenine dinucleotide (NAD^{+}) (Sigma) in 10mM phosphate buffer, pH 8.0 at 37°C. The reaction was incubated at 37°C for 18 hours after which the mixture was boiled for 3 minutes to halt the reaction.

The labelled lactate was filtered and purified on a Dowex 1 x 8 - 200 ion exchange column (2 x 8cm) equilibrated in deionised water and eluted using a linear gradient of deionised water and 3.6M formic acid (Sigma). Fractions were tested for pyruvate using a diagnostic kit (Sigma). Pyruvate-free fractions were pooled and concentrated using a rotary evaporator before being diluted with Tris.HCl buffer, pH 7.5, I=0.10M, checking and adjusting the pH if

necessary before use.

The isotopic purity of the L-[2-^{2}H] lactate was confirmed by NMR spectroscopy. L-[2-^{2}H] lactate concentration was determined enymatically by measuring the amount of ferricyanide reduced by a limiting amount of L-[2-^{2}H] lactate in the presence of a catalytic amount of flavocytochrome $\underline{b}_2$ [7].

8.8.3 INHIBITORS

Pyruvic acid (sodium salt) (Fluka) and sodium oxalate (Fisons SLR) were used to prepare inhibitor solutions.

8.8.4 ELECTRON ACCEPTORS

Ferricyanide (potassium salt) (Fisons SLR) was used as the electron acceptor in all steady-state kinetic studies.

8.9 STEADY-STATE KINETICS

8.9.1 THEORY

When an enzyme is mixed with a large excess of substrate, enzyme-bound intermediates quickly build up to a constant concentration. When this is reached the system is said to be in a steady state, and kinetic parameters can be measured.

The expressions used to calculate steady-state kinetic parameters assume that the concentration of enzyme is negligible compared with that of the substrate, and also that the rate being measured, v, is the initial rate of formation of products. v generally follows saturation kinetics with respect to the concentration of substrate, [S], as illustrated in Figure 8.1(a).

At low [S], v increases linearly with [S]. As [S] increases the relationship ceases to be linear until, at saturating [S], v tends towards a limiting value V_{max}. This is expressed in the Michaelis-Menten equation (1) [8]:

$$v = \frac{[E]_o\ [S]\ k_{cat}}{K_m + [S]} \qquad (1)$$

where $[E]_o$ is the total concentration of enzyme initially introduced into the system, $k_{cat}\ [E]_o = V_{max}$, and K_m is the value of [S] at which $v = \frac{1}{2}V_{max}$.

The equation was derived from the scheme:

$$E + S \underset{}{\overset{K_s}{\rightleftharpoons}} ES \xrightarrow{k_{cat}} E + P \qquad (2)$$

where E = enzyme, S = substrate and P = product.

The first stage of catalysis in (2) is reversible formation of an enzyme-substrate complex ES, for which the rate equation is:

$$\frac{[E]\ [S]}{[ES]} = K_s \qquad (3)$$

This is followed by a second step in which the product P is formed. This step is irreversible and has a pseudo-first order rate constant, k_{cat}. The rate equation for the second step is:

$$v = k_{cat}\ [ES] \qquad (4)$$

The concentration of free enzyme, [E], at the steady state is:

$$[E] = [E_o] - [ES] \qquad (5)$$

Substituting for [E] in (3) and rearranging:

$$[ES] = \frac{[E]_o\ [S]}{K_s + [S]} \qquad (6)$$

and using (4) to substitute for [ES] in (6),

$$v = \frac{[E]_o\ [S]\ k_{cat}}{K_s + [S]} \qquad (7)$$

(7) is identical to (1), where K_m is equivalent to the dissociation constant of the enzyme-substrate complex, K_s.

The Michaelis-Menten equation can be represented in a linear form using the Lineweaver-Burk, or double-reciprocal plot (Figure 8.1 (b)). Inverting both sides of equation (1) and using (2) to substitute for $[E_o]$ gives:

$$\frac{1}{v} = \frac{1}{V_{max}} + \frac{K_m}{V_{max}\ [S]} \qquad (8)$$

Thus a plot of 1/v against 1/[S] is linear, with a gradient of k_m/V_{max} and intercept $1/V_{max}$.

The two kinetic parameters evaluated from the Michaelis-Menten equation are K_m and k_{cat}. k_{cat} is called the catalytic constant, or turnover number, and is the velocity of the reaction at infinite substrate concentration. In the case of flavocytochrome $\underline{b}_2$ K_m, the Michaelis-Menten constant, approximates to the dissociation constant of the enzyme-substrate complex, K_s.

8.9.2 GENERAL

The reaction catalysed by $\underline{b}_2$-flavin domain is the two-electron oxidation of L-lactate to pyruvate. The enzyme then transfers electrons to a one-electron acceptor, ferricyanide (Chapter 5). The rate of electron turnover can therefore be measured by monitoring the rate of reduction of ferricyanide in an assay containing excess ferricyanide and substrate with a known quantity of enzyme.

Steady-state kinetics experiments were carried out using a

FIGURE 8.1 MICHAELIS-MENTEN AND LINEWEAVER-BURK (DOUBLE RECIPROCAL) PLOTS

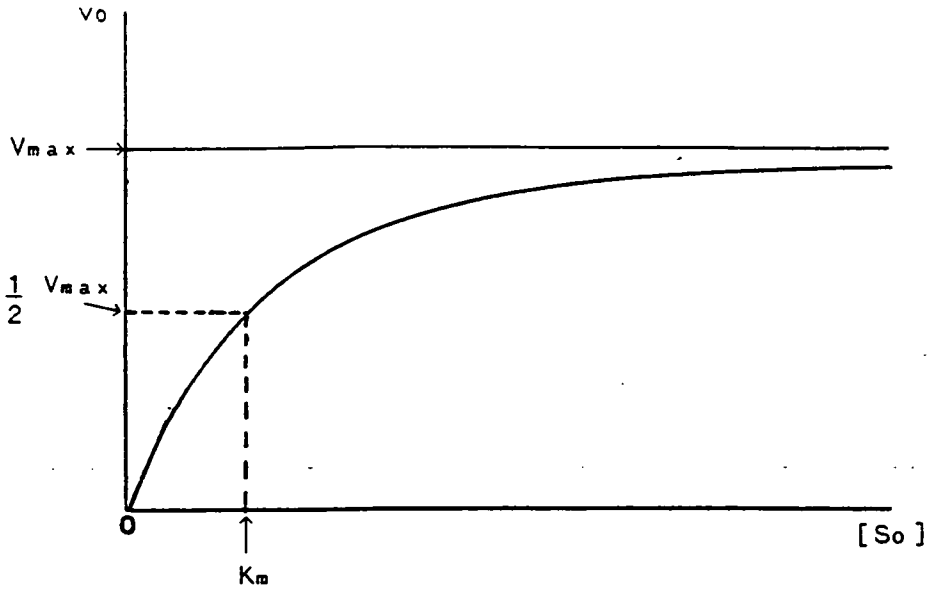

(a) GRAPHICAL REPRESENTATION OF THE MICHAELIS-MENTEN EQUATION

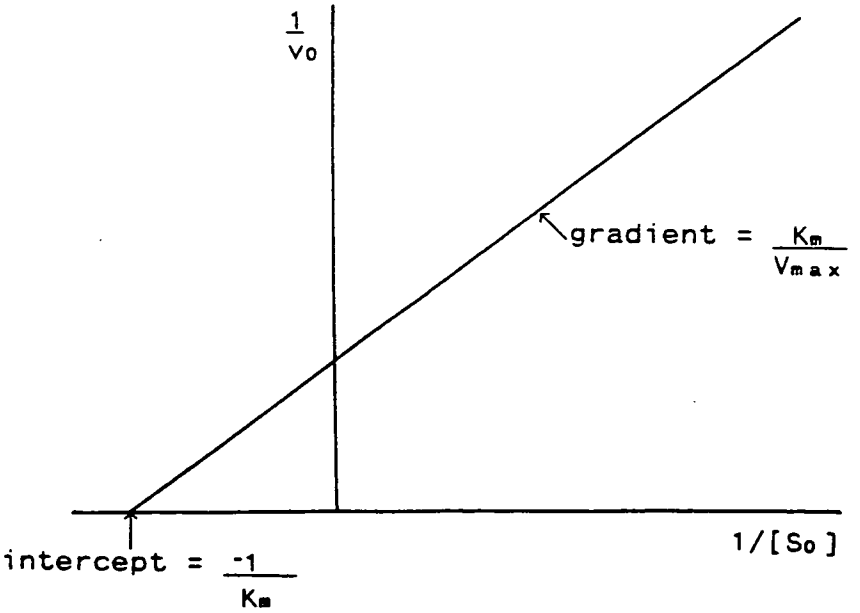

(b) THE LINEWEAVER-BURK PLOT

v_o = initial velocity of reaction
$[S_o]$ = initial concentration of substrate
V_{max} = limiting initial velocity
K_m = Michaelis constant

Beckman DU-62 UV/visible spectrometer thermostatted at 25 ± 0.1°C to measure ferricyanide reduction at 420nm ($\epsilon_{Fe(CN)_6^{3-}}$ = 1010 $M^{-1}cm^{-1}$).

All assays were performed in cuvettes of 0.2cm pathlength. Tris. HCl buffer, pH 7.5 I=0.10M (Section 8.2.3) was used throughout. All solutions were thermostatted at 25 ± 0.1°C throughout the experiment with the exception of protein solutions, which were kept on ice.

Kinetics parameters were calculated using a linear least-squares program to fit double-reciprocal plots or by using a non-linear regression program to fit Michaelis-Menten plots.

8.9.3 PROTEIN CONCENTRATION DETERMINATION

Protein concentration was determined spectrophotometrically with oxidized $\underline{b}_2$-flavin domain, using previously-published extinction coefficients for haem-free flavocytochrome $\underline{b}_2$ [9] (ϵ_{453} = 11.1 mM^{-1} cm^{-1}). The enzyme was then reduced by the addition of solid sodium L(+)lactate to minimise any loss of activity during the course of the experiment.

8.10 STOPPED-FLOW KINETICS

8.10.1 GENERAL

Pre-steady state kinetic methods such as stopped-flow are used to monitor the approach to the steady state. Stopped-flow kinetic studies were used to directly monitor the rate of reduction of the FMN prosthetic group by the rapid mixing of oxidized enzyme and substrate in the absence of electron acceptors.

Experiments were performed using an Applied Photophysics

SF.17mV stopped-flow spectrofluorimeter which has a dead time (the interval between mixing and initial observation) of $\leq$ 1ms. Flavin reduction was monitored by observing the decrease in absorbance at 453nm. The temperature was maintained at 25 $\pm$ 0.1°C throughout. Mixing was initiated by a gas drive unit under a pressure of approximately 70 p.s.i., the total mixing volume being 50 μl. Data were collected in the software absorbance mode and were automatically collected and displayed in absorbance units. The SF.17 MV software was used to analyse data by non-linear regression analysis of stopped-flow traces to analytical equations.

8.10.2 PROTEIN PREPARATION

Enzymes (b_2-flavin domain and FD/Y143F) were purified by DE-52 column chromatography (Section 4.3.2). Prior to use, the enzyme was oxidized by passing through a Sephadex G-25 gel filtration column equilibrated in Tris.HCl buffer, pH 7.5, I=0.10M (Sections 8.2.3 and 8.5.4), which removed ammonium sulphate and lactate.

8.11 REDOX POTENTIAL DETERMINATION

8.11.1 GENERAL

Haem midpoint potentials were determined spectrophotometrically using a previously-published technique [10]. The apparatus used consisted of a 3ml Pyrex cuvette with an adaptor fused onto it. Potentials were recorded using a platinum working electrode with a sliver/silver chloride reference electrode. The degree of oxidation or reduction was monitored by recording the absorbance at 557nm.

8.11.2 REDOX SOLUTIONS

Fe^{3+}/EDTA standard solution

48.2mg ferric ammonium sulphate was dissolved in 25ml of 40mM EDTA solution previously neutralised to pH 7.0. After gentle heating to dissolve the salt, the solution was made up to 50ml with deionised water to make a standard 2mM Fe^{3+}/20mM EDTA solution.

Fe^{2+} standard solution

Ferrous ammonium sulphate (1.96g) was dissolved in 40 ml previously-degassed water (deionised water which had been bubbled with oxygen-free argon), made up to 50ml volumetrically, and degassed thoroughly by bubbling with argon. This produced a standard solution of 100mM Fe^{2+}.

Redox mediators

Redox mediators effectively act as "go-betweens" connecting the measuring electrode to the biological redox centre, which would not otherwise gain proper contact with the electrode surface due to the shielding by the surrounding protein. The redox mediators used are summarised in Table 8.1.

Dithionite solution

Sodium dithionite (Fisons SLR) (30mg) was dissolved in Tris.HCl buffer pH 7.5 I=0.10M (Section 8.2.3) (5ml) immediately prior to use. The solution was degassed and sealed with a rubber septum.

Ferricyanide solution

Potassium ferricyanide (Fisons SLR) (30mg) was dissolved in Tris.HCl buffer, pH 7.5 I=0.10M (5ml).

8.11.3 CALIBRATION OF THE REDOX ELECTRODE

The Pt pin of the electrode was cleaned with acetone prior to

TABLE 8.1: MEDIATORS USED IN REDOX TITRATIONS

Mediator	E_m (mV) [10]
2-hydroxy-1,4,naphthaquinone (HNQ)	-145
N-ethylphenazonium ethosulphate (PES)	+55
N-methylphenazonium methosulphate (PMS)	+80
2,3,5,6-tetramethylphenylenediamine (DAD)	+260

PMS and PES were dissolved in deionised water and HNQ and DAD were dissolved in 20% ethanol to make 5mM stock solutions.

Mediator solutions were stored in the dark.

use. The calibration solution was prepared in the cuvette using the Fe^{3+}/EDTA standard (1.25ml), 1M acetate buffer pH 5.0 (1.25ml) and deionised water (2.5ml). The redox electrode was put in place and the solution was degassed for at least 20 minutes by continuously flushing O_2-free Ar over the surface of the solution with constant stirring. Fe^{2+} standard solution (10 μl) was injected into the calibration solution and the potential recorded. A further 15 μl of Fe^{2+} standard solution was injected and the potential recorded. These values were used to draw a Nernst plot (potential vs. log [ox]/[red], where [ox] and [red] are the total concentration of oxidized and reduced species respectively). Calibration was repeated until a Nernst plot was achieved with a slope and intercept close to the ideal values of 59mV and 108mV respectively.

8.11.4 HAEM REDUCTION AND OXIDATION

The reaction mixture containing oxidized enzyme (10-20 μM), redox mediators (PES, DAD, HNQ and PMS, all 14 μM) and Fe^{3+}/EDTA solution (20 μM) in Tris.HCl buffer, pH 7.5, I=0.10M, was degassed, with stirring, for at least one hour. Stirring and degassing was maintained throughout the experiment. The haem was reduced by titrating with dithionite, adding sufficient reductant to induce a decrease in potential of 20-40mV. After each addition, the visible absorption spectrum was recorded between 530nm and 575nm, noting the electrode potential at 557nm (the haem absorbance). The absorbance was zeroed at 546nm, a haem isosbestic point, prior to each recording. When the protein had become fully reduced it was reoxidized by titrating with ferricyanide, taking spectra and recording potentials as before. Potentials were corrected for

Ag/AgCl (E_m = +196mV) and Nernst plots were made for oxidative and reductive titrations.

8.12 ELECTRONIC ABSORPTION SPECTROSCOPY

8.12.1 GENERAL

All molecules absorb electromagnetic radiation in the UV/visible region to different extents depending on their structure, making absorption spectroscopy a valuable qualitative and quantitative technique.

At a fixed wavelength, dilute solutions obey the Beer-Lambert law:

$$\log_{10} I_0/I = \epsilon c l$$

where I_0 and I are the respective intensities of the incident and transmitted radiation, l is the path length (the length of the sample in the beam), c is the sample concentration and ϵ is the molar extinction coefficient. log I_0/I is the absorbance of the sample. Therefore, the absorbance of a sample of known extinction coefficient can be used to calculate its concentration.

8.12.2 EXPERIMENTAL DETAILS

All UV/visible spectra were recorded on either a Pye Unicam SP8-400 or a Beckman DU-62 UV/visible spectrometer. Spectrometers were thermostatted at 25 $\pm$ 0.1°C. All assays were carried out at 420nm on a Beckman DU-62 UV/visible spectrometer.

8.13 NUCLEAR MAGNETIC RESONANCE (N.M.R) SPECTROSCOPY

All the NMR studies reported in this thesis were carried out as

part of a collaboration with Drs. G.R. Moore and A.J.P. Thurgood and Mr. M.C. Cox.

8.13.1 SAMPLE PREPARATION

Oxidized flavocytochrome $\underline{b}_2$ and $\underline{b}_2$-haem domain were transferred to various ^2H_2O/phosphate buffers by repeated concentration and dilution using a Centricon 10 microconcentrator (Amicon). ^2HCl and NaO^2H (both 1%) were used to adjust pH. A Radiometer pH meter and Russel electrode were used to measure pH, which was uncorrected for the small isotope effect.

8.13.2 EXPERIMENTAL

NMR spectra were run on a Jeol GX-400 spectrometer (University of East Anglia) or a Varian VXR 600S spectrometer. 1,4-dioxan was used as an internal standard.

8.14 REFERENCES

[1] Gomori, G., Methods Enymol. **1**, 67-90 (1955)

[2] Freifelder, D., "Physical Biochemistry: Applications to Biochemistry and Molecular Biology", W.H. Freeman & Co., San Francisco, p.256 (1976)

[3] Freifelder, D., "Physical Biochemistry: Applications to Biochemistry and Molecular Biology", W.H. Freeman & Co., San Francisco, p.202 (1976)

[4] Weber, K. & Osborn, M., J. Biol. Chem. **244**, 4406-4412 (1969)

[5] Freifelder, D., "Physical Biochemistry: Applications to Biochemistry and Molecular Biology", W.H. Freeman & Co., San Francisco, p.218 (1976)

[6] Shapiro, S.S. & Dennis, D., Biochemistry **4**, 2283-2288 (1965)

[7] Miles, C.S., PhD Thesis, University of Edinburgh (1992)

[8] Fersht, A., "Enzyme Structure and Mechanism" (2nd Edition), W.H. Freeman & Co., New York, 99-100 (1985)

[9] Iwatsubo, M., Mevel-ninio, M. & Labeyrie, F., Biochemistry **16**, 3558-3566 (1977)

[10] Dutton, P.L., Methods Enzymol. **54**, 411-435 (1978)

APPENDIX

COURSES AND MEETINGS ATTENDED

COURSES

German Introductory Reading Course
G.M. Burnett, University of Edinburgh, 1989

Inorganic Medicinal Chemistry
Drs. S.K. Chapman and A.J. Welch, University of Edinburgh, 1990

Federation of European Biochemical Societies Advanced Course on Inorganic and Physical Biochemistry
Louvain-la-Neuve, Belgium, 1990

Departmental Postgraduate Lectures
University of Edinburgh, 1989-1992

Research Seminars and Colloquia
University of Edinburgh, 1989-1992

MEETINGS

Scottish Protein Group Meeting
Stirling University, 1990

Royal Society of Chemistry Fifth International Conference on Mechanism of Reactions in Solution
University of Kent, 1990

Royal Society of Chemistry Inorganic Biochemistry Discussion Group Christmas Meeting
King's College, London, 1990

Fifth International Conference on Bioinorganic Chemistry
Oxford University, 1991

Inorganic Biochemistry Discussion Group/Scottish Protein Structure Group Joint Meeting on Metalloproteins: Genetic, Biochemical and Structural Approaches
University of Edinburgh, 1992

University of Strathclyde Inorganic Club (USIC) Meetings
1989-1992 (Speaker, 1992)

PUBLICATIONS

PAPERS

Isolation and characterization of the cytochrome domain of flavocytochrome b_2 expressed independently in Escherichia coli

C.E. Brunt, M.C. Cox, A.G.P. Thurgood, G.R. Moore, G.A. Reid and S.K. Chapman, Biochem. J. **283**, 87-90 (1992)

The importance of the hinge in interdomain electron transfer in flavocytochrome b_2

P. White, F.D.C. Manson, C.E. Brunt, G.A. Reid and S.K. Chapman (in press)

ABSTRACTS

Isolation and purification of the flavin domain of flavocytochrome b_2 expressed independently in E.coli

R.L. Pallister, G.A. Reid, C.E. Brunt, C.S. Miles and S.K. Chapman, in "Flavins and Flavoproteins 1990" (B. Curti, S. Ronchi and G. Zanetti, eds.), Walter de Gruyter, Berlin, New York, 787-790 (1991)

Isolation and characterisation of the cytochrome domain of flavocytochrome b_2 expressed independently in E.coli

C.E. Brunt, M.C. Cox, A. Thurgood, G.R. Moore, G.A. Reid and S.K. Chapman, J. Inorg. Biochem. **43**, 312 (1991)

Biochem. J. (1992) 283, 87–90 (Printed in Great Britain)

Isolation and characterization of the cytochrome domain of flavocytochrome b_2 expressed independently in *Escherichia coli*

Claire E. BRUNT,* Mark C. COX,† Andrew G. P. THURGOOD,† Geoffrey R. MOORE,† Graeme A. REID‡ and Stephen K. CHAPMAN*§

*Edinburgh Centre for Molecular Recognition, Department of Chemistry, University of Edinburgh, West Mains Road, Edinburgh EH9 3JJ, Scotland, U.K., †Centre for Metalloprotein Spectroscopy and Biology, School of Chemical Sciences, University of East Anglia, Norwich NR4 7TJ, U.K., and ‡Edinburgh Centre for Molecular Recognition, Institute of Cell and Molecular Biology, University of Edinburgh, Edinburgh EH9 3JR, Scotland, U.K.

The cytochrome domain of flavocytochrome b_2 (L-lactate dehydrogenase) was expressed in the bacterium *Escherichia coli* and a purification procedure was developed. When expressed in *E. coli*, the b_2-cytochrome domain contains protohaem IX and has an electronic absorption spectrum identical with that of the cytochrome b_2 'core' produced by proteolytic cleavage of the enzyme isolated from yeast. The b_2-cytochrome domain isolated from *E. coli* has an M_r of 10500 and a redox potential of -31 ± 2 mV. High-field n.m.r. studies indicate pK_a values for the haem propionate groups to be 4.8 and 4.6, consistent with these groups being exposed to solvent rather than buried inside the protein. Using n.m.r. spectroscopy, we have determined an electron self-exchange rate constant for the b_2-cytochrome domain of 2.3×10^6 $M^{-1} \cdot s^{-1}$, which is more than two orders of magnitude larger than the value obtained for microsomal cytochrome b_5, a homologue of b_2-cytochrome domain.

INTRODUCTION

Flavocytochrome b_2 (L-lactate:cytochrome *c* oxidoreductase, EC 1.1.2.3) from baker's yeast (*Saccharomyces cerevisiae*) is a tetramer of identical subunits, with M_r 57500 [1]. The enzyme is a soluble component of the mitochondrial intermembrane space [2], where it catalyses the oxidation of L-lactate to pyruvate and transfers electrons to cytochrome *c* [3]. The crystal structure of flavocytochrome b_2 has been solved to 0.24 nm resolution [4] and reveals that each subunit consists of two distinct domains: an *N*-terminal haem-containing, or cytochrome, domain; and a *C*-terminal flavin mononucleotide-containing domain. Various attempts have been made to isolate these functionally distinct domains independently by using proteolytic methods [5–7]. Labeyrie *et al.* [5] isolated a tryptic fragment of M_r 11000 that contained haem but was devoid of flavin and had no lactate dehydrogenase activity. The fragment, referred to as the 'cytochrome b_2 core', was found to have spectral properties very like those of microsomal cytochrome b_5 [5]. The isolated cytochrome b_2 core was subsequently shown to consist of residues 8–103 of the mature flavocytochrome b_2 amino acid sequence [6].

An alternative, 'cleaner', method of obtaining the b_2-cytochrome domain alone would be to express this domain independently in *Escherichia coli*. In the present paper we describe the expression of the b_2-cytochrome domain in *E. coli* and its purification, and report initial biophysical characterization of this protein by spectroscopic and other methods.

MATERIALS AND METHODS

DNA manipulation, strains, media and growth

We have previously described a system for efficient expression of active flavocytochrome b_2 in *E. coli* [8]. To express the b_2-cytochrome domain alone we have used the same parent vector, pDS6 [9], and have modified the flavocytochrome b_2 gene by site-directed mutagenesis, introducing a TGA stop codon immediately after the codon for Gly-100. An *Eco*RI-cleavage site was also introduced overlapping with the TGA codon so that the DNA encoding the haem domain could be excised from a mutant clone as an *Eco*RI restriction fragment. Mutagenesis was performed as previously described [10] with the use of the oligonucleotide *074*A (CTCCTGGTTGAATTCA-TGGAAACTAAG) with single-stranded DNA from an M13mp19 clone containing the entire flavocytochrome b_2 coding sequence. Resulting clones were screened for the introduction of the novel *Eco*RI-cleavage site, and one positive clone was then subjected to DNA sequencing, which showed that the stop codon had been introduced as expected and that no further, unwanted, mutations had been introduced into the coding sequence. The *Eco*RI fragment containing the b_2-cytochrome domain coding sequence was inserted in the *Eco*RI site of pDS6, and a recombinant was selected with the correct orientation of the insert for expression.

E. coli MM294 harbouring the recombinant pDS-core was found to express the b_2-cytochrome domain at a high level. Standard methods for growth of *E. coli*, plasmid purification, DNA manipulation and transformation were performed as described in Maniatis *et al.* [11].

b_2-cytochrome domain isolation

Frozen *E. coli* cells were resuspended in 100 mM-sodium phosphate buffer, pH 7.0, containing 10 mM-EDTA. Lysozyme (Sigma) was added to approx. 0.2 mg/ml and the mixture was incubated, with stirring, for 30 min at 4 °C. The solution was centrifuged at 39000 *g* for 20 min. The red supernatant was retained, and the pellet, consisting of cell debris and unlysed cells, was resuspended and subjected to a second lysis followed by a second centrifugation. The supernatant from this second lysis (again red in colour) was combined with that from the first and the solution was adjusted to 30% $(NH_4)_2SO_4$ saturation and centrifuged at 39000 *g* for 10 min. The pellet from this was discarded, and the supernatant was adjusted to 70% $(NH_4)_2SO_4$ saturation, at which point the b_2-cytochrome domain was precipitated. The precipitate was collected by centrifugation at 39000 *g* for 10 min. The red precipitate was redissolved in a minimum volume of 10 mM-sodium phosphate buffer, pH 7.0, and dialysed against this same buffer overnight at 4 °C.

§ To whom correspondence should be addressed.

Table 1. Purification data for isolation of the b_2-cytochrome domain from *E. coli*

A detailed description of the procedure is given in the Materials and methods section.

Purification step	Total protein (mg)	b_2-cytochrome domain (mg)	Recovery (%)	A_{275}/A_{413} ratio
Supernatant after cell lysis	500	8	100	> 6
After $(NH_4)_2SO_4$ and dialysis	160	7.1	89	1.9
After hydroxyapatite column chromatography	28	4.3	54	0.56
After DE-52 DEAE-cellulose column chromatography	3.2	2.2	27	0.27
After Sephadex G-75 column chromatography	2.0	2.0	25	0.19

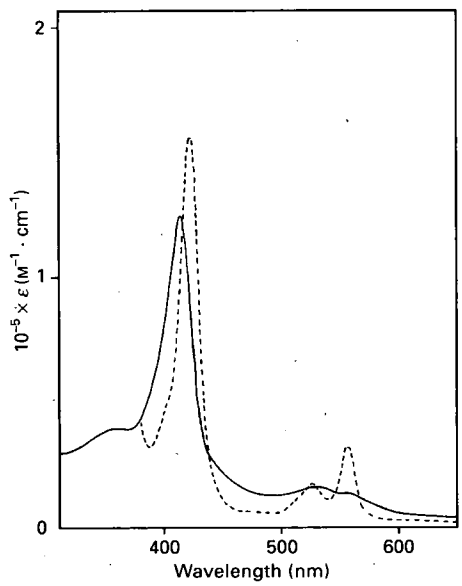

Fig. 1. Visible absorption spectrum of the b_2-cytochrome domain after isolation from *E. coli*

The oxidized and reduced states are denoted by the continuous and broken lines respectively.

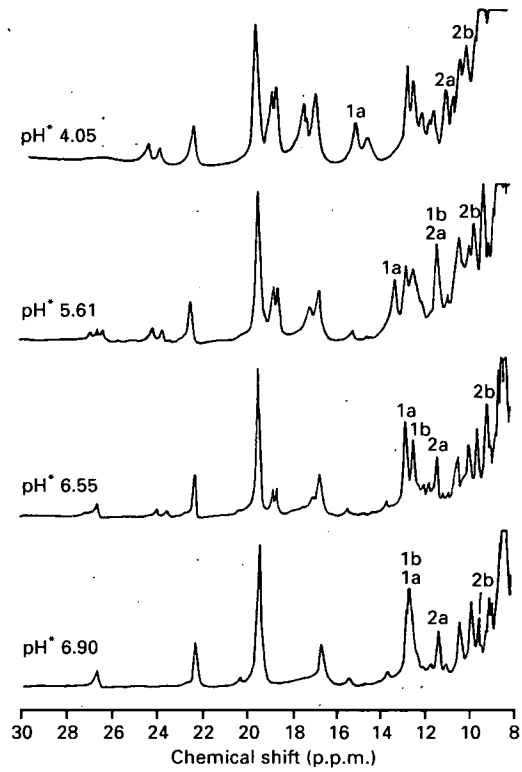

Fig. 2. N.m.r. pH* titration of 2 mM-b_2-cytochrome domain at 25 °C

Spectra were recorded over a frequency range of 25000 Hz with 16 k data points and transformed with an exponential line-broadening function of 2 Hz. They are the sum of 1000 scans.

After dialysis, the solution was centrifuged at 39000 *g* for 2 min, to remove any insoluble material, and then loaded on to a hydroxyapatite (Fluka, fast-flow) column (80 cm × 2.5 cm) previously equilibrated in 10 mM-sodium phosphate buffer, pH 7.0. The column was washed with 2 column volumes of the phosphate buffer and the protein was then eluted by using a gradient of 0–5 %-saturated $(NH_4)_2SO_4$ in the 10 mM-phosphate buffer. Fractions were collected and their purity was evaluated by measuring the ratio of u.v.–visible absorptions at 275 nm and 413 nm. Those fractions with A_{275}/A_{413} ratios < 1.0 were pooled and precipitated at 70 % $(NH_4)_2SO_4$ saturation. After centrifugation at 39000 *g* for 10 min, the precipitate was re-dissolved in 2 mM-sodium phosphate buffer, pH 8.5, and dialysed overnight against this buffer at 4 °C.

After dialysis, the solution was centrifuged at 39000 *g* for 2 min to remove insoluble material and then loaded on to a DE-52 DEAE-cellulose (Whatman) column (50 cm × 2.5 cm) equilibrated in 2 mM-sodium phosphate buffer, pH 8.5. The column was washed with 2 column volumes of the same buffer and the protein was eluted with a gradient of 2–20 mM-sodium phosphate buffer, pH 8.5. Fractions were collected as before and those with A_{275}/A_{413} ratios < 0.3 were pooled. This protein solution was adjusted to 70 % $(NH_4)_2SO_4$ saturation and centrifuged at 39000 *g* for 10 min. The resulting precipitate was dissolved in a minimum volume of 20 mM-sodium phosphate buffer, pH 7.0, and passed through a Sephadex G-75 gel-filtration column (130 cm × 2.5 cm) in the same buffer. Fractions with A_{275}/A_{413} ratio 0.2 ± 0.01 were pooled. Protein purified to this stage showed a single band of M_r 10500 on SDS/PAGE.

The b_2-cytochrome domain concentration was calculated from the absorbance at 413 nm by using the previously published molar absorption coefficient, ε_{413}, of 121500 $M^{-1} \cdot cm^{-1}$ [12].

Further details of the purification procedure, including yields etc., are given in Table 1.

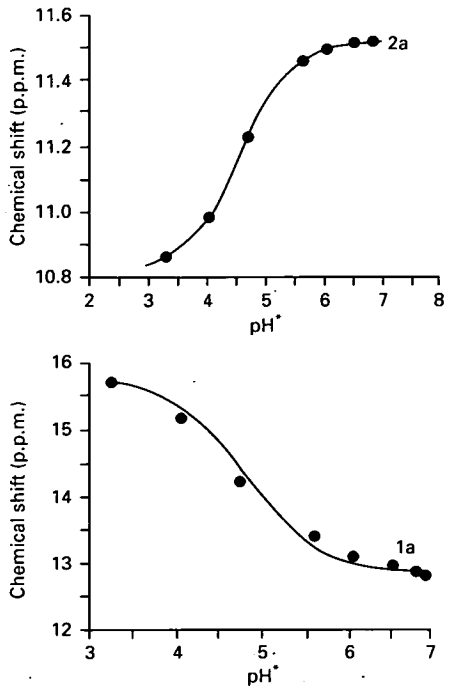

Fig. 3. Shifts of the haem propionate resonances with change in pH*

The points are experimental data obtained from spectra of the type shown in Fig. 2.

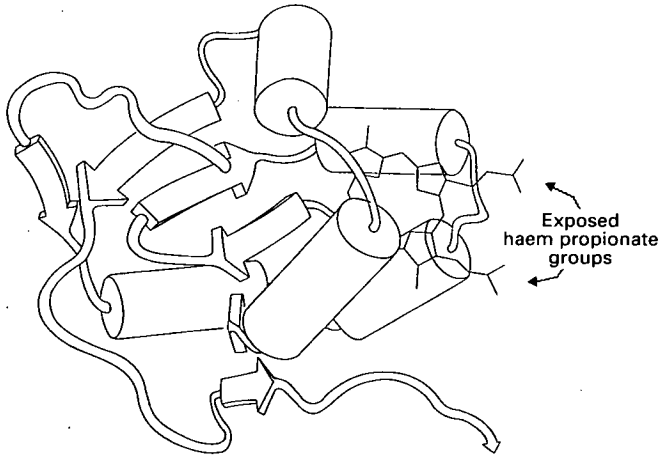

Fig. 4. Schematic diagram of the b_2-cytochrome domain based on the three-dimensional structure of flavocytochrome b_2 determined by Xia & Mathews [4]

Cylinders represent helices and arrows represent β-strands. The exposed propionate groups are indicated.

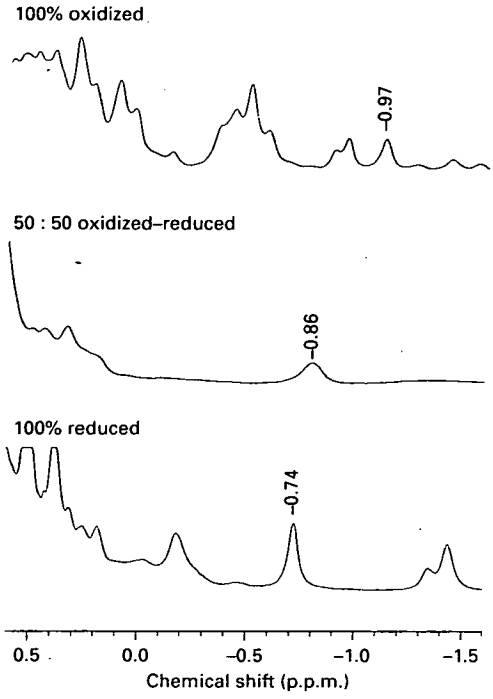

Fig. 5. Oxidation–reduction titration of b_2-cytochrome domain

A 1.1 mM solution of oxidized b_2-cytochrome domain in 5 mM-phosphate buffer, pH 7, was reduced in stages by the addition of $Na_2S_2O_4$ solution (3%, w/v) in ^2H_2O. The electron self-exchange rate was calculated from the excess linewidth at half-height ($\Delta\nu_{\frac{1}{2}}^{e}$) of peaks in the 50:50 oxidized–reduced mixture by using eqn. (1)

$$\Delta\nu_{\frac{1}{2}}^{e} = \frac{2\pi(\nu_A - \nu_B)^2}{k_e} \quad (1)$$

where ν_A is the chemical shift of a peak in the oxidized spectrum, ν_B the chemical shift of a peak in the reduced spectrum and k_e is the first-order self-exchange rate constant [16]. The Figure shows the linewidth change for one of the peaks used to determine k_e.

Measurement of redox potential

The midpoint potential of the cytochrome domain was determined spectrophotometrically by using a previously published redox potentiometry method [13]. The mediators *N*-ethylphenazonium sulphate, *N*-methylphenazonium sulphate, 2,3,5,6-tetramethylphenylenediamine and 2-hydroxy-1,4-naphthoquinone were used as previously described [13]. The cytochrome domain was reduced by titrating with $Na_2S_2O_4$ under anaerobic conditions and oxidized by titrating with $K_3Fe(CN_6)$. Changes in the haem absorbance at 557 nm were measured with changing electrode potential. The system was buffered with 100 mM-sodium phosphate buffer, pH 7.0. The Nernst plots for both reductive and oxidative sequences showed no hysteresis, implying that the system was at equilibrium.

N.m.r. measurements

^1H n.m.r. spectra were recorded with a JEOL GX-400 n.m.r. spectrometer operating at 400 MHz. 1,4-Dioxan was used as an internal standard, but chemical shifts are reported in p.p.m. downfield from the methyl resonance of 4,4-dimethyl-4-silapentane-1-sulphonate. Samples were prepared for n.m.r. with Amicon Centricon devices for exchange of solvent. Three to five cycles of dilution and concentration were used to obtain samples with solvent > 98% ^2H_2O. ^2HCl and NaO^2H were used to adjust pH values. Reported pH values are direct meter readings uncorrected for the small isotope effect and they are designated as pH*. Other conditions are given in Figure legends.

RESULTS AND DISCUSSION

By introducing a termination codon immediately after the Gly-100 codon of the *S. cerevisiae* flavocytochrome b_2 coding region, it has been possible to express the b_2-cytochrome domain with the pDS–b_2 vector previously used for efficient expression of the holoenzyme in *E. coli* [9]. As in the case of the holoenzyme, the cytochrome domain expressed in *E. coli* commences at the amino acid position equivalent to Met-6 of the mature yeast protein (confirmed by determination of the *N*-terminal sequence

with an Applied Biosystems 477 sequencer by the WELMET protein characterization facility at the University of Edinburgh). A purification procedure (see Table 1 and description in the Materials and methods section) has been developed and this has provided good yields of the cytochrome domain. After purification a single band of M_r 10500 can be seen on an SDS/PAGE gel. The electronic absorption spectrum of the b_2-cytochrome domain expressed in *E. coli* (Fig. 1) was superimposable on the spectrum for the cytochrome b_2 core produced by trypsin digest of the holoenzyme from yeast [5], with peaks at 557, 528 and 423 nm in the reduced form and 560, 530 and 413 nm in the oxidized form. The reduction potential (at pH 7.5) of the b_2-cytochrome domain was measured as -31 ± 2 mV, which is very close to the previously published value of -28 mV determined for the proteolytically produced cytochrome b_2 core. These results are consistent with the idea that the b_2-cytochrome domain (residues 6–100 of the mature protein) expressed in *E. coli* and the cytochrome b_2 core (residues 8–103 of the mature protein [6]) produced by proteolysis of the holoenzyme from yeast are essentially identical in terms of their physical properties. This is supported by analysis of the n.m.r. spectra of the two proteins. The general appearance of the b_2-cytochrome domain n.m.r. spectrum resembles that of the proteolytically produced b_2 core as reported by Keller *et al.* [14], particularly with respect to the chemical shift of the haem methyl resonance at 19.5 p.p.m. However, other peaks in the high-frequency region with chemical shifts greater than 14 p.p.m., which were assigned to methyl groups by Keller *et al.* [14], do not have sufficient intensity to arise from methyl groups.

The isolated b_2-cytochrome domain is stable over a wide pH range with no significant change in the electronic absorption spectrum of the oxidized protein between pH 4.0 and 10.0. This pH stability made it possible to use high-field n.m.r. to determine the pK_a values for the ionization of both of the haem propionate groups. Fig. 2 shows n.m.r. spectra of the ferricytochrome domain between 8 and 30 p.p.m. at various pH* values. The peaks assigned to the propionate are labelled 1a, 1b, 2a and 2b. The positions of these peaks shift significantly with pH*. Plots of chemical shift against pH* for peaks 1a and 2a are shown in Fig. 3; these give rise to pK_a values of 4.8 ± 0.1 (1a) and 4.6 ± 0.1 (2a). These values are close to that for free haem propionic acid groups [15], indicating that the propionate groups of the isolated b_2-cytochrome domain must be exposed to solvent rather than buried inside the protein. In the X-ray crystal structure of the holoenzyme, the haem propionate groups point directly into the flavin-binding domain [4]. Thus the isolated b_2-cytochrome domain, independently of the flavin-binding domain, should have exposed propionate groups, as illustrated in Fig. 4 and consistent with the n.m.r. observations.

The electron self-exchange rate constant, k_{11} (at relatively low ionic strength, 5 mM-phosphate), for the b_2-cytochrome domain was determined from a redox titration as described in Fig. 5. At 25 °C and pH 7.4, k_{11} was found to be 2.3×10^6 M^{-1}·s^{-1}. This value is around 600 times larger than the value found for the homologous protein cytochrome b_5 [17]. Cytochrome b_5 and the b_2-cytochrome domain both share a common folding topology, the so-called 'cytochrome b_5 fold' [18]. The two proteins have a high degree of sequence similarity, with 13 residues invariant between the two proteins. One significant difference, however, is the overall charge; this is around -8 in cytochrome b_5 but close to zero in the b_2-cytochrome domain. This difference in charge may be one of the reasons for the large difference in the values of the self-exchange rate constants for the two proteins. In the case of cytochrome b_5 a larger coulombic barrier would have to be overcome to allow electron transfer to take place, and thus one might expect the electron self-exchange rate in cytochrome b_5 to be slower than in the b_2-cytochrome domain, and this is indeed reflected in the values of the measured rate constants.

In conclusion, we have demonstrated an expression system for the b_2-cytochrome domain in *E. coli* and have described an efficient purification procedure for the protein. Biophysical and biochemical properties of the b_2-cytochrome domain, determined by spectroscopic and other methods, have been reported.

We thank the WELMET protein characterization facility at the University of Edinburgh for *N*-terminal sequencing and Dr. G. W. Pettigrew for help in determining redox potentials. This work was supported by the Molecular Recognition Initiative of the Science and Engineering Research Council through research grants and funding for the Edinburgh Centre for Molecular Recognition and the U.E.A. Centre for Metalloprotein Spectroscopy and Biology.

REFERENCES

1. Jacq, C. & Lederer, F. (1974) Eur. J. Biochem. **41**, 311–320
2. Daum, G., Böhni, P. C. & Schatz, G. (1982) J. Biol. Chem. **257**, 13028–13033
3. Appleby, C. A. & Morton, R. K. (1954) Nature (London) **173**, 749–752
4. Xia, Z.-X. & Mathews, F. S. (1990) J. Mol. Biol. **212**, 837–863
5. Labeyrie, F., Groudinsky, O., Jacquot-Armand, Y. & Naslin, L. (1966) Biochem. Biophys. Acta **128**, 492–503
6. Guiard, B. & Lederer, F. (1976) Biochimie **58**, 305–316
7. Celerier, J., Risler, Y., Schwencke, J., Janot, J.-M. & Gervais, M. (1989) Eur. J. Biochem. **182**, 67–75
8. Black, M. T., White, S. A., Reid, G. A. & Chapman, S. K. (1989) Biochem. J. **258**, 255–259
9. Stueber, D., Ibrahimi, I., Cutler, D., Dobberstein, B. & Bujard, H. (1984) EMBO J. **3**, 3143–3148
10. Reid, G. A., White, S. A., Black, M. T., Lederer, F., Mathews, F. S. & Chapman, S. K. (1988) Eur. J. Biochem. **178**, 329–333
11. Maniatis, T., Fritsch, E. F. & Sambrook, J. (1982) Molecular Cloning: A Laboratory Manual, Cold Spring Harbor Laboratory Press, Cold Spring Harbor
12. Pajot, P. & Groudinsky, O. (1970) Eur. J. Biochem. **120**, 158–164
13. Dutton, P. L. (1978) Methods Enzymol. **54**, 411–435
14. Keller, R. M., Groudinsky, O. & Wüthrich, K. (1973) Biochim. Biophys. Acta **328**, 233–238
15. Moore, G. R. & Pettigrew, G. W. (1990) Cytochromes *c*: Evolutionary, Structural and Physicochemical Aspects, p. 14, Springer-Verlag, Berlin
16. Wüthrich, K. (1976) NMR in Biological Research: Peptides and Proteins, Elsevier, Amsterdam
17. Dixon, D. W., Hong, X., Woehler, S. E., Mauk, A. G. & Sishta, B. P. (1990) J. Am. Chem. Soc. **112**, 1082–1088
18. Guiard, B. & Lederer, F. (1979) J. Mol. Biol. **135**, 639–650

Received 31 July 1991/19 September 1991; accepted 4 October 1991